



HAL
open science

Structure-function relationship of FUS, an RNA-binding protein, in DNA repair

Evgeniya Mamontova

► To cite this version:

Evgeniya Mamontova. Structure-function relationship of FUS, an RNA-binding protein, in DNA repair. Molecular biology. Université Paris-Saclay; Novosibirsk State Technical University (Novosibirsk, Russie), 2023. English. NNT : 2023UPASL051 . tel-04195352

HAL Id: tel-04195352

<https://theses.hal.science/tel-04195352>

Submitted on 4 Sep 2023

HAL is a multi-disciplinary open access archive for the deposit and dissemination of scientific research documents, whether they are published or not. The documents may come from teaching and research institutions in France or abroad, or from public or private research centers.

L'archive ouverte pluridisciplinaire **HAL**, est destinée au dépôt et à la diffusion de documents scientifiques de niveau recherche, publiés ou non, émanant des établissements d'enseignement et de recherche français ou étrangers, des laboratoires publics ou privés.

Structure-function relationship of FUS, an RNA-binding protein, in DNA repair

*Relation structure-fonction de FUS, une protéine de liaison à l'ARN, dans la
réparation de l'ADN*

Thèse de doctorat de l'université Paris-Saclay

École doctorale n° 577 : structure et dynamique des systèmes vivants (SDSV)
Spécialité de doctorat : Biologie moléculaire et cellulaire
Graduate School: Life Sciences and Health
Réfèrent : Université d'Évry Val d'Essonne

Thèse préparée dans les unités de recherche **Structure-Activité des Biomolécules Normales et Pathologiques (Université Paris-Saclay, Inserm, Univ Evry) et Institute of Chemical Biology and Fundamental Medicine SB RAS**
Sous la direction de **David PASTRE**, Professeur, la co-direction de **Olga LAVRIK**, Professeure

Thèse soutenue à Paris-Saclay, le 22 mai 2023, par

Evgeniya M. MAMONTOVA

Composition du Jury

Loïc HAMON Professeur, Université d'Évry/Université Paris-Saclay	Président
Françoise DANTZER Directrice de recherche, Université de Strasbourg	Rapporteur & Examinatrice
Stefania MILLEVOI Directrice de recherche, Cancer Research Center of Toulouse, INSERM, Université Toulouse III	Rapporteur & Examinatrice
Partho S. RAY Directeur de Recherches, Indian Institute of Science Education and Research Kolkata	Examineur

Titre : Relation structure-fonction de FUS, une protéine de liaison à l'ARN, dans la réparation de l'ADN

Mots clés : Réparation de l'ADN, protéines de liaison à l'ARN, PARP1, FUS

Résumé : Les cellules ont développé des mécanismes de réparation complexes pour maintenir l'intégrité de leurs génomes, et l'un de ces mécanismes implique l'enzyme PARP-1 et la synthèse de poly(ADP-ribose) (PAR). PARP-1 est recruté sur les sites de dommages à l'ADN, où il synthétise de longues chaînes PAR chargées négativement attachées à lui-même et à d'autres protéines. Les chaînes PAR agissent alors comme un échafaudage pour le recrutement d'autres protéines, qui sont nécessaires à une réparation correcte de l'ADN.

Dans des études récentes, diverses protéines de liaison à l'ARN se sont avérées jouer un rôle dans la réparation de l'ADN. Lorsque l'on considère les mécanismes de réparation de l'ADN qui dépendent de l'activation de PARP-1, il semble que les membres de la famille FET, en particulier FUS, jouent un rôle central. FUS est recruté sur les sites de dommages à l'ADN après exposition au faisceau laser. Il a été identifié dans des analyses par spectrométrie de masse de protéines PARylées suite à un stress génotoxique et il a été démontré qu'il interagit directement avec le PAR. De plus, FUS a été démontré comme formant des compartiments grâce à des interactions entre ses domaines de faible complexité, comme observé au niveau des sites de dommages à l'ADN suite à l'activation de PARP-1.

Le but de cette étude est d'étudier les fonctions biologiques de FUS dans les mécanismes de réparation de l'ADN liés à l'activation de PARP-1. FUS est connu pour participer à la transcription en interagissant avec l'ARN Pol II et en se liant à l'ARNm naissant. Étant donné que les dommages à l'ADN se produisent souvent dans la chromatine ouverte et transcriptionnellement active, FUS est situé à proximité des sites de dommages à l'ADN et peut être rapidement dirigé vers eux. À cet égard, la première question abordée dans cette étude était le lien entre la transcription et la réparation de l'ADN dans le contexte des fonctions FUS dans le noyau. Deuxièmement, la fonction de FUS dans la réparation

de l'ADN dépendante de PARP-1 est basée sur sa capacité à se lier à PAR. Alors que d'autres protéines de liaison à l'ARN peuvent également se lier au PAR par le biais d'interactions électrostatiques, FUS a une propension unique à se lier et à être PARylé. Par conséquent, comprendre les caractéristiques structurales qui rendent FUS unique parmi les autres protéines de liaison à l'ARN et la nature des interactions FUS-PAR peut aider à faire la lumière sur son rôle dans la réparation de l'ADN.

Dans cette étude, nous avons utilisé une approche structurale pour démontrer l'interaction spécifique du domaine RRM unique de FUS avec PAR. Contrairement à d'autres protéines de liaison à l'ARN, les RRM de FUS manquent de résidus aromatiques qui interagissent généralement avec les bases de l'ARN. Notre analyse par spectroscopie RMN montre que cela fournit une base pour l'interaction similaire du FUS RRM avec l'ARN et le PAR. De plus, nous avons cherché à savoir si FUS jouait un rôle dans le contrôle du niveau global de PAR dans le noyau des cellules HeLa suite au stress oxydatif et à l'arrêt de la transcription. Nos résultats indiquent que FUS peut augmenter de manière significative le niveau de PARylation dans les cellules exposées à de faibles concentrations de peroxyde d'hydrogène, un agent de stress oxydatif connu pour activer fortement PARP-1. Cette découverte est cohérente avec le lien entre la transcription et la réparation de l'ADN, car le blocage de la transcription augmente considérablement la capacité de FUS à augmenter le niveau de PAR dans les cellules HeLa exposées au peroxyde d'hydrogène. De plus, nous avons identifié certains résidus situés dans le RRM de FUS, précédemment identifiés comme PARylés, qui contrôlent l'autoPARylation de PARP-1 in vitro et le niveau d'activité de PARP-1 dans les cellules. Dans l'ensemble, ces résultats fournissent une base pour comprendre le rôle spécifique de FUS dans les mécanismes de réparation de l'ADN liés à PARP-1.

Title : Structure-function relationship of FUS, an RNA-binding protein, in DNA repair

Keywords : DNA repair, RNA binding proteins, PARP1, FUS (Fused in Sarcoma)

Abstract : Cells have evolved complex repair mechanisms to maintain the integrity of their genomes, and one of these mechanisms involves the PARP-1 enzyme and the synthesis of poly(ADP-ribose) (PAR). PARP-1 is recruited to the sites of DNA damage, where it synthesizes long negatively charged PAR chains attached to itself and other acceptor proteins. The PAR chains then act as a scaffold for the recruitment of other proteins, such as DNA repair factors, which are required for proper DNA repair.

In recent studies, various RNA-binding proteins (RBPs) have been found to play a role in DNA repair. When considering DNA repair mechanisms that are dependent on PARP-1 activation, it appears that members of the FET family, particularly FUS, play a central role. FUS is recruited to DNA damage sites after laser beam exposure, and this recruitment depends on PARP-1 activity. FUS was identified in mass-spectrometry analyses of PARylated proteins following genotoxic stress and was shown to interact directly with PAR. In addition, FUS was shown to form the compartments through the interactions occurring between its low-complexity domains. Particularly, the formation of such compartments was observed at DNA damage sites following PARP-1 activation.

The aim of this study is to investigate the biological functions of FUS in DNA repair mechanisms related to PARP-1 activation. FUS is known to participate in transcription by interacting with the C-terminal domain of RNA pol II and binding to nascent mRNA. Given that DNA damages often occur in open, transcriptionally-active chromatin, FUS is located in close proximity to DNA damage sites and can be rapidly directed to them. In this regard, the first question addressed in this study was the link between transcription and DNA repair in the context of FUS functions in the nucleus. Secondly, we asked whether FUS's function in PARP-1-dependent DNA repair is based on its ability to bind PAR. While other

RNA-binding proteins can also bind to PAR through electrostatic interactions, FUS has a unique propensity for binding to and being PARylated. Therefore, understanding the structural characteristics that make FUS unique among other RNA-binding proteins and the nature of FUS-PAR interactions can help shed light on its role in DNA repair.

In this study, we utilized a structural approach to demonstrate the specific interaction of the single RRM domain of FUS with protein-free PAR. Unlike other RNA-binding proteins, FET protein RRM domains lack several aromatic residues that usually interact with RNA bases. Our NMR spectroscopy analysis shows that this provides a basis for the similar interaction of FUS RRM with RNA and PAR. Furthermore, we investigated whether FUS plays a role in controlling the overall level of PAR in the nucleus of HeLa cells following oxidative stress and transcription arrest. Our results indicate that FUS can significantly increase the level of PARylation in cells exposed to mild concentrations of hydrogen peroxide, an oxidative stress agent known to strongly activate PARP-1. This finding is consistent with the link between transcription and DNA repair, as stalling transcription significantly increases the capacity of FUS to increase the PAR level in HeLa cells exposed to hydrogen peroxide. Additionally, we identified certain residues located in the RRM of FUS, previously identified as PARylated, that control the autoPARylation of PARP-1 in vitro and the level of PARP-1 activity in cells. Overall, these results provide a basis for understanding the specific role of FUS in PARP-1-related DNA repair mechanisms.

TABLE OF CONTENT

TABLE OF CONTENT	4
ACKNOWLEDGEMENTS	6
AUTHOR'S DECLARATION	8
LIST OF FIGURES	9
LIST OF TABLES	13
LIST OF ABBREVIATIONS	14
LITERATURE REVIEW	18
1. INTRODUCTION.....	18
2. THE ROLE OF PARP-1 AND POLY(ADP-RIBOSYLATION) IN DNA REPAIR.....	21
2.1 The PARPs superfamily	21
2.2 The structural basis of poly(ADP-ribosylation).....	23
2.3 The role of PARP-1 in DNA repair.....	36
3. FET PROTEIN STRUCTURE AND FUNCTIONS.....	46
3.1 FET protein structure	47
3.2 Functions of FET proteins.....	54
3.3 FET proteins - driven liquid-liquid phase separation and the formation of aggregates.....	65
3.4 FET proteins mutations and post-translational modifications and their role in the development of amyotrophic lateral sclerosis and frontotemporal lobar degeneration	80
4. The role of FUS proteins in DNA damage response.....	90
OBJECTIVES OF WORK	93
RESULTS	96
Chapter 1: FUS interacts with poly(ADP-ribosyl)ated PARP-1 under oxidative stress conditions that prevents aberrant FUS self-assemblies after transcription inhibition...	96
Chapter 2: FUS increases the poly(ADP-ribose) level in H ₂ O ₂ -treated cells in a transcription-dependent manner.....	103
Chapter 3: FUS is significantly PARylated and also increases total protein PARylation level <i>in vitro</i> and in cells	110
Chapter 4: Structural basis of the recognition of PAR by FUS RRM.....	113
Chapter 5: FUS RRM is important to increase the PARylation level in cells.....	121

Chapter 6: D343A mutation interferes with the interaction of FUS RRM with activated PARP-1	124
Supplementary information	129
Discussion	137
MATERIALS AND METHODS	142
CONCLUSIONS AND PERSPECTIVES	159
SYNTHESE EN FRANÇAIS	166
BIBLIOGRAPHY	179

ACKNOWLEDGEMENTS

Before delving into the subject matter, I would like to express my heartfelt gratitude to the individuals who have supported me throughout this interesting journey and contributed significantly to the completion of this doctoral thesis.

First and foremost, I extend my deepest appreciation to my research supervisors, Dr. Olga Lavrik and Dr. David Pastré. This journey would not have been possible without the trust and belief given to me by Dr. Olga Lavrik, who four years ago proposed me this thesis topic. Her profound knowledge in the field and her commitment to excellence were invaluable for this work. I am immensely grateful to Dr. David Pastre for his guidance and constant encouragement throughout my research journey. His exceptional expertise, insightful perspectives, and brilliant ideas have played a pivotal role in defining the course of this thesis. Without their assistance and dedicated involvement in every step throughout the process, this thesis would have never been accomplished. Both of you have served as a profound source of inspiration, and I have gained immeasurable knowledge from your mentorship. Thank you, from the depths of my heart.

I would also like to show gratitude to the members of my thesis committee, Gilles Lemaitre and Svetlana Dokudovskaya, for their invaluable feedback and constructive criticism. Their input has played a crucial role in refining and enhancing the quality of my work.

Furthermore, I would like to express my heartfelt appreciation to the members of the jury: Loïc Hamon, the president of the jury, Françoise Dantzer and Stefania Millevoi, the reporters, and Ray Partho, the examiner. I am deeply grateful for their time and effort in carefully reviewing my thesis and providing invaluable suggestions. The engaging discussions and thought-provoking questions during the defense have greatly deepened my understanding of the field and expanded my perspective on research.

I am grateful to Paris-Saclay University for providing me with the opportunity to conduct collaborative research between two laboratories. Their resources and support, particularly the IDEX Paris-Saclay ADI 2019 grant, have been pivotal in the realization of my work.

Many thanks to Maria Sukhanova, whose teaching and guidance have been crucial for successful completion of my work. Not only has she taught me numerous techniques and methods that I have utilized in my work, but she has also been an unwavering source of support throughout these four years. I would also like to express my thanks to Vandana Joshi, whose expertise in plasmid preparation techniques has been invaluable. I have learned a great deal about cell culture methods from her, and her assistance has greatly contributed to the progress of my research. Marie-Jeanne Clément deserves special recognition for her diligent efforts in obtaining all the NMR data presented in this work. I am grateful for her contributions. I would also like to thank Ahmed Bouhss and Juan Carlos Renfigo-Gonzalez for their help with protein production and purification and Benedicte Desforges for her help

with cell culture experiments. Additionally, my sincere thanks go to Lydia Lebouil, the SABNP lab's secretary, for her assistance with administrative procedures. Navigating the intricacies of the French administrative systems would have been significantly more challenging without her help.

I would like to express my gratitude to my fellow doctoral students, especially Virginie Bernard and Diane Valenti in France, and Irina Chernyshova and Tatiana Kornienko in Russia, with whom I have shared an office. Our engaging discussions have been a source of inspiration and motivation, even during challenging times.

I had the pleasure of working with Anastasiia Samsonova and Karina Budkina (already PhD) during my first year of thesis. I am thankful for their assistance during those crucial initial steps.

Lastly, I would be remiss if I did not mention my family, especially my parents and my husband. Their belief in my abilities has kept my spirits high throughout this process. Their love and support have been the foundation of my journey, and for that, I am eternally grateful.

AUTHOR'S DECLARATION

The content presented here is based on work mostly done by myself, although there are a few exceptions. NMR data presented in Chapter 4 and 6 of Results were obtained by Marie-Jeanne Clément (SABNP, Université d'Evry). Recombinant proteins used by me in radioactive assays of protein PARylation were produced and purified by Maria Sukhanova (LBCE, Institute of Chemical Biology and Fundamental Medicine SB RAS), Ahmed Bouhss and Juan Carlos Renfigo-Gonzalez (SABNP, Université d'Evry). I would also like to acknowledge the valuable contribution of Vandana Joshi and Benedicte Desforges (SABNP, Université d'Evry), who provided significant assistance with cell culture experiments.

LIST OF FIGURES

Figure 1: PARP family members: their structure, enzymatic activity, and localization

Figure 2: PARP-1 domain organisation.

Figure 3: PARP-1 catalytic mechanism.

Figure 4: Reversal of protein ADP-ribosylation by MAR and PAR erasers.

Figure 5: PAR readers and the binding sites of PAR that they recognize.

Figure 6: The roles of PARP-1 in excision repair.

Figure 7: The roles of PARP-1 in the detection (a) and repair of double-strand breaks by HR (b), cNHEJ (c) and aNHEJ (d)

Figure 8 : FET protein domain structure.

Figure 9: The solution structure of FUS RRM domain.

Figure 10: The atypical PY-NLS of FET proteins.

Figure 11: Roles of FUS in transcription.

Figure 12: Roles of FUS in splicing.

Figure 13: A monolayer protein recruitment mechanism of nucleic-acid-mediated FUS condensation.

Figure 14: A catalyst-like mechanism of PAR-mediated FUS condensation.

Figure 15: Schematic representation of the *FUS* transcript, and functional domains of the FUS protein with gene mutations identified in patients with neurodegenerative diseases.

Figure 16: Post-translational modifications (PTMs) of FUS and disease-associated mutations that alter PTM sites.

Results

Figure 1: FET proteins have been identified to be PARylated in two large scale analyses.

Figure 2: FUS mixes well along microtubules with PARP-1, as well as XRCC1.

Figure 3: PAR can be detected on microtubule when PARP-1 is fused to a microtubule binding domain.

Figure 4: PLA assay shows the interaction between FUS and PARP-1 whose occurrence increase upon PARP-1 activation with H₂O₂.

Figure 5. The interaction of FUS with PARylated PARP-1 prevents aberrant FUS self-assemblies after transcription inhibition.

Figure 6: No enrichment in Poly(A) mRNAs inside nuclear FUS granules appearing after ActD and olaparib treatment.

Figure 7: No difference in the global PAR level was detected by comparing siRNA- with siNeg-treated in cells exposed to H₂O₂.

Figure 8: Overexpression of FUS increases PARP-1 mediated PAR synthesis in cells.

Figure 9: Relative increase in nuclear PAR/MAR level in HeLa cells expressing FUS-HA at various H₂O₂ concentrations.

Figure 10: FUS expression does not significantly change γ H2AX fluorescence level.

Figure 11: Only long ActD treatments (≥ 45 min) lead to an increased PARylation in the nuclei after H₂O₂ treatments.

Figure 12: Global transcription significantly decreases after H₂O₂ treatment at higher concentrations than 100 μ M.

Figure 13: DRB but not Oxaliplatin increase the PARylation level in HeLa cells exposed to ActD and H₂O₂.

Figure 14: FUS is PARylated in cells-treated with H₂O₂ but not HuR and TDP-43 under our experimental conditions.

Figure 15: The increase in PAR level in HA-FUS-expressing HEK293 cells demonstrated by Western blot analysis.

Figure 16: Serving as an acceptor protein, FUS increases significantly the level of PAR, synthesized by PARP-1 in a reconstituted system.

Figure 17: Sequence alignment of different RRM of human RBPs.

Figure 18: Structural basis of the interaction of FUS RRM, TDP-43 RRM2 and HuR RRM1 with PAR.

Figure 19: Structural basis of the interaction of FUS RRM, TDP-43 RRM2 and HuR RRM1 with PAR: CSP values.

Figure 20: FUS RRM structure (PDB DOI: 10.2210/pdb2LCW/pdb) in which the CSPs in presence of hnRNP RNA loop and PAR are indicated by colors according to their amplitude (σ of the CSP values).

Figure 21: HuR RRM1 binds to C20 but to a very low extent to PAR.

Figure 22: K315A/K316A mutations decrease FUS RRM binding to PAR.

Figure 23: PAR interacts with FUS RRM and can outcompete DNA T10.

Figure: 24. WaterLOGSY analysis of the interaction of FUS RRM with PAR and T10

Figure 25: Cell pretreatment with ActD does not affect PAR level in control cells.

Figure 26: Exchanging FUS RRM with the RRM1 of TDP-43 completely alleviates the increase of PAR level observed in HA-FUS-expressing cells.

Figure 26: Exchanging FUS RRM with the RRM1 of TDP-43 completely alleviates the increase of PAR level observed in HA-FUS-expressing cells.

Figure 27: D343A mutation of FUS significantly decreases PAR level in ActD and H₂O₂-treated cells.

Figure 28: 1D NMR spectra showing the gradual consumption of NAD⁺ upon the activation of PARP-1 in the presence of damaged DNA.

Figure 29: A significant difference in the interaction of D343A FUS RRM mutant and wild-type FUS RRM with activated PARP-1.

Figure 30: Zoom in on several residues experiencing doubling peaks in D343A FUS RRM after PARP-1 activation.

Figure 31: D343A FUS RRM is hyperPARylated *in vitro* compared to wild-type FUS RRM.

Figure 32: Full length FUS but not TDP-43 is highly PARylated by PARP-1 *in vitro*.

Figure 33: D343A mutation in full length FUS protein increases PARP-1 autoPARylation *in vitro*.

Figure 34: Schematic view of the role of FUS in PARP-1-mediated DNA repair.

Figure 35: Steps of the preparation of RFP-MBD expression vectors using the gateway strategy.

Figure 36: Quantification of FUS silencing and overexpression levels in HeLa cells.

Figure 37: Detection scheme allowing to score the mixing between two proteins.

Figure 38: Schematic of Duolink® PLA reaction.

Figure 39: The model of FUS stimulation of PARP-1 activity in H₂O₂-treated cells in a transcription-dependent manner.

Figure 40: Schematic of FUS formation of nuclear condensates in the absence of PAR and mRNA.

Supplementary information

Figure S1: Representative scatter plots of relative GFP and RFP fluorescence intensity in each spot on the microtubules of HeLa cells co-transfected with indicated plasmids.

Figure S2: PARP-1 mixes well along microtubules with FET proteins but less so with the other RBPs tested.

Figure S3: FUS mixes well along microtubules with PARP-1, XRCC1 and LIG3 but less with other DNA repair proteins tested.

Figure S4: D343A changes the balance between PARP-1 and acceptor protein PARylation (A. FUS WT, B. FUS D343A).

Figure S5: D343A favors PARP-1 autoPARylation at the expense of FUS PARylation.

Figure S6: NMR analysis of the binding of FUS , TDP and HuR RRMs to various nucleic acids (RNA and ssDNA).

Figure S7: Varying CSPs induced by point mutation in the RMM of FUS (N284A, D342A, D343A and K315A/K316A).

Figure S8: D343A RRM still binds to PAR while K315A/316A RRM displays a reduced affinity for PAR, RNA and ssDNA.

LIST OF TABLES

Literature review

Table 1: PAR reader modules.

Results

Table 1: List of the primers used for PCR amplification of cDNAs.

Table 2: Recombinant DNAs.

Table 3: Mammalian expression vectors.

Table 4: siRNA oligonucleotides.

Table 5: List of antibodies.

LIST OF ABBREVIATIONS

ActD – Actinomycin D;

ADPr - ADP-ribose;

ALS - amyotrophic lateral sclerosis;

aNHEJ – alternative non-homologous end joining;

APE1 – apurinic/apirimidinic endonuclease 1;

APTX – aprataxin;

ARH - ADP-ribosyl hydrolase;

ART - ADP-ribose transferases;

ART domain - (ADP-ribosyl)transferase domain;

ATM - ataxia telangiectasia mutated;

BER – base excision repair;

BRCT - BRCA1 C-terminal domain;

CLIP-seq - crosss-linking immunoprecipitation sequencing;

cNHEJ – classical non-homologous end joining;

CSP - Chemical shift perturbation;

CTD RNA Pol II – C-terminal domain of RNA polymerase II;

DAPI - 4',6-diamidino-2-phénylindole;

DDR – DNA damage response;

DNA-PK - DNA-dependent protein kinase;

DRB - 5,6-Dichlorobenzimidazole 1-β-D-ribofuranoside;

DRP – DNA repair protein;

DSB – double strand break;

dsDNA – double-stranded DNA;

EWS - Ewings sarcoma;

EWSR1 - EWS RNA-binding protein 1;

fALS – familial ALS;

FEN1 - flap endonuclease 1;

FHA domain - Forkhead-associated domain;

FTLD - frontotemporal lobar degeneration;

FUS/TLS – Fused is sarcoma/Translocated in liposarcoma;

G3BP1 - Ras GTPase-activating protein-binding protein 1;

GFP/RFP – green/red fluorescent protein;

GG-NER - global genomic NER;

HA-tag – hemagglutinin tag;

HD - helical subdomain;

hnRNP - heterogeneous nuclear ribonucleoprotein;

HPF1 - histone PARylation factor 1;

HR – homologous recombination;

HuR - Human antigen R;

IDR – intrinsically disordered region;

Kap β 2 - karyopherin β 2;

KAT - lysine acetyltransferase;

KDAC - lysine deacetylases;

LCD – low-complexity domain;

LIG3 – DNA ligase 3;

LLPS – liquid-liquid phase separation;

lncRNA – long non-coding RNA;

MacroDs - macrodomain-containing enzymes;

MALAT1 - metastasis associated lung adenocarcinoma transcript 1;

MAR – mono(ADP-ribose);

miRNA – micro RNA;

MRE11 - meiotic recombination 11;

MRN complex - MRE11-RAD50-NBS1 complex;

mRNA – messenger RNA;

NAD⁺ - nicotinamide adenine dinucleotide;

NAM – nicotinamide;

NAT - N-terminal acetyltransferase;

NBS1 - Nijmegen breakage syndrome protein 1;

NEAT1 - nuclear paraspeckle assembly transcript 1;

NER – nucleotide excision repair;

NLP4 - nuclear protein localization protein 4 homolog;

NONO - Non-POU domain-containing octamer-binding protein;

NUDIX - nucleoside diphosphates linked to moiety-X;

OB-fold - oligonucleotide/oligosaccharide-binding fold;

OGG1 - 8-oxoguanine glycosylase 1;

PAR - poly(ADP-ribose);

PARG - poly(ADP-ribose) glycohydrolase;

PARP - Poly(ADP-ribose) polymerase;

PBM - PAR-binding motif;

PBZ - PAR-binding zinc fingers;

PCNA - proliferating cell nuclear antigen;

PDEs - phosphodiesterases;

PIN protein - PiIT N-terminus protein;

PLA – proximity ligation assay;

PNKP - polynucleotide kinase-3'-phosphatase;

PP1 α - protein phosphatase 1 alpha;

pre-mRNA - pre-mature RNA;

PRMT - protein arginine methyltransferases;

pTEFb - positive transcription elongation factor b;

PTM – post-translational modification;

PY-NLS - proline-tyrosine nuclear localization signal;

RanB2 ZnF family - Ran-binding protein zink finger type family;

RanGTP/RanGDP – GTP/GDP-binding nuclear protein Ran;

RBMX - RNA binding motif protein X-linked;

RBP – RNA-binding protein;

RISC - RNA-induced silencing complex;

RRM - RNA recognition motif;

sALS – sporadic ALS;

SAM - S-Adenosyl methionine;

Sam68 - Src-associated in mitosis 68 kDa protein;

SG – stress granule;

siRNA - small interfering RNA;

snRNA – small nuclear RNA;

SSB – single strand break;

SSBR – single-strand break repair;

ssDNA – single-stranded DNA;

TAF15 - TATA-box binding protein associated factor 15;

TARG - terminal ADPr protein glycohydrolase;

TC-NER - transcription-coupled NER;

TDP1 - tyrosyl-DNA phosphodiesterase 1;

TDP-43 - TAR DNA-binding protein 43;

TERRA - telomeric repeat-containing RNA;

TFIID - transcription factor II D;

TNK – tankyrase;

TOP1 – DNA topoisomerase 1;

TOP1cc - TOP1-DNA cleavage complexes;

TRN – transportin;

XPC - xeroderma pigmentosum group C-complementing protein;

XRCC1 - X-ray repair cross-complementing protein 1;

ZnF – zinc finger.

LITERATURE REVIEW

1. INTRODUCTION

DNA damage is an inevitable consequence of everyday life, as our genetic material is continuously exposed to a variety of damaging agents such as radiation, toxins, and metabolic byproducts. These agents can cause genetic mutations and chromosomal abnormalities, leading to the development of severe diseases such as cancer and neurological disorders. Fortunately, our cells have developed sophisticated mechanisms to detect and repair DNA damage, ensuring the preservation of genomic integrity and preventing the onset of such diseases (*Ciccia & Elledge, 2010*).

DNA repair refers to the collection of cellular processes that recognize and correct DNA damages. In case of single strand breaks (SSBs), the enzyme poly(ADP-ribose) polymerase 1 (PARP-1) serves as a key player of DNA repair of SSBs. PARP-1 is a DNA damage sensor that is rapidly recruited to DNA damage sites where it catalyzes the synthesis of poly(ADP-ribose) using NAD⁺ as a substrate. Thus, PARP-1 transfers ADP-ribose units from NAD⁺ to itself or other target proteins, forming a poly(ADP-ribose) (PAR) chain (*Schreiber et al., 2006; Alessova & Lavrik, 2019*). Many functional roles have been attributed to the formation of PAR chains. One of the primary roles of PAR is to recruit and activate other DNA repair factors to the sites of DNA damage by serving as a scaffold molecule for them (*Haince et al., 2008; Hanzlikova et al., 2017*). PAR also plays a critical role in the regulation of chromatin condensation. PARylation of histones and other chromatin-associated proteins can alter chromatin structure and regulate gene expression (*Luo et al., 2012; Chaudhuri & Nussenzweig, 2017*). PAR participates in several other cellular processes, such as cell cycle regulation, apoptosis, and inflammation. Long PAR chains have a very short life, from seconds to minutes, thanks to the permanent action of poly(ADP-ribose) glycohydrolase (PARG), an enzyme that hydrolyzes polymer of poly(ADP-ribose) (*Illuzzi et al., 2014*). The reversible nature of PARylation allows for dynamic regulation of cellular processes, with the balance between PARylation and PAR degradation tightly controlled.

Activation of PARP-1 recruits several protein factors, which have been identified through large-scale analyses by mass spectrometry. These factors have been found to have an affinity for PAR (PAR readers) or are themselves PARylated (*Kliza et al., 2021; Jungmichel et al., 2013; Martello et al., 2016; Zhang et al., 2013; Gagne et al., 2012*). In addition to DNA repair factors like XRCC1 and DNA polymerase β , several other proteins whose connection to DNA repair is less clear have also been identified, generating considerable interest. One such group is the RNA-binding proteins (RBPs). When considering DNA repair mechanisms that are dependent on PARP-1 activation, it appears that members of the FET family of RNA-binding proteins, FUS, EWSR1 and TAF15 play a central role. All three FET family members are recruited to DNA damage sites after laser beam exposure, and this recruitment depends on PARP-1 activity (*Izhar et al., 2015; Rulten et al., 2014*). They were identified in mass-spectrometry analyses of PARylated proteins following genotoxic stress and, additionally, as PAR readers (*Jungmichel et al., 2013; Zhang et al., 2013; Rhine et al., 2022; Teloni & Altmeyer, 2015*). FUS stands out among FET family members due to its ability to form compartments at DNA damage sites through interactions occurring between its low-complexity domains (*Rhine et al., 2022; Teloni et al., 2015; Patel et al., 2015; Schwartz et al., 2013*). The formation of such compartments at DNA damage sites was observed in a reconstituted system following PARP-1 activation (*Singatulina et al., 2019*). Moreover, in addition to its roles in RNA biogenesis and DNA repair which overlap with the roles of other two FET proteins, FUS cellular function is associated with the development of neurological disorders such as amyotrophic lateral sclerosis (ALS) and frontotemporal lobar degeneration (FTLD), making it an intriguing target for further investigation (*Zhao et al., 2018; Van Langenhove et al., 2010*).

The aim of this study is to investigate the biological functions of FUS in DNA damage response related to PARP-1 activation. FUS is known to participate in the regulation of transcription by interacting with the C-terminal domain of RNA Pol II and binding to nascent mRNA (*Schwartz et al., 2012; Burke et al., 2015*). Given that DNA damages often occur in open, transcriptionally-active chromatin, FUS is located in close proximity to DNA damage sites and can be rapidly directed to them (*Pankotai et al., 2013; Dinant et al., 2008; Van Attikum & Gasser, 2009*). In this regard, the first question described in this study

was the link between transcription and DNA repair in the context of FUS functions in the nucleus. Secondly, FUS's function in PARP-1-dependent DNA repair is based on its ability to bind PAR. While other RNA-binding proteins can also bind to PAR through electrostatic interactions, FUS has a unique propensity for binding to and being PARylated (*Teloni & Altmeyer; 2015*). Therefore, understanding the structural characteristics that make FUS unique among other RNA-binding proteins and the nature of FUS-PAR interactions can help shed light on its role in PAR-dependent DNA repair.

To provide a comprehensive background for the investigation of the interplay between FUS and PARP-1, this literature review will be divided into three parts. The first part will focus on PARP-1, including its structure, enzymatic mechanisms, and its crucial role in DNA repair processes (Chapter 2). Additionally, the nature of poly(ADP-ribose) polymer will be discussed in relation to PARP-1 function. The second part of this review will explore the structure and diverse functions of FET proteins, which include FUS, EWSR1, and TAF15 (Chapter 3). The review will cover their roles in RNA biogenesis and transcriptional regulation, with a specific emphasis on FUS protein. The final part of the literature review will examine the interplay between FUS functions and DNA damage response mechanisms that are orchestrated by PARP-1 (Chapter 4).

2. THE ROLE OF PARP-1 AND POLY(ADP-RIBOSYLATION) IN DNA REPAIR

2.1 The PARPs superfamily

Poly(ADP-ribose) polymerases (PARPs), also known as diphtheria toxin-type ADP-ribose transferases (ARTDs), are a crucial family of enzymes that are involved in numerous cellular processes, including DNA repair, genomic stability, and cell death. There are 17 known PARP family members in humans, which are grouped into four main subfamilies based on their structure and functions (Figure 1).

The first subfamily comprises PARP-1, PARP-2, and PARP-3, which are activated by damaged DNA and involved in DNA repair and maintenance of genomic stability.

The second subfamily consists of tankyrase 1 (TNK1, also called PARP5a) and tankyrase 2 (TNK2, also called PARP5b), which are characterized by ankyrin repeats.

The third subfamily, which includes PARP9, PARP14, and PARP15, is distinguished by the presence of the ADP-ribose-binding macro domain.

Lastly, the CCCH subfamily contains PARP7, PARP12, and PARP13, characterized by the Cys-Cys-Cys-His zinc-finger (ZnF) motifs that are known to bind RNA (*Ummarino et al., 2021; Bai et al., 2015; Hottiger et al., 2010*).

The enzymatic activity of PARPs involves the cleavage of NAD⁺ into nicotinamide (NAM) and ADP-ribose (ADPr), followed by the transfer of ADPr units to target proteins. This modification process alters the function and activity of the target proteins and is referred to as mono, oligo, or poly(ADP-ribosyl)ation (or simply PARylation), depending on the number of ADPr units transferred (*Bai et al., 2015*). Poly(ADP-ribose) chains are synthesized by only five family members, namely PARP1, PARP2, PARP4, TNK1, and TNK2. Other PARP family members have the ability to produce mono or oligo(ADP-ribose) instead. Notably, PARP9 is an exception as it has been found to lack enzymatic activity (*Bai et al., 2015; Hottiger et al., 2010*). Most of the cellular PARP activity is concentrated in

the nucleus, but some PARP activity has also been observed in the cytoplasm. PARylation can be categorized into two types, depending on the recipient protein. AutoPARylation occurs when PAR chains are transferred to PARP proteins themselves, while transPARylation involves the transfer of PAR chains to other proteins (Bai et al., 2015). PARylation is a reversible process. The degradation of PAR is mainly carried out by two enzymes, poly(ADP-ribose) glycohydrolase (PARG) and ADP-ribosylhydrolase 3 (ARH3), which cleave PAR chains into ADP-ribose monomers. The resulting mono(ADP-ribose) moieties can be further degraded by the action of terminal ADPr protein glycohydrolase (TARG1), MacroD1 and MacroD2 (Chapter 2.2.3) (Palazzo et al., 2016; Rosenthal et al., 2013; Jankevicius et al., 2013). The degradation of PAR is critical for regulating the duration and intensity of PARylation.

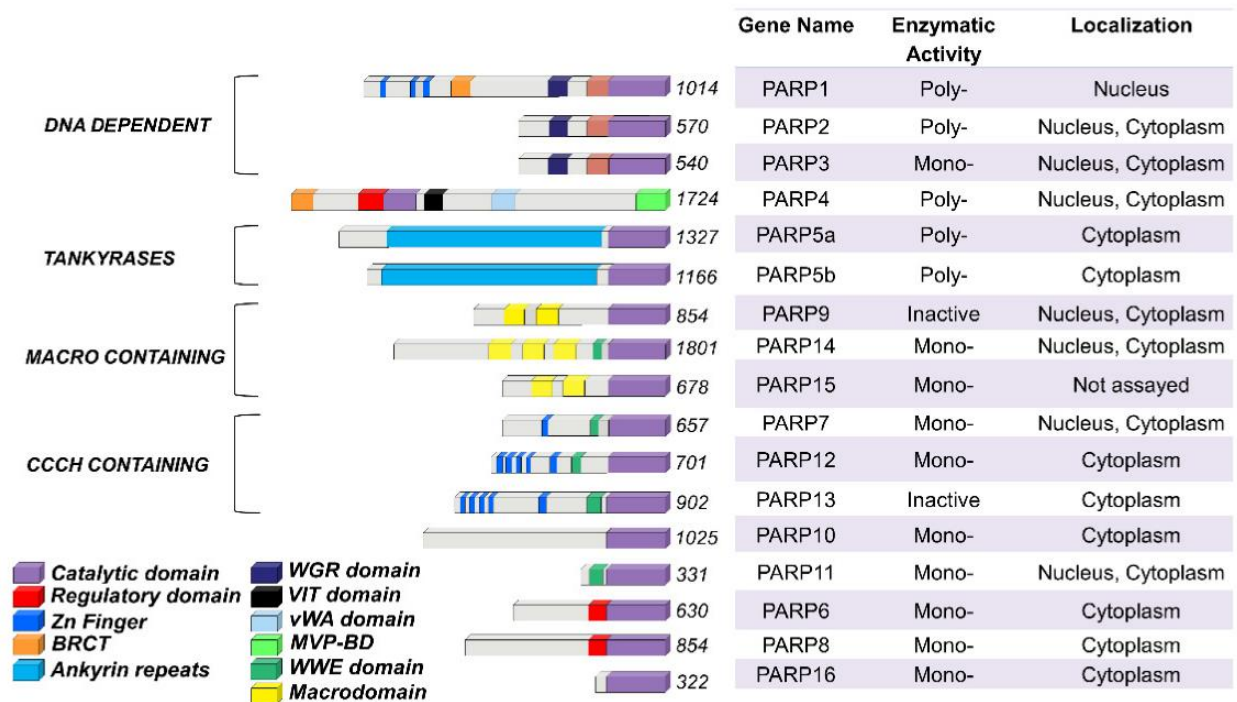


Figure 1: PARP family members: their structure, enzymatic activity, and localization. Left: the domain organization of PARP family members and their affiliation with four PARP subfamilies (DNA dependent, tankyrases, macro containing and CCCH containing subfamily). Right: the enzymatic activity and localization of 17 PARP family members (with modifications from Ummarino et al., 2021).

PARP-1 is the most extensively researched member of the PARP family and is responsible for 85-90% of PAR synthesis in cells. This essential protein is involved in numerous cellular processes, including DNA repair, DNA replication, modulation of chromatin and gene expression, ribosome biogenesis, and RNA transcription (Huang et al., 2022). However, for

the purpose of this literature review focusing on the role of FUS protein in PARP-1-dependent DNA repair, the discussion will center on PARP-1 and its specific functions in DNA repair and modulation of chromatin structure.

2.2 The structural basis of poly(ADP-ribosylation)

2.2.1 The domain structure of PARP-1 and mechanism of its activation

PARP-1 refers to the subfamily of DNA-dependent PARPs meaning that it requires damaged DNA to be activated. PARP-1 contains from six domains connected by flexible linkers: two zinc-finger (ZnF1-ZnF2) domains are involved in DNA binding; BRCA1 C-terminal domain (BRCT) performs protein-protein interactions and required for the automodification of the protein; helical subdomain (HD) together with (ADP-ribosyl)transferase (ART) domain form a catalytically active site of the enzyme; Trp-Gly-Arg (WGR) domain mediates interaction between DNA recognition domains and catalytic domain (Figure 2) (*de Murcia et al., 1994; Khodyreva & Lavrik, 2016*).

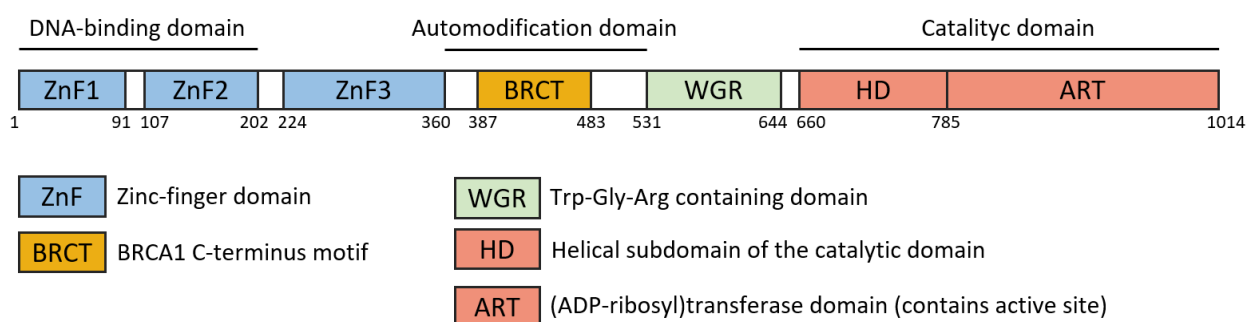


Figure 2: PARP-1 domain organisation. Zn1, Zn2, and Zn3 are zinc finger domains, BRCT is the C-terminal BRCA1 domain, WGR is a domain containing Trp-Gly-Arg motif, HD (also referred to as PRD) is a regulatory helical subdomain domain, ART is a (ADP-ribosyl)transferase catalytic domain responsible for PAR synthesis. A nuclear localization signal and a caspase-3 cleavage site (NLS, caspase) are located between Zn2 and Zn3.

When PARP-1 is in its inactive state, the HD domain acts as an inhibitory region of the protein by entirely blocking the NAD^+ binding site. However, upon recognition of damaged DNA by the ZnF1 and ZnF2 domains, PARP-1 undergoes conformational changes that cause the NAD^+ binding site to become accessible, allowing NAD^+ to bind. It is worth noting that PARP-1 may undergo transient conformational changes that enable the interaction between its ART domain and NAD^+ even in the absence of damaged DNA,

explaining the enzyme's low basal activity (*Alemasova & Lavrik, 2019; Dawicki-McKenna et al., 2015; Langelier et al., 2018*).

The catalytic ART domain is highly conserved among all members of the PARP family (*Hottiger et al., 2010*). It can be subdivided into two components: a donor NAD⁺-binding site and an acceptor site that binds to either the target protein or the distal ADP-ribose monomer of a growing PAR chain. The donor site consists of a nicotinamide-binding pocket (Figure 3, in yellow), a pyrophosphate binding site (Figure 3, in pink), and an adenine binding site (Figure 3, in orange) (*Alemasova & Lavrik, 2019; Barkauskaite et al., 2015*). The nicotinamide-binding site contains the ART signature triad (H-Y-E) which is responsible for catalysis. H862 interacts with the 2'-OH group of adenine-ribose, while Y896 forms a stacking interaction with the nicotinamide moiety. E988 plays a dual role, both in coordinating NAD⁺ by forming a hydrogen bond with the 2'-OH group of the nicotinamide ribose, and in some cases, in coordinating the glutamate or aspartate acceptor amino acids by forming a hydrogen bond with them during the initiation step. Although coordination with the latter is not always necessary since carboxyl groups are mostly ionized at physiological pH. E988 is crucial in coordinating NAD⁺ and pulling electron density from the N-glycosidic bond, thus facilitating nucleophilic attack by the acceptor amino acid (*Alemasova & Lavrik, 2019; Steffen et al., 2013*). Interestingly, natural substitutions of Glu988 to Leu, Ile, Tyr, Val, or Thr result in the loss of poly(ADP-ribose) transferase activity of the protein, which has been observed for mono(ADP-ribosyl)transferases such as PARP6, PARP7, PARP8, PARP10, PARP11, PARP12, PARP14, PARP15, and PARP16 (*Alemasova & Lavrik, 2019; Barkauskaite et al., 2015*).

The PAR synthesis process catalyzed by PARP-1 ART domain can be divided into three steps:

1. Initiation: This involves the attachment of the first mono(ADP-ribose) to the acceptor amino acid residue (Figure 3A).
2. Elongation: In this step, additional (ADP-ribose) monomers are attached through (2'-1'') ribose-ribose glycosidic bond (Figure 3B).

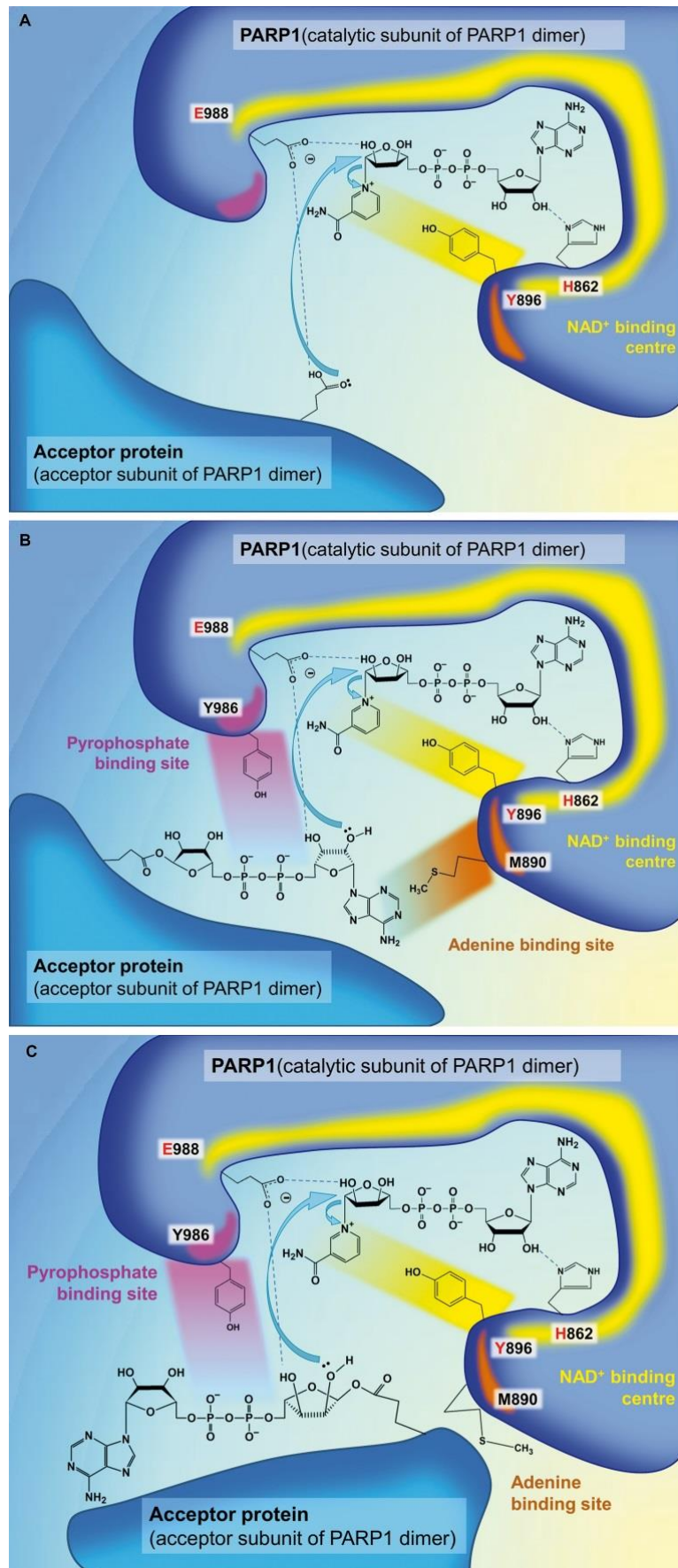


Figure 3: PARP-1 catalytic mechanism. A. Initiation: the attachment of the first mono(ADP-ribose) to the acceptor amino acid residue. B. Elongation: the attachments of (ADP-ribose) monomers through (2'-1'') ribose-ribose glycosidic bond. C. Branching: the attachments of (ADP-ribose) monomers through (2''-1''') ribose-ribose glycosidic bond (from Alemasova & Lavrik, 2019).

3. Branching: This step involves the attachment of further (ADP-ribose) monomers through (2''-1''') ribose-ribose glycosidic bond (Figure 3C).

During the initiation step, the acceptor protein residue performs a nucleophilic attack on the polarized N-glycosidic bond, resulting in the attachment of the first ADP-ribose monomer to the target protein (*Alemasova & Lavrik, 2019; Marsischky et al., 1995*). To promote further elongation, mono(ADP-ribose) is positioned through additional hydrogen bonding between the E988 residue and the 3'-OH of the adenosine ribose, the interaction of the M890 residue in the adenine-binding site with adenine, and the interaction of the Y986 residue in the pyrophosphate-binding site with the pyrophosphate of the ADP-ribose attached to the target protein. The elongation occurs when the 2'-OH nucleophile of the adenosine ribose of the terminal PAR unit attacks the C1' atom of the nicotinamide ribose (*Marsischky et al., 1995; Ruf et al., 1998*). During the branching step, the synthesized PAR chain must be reversed by 180 degrees compared to its orientation in the elongation step. In this case, the pyrophosphate of ADP-ribose is tightly bound by the PARP-1 Y986 residue, while the binding of adenine by M890 is lacking. The additional coordination of (ADP-ribose) in this reversed orientation can be strengthened by amino acids located on the surface of the PARP-1 protein, suggesting that PAR branching may be affected by protein-protein interactions (*Ruf et al., 1998; Rolli, 1997*).

The length and branching of PAR chains synthesized by PARP-1 can vary widely, ranging from just a few ADP-ribose units to over 200 units in length, with branching sites occurring approximately every 20-50 ADP-ribose units (*Leung, 2014; Alvarez-Gonzalez & Jacobson, 1987*). Numerous factors can impact the length of PAR chains, including the concentration of NAD⁺ and the activity of other enzymes involved in PAR metabolism. Initially, it was believed that autoPARylation of PARP-1 caused the protein to dissociate from DNA damage sites due to electrostatic repulsion between negatively charged DNA and PAR (*Satoh & Lindahl, 1992*). This was thought to allow other DNA repair proteins to access the damaged site. However, recent studies have revealed a more complex relationship between PARylation and DNA repair. It is now understood that PARylation plays a critical role in the recruitment and retention of DNA repair factors at damaged sites. This process

is mediated by the recruitment of PAR-binding proteins that recognize and bind to PAR chains, creating a scaffold for the assembly of a multi-protein repair complex (*El-Khamisy et al., 2003; Okano et al., 2003*). The recruited DNA repair proteins can displace PARP-1 from the lesion site, as demonstrated by the recruitment of XRCC1 (X-ray repair cross-complementing protein 1), a protein involved in DNA base excision repair, which competes with PARP-1 for binding to DNA lesions, thus preventing excessive PARP-1 activation (*Demin et al., 2021*). This topic will be further discussed in the upcoming chapter 2.3.1. Overall, PARylation is considered a post-translational modification (PTM) that can affect the function, localization, and stability of target proteins and, additionally, serve as a scaffold for PAR binding proteins (further referred to as PAR readers).

2.2.2 Amino acid specificity of poly(ADP-ribosyl)ation by PARP-1

In the early studies of PARylation target specificity, it was proposed that glutamate (E) and aspartate (D) were the primary amino acid residues targeted by PARPs, accounting for 70% of PAR modifications (*Hottiger, 2015; Bredehorst et al., 1978; Smith & Stocken, 1975*). However, with the development of proteomics technologies over time, multiple other acceptor sites have been discovered, including lysine (K), arginine (R), cysteine (C), diptamide (Dph), phospho-serine (pS), and asparagine (N) residues (*Rosenthal & Hottiger, 2014; Daniels et al., 2014; McDonald & Moss, 1994; Manning et al., 198; Laing et al., 2011; Altmeyer et al., 2009; Oppenheimer & Bodley, 1981*). Despite the wide range of amino acid targets for PARylation, the accessibility of the acceptor residue is believed to be the main determinant of whether a residue is PARylated. For example, the importance of the availability of the acceptor residue was demonstrated for Glu residues (*Zhang et al., 2013*). However, it is interesting to note that the resulting ADP-ribosylated acceptors may differ in their chemical and enzymatic sensitivities, as well as impact PAR recognition by other PAR-binding proteins. For example, acidic amino acids such as Glu and Asp lose ADP-ribose in the presence of high pH or hydroxylamine, while basic amino acids such as Arg and Lys are less sensitive to hydroxylamine treatment (*Adamietz & Hilz, 1976; Messner & Hottier, 2011*). This difference in sensitivity may play a biological role in cellular processes. Moreover, several PAR degrading enzymes have been shown to exhibit

specificity towards certain acceptor residues, further emphasizing the importance of the specificity of the PARylation site (Chapter 2.2.3). Additionally, it has been found that there are sequence constraints that restrict the location of modification sites in target substrates. One such constraint is the presence of consensus motifs surrounding ADP-ribosylated Glu residues, including PXE*, EP, PXXE, and E*XXG (*Alemasova & Lavrik, 2019; Zhang et al., 2013*).

In the field of PARylation studies, a new wave has recently emerged, which involves the targeting of serine residues by PARP-1 in the presence of HPF1 (*Leung, 2017*). HPF1, also known as histone PARylation factor 1, is a binding partner of PARP-1 that has been shown to enhance PARP-1 activity and promote PARylation on serine residues in target proteins. The proposed mechanism for this new type of modification involves the activation of PARP-1 by damaged DNA, followed by direct binding of HPF1 to the PARP-1 catalytic domain. This binding then enables the initiation of ADP-ribosylation of serine residues, which has been demonstrated to be particularly important for PARylation of serine residues in histones (*Gibbs-Seymour et al., 2016; Bonfiglio et al., 2017; Kurgina et al., 2021*).

2.2.3 The reversibility of PARylation: PAR erasers

Protein PARylation is a tightly regulated process within cells, and like other post-translational modifications (PTMs), its turnover depends on the interplay between synthesis and degradation mechanisms (*Palazzo et al., 2017; Perina et al., 2014*). Enzymes involved in these functions can be thought of as "writers" and "erasers," borrowing terminology from the classification of proteins involved in epigenetic regulation. Accordingly, PAR writers are members of the PARP family, while PAR erasers are primarily represented by poly(ADP-ribose) glycohydrolase (PARG) (*O'Sullivan et al., 2019*).

PARG is the major enzyme involved in the removal of PARylation from target proteins. Its primary role is to hydrolyze the glycosidic linkages between ADP-ribose units of PAR polymers, resulting in the generation of free ADP-ribose monomers (*O'Sullivan et al., 2019*) (Figure 4). It is localized in both the nucleus and cytoplasm, with a predominant perinuclear distribution in the cytoplasm (*Winstall et al., 1999*). PARG primarily functions

as an exoglycosidase, catalyzing the hydrolysis of PAR from the protein-distal end. However, around 20% of its activity is attributed to endoglycosidase activity, allowing for in-chain hydrolysis (Davies & Henrissat, 1995; Braun et al., 1994).

PARG plays an essential role in cellular homeostasis. Firstly, when cells are depleted of PARG, they become hypersensitive to genotoxic stress (Cortes et al., 2004; Min et al., 2010). Secondly, Illuzzi et al. have shown that PARG is also necessary to prevent the accumulation of detrimental PAR production upon prolonged replicative stress. In particular, the accumulation of PAR prevents RPA loading on single-stranded DNA (ssDNA), which can eventually lead to the formation of double-strand breaks (DSB), thus promoting apoptosis and/or necrotic cell death in proliferating cells (Illuzzi et al., 2014). Finally, it has been demonstrated that PARG^{-/-} mice are embryonically lethal (Koh et al., 2004).

While PARG is essential in maintaining cellular homeostasis, it has its limitations. One such limitation is its inability to remove MARylation modifications, which necessitates the involvement of other enzymes in this process. There are three classes of additional PAR erasers that have been identified: macrodomain-containing enzymes (MacroDs), ADP-ribosyl hydrolases (ARHs), and phosphodiesterases (PDEs) (O'Sullivan et al., 2019).

The ARH family consists of three proteins: ARH1-3 (Oka et al., 2006). ARH1 has a specificity for arginine-linked ADP-ribose, while ARH3 is specific to ADP-ribosyl-serine (Laing et al., 2010; Mashimo et al., 2014). The substrates for ARH2 have not been identified yet. In addition to its ability to remove MARylation, ARH3 possesses activity toward the O-glycosidic bond of PAR, which is similar to PARG (Figure 4) (Mashimo et al., 2014).

The macrodomain-containing enzymes with ADP-ribose hydrolase activity include MacroD1, MacroD2, and TARG1 proteins. While MacroD1 and MacroD2 are non-specific MAR erasers, TARG1 has the unique ability to act as both MAR and PAR erasers with specificity to aspartate and glutamate acceptor residues (Figure 4) (O'Sullivan et al., 2019; Sharifi, 2013).

Recent studies have identified several phosphodiester ADP-ribose hydrolases that are capable of reversing ADP-ribosylation modifications of proteins. These enzymes include members of the NUDIX (nucleoside diphosphates linked to moiety-X) superfamily, such as NUDT9 and NUDT16, as well as ectonucleotide pyrophosphatase/phosphodiesterase 1 (ENPP1). These enzymes are responsible for the cleavage of phosphodiester bonds in PAR and MAR (Figure 4) (O'Sullivan et al., 2019; Palazzo et al., 2015; Daniels et al., 2016; Palazzo et al., 2016).

The identification of these PAR erasers and their specificities highlights the complexity of PARylation and the need for further research to fully understand the mechanisms involved.

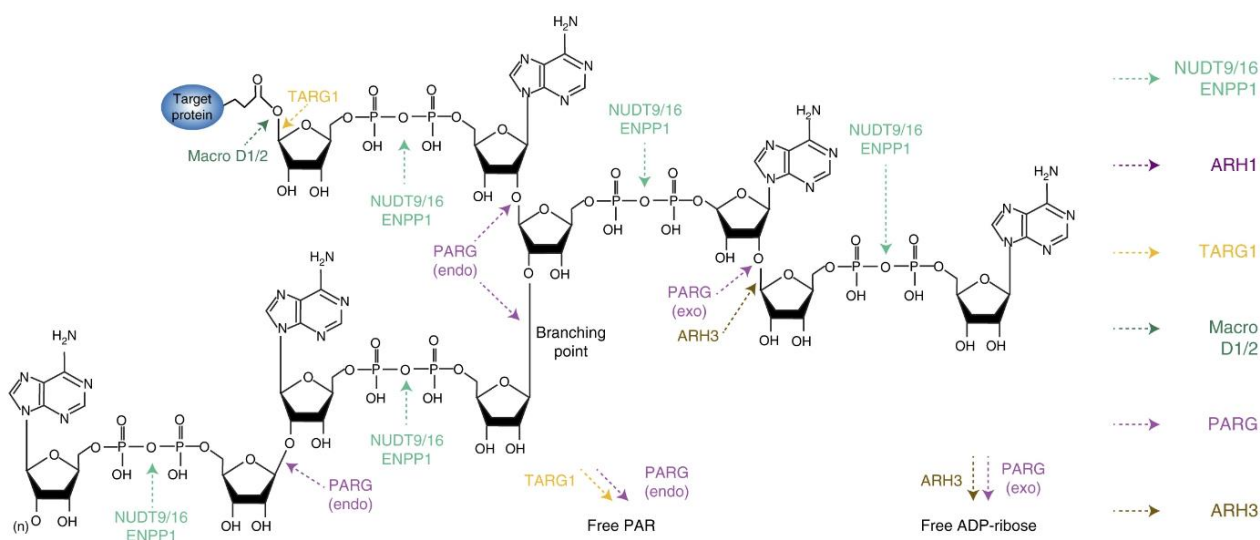


Figure 4: Reversal of protein ADP-ribosylation by MAR and PAR erasers. The diagram represents PAR and MAR eraser enzymes PARG, ARH3, Macro D1/2, TARG1, ARH1, NUDT9/16, ENPP1 and their cleavage sites (with modifications from O'Sullivan et al., 2019).

2.2.4 PAR-binding proteins: PAR readers

PAR readers refer to proteins that have the capability to bind to poly(ADP-ribose) (PAR) molecules. Hundreds of proteins that interact either directly or indirectly with PAR have been identified (Gagné et al., 2008; Isabelle et al., 2012). This diverse group of proteins plays a role in a variety of cellular processes such as DNA repair, chromatin remodeling, transcriptional regulation, and cell death (Krietsch et al., 2012; Gagné et al., 2011; Malanga

& Althaus, 2011; Kalisch et al., 2012). PAR readers typically contain one or more PAR-binding modules that enable them to recognize and bind to PAR. These PAR-binding modules include PAR-binding motif (PBM), PAR-binding zinc fingers (PBZ), macrodomains, WWE domains, FHA and BRCT domains, RNA recognition motif (RRM), SR repeats and KR-rich motifs, the OB-fold, PIN domains and RG/RGG motifs (Table 1) (Teloni & Altmeyer, 2016; Kalisch et al., 2012).

Table 1: PAR reader modules (with modifications from Teloni & Altmeyer, 2016)

Reader Module	Module size	Defined protein fold	Interaction mode	Main functions	Examples
PBM	≈20 residues	no	unknown, potentially electrostatic interactions	DNA replication and repair, cell cycle regulation, chromatin architecture, RNA metabolism	H1, H2A, H2B, H3, H4, p21, p53, XRCC1, XPA, MSH6, ERCC6, ATM, MRE11, DNA-PKcs, KU70, WRN, DNA Ligase 3, Polymerase epsilon, TERT, DEK, CAD, CENP-A, CENP-B, Lamin A/C, BUB3, hCAP-D2, HK1, HKDC1, G3BP1, hnRNPA1, hnRNPK, hnRNPH, hnRNPG, hnRNPM, hnRNPA2B1, hnRNPC1C2, AURKAIP1, NF-kappaB, iNOS
PBZ	≈30 residues	yes	C2-H2-type zinc finger binds to two consecutive ADP-ribose moieties	DNA damage signaling and repair	APLF, CHFR
Macrodomains	≈130–190 residues	yes	Recognizes the terminal ADP-ribose unit	Chromatin remodeling	macroH2A, ALC1/CHD1L, C6orf130/TARG
WWE	≈80–100 residues	yes	Binds to iso-ADP-ribose	Protein turnover	RNF146/Iduna
FHA/BRCT	≈80–100 residues	yes	Phosphate-binding pockets interact with ADP-ribose or iso-ADP-ribose	DNA damage signaling and repair	APTX, PNKP, XRCC1, NBS1, BARD1, DNA Ligase 4
RRM	≈60–80 residues	yes	unknown, potentially electrostatic interactions	DNA damage signaling and repair, RNA metabolism	ASF/SF2, NONO, RBMX, TAF15
SR repeats and KR-rich motifs	variable	no	unknown, potentially	Gene expression, RNA metabolism	ASF/SF2, dMi-2

			electrostatic interactions		
OB-fold	≈70–150 residues	yes	Binds to iso-ADP-ribose	DNA damage signaling and repair	SSB1, BRCA2
PIN domains	≈130–150 residues	yes	unknown, potentially electrostatic interactions	DNA damage signaling and repair	EXO1
RG/RGG repeats	variable	no	unknown, potentially electrostatic interactions	Stress granule assembly, liquid demixing, DNA repair	MRE11, G3BP1, SAFB1, FUS/TLS, EWS/EWSR1, TAF15

The basic PAR-binding motif (PBM). The PAR-binding motif (PBM) is a 20-amino acid sequence that was discovered in 2000 as the first known PAR-binding domain. The motif contains two regions that are highly conserved: a cluster of basic amino acids and a pattern of hydrophobic amino acids interspersed with basic residues (*Pleschke et al., 2000*). In 2008, refined *in silico* prediction of PAR binding proteins and mass spectrometry-based proteome analysis revealed more than 800 proteins containing the PBM (*Gagné et al., 2008*). These proteins likely bind to PAR through electrostatic interactions between the positively charged amino acids of the consensus sequence ([HKR]-X-X-[AIQVY]-[KR]-[KR]-[AILV]-[FILPV]) and the negatively charged phosphates in the PAR chains. The PBM has a relatively high affinity to PAR, with Kd values ranging from 10^{-7} to 10^{-9} (*Krietsch et al., 2013; Teloni & Altmeyer, 2016*).

The PAR-binding zinc finger (PBZ). The PAR-binding Cys2-His2 type zinc finger motif has initially been identified in only two proteins: aprataxin and PNK-like factor (APLF) and checkpoint with forkhead and ring finger domains (CHFR) (*Ahel et al., 2008*). Both proteins participate in the processes dependent on PAR synthesis. APLF is involved in DNA repair by non-homologous end joining (NHEJ), and its recruitment to the sites of DNA damage was shown to be dependent on the PAR synthesis and PAR binding (*Rulten et al., 2011; Rulten, 2008*). Similarly, the CHFR-dependent antepause checkpoint is dependent on PAR amplification and interaction between PBZ and PAR (*Ahel et al., 2008; Oberoi et al., 2010*). The motif consists of around 30 amino acids and has the consensus sequence [K/R]-X-X-C-X-[F/Y]-G-X-X-C-X-[K/R]-[K/R]-X-X-X-X-H-X-X-X-[F/Y]-X-H (*Isogai et al., 2010; Oberoi*

et al., 2010; Eustermann et al., 2010). It is involved in PAR binding through interaction with the ADP-ribose-ADP-ribose junction (Figure 5) (*Eustermann et al., 2010*). PBZ is not a common PAR-binding motif found in only a few proteins.

Macrodomains. Macrodomain is a comparatively big globular domain consisting of 130-190 amino acids. It should be called rather a MAR reader than a PAR reader, as it recognizes only the terminal ADP-ribose moiety of PAR according to the structural data (Figure 5) (*Timinszky et al., 2009*). The affinity of the macrodomain to PAR reaches $K_d \sim 10^{-7}$ (*Krietsch et al., 2013*). Eleven human proteins containing the macrodomain have been identified, including PARP family members (PARP9, PARP14, and PARP15), histone variants (macroH2A1.1, macroH2A1.2, macroH2A2), PAR erasers (macroD1, macroD2, TARG1), and other proteins (such as ALC1/CHD1L and GDAP2) (*Teloni & Altmeyer, 2016*). PARP family members can contain either two (PARP9, PARP15) or three (PARP14) macrodomains (*Aguiar et al., 2005*). In addition to their PAR-binding properties, the macrodomain of PAR erasers possesses catalytic activity that is necessary for PAR degradation (for more information, see Chapter 2.2.3).

WWE domain. The WWE domain is named after the consensus amino acid sequence containing tryptophan and glutamate residues (*Teloni & Altmeyer, 2016*). It is found in 12 human proteins, including PARP family members and ubiquitin ligases (*Wang et al., 2012*). WWE domain interacts predominantly with iso-ADP-ribose ($K_d \sim 10^{-7}$), however, the binding to ADP-ribose is also possible, although with much lower affinity ($K_d \sim 10^{-3}$) (Figure 5) (*Wang et al., 2012; Krietsch et al., 2013*). While the role of the WWE domain in PARP family members is not fully understood, there is enough data describing the link between the interaction with PAR and ubiquitin ligase activity. For example, the WWE domain of E3 ligase RNF146/Iduna has been shown to bind to PAR, which activates the PAR-dependent ubiquitylation of target proteins and their subsequent proteasomal degradation (*Kang et al., 2011*). Interestingly, another ubiquitin E3 ligase, TRIP12, which also harbors the WWE domain, has been recently found to catalyze PAR-dependent polyubiquitylation of PARP-1, leading to its proteasomal degradation and preventing PARP-1 accumulation. Loss of TRIP12 in cells treated with PARP-1 inhibitors leads to

elevated PARP-1 trapping on DNA, increased DNA replication stress, DNA damage, and cell death (*Gatti et al., 2020*). In summary, PAR-dependent ubiquitylation is an emerging and exciting topic.

FHA and BRCT domains. The FHA (Forkhead-associated) and BRCT (BRCA1 C-terminal) domains were initially identified as domains that bind to phospho-Ser/Thr residues. However, it has since been discovered that these domains can also recognize negatively charged PAR polymers. Similar to the WWE domain, the FHA domains of aprataxin (APTX) and polynucleotide kinase-3'-phosphatase (PNKP) interact with iso-ADP-ribose, while the BRCT domain of XRCC1 or DNA LIG4 binds to ADP-ribose (Figure 5).

RNA recognition motif (RRM). Due to structural similarities between RNA and PAR, it is not surprising that this abundant RNA-binding domain has an affinity towards PAR. The FET protein family, which includes FUS, EWSR1, and TAF15, is an excellent example of RRM-containing proteins. While previous studies demonstrated that FUS could form multiple interactions with PAR, it remained unclear whether the RRM domain played a role in this binding (*Rhine et al., 2022; Singatulina et al., 2019; Altmeyer et al., 2015*). In addition to the FET proteins, there are several other RNA-binding proteins with the RRM domain, including members of the heterogeneous nuclear ribonucleoprotein (hnRNP) family, RNA processing factors such as NONO and RBMX, and several transcription factors. Some of these proteins have been shown to be recruited to DNA damage sites in a PAR-dependent manner and function in DNA damage response (DDR) mechanisms (*Gagné et al., 2003; Ji & Tulin, 2009; Krietsch et al., 2012; Adamson et al., 2012; Izhar et al., 2015*).

SR repeats and KR-rich motifs. Serine/Arginine (SR) repeats are primarily found in splicing factors. Certain splicing factors, such as SF3A1, SF3B1, SF3B2, and ASF/SF2, have been demonstrated to interact with PAR via electrostatic interactions (*Isabelle et al., 2012; Malanga et al., 2008*). Additionally, nucleosome remodeler dMi-2 in *Drosophila* was found to bind PAR through KR-rich motifs (*Murawska et al., 2011*).

The OB-fold. The oligonucleotide/oligosaccharide-binding fold (OB-fold) is a motif that binds to single-stranded DNA (ssDNA) or RNA, and has also been found to bind to PAR (Zhang *et al.*, 2014; Zhang *et al.*, 2015). This fold is present in the ssDNA-binding protein SSB1, which is recruited to DNA damage sites through recognition of the iso-ADP-ribose moiety of PAR by its OB-fold (Figure 5) (Zhang *et al.*, 2014).

PIN domains. The name "PIN" derives from the founding members of this domain family, the PiIT N-terminus (PIN) proteins. PIN domains are ssDNA and RNA-recognition domains, having ribonuclease activity. The PIN domains of SMG5, EXO1 and GEN1 were shown to interact with PAR. These proteins, like other PAR-binding proteins, are recruited to DNA damage sites through their binding to PAR (Zhang *et al.*, 2015).

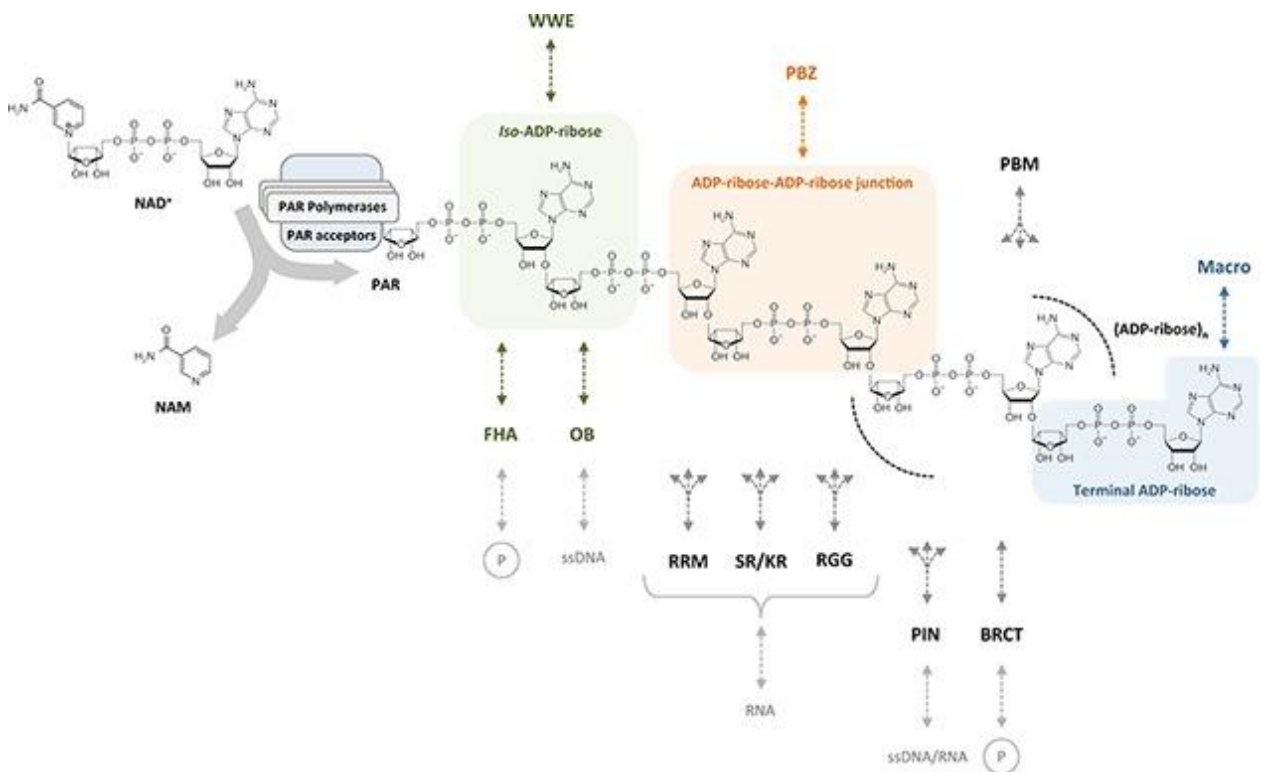


Figure 5: PAR readers and the binding sites of PAR that they recognize Well characterized PAR reader domains WWE, PBZ, PBM and macrodomains and the sites of PAR they recognize are showed on the top. Newly emerging PAR reader domains FHA, OB-fold, PIN domain, RRM, SR/KR repeats are shown on the bottom. Multi-branch arrows indicate that the exact binding sites have not been identified (from Teloni & Altmeyer, 2016).

RG/RGG motifs. Over 1000 proteins contain RG/RGG motifs, many of which are RNA-binding proteins. Members of the FET family, including FUS, EWSR1, and TAF15, are also among these proteins (Thandapani *et al.*, 2013). The RG/RGG motifs interact with RNA

through multiple electrostatic interactions between positively charged arginines and negatively charged phosphates. It's therefore not surprising that these motifs are also involved in PAR binding. Indeed, all three FET family members are recruited to DNA damage sites in a PAR-dependent manner. In the case of FUS protein, recruitment is mediated by the RGG domains, which have been shown to directly interact with PAR (*Izhar et al., 2015; Mastrocola et al., 2013; Rulten et al., 2014*). Interestingly, the RGG motifs are regarded as low complexity domains which play a critical role in the promotion of liquid-liquid phase separation and the formation of protein-RNA or protein-PAR assemblies in cells (Chapter 3.3).

2.3 The role of PARP-1 in DNA repair

DNA repair is an essential process that maintains the integrity of the genetic information in all living organisms. DNA damage can occur due to a variety of exogenous (ionizing radiation, chemical mutagens, reactive oxygen species) and endogenous (errors during DNA replication) factors (*Ciccia & Elledge, 2010*). If left unrepaired, DNA damage can lead to mutations and genomic instability, which can cause cancer and other diseases (*Torgovnick & Schumacher, 2015*).

PARP-1 is a pivotal enzyme involved in the DNA damage response (DDR) (*Chaudhuri & Nussenzweig, 2017*). It recognizes sites of DNA damage, resulting in the activation of its enzymatic activity and synthesis of PAR chains on itself (a process known as automodification), histones, and other proteins (*D'Amours et al., 1999, PMID: 10455009; Huambachano et al., 2011; Gagné et al., 2008; Jungmichel et al., 2013*). Proteins participating in DDR can be recruited to DNA damage sites via their PAR-binding capabilities or protein-protein interactions with PARP-1 (*Krietsch et al., 2012*). These proteins, also known as PAR readers (Chapter 2.2.4), are impacted by their binding to PAR, potentially affecting their ability to bind DNA, participate in protein-protein interactions, localize within the cell, and perform other vital functions necessary for the cell's DDR (*Althaus et al., 1999; Malanga et al., 1998; Pleschke et al., 2000*). PARylation of histones by PARP-1 leads to nucleosome disassembly, ultimately resulting in chromatin relaxation.

The accessibility of chromatin is essential for the easy recruitment of DNA repair factors and successful DNA repair (Messner *et al.*, 2010; Poirier *et al.*, 1982). Once the DNA repair process is completed, PAR is hydrolyzed by PAR-degrading enzymes, mainly PARG, resulting in the disassembly of DNA repair complexes (Erdélyi *et al.*, 2009; Fisher *et al.*, 2007).

The upcoming chapter will delve into the role of PARP-1 in repairing single-strand and double-strand breaks in DNA.

2.3.1 PARP-1 in excision repair

Around 50000 of base and nucleotide lesions, as well as single-strand DNA breaks (SSBs), occur each day in the DNA of living cells (Lindahl & Barnes, 2000; De Bont & van Larebeke, 2004). These lesions and DNA breaks can result from reactive endogenous metabolites, such as free radicals and reactive oxygen species (ROS), as well as from spontaneous decay of DNA (Chaudhuri & Nussenzweig, 2017; Caldecott, 2008). The resulting DNA lesions include oxidated and alkylated bases, apurinic/apyrimidinic sites, SSBs, and other modifications. To maintain the integrity of the genome, cells have developed several distinct mechanisms to repair these DNA lesions. These repair pathways include single strand breaks repair (SSBR), base excision repair (BER), and nucleotide excision repair (NER) (Chaudhuri & Nussenzweig, 2017).

PARP-1 in single-strand break repair

SSBs are recognized directly by PARP-1 (Figure 6a) (Sato & Lindahl, 1992). As mentioned earlier, this recognition results in the synthesis of PAR chains and the recruitment of DNA repair factors. One such crucial component in SSB repair is the X-ray repair cross-complementing protein 1 (XRCC1), which is recruited to SSBs in a PARP-1-dependent manner (Hanzlikova *et al.*, 2017; El-Khamisy *et al.*, 2003). XRCC1 serves as a scaffold for DNA ligase 3 (LIG3), DNA polymerase β , and bifunctional polynucleotide kinase 3'-phosphatase (PNKP) – all DNA repair proteins involved in DNA end processing to restore SSBs to conventional 3'-hydroxyl (3'-OH) and 5'-phosphate moieties for further gap filling

(Caldecott *et al.*, 1994; Marintchev *et al.*, 2000; Whitehouse *et al.*, 2001). To fill the gaps, DNA polymerase δ (Pol δ), Pol ϵ , and Pol β are employed (Caldecott, 2007). This process also requires PARP-1 to stimulate the 5' flap endonuclease activity of flap endonuclease 1 (FEN1) (Prasad *et al.*, 2001). In the end, LIG1 ligates DNA to complete the repair process (Mortusewicz *et al.*, 2006).

Using PARP-1 depletion, it was demonstrated that PARP-1 activity is essential for rapid rates of SSBR in cells, and PAR synthesis accelerates the process (Fisher *et al.*, 2007). In addition to its role in the recruitment of other proteins, PAR can serve as an ATP source for the final step of SSBR, DNA ligation catalyzed by LIG3 (Oei & Ziegler, 2000; Petermann *et al.*, 2003).

Interestingly, recent research has shown that the proper functioning of XRCC1 is crucial for maintaining normal neurological function. Mutations in XRCC1 in both human and mice lead to PARP-1 hyperactivity, elevated PAR levels, and reduced rates of SSB repair, which can result in neuropathological defects (Hoch *et al.*, 2017). XRCC1's role in assembling complexes containing DNA Pol β and LIG3 has been suggested as a preventative measure against excessive PARP-1 activation during SSBR. Conversely, the deficiency of XRCC1 can lead to PARP-1 "trapping" on DNA damage sites, which causes PARP-1 overactivation and hinders DNA repair (Demin *et al.*, 2021).

PARP-1 also plays an additional role in repairing DNA lesions that arise from the abortive activity of DNA topoisomerase I (TOP1) (Figure 6b). While TOP1 is an essential enzyme that helps regulate DNA supercoiling, it can become trapped on DNA during its catalytic cycle, leading to the formation of covalent TOP1-DNA adducts known as cleavage complexes (TOP1cc). If left unresolved, these complexes can cause DNA strand breaks and genomic instability. The removal of TOP1 from DNA is carried out by a specialized DNA repair pathway called the tyrosyl-DNA phosphodiesterase 1 (TDP1) pathway. TDP1 cleaves the phosphodiester bond between the TOP1 adduct and DNA, releasing TOP1 from the DNA and generating a DNA single-strand break (SSB). The resulting SSB is then repaired in the SSBR pathway. PARP-1's role in the regulation of TOP1cc repair involves the

PARylation of TDP1. This results in TDP1's stabilization and facilitates its recruitment to TOP1cc, promoting its efficient removal (*Pommier, 2006; Pouliot et al., 1999; Yang et al., 1996*).

PARP-1 in base excision repair

Base excision repair (BER) is a cellular mechanism that repairs damaged DNA bases and abasic sites. BER is initiated by DNA glycosylases that recognize and cleave the damaged base from the sugar-phosphate backbone, generating an abasic site, or one nucleotide gap, in the DNA strand. The abasic site is subsequently recognized and cleaved by apurinic/apyrimidinic endonuclease 1 (APE1), creating one nucleotide gap in the DNA. SSBs in DNA are repaired through two different pathways: short-patch repair and long-patch repair. These pathways differ in terms of the quantity of inserted nucleotides and the DNA repair factors involved in the repair process (*Caldecott, 2008*).

Several studies suggest PARP-1 plays an important role in BER. For example, PARP-1-deficient cells demonstrated half as efficient short-patch BER as wild-type cells, and inefficiency in long-patch BER (*Dantzer et al., 2000*). Additionally, PARP knockout mice and the derived mouse embryonic fibroblasts were shown to be sensitive to DNA-damaging agents triggering the BER process (*Dantzer et al., 1999*).

PARP-1 is involved in BER through interactions with various BER factors, including XRCC1, DNA Pol β , and LIG3 (as previously mentioned), as well as 8-oxoguanine DNA glycosylase 1 (OGG1), proliferating cell nuclear antigen (PCNA), aprataxin, and condensin I (*Hooten et al., 2011; Frouin et al., 2003; Harris et al., 2009; Moor et al., 2015*).

PARP-1 in nucleotide excision repair

Nucleotide excision repair (NER) is a cellular mechanism that repairs bulky adducts caused by environmental factors such as UV light, ionizing irradiation and chemical mutagens. NER can be divided into two sub-pathways: global genomic NER (GG-NER) and transcription-coupled NER (TC-NER) (*de Laat et al., 1999*). GG-NER operates throughout

the genome and can recognize and repair lesions in both transcribed and non-transcribed DNA strands. TC-NER is specific to transcribed DNA strands and primarily repairs lesions that stall RNA polymerase during transcription (Chaudhuri & Nussenzweig, 2017).

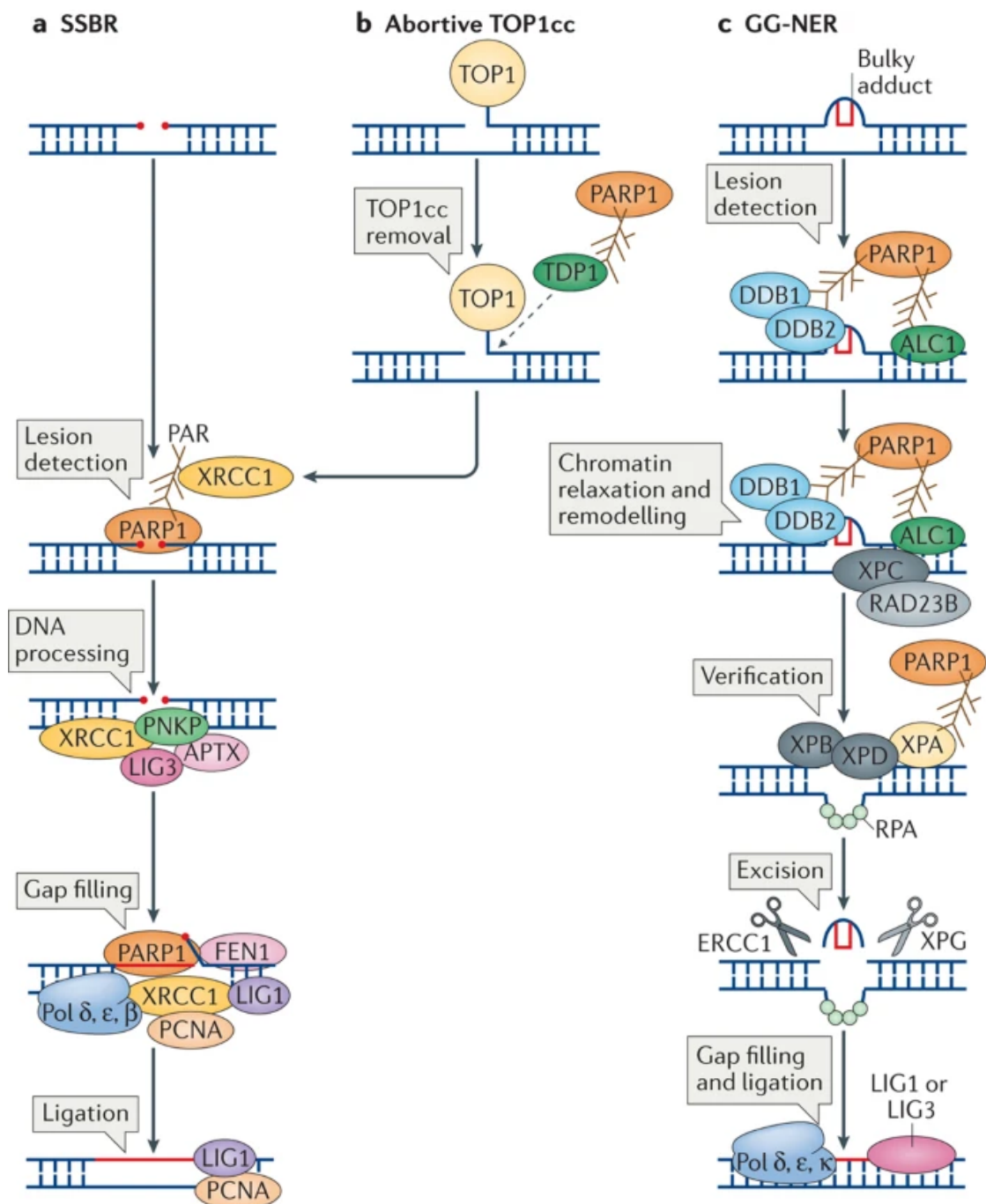


Figure 6: The roles of PARP-1 in excision repair. a. Single-strand break repair (SSBR) mechanism. PARP-1 plays a role in the detection of SSBs and in the recruitment of XRCC1 which then serves as a scaffold for the recruitment of other DNA repair factors. b. Mechanism of the abortive TOP1cc repair. PARP-1 recruits and activates tyrosyl-DNA phosphodiesterase 1 (TDP1), which cleaves the TOP1cc from the DNA. c. Global genome nucleotide excision repair (GG-NER) mechanism. AutoPARylated PARP-1 mediates the recruitment of DDB1-DDB2 complex, ALC1 and XPA (from Chaudhuri & Nussenzweig, 2017).

In NER, damage is first detected and recognized by a complex of proteins, including xeroderma pigmentosum group C-complementing protein (XPC) and RAD23B, which associate with the DNA damage-binding protein 1 (DDB1)–DDB2 complex. The complex recruits and unwinds the DNA around the lesion, creating a bubble-like structure. The lesion is then excised from the DNA strand by the action of endonucleases, which cleave the phosphodiester backbone on either side of the lesion. The gap is subsequently filled in by DNA polymerases and sealed by DNA ligases (Figure 6c) (*Chaudhuri & Nussenzweig, 2017; Marteijn et al., 2014*).

Recent studies have revealed that PARP-1 plays a role in GG-NER. It is involved in the recruitment of XPC to the lesions resulting from its interaction with synthesized PAR. PARP-1 also interacts with DDB2, stimulating its catalytic activity (*Pines et al., 2012; Robu et al., 2013*). Another interesting finding is that DDB2 can stimulate PARP-1-mediated PARylation of histones, leading to the recruitment of ALC1, a chromatin-remodeling helicase that, in its turn, stimulates NER (*Pines et al., 2012*). Moreover, the recruitment of XPA, which is involved in the verification step of NER, has been shown to be PAR-dependent (*King et al., 2012*). The significance of PARP-1 in NER is underscored by the observation that cells become sensitive to UV irradiation when PARP-1 is inhibited (*Pines et al., 2012*).

2.3.2 PARP-1 in DNA double-strand break repair

Double-strand breaks (DSBs) can be caused by various factors, including exposure to DNA-damaging agents like ionizing radiation and chemotherapeutics, or spontaneously during DNA replication when the DNA replication forks encounter obstacles like unrepaired DNA lesions (*Mehta & Haber, 2014*). To repair these DSBs, cells choose between two DNA DSB repair pathways: homologous recombination (HR) and non-homologous end joining (NHEJ) (*Chapman et al., 2012*).

Studies have revealed that the recognition of DNA breaks by PARP-1 and subsequent PAR synthesis are involved in the recruitment of DSB repair factors (Figure 7a) (*Ali et al., 2012; Langelier & Pascal, 2013; Polo & Jackson, 2011; Sukhanova et al., 2016*). For instance, it

was found that the interaction of the ataxia telangiectasia mutated (ATM) kinase with PAR can stimulate its activity *in vitro*, thereby impacting the early DNA damage-induced signaling cascade initiated by ATM. The activity of ATM is essential for the phosphorylation of key proteins involved in DDR, such as p53, SMC1, and histone H2AX. As a result, PARP-1 deficiency or inhibition has been shown to lead to delayed activation of these DDR proteins (*Haince et al., 2007*). Additionally, studies have revealed that the recruitment of two other DNA damage sensors, meiotic recombination 11 (MRE11) and Nijmegen breakage syndrome protein 1 (NBS1), to DSBs is dependent on PARP-1 activity (*Haince et al., 2008*). However, it should be noted that the recruitment of all mentioned above DDR factors is only delayed in PARP-1 deficit cells, not abolished. This suggests the existence of other DDR activation pathways that can partially compensate for the loss of PARP-1 activity (*Haince et al., 2007*).

PARP-1 in homologous recombination

Homologous recombination (HR) is a highly conserved DSB repair mechanism that involves several steps, including resection, strand invasion, synthesis, and resolution. The MRE11-RAD50-NBS1 (MRN) complex, binding to the DSB ends, recruits the exonuclease to initiate the process of resection. During the resection step the 5' end of the broken DNA strand is degraded, creating a 3'-OH ending single-stranded tail which will be further used as a primer for DNA synthesis. The resulting ssDNA is rapidly covered by replication protein A (RPA), and this reaction also requires breast cancer type 1 susceptibility protein (BRCA1). The next step is the strand invasion, in which the single-stranded tail invades the homologous DNA duplex, forming a displacement loop (D-loop). The D-loop serves as a template for DNA synthesis. In the synthesis step, DNA polymerases extend the invading strand using the homologous duplex as a template, resulting in the formation of a new DNA strand. The final step is resolution, in which the D-loop is resolved, and the new DNA strand is ligated to the repaired DNA duplex (Figure 7b) (*Chaudhuri & Nussenzweig, 2017*).

PARP-1 activity contributes to the early recruitment of MRE11, and the HR after the treatment with genotoxic agents leading to the formation of DSBs was impaired in PARP-

1-deficient cells (*Hochegger et al., 2006*). Besides MRE11, PARP-1 is also involved in BRCA1 recruitment to DSBs (*Li & Yu, 2013*). However, while BRCA1 recruitment is regulated through a ubiquitin-dependent mechanism, it remains unclear if there is any interdependence between this mechanism and the PARylation-dependent mechanism (*Schwertman et al., 2016*).

In addition, it was recently demonstrated that PARylation of BRCA1 by PARP-1 regulates its function in HR DNA repair (*Chaudhuri & Nussenzweig, 2017; Hu et al., 2014*). PARylation enables BRCA1 to bind to receptor-associated protein 80 (RAP80), which stabilizes the BRCA1-RAP80 complex and limits HR. When PARylation of BRCA1 is lost in PARP-1 deficient cells, recombination level is increased, indicating that PARP-1 may fine-tune the HR process. However, the increased HR level in PARP-1 deficient cells may also result from a deficiency in SSBR, as unrepaired SSBs can lead to increased levels of DSBs that activate HR (*Hu et al., 2014*).

PARP-1 in non-homologous end joining

Classical non-homologous end joining pathway (cNHEJ) involves several proteins, including the Ku70/80 heterodimer, DNA-dependent protein kinase catalytic subunit (DNA-PKcs), XRCC4, and DNA ligase IV (LIG4). The Ku70/80 heterodimer binds to the broken ends of DNA and recruits DNA-PKcs, which phosphorylates several proteins to facilitate DSB repair. XRCC4 and LIG4 are then recruited to the site of the break to facilitate ligation (Figure 7c). NHEJ can occur throughout the cell cycle but is particularly active during G1 phase. It is also used as a backup mechanism when homologous recombination is not possible (*Chaudhuri & Nussenzweig, 2017*).

PARP-1 can PARylate DNA-PKcs *in vitro*, enhancing its kinase activity independently of the Ku70/80 heterodimer (*Ruscetti et al., 1998*). Furthermore, PARP-1 was demonstrated to form a complex with DNA-PKs *in vivo* (*Luijsterburg et al., 2016*). In another study, PARP-1 was shown to recruit the chromatin remodeler CHD2 through a poly(ADP-ribose)-binding domain (*Spagnolo et al., 2012*). Overall, these data suggest that PARP-1 activity may impact the efficiency of cNHEJ (*Chaudhuri & Nussenzweig, 2017*).

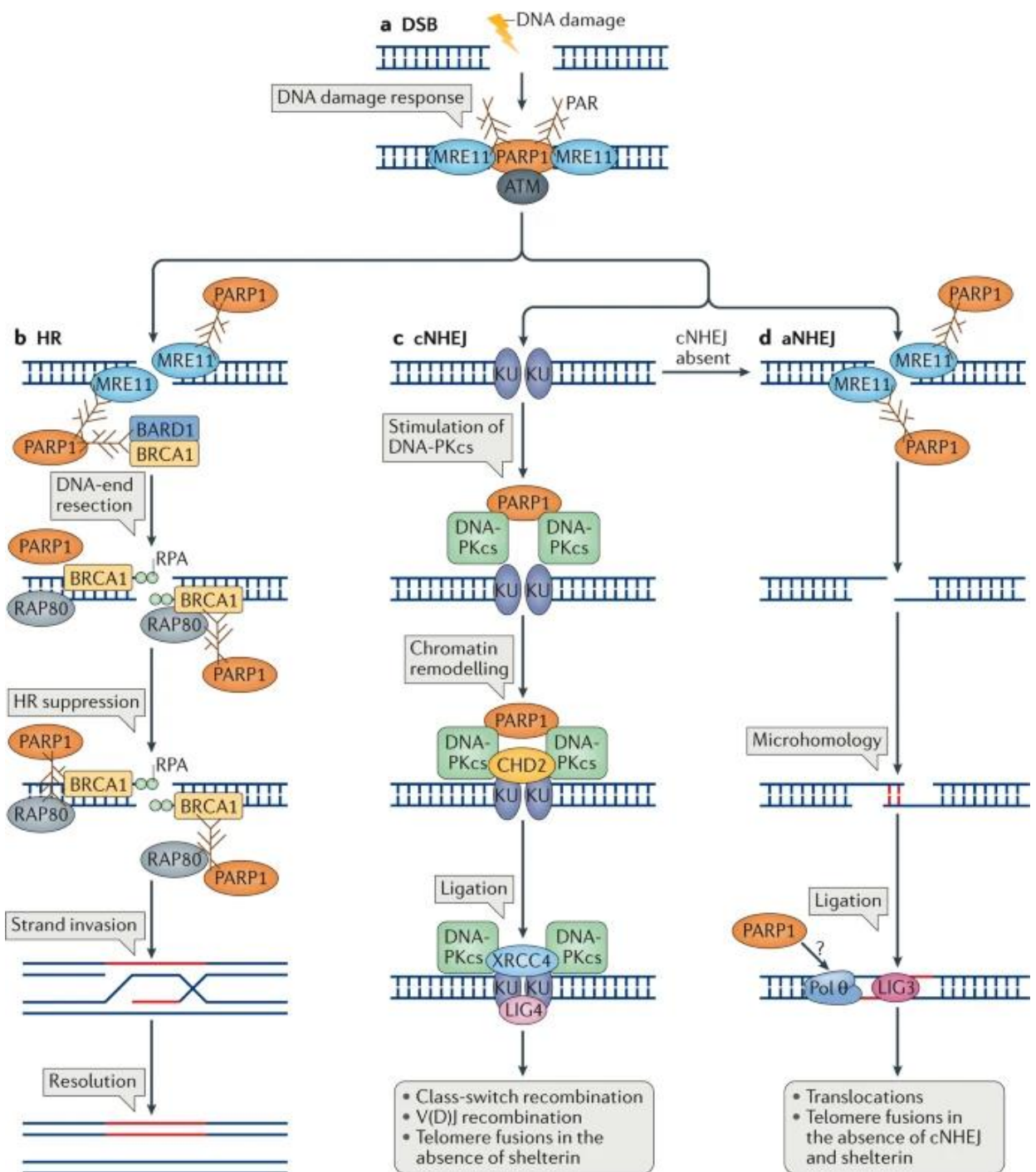


Figure 7: The roles of PARP-1 in the detection (a) and repair of double-strand breaks by HR (b), cNHEJ (c) and aNHEJ (d). a. PARP-1 is required for the robust detection of DSBs and for the initial DNA damage response through its interaction with MRE11 and ATM b. PARP-1 plays a role in the recruitment of MRE11 and BRCA1 through the interaction with its binding partner BARD1. c. PARP-1 interacts with DNA-PKcs and stimulates its activity. Additionally, it plays a role in the recruitment of CHD2 to DSBs. d. PARP-1 recruits MRE11 to DSBs thus playing a role in aNHEJ. Possibly, the recruitment of Pol θ is also dependent on PARP-1 (question mark) (from Chaudhuri & Nussenzweig, 2017).

Unlike cNHEJ, which rejoins broken DNA ends with minimal processing, alternative NHEJ (aNHEJ) relies on end resection and annealing of complementary sequences for repair (Figure 7d). aNHEJ is an error-prone mechanism that can introduce mutations, deletions, or insertions at the site of the double-strand breaks (*Deriano & Roth, 2013*). aNHEJ does not rely on the activity of LIG4 and Ku70/80 proteins (Figure 7c), instead it requires processing of DSB by MRN complex (Figure 7d) (*Truong et al., 2013*).

PARP-1 has the ability to bind to sites of double-stranded breaks (DSBs), competing with the Ku70/80 complex and thereby promoting aNHEJ. Studies have demonstrated that PARP-1 is recruited to DSBs when the Ku heterodimer is absent (*Cheng et al., 2011; Fattah et al., 2010; Mansour et al., 2010; Wang et al., 2006*). Inhibition of PARP-1 leads to a decrease in the efficiency of aNHEJ in cells deficient in Ku or LIG4 (*Wang et al., 2006*). Moreover, PARP-1 is also involved in the recruitment of DNA polymerase θ (Pol θ), which catalyzes DNA synthesis during aNHEJ (*Kent et al., 2016; Mateos-Gomez et al., 2015*).

To sum up, PARP-1 can facilitate the recruitment of MRN complex to DSBs, which, in the absence of Ku70/80 heterodimer, may initiate the processing of DNA ends and trigger aNHEJ pathway choice (*Chaudhuri & Nussenzweig, 2017*).

3. FET PROTEIN STRUCTURE AND FUNCTIONS

Before embarking on a comprehensive analysis of the structure and functions of FET proteins, it would be beneficial to briefly delve into their history of discovery.

In 1992 the analysis of chromosomal translocation in Ewing's sarcoma resulted in the discovery of the gene encoding one of the proteins of FET family, EWSR1 (*Delattre et al., 1992*). This specific t(11;22) (q24;q12) chromosomal translocation leads to the expression of fusion protein EWS-FLI-1 which harbors the N-terminal non-structured domain of EWSR1 and C-terminal domain of the transcription factor FLI-1 (*Delattre et al., 1992*). It was further demonstrated that the N-terminal domain of EWSR1 functions as a transcriptional activation domain, and the resulting fusion oncoprotein EWS-FLI-1 with aberrant transcriptional activator properties is responsible for the genesis of Ewing's sarcoma (*Ohno et al., 1993*).

One year later, in 1993, a chromosomal translocation t(12;16)(q13;p11) occurring in human myxoid liposarcomas was discovered and characterized. Similar to Ewing's sarcoma, this translocation leads to the expression of fusion oncoprotein, whose N-terminal domain is a transcriptional activator domain of FUS/TLS (Fused in Sarcomas/Translocated in Liposarcomas) and C-terminal domain is a DNA-binding domain of the transcription factor CHOP (*Crozat et al., 1993*). The amino acid sequences of FUS and EWSR1 appeared to share high homology (~70%). FUS is an RNA-binding protein (*Crozat et al., 1993; Prasad et al., 1994*), being also the partner of several other RNA-binding proteins. Thus, FUS was shown to co-immunoprecipitate with hnRNPA1 and hnRNPC1/2 (*Zinszner et al., 1994*) and was identified as hnRNP P2 (*Calvio et al., 1995*). It was further demonstrated that FUS is directly involved in transcription serving as a specific component of TFIID and RNA polymerase II preinitiation complexes (*Bertolotti et al., 1996*).

Later in 1996, the third protein with properties similar to FUS and EWSR1 was discovered. TAF15 is another RNA-binding protein, included in the TFIID preinitiation complex and associated with RNA Pol II transcription system (*Bertolotti et al., 1996*).

Based on the similar domain structure of the three proteins (FUS, EWSR1, and TAF15) and their high amino acid sequence homology (~70%), they were assigned to the same FET protein family.

3.1 FET protein structure

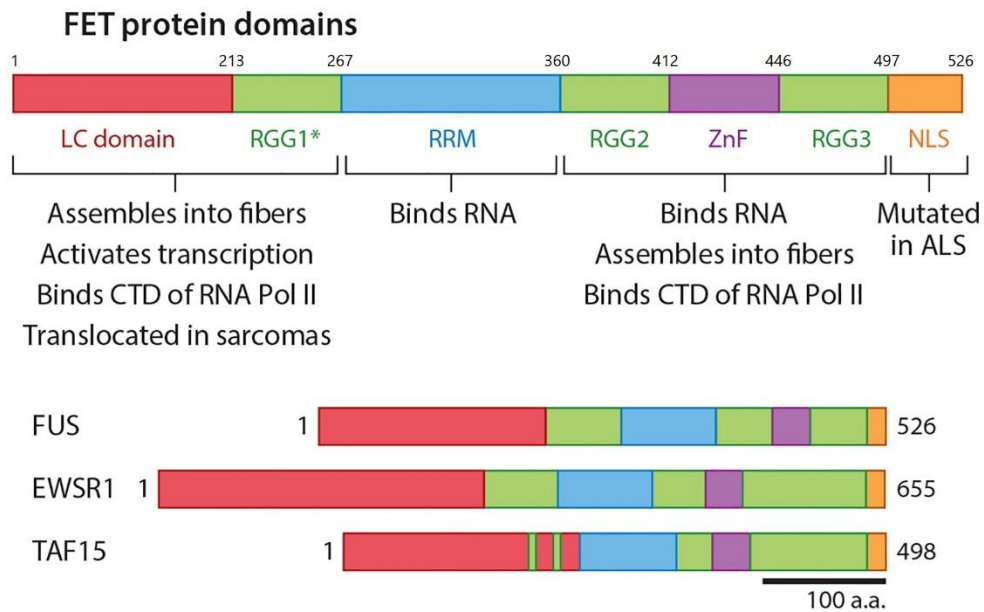


Figure 8 : FET proteins domain structure. ALS, amyotrophic lateral sclerosis; CTD, C-terminal domain; NLS, nuclear localization signal; RNA Pol II, RNA polymerase II; RRM, RNA recognition motif; ZnF, zinc-finger domain (with modifications from Schwartz et al., 2015).

FET family members have similar domain organizations. They contain two structured domains, a conservative RNA-recognition motif (RRM) and a zinc finger domain (ZnF), several non-structured regions, N-terminal intrinsically disordered region containing serine/tyrosine/glycine/glutamine repeats (SYGQ-rich domain or low-complexity (LC) domain) and three areas rich in Arg and Gly (the RGG domains), and a proline-tyrosine nuclear localization signal (PY-NLS) at the C-terminus (Figure 8).

RRM

The RRM domain is a common RNA-binding domain in eukaryotes and contains the RNP1 and RNP2 consensus sequences that are featured in RNP proteins (Clery et al., 2008). A canonical RRM domain has a $\beta 1-\alpha 1-\beta 2-\beta 3-\alpha 2-\beta 4$ structure with a four-stranded β -sheet and two perpendicular α -helices (Dreyfuss et al., 1988). The RRM domains of hnRNP A1, hnRNP D, and TDP-43 contain the nucleic acid binding pocket formed by the central four-

stranded sheet consisting of conserved aromatic and positively charged residues. Therefore, the RRM domain binds nucleic acids by forming “stacking” interactions between its aromatic residues and nucleobases and electrostatic interactions between its positively charged amino acids and the sugar-phosphate backbone.

The RRM domains of FET proteins (FUS, EWSR1 and TAF15) adopt the classical $\beta 1$ – $\alpha 1$ – $\beta 2$ – $\beta 3$ – $\alpha 2$ – $\beta 4$ fold but have several specific features compared to canonical RRM domains of other RNA-binding proteins (Figure 9).

1. RRM domains of FET proteins lack essential aromatic residues shown to interact directly with nucleic acids through ring stacking and hydrogen bonding for canonical RRM domains. In particular, FUS has residues E336 and T338 in RNP1 instead of F147 and F149 in TDP-43, which are crucial for RNA binding and toxicity in TDP-43 (Voigt *et al.*, 2010). These non-canonical residues E336 and T338 are highly conserved in FUS from different organisms (Figure 9).
2. RRM domain of FET proteins contains an extra-long lysine-containing loop between $\alpha 1$ and $\beta 2$ which is called the “KK-loop”. Its name originates from the fact that the KK-loop comprises several evolutionary conserved lysine residues. The “KK-loop is absent in canonical RRM domains of TDP-43 and other RBPs, and it is involved in the direct interaction of FET RRM with nucleic acids. Moreover, the mutations of lysine residues located in the KK-loop (K312A, K315A, and K316A) of FUS RRM greatly reduce or abolish FUS RRM binding to both 24-mer DNA and RNA, suggesting that the KK-loop region plays a critical role in nucleic acid binding (Figure 9) (Liu *et al.*, 2012).

The lack of two essential aromatic residues in RNP1 and the presence of the additional KK-loop leads to the distortion of the conventional nucleic acid binding surface. It further leads to the following consequences:

- the lack of π -stacking interactions between RRM domains and RNA bases;
- the KK-loop with other charged residues forms a positively charged surface area that undergoes electrostatic interactions with negatively charged nucleic acids.

In conclusion, the additional positively charged KK-loop boosts the nucleic acid binding ability of the RRM domains of FET proteins, despite the lack of critical aromatic residues. The presence of multiple positively charged residues on the nucleic acid binding surface and the dependence of the interaction on salt concentrations imply the electrostatic nature of RRM-nucleic acid interactions (Liu et al., 2012).

3. Unlike the canonical RRM domains, the RRM domain of FET proteins contains two conserved D343 and D344 residues. In the study of Zhang et al. these aspartate residues were shown to be PARylated for all three FET proteins RRMs, FUS, EWSR1, and TAF15. Aspartate and glutamate are commonly PARylated residues in proteins (Chapter 2.2.2). The presence of these two DD residues in the RRM domain of FET proteins, in contrast to other RRM domains, makes them unique among different RNA-binding proteins.

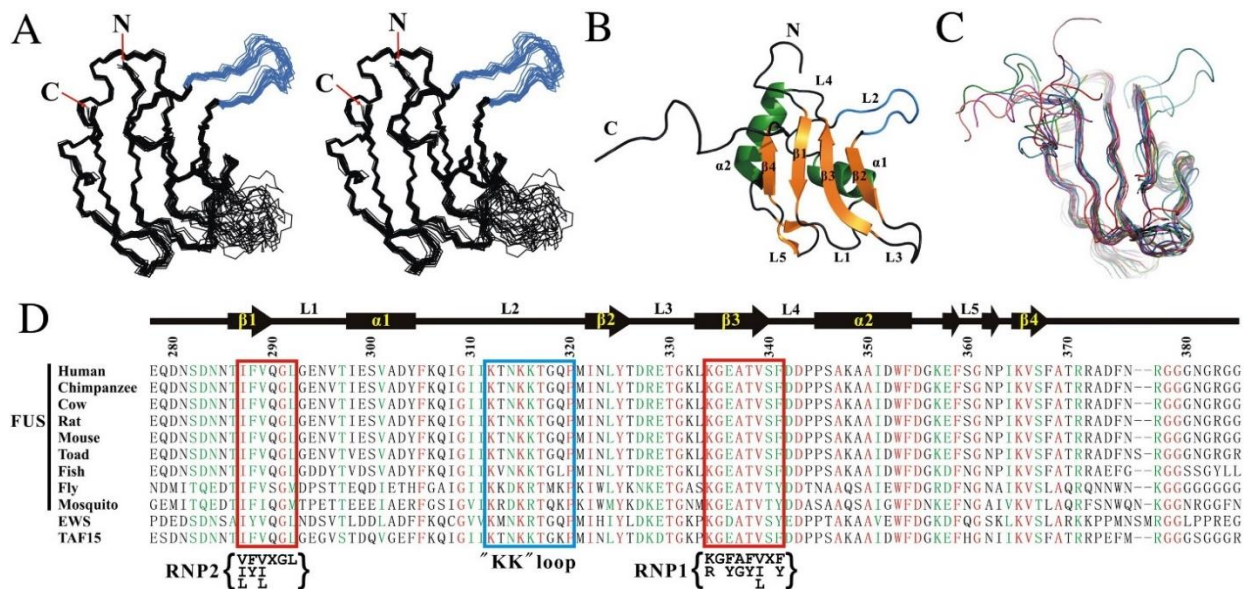


Figure 9: The solution structure of FUS RRM domain (PDB ID: 2LCW). A. Stereo-view showing the backbones of 20 superimposed NMR-derived structures of the FUS RRM domain. The KK-loop is shown in blue. B. Ribbon diagram of a representative NMR structure of FUS RRM with labelled secondary structures. C. Superimposed plot of the FUS RRM domain with other RRM domain structures randomly selected from the Protein Data Bank (PDB IDs: 1H2V, 1HD0, 1L3K, 1S1Q, 1U1P, 1WF2, 1X4B, 2DH9, 2DO0, 2HGL, 2X1A, 3BS9, 3HI9 and 2DGV). The FUS RRM domain contains a long KK-loop (L2) whereas most of the other RRM domains contain a single residue in the place of this loop. D. Sequence alignment of the FUS-RRM domain from different species and RRM domains from human EWS and TAF15. (with modifications from Liu et al., 2013)

All the discussions above concerning FET proteins' interactions with RNA and DNA. In the present work, the interaction of FUS RRM with PAR will be discussed.

ZnF domain

The ZnF domain of FET family proteins belongs to the Ran-binding protein 2 zinc finger type family (RanB2 type ZnF). The Ran-binding protein zinc finger domain itself interacts with the GDP-bound form of the Ran GTPase and is involved in the transport across the nuclear membrane. This type of zinc finger domain is found in over 200 proteins with different functions and domain organizations. Among them, ZnF domains of the nuclear pore complex proteins Nup358 and Nup153 that have also been shown to bind RanGDP, ZnF of the nuclear protein localization protein 4 homolog (NLP4) interacting with ubiquitin and ZnFs of several RNA-binding proteins such as FUS, EWSR1, TAF15, RBM5, RBM10 and TEX13A binding to RNA (*Iko et al., 2004; Nguyen et al., 2011*).

RanB2 ZnF consists of two crossed β -hairpins and a zinc atom bound by four cysteines. As it was demonstrated in several CLIP experiments the ZnF of FUS has a sequence-specific RNA binding mode, preferentially recognizing the UGGU motif (*Ishigaki et al., 2012; Lagier-Tourenne et al., 2012*). The solution structure of FUS ZnF bound to RNA and binding studies with different RNA sequences recently performed by F. E. Loughlin further confirmed this binding motif (*Loughlin et al., 2018*). The central guanines of the sequence are positioned in sequence-specific pockets, with U4 being recognized by side chains that could also accommodate a G, while U1 is not recognized specifically. Thus, the consensus sequence bound by FUS ZnF is NGGK. The fact that the ZnF structure is conserved within other FET proteins, including EWSR1 and TAF15, and that the same GGU binding motif was identified in the TAF15 CLIP-seq experiment imply that this sequence specificity extends to all FET family proteins (*Kapeli et al., 2016*).

RGG

The arginine/glycine-rich (RGG) domain is one of the most common RNA-binding domains in the human genome. The RGG domains are known to be intrinsically disordered, meaning they do not have a fixed, stable structure. Instead, they have the ability to adopt various conformations, giving them a high degree of flexibility and adaptability. This characteristic is particularly useful in RNA-binding proteins as it allows

them to interact with a diverse range of RNA molecules. Each FET protein has three RGG domains: the RRM domain is flanked by RGG1 and RGG2 motifs, while the ZnF domain is flanked by RGG2 and RGG3 (Figure 8).

The RGG domains, together with RRM and ZnF domains, contribute to the binding of FET proteins to RNA. The nature of these interactions is mostly electrostatic. Even though the majority of data show that the RNA recognition by FET proteins is performed in a non-sequence-specific manner, recent studies indicate that these domains exhibit a preference for RNA molecules that have GC-rich sequences and intricate structures that include double-stranded helices (Ozdilek *et al.*, 2017, Schwartz *et al.*, 2015; Wang *et al.*, 2015; Schwartz *et al.*, 2012; Schwartz *et al.*, 2013, Colombrita *et al.*, 2012). Likewise, it has been demonstrated that the nucleic acid-binding behavior of RGG-containing proteins in cells is not completely non-specific (Schwartz *et al.*, 2015; Wang *et al.*, 2015; Schwartz *et al.*, 2012; Hoell *et al.*, 2011).

The RGG domain is a conserved domain that was shown to be involved in the binding of several RNA-binding proteins to the G-quadruplex structures both in DNA and RNA. G-quadruplexes are noncanonical DNA or RNA structures formed by guanine-rich sequences. In these structures, four guanine bases are connected through Hoogsteen hydrogen bonding resulting in a planar arrangement that can be stabilized by a cation (K^+ , Na^+ or Li^+) (Millevoi *et al.*, 2012). G-quadruplex sequences play important roles in numerous cellular processes, particularly in telomere homeostasis, regulation of transcription, pre-mRNA processing and translation (Millevoi *et al.*, 2012). In 2009 based on the purification of human telomeric chromatin using proteomics of the isolated chromatin segments Déjardin and Kingston first demonstrated that FUS binds telomers (Déjardin *et al.*, 2008). Later in 2011 Takahama *et al.* reported that another protein of the FET family, EWSR1, binds to G-quadruplex-formed human telomeres and TERRA (telomeric repeat-containing RNA) through RGG3 domain (Takahama *et al.*, 2011). The mutations of arginine residues within the RGG3 domain to lysines resulted in the disruption of this interaction suggesting the role of positively charged arginines in the binding of EWSR1 to G-quadruplexes. Two years later by the same group, it was

demonstrated that similar to EWSR1, FUS interacts with both G-quadruplex human telomere DNA and TERRA and that tyrosines in the FUS RGG3 domain are involved in this interaction by recognizing 2'-OH groups of the riboses in TERRA (*Takahama et al., 2013; Takahama et al., 2013*).

RGG domains of FET proteins have been shown to undergo extensive asymmetric arginine dimethylation which can affect their interactions with other proteins and are critical for phase separation of FUS (*Hofweber et al., 2018*). Two protein arginine methyltransferases (PRMTs) were reported to be responsible for such methylation: PRMT1 and PRMT8 (*Ong et al., 2004; Scaramuzzino et al., 2013*). The influence of RGG dimethylation on the nuclear-cytoplasmic shuttling of FET proteins and the effect of the mutations in the RGG domain on the phase separation and the development of ALS and FTLD will be further described in the chapter 3.3 and the chapter 3.4.

N-terminal low-complexity domain

The SYGQ-rich domain, also known as the low-complexity domain (LCD), is an intrinsically disordered region located at the N-terminal of FET proteins. It is characterized by a high content of amino acids such as serine, tyrosine, glycine, and glutamine, which are repeated multiple times throughout the N-terminal region of the protein. This region has been the subject of extensive research due to its involvement in two key processes.

Firstly, the SYGQ-rich domain is involved in transcriptional regulation and has been shown to interact with RNA polymerase II and other transcription factors. The N-terminal region of FUS interacts with the C-terminal domain (CTD) of RNA Pol II which prevents premature hyperphosphorylation of Ser2 in the CTD required for a transition from the initiation of transcription to elongation (*Schwartz et al., 2012; Schwartz et al., 2013; Bertolotti et al., 1996; Yang et al., 2000*).

Secondly, the SYGQ-rich domain mediates liquid-liquid phase separation of FET proteins, leading to the formation of non-membrane compartments within cells. This process is regulated by numerous factors such as protein concentration, post-translational

modifications, and interactions with other proteins and RNA molecules. The ability of the SYGQ-rich domain to undergo phase separation is thought to play an important role in the organization and function of these membraneless compartments within cells. The role of the SYGQ-rich domain in the formation of higher-order assemblies will be further discussed in detail in the Chapter 3.3.

PY-NLS

Proline-Tyrosine NLS is a non-classical NLS that is bound by nuclear import receptor Transportin (TRN), also known as Karyopherin $\beta 2$ (Kap $\beta 2$), and translocated across the nuclear pore complex (*Dormann et al., 2012*). This nuclear-cytoplasmic trafficking is mediated by RanGTP. RanGTP is mostly located in the nucleus, whereas RanGDP is located in the cytoplasm. In import pathways, protein cargo containing the PY-NLS sequence binds to Kap $\beta 2$ in the cytosol and is displaced from Kap $\beta 2$ by nuclear RanGTP after translocation to the nucleus. By contrast, in export pathways, protein cargo and RanGTP bind Kap $\beta 2$ cooperatively. Such complex is translocated to the cytoplasm, where it is dissociated through the hydrolyzation of RanGTP with the formation of RanGDP (*Lee et al., 2006*).

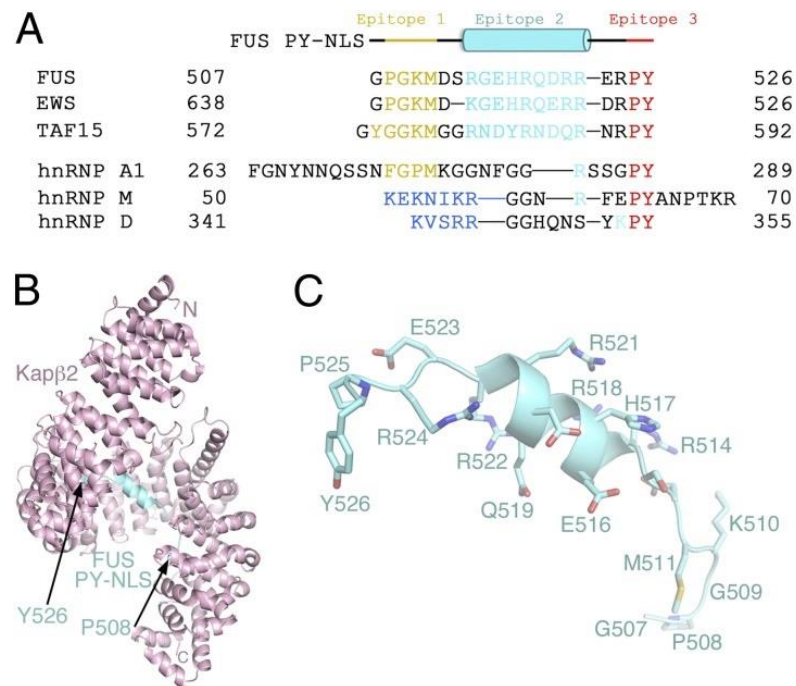


Figure 10: The atypical PY-NLS of FET proteins. A. Aligned sequences of PY-NLS of FET proteins, hnRNP A1, M, and D with three epitopes involved in the interaction of proteins with Kap $\beta 2$ showed in yellow, cyan and red. B. The structure of the Kap $\beta 2$ -FUS PY-NLS complex. C. Side chains of FUS PY-NLS. (with modifications from Zhang and Chook, 2012)

There are four epitopes contributing to binding of FET proteins to Kap β 2. Three of them are localized in PY-NLS (residues 498-526): (1) a C-terminal PY motif, (2) RG-rich polarized α -helix, and (3) an N-terminal hydrophobic motif (Figure 10) (Süel *et al.*, 2008). Later the RGG repeat region preceding the PY-NLS was shown to be a novel Kap β 2 binding epitope (Dormann *et al.*, 2012). When unmethylated, it interacts directly with Kap β 2 stabilizing the interaction of epitopes (1)-(3) of FUS. Methylation of RGG repeats impairs FUS-Kap β 2 interaction however in the methylated protein PY-NLS epitopes bind tightly enough to enable FUS to be imported to the nucleus (Dormann *et al.*, 2012).

The mutations in PY-NLS and RGG-rich regions of FUS affect its translocation and were found in several cases of ALS and FTL (Chapter 3.4).

3.2 Functions of FET proteins

3.2.1 Transcription

FET proteins have been extensively studied for their role in the regulation of transcription, which was suggested early on in the discovery of these proteins. At the beginning of the 1990s, it was proposed that FET proteins affect transcription, as genomic translocations of the N-terminal LC domain of FET proteins observed in leukemia and sarcomas were associated with the activation of transcription (Crozat *et al.*, 1993; Zinszner *et al.*, 1994; Ichikawa *et al.*, 1994; Rabbits *et al.*, 1993; Panagopoulos *et al.*, 1994). In these cases, the chromosomal translocations led to the expression of a fusion protein consisting of the N-terminal domain of FUS, EWSR1, or TAF15 fused to the C-terminal DNA-binding domain from ERG, CHOP, or FLI1. These fusion proteins acted as potent oncoproteins by increasing the activation of CHOP-, ERG-, or FLI1-specific genes via the N-terminal domain of FET proteins. Further supporting the notion that the LC domain can activate transcription, is the finding that a genetically engineered fusion protein consisting of the LC domain and the DNA-binding domain of Gal4 can recruit RNA Pol II and induce transcription (Kwon *et al.*, 2013; Zhang *et al.*, 1998; Bertolotti *et al.*, 1999).

RNA-seq and microarray experiments have provided further evidence for the role of FET proteins in transcriptional regulation. Knockdown of FET proteins has been shown to

result in changes in the mRNA levels of numerous genes, indicating that FET proteins can both positively and negatively affect gene expression (*Tan et al., 2012; Araya et al., 2003; Lee et al., 2005*). In particular, FUS was demonstrated to bind to single-stranded DNA (ssDNA) response elements in the promoter regions of target genes, including several cell cycle-related genes (RAS family genes, PRAP and SAC3D1), MECP2 (encodes methyl CpG-binding protein 2), INTS3 (plays a crucial role in the 3'-end processing of snRNAs and mRNAs), and ZNF397. FUS primarily acts as a negative regulator of the studied genes, with increased FUS levels leading to a decrease in mRNA transcription and vice versa, though there are exceptions. In another study, ChIP-seq analysis has shown that FUS is highly enriched near the transcription start site (TSS) and is associated with thousands of genes (*Schwartz et al., 2012*).

FUS, EWSR1, and TAF15 were discovered to interact with several transcription components. FET proteins co-purify with distinct and separate TFIID complexes (*Bertolotti et al., 1996; Bertolotti et al., 1998*). TFIID is a multi-subunit complex that includes TBP and is responsible for recognizing and binding to the promoter regions of many genes transcribed by RNA Pol II. It has been hypothesized that the association of different FET proteins with specific populations of TFIID may have an impact on transcription initiation and promoter selection. Importantly, a number of evidence report that FET proteins interact directly with RNA Pol II, with the N-terminal domain of FET proteins being responsible for this interaction (*Schwartz et al., 2012; Schwartz et al., 2013; Bertolotti et al., 1996; Yang et al., 2000*). Specifically, FUS was demonstrated to bind the C-terminal domain (CTD) of RNA Pol II and prevent premature hyperphosphorylation of Ser2 in the RNA Pol II CTD. The loss of FUS leads to RNA Pol II accumulation at the transcription start site and a shift in mRNA isoform expression toward early polyadenylation sites (*Schwartz et al., 2012*). Finally, FUS has been found to inhibit RNA Pol III transcription. In a study using small interfering RNA (siRNA) to deplete FUS in HeLa cells, increased steady-state levels of RNA Pol III transcripts were observed (*Tan et al., 2010*). Conversely, overexpression of FUS led to a decreased accumulation of RNA Pol III-generated transcripts. These findings were unexpected and suggested that FUS has a role in regulating both RNA Pol II and III

mediated transcription, highlighting the possibility of cross-regulation between these RNA polymerases in maintaining normal cell growth.

The observation that FUS preferentially localizes to active chromatin is consistent with its role in transcription. Immunofluorescence studies have shown that *cabeza*, the FET protein homolog in *D. melanogaster*, is sequestered to regions of loose chromatin compaction on polytene chromosomes that are actively transcribed (Immanuel *et al.*, 1995). Furthermore, results of immunofluorescence-based assay suggests that FUS is not bound to chromatin during mitosis when transcription is turned off (Kuroda *et al.*, 2000).

In summary, there is considerable evidence for the involvement of FET proteins in transcription, including their:

- interaction with ssDNA in promoter regions of certain genes (Figure 11B);
- co-immunoprecipitation with several components of TFIID complex (Figure 11A);
- binding to CTD of RNA Pol II and suppression of its phosphorylation on Ser2 (Figure 11A);
- suppression of RNA Pol III mediated transcription (Figure 11C);
- localization on the active chromatin region;
- RNA-dependent oligomerization promoting RNA Pol II-dependent transcription.

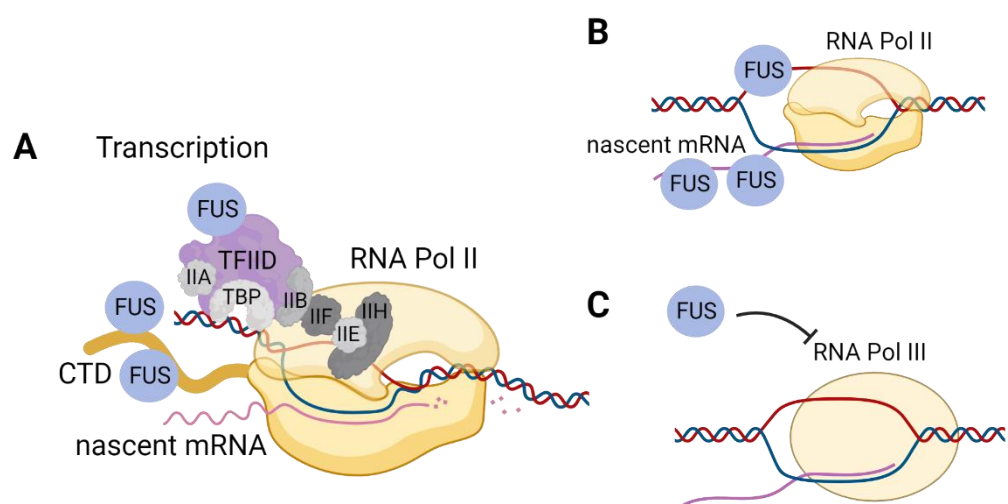


Figure 11: Roles of FUS in transcription. A. FUS interacts with several components of TFIID complex and binds to the C-terminal domain of RNA Pol II regulating its activity. B. FUS interacts with nascent mRNA and ssDNA in promoter regions of certain genes. C. FUS plays a role in the suppression of RNA Pol III activity.

3.2.2 Pre-mRNA processing and splicing

The RNA-processing functions of FET proteins could be linked to their role in transcription. Recent data further strengthen the idea that transcription and following splicing and processing of pre-mRNA are tightly connected processes (*Maniatis et al., 2002; Bentley et al., 2014*). RNA-binding proteins, such as FET family members, can act as a bridge between these different steps in mRNA synthesis and maturation.

Splicing is a critical process that involves the removal of non-coding introns from pre-mRNA and the joining of coding exons to form mature mRNA transcripts. This process is regulated by a complex interplay of various factors, including splice site recognition sequences, splicing factors, and RNA-binding proteins. FET proteins are primarily known for their role in regulating alternative splicing, which is the process by which different combinations of exons are spliced together to generate multiple mRNA transcripts from a single gene. FET proteins can either promote or inhibit alternative splicing depending on the specific context and the interacting partners involved.

FET proteins could affect splicing and RNA processing by interacting directly with pre-mRNA or with splicing factors and other proteins affecting splicing. In the first case, FET proteins are implicated in splicing because they bind to introns and other parts of mRNA, as seen in numerous CLIP-seq studies. (*Hoell et al., 2011; Ishigaki et al., 2012; Rogelj et al., 2012*). This interaction can alter the availability of splice sites and binding sites for other factors. In the second case, FET proteins interact with the splicing machinery, including serine and arginine-rich (SR) proteins (SC35, SRp75, and TLS-associated SR protein) (*Yang et al., 1998; Yang et al., 2000; Das et al., 2007*) and the U1 snRNP complex (*Calvio et al., 1995; Hackl et al., 1996; Yamazaki et al., 2012; Leichter et al., 2011*). Additionally, they have been shown to interact with several hnRNP proteins that also affect splicing. (*Calvio et al., 1995; Zinszner et al., 1994; Yamazaki et al., 2012; Das et al., 2007*). As it was mentioned in the previous chapter (Chapter 3.2.1), FUS regulates Ser2 phosphorylation on the CTD of RNA Pol II. This PTM, in its turn, regulates the interaction of splicing factors with RNA Pol II and splicing itself (*Muñoz et al., 2009; Brès et al., 2008*). Furthermore, FET proteins, such

as FUS and EWSR1, are known to interact with SMN proteins, suggesting they may also affect snRNA biogenesis (*Yamazaki et al., 2012; Tsuji et al., 2013*).

One powerful piece of evidence supporting the role of FET proteins in splicing is the observation that the knockdown of FUS (*Ishigaki et al., 2012; Rogelj et al., 2012*) or EWSR1 (*Paronetto et al., 2011*) alters splicing for numerous gene products, as demonstrated by RNA-seq analysis. In addition, RNA-seq of FUS-depleted cells shows multiple changes in the site of polyadenylation (*Schwartz et al., 2012*)

Interestingly, FUS CLIP-seq data also reveals that FUS binds RNA-encoding genes crucial for DNA damage response and repair pathways. Thus, in the FUS CLIP-seq study of Zhou (*Zhou et al., 2014*), 382 genes were identified, many of which involved in the BRCA1 breast cancer signaling, ATM signaling, DNA double-strand break repair, and cell cycle checkpoints. Remarkably, about 60% of the genes in the DNA double-strand break repair HR pathway and NHEJ pathway are FUS RNA targets. Another study demonstrated that EWSR1 modifies the alternative splicing of genes responsible for DNA repair and genotoxic stress signaling, such as ABL1, CHEK2, and MAP4K2, in response to UV-induced single-strand DNA damage (*Paronetto et al., 2011*). FET proteins, FUS in particular, play an important role in DNA damage response and DNA repair mechanisms, which will be further described in the subsequent chapters of the literature review and in the present study. Data described above suggest that FET proteins may regulate the alternative splicing of DNA damage response or repair genes in response to DNA breaks and cellular stress.

Taken together, substantial evidence supports the involvement of FET proteins in RNA processing and splicing (Figure 12):

- FET proteins directly interact with introns on pre-mRNA which was shown by ChIP-seq analyses;
- FET proteins interact with several splicing factors (SR proteins, U1 snRNP complex) as well as other proteins (hnRNP) that can affect splicing;

- Knockdown of FET proteins affects the splicing of many gene products, genes important for DNA damage response being of particular interest.

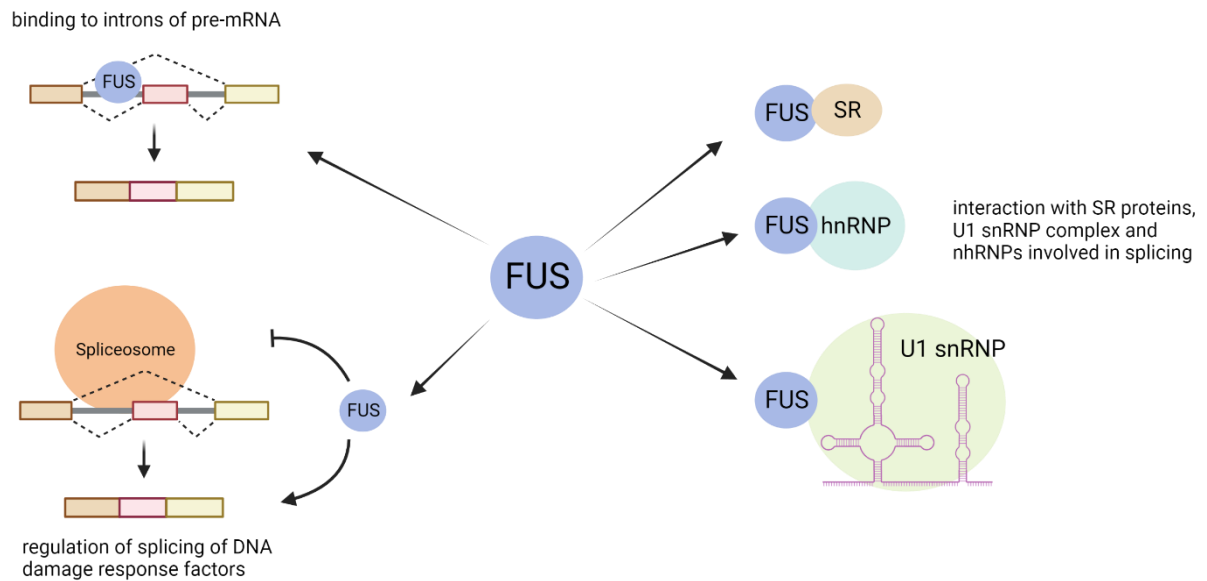


Figure 12: Roles of FUS in splicing. FUS directly interacts with introns on pre-mRNA. FUS interacts with several splicing factors (SR proteins, U1 snRNP complex) and hnRNPs. Differences in FUS expression level affect splicing of DNA damage response genes,

3.2.3 Nuclear-cytoplasmic shuttling of FET proteins

FET proteins are primarily expressed in the nucleus, but they have been shown to move between the nucleus and cytoplasm. The first evidence of FET proteins' ability to translocate to the cytoplasm was observed in 1994 when Zinszner et al. demonstrated the translocation of FUS in cells treated with transcription inhibitors, namely α -amanitin, 5,6-dichloro-1-beta-D-ribofuranosylbenzimidazole (DRB) and Actinomycin D (ActD) (Zinszner et al., 1994). Later, in 1997, the authors demonstrated that the nucleocytoplasmic shuttling of FUS is functionally linked to mRNA transport from the nucleus to the cytoplasm, using heterokaryons, which are fusions of mouse and human cells (Zinszner et al., 1997). In the heterokaryons, proteins located exclusively in the nucleus can remain only in the original nucleus, whereas proteins shuttling between the nucleus and cytoplasm can equally be found in either the mouse or human nucleus. The presence of human FUS protein in the mouse nucleus confirmed FUS's ability to shuttle between the nucleus and cytoplasm.

FET proteins have an unusual C-terminal PY nuclear localization signal (PY-NLS) which is responsible for the interaction with Karyopherin β 2 (Kap β 2) and their nuclear import

(Chapter 3.1). This interaction is regulated by the methylation of arginine residues in the RGG3 domain, which is adjacent to the PY-NLS (Figure 8) (*Dormann et al., 2012*). Arginine methylation, a post-translational modification catalyzed by protein arginine methyltransferases (PRMTs), plays a critical role in the regulation of protein function and subcellular localization. It is important to note that mutations or alterations in the PY-NLS sequence can result in abnormal cytoplasmic localization of the protein, which is associated with the development of ALS. However, PRMT1 knockdown can partially restore the nuclear localization of FET proteins (*Dormann et al., 2012; Tradewell et al., 2012; Yamaguchi et al., 2012*).

There have been numerous studies investigating the translocation of FET proteins to the cytoplasm under different stress conditions. However, a consensus on the underlying mechanisms and reasons behind this phenomenon has not been reached. This topic is particularly significant as cytoplasmic mislocalization and aggregation of FUS have been linked to ALS and FTD (*Urwin et al., 2012; Tyzack et al., 2019*). Although two main reasons for FET protein translocation have been identified, namely DNA damage and transcriptional inhibition, the results from studies are often contradictory. For instance, while one study showed that FUS translocated to the cytoplasm following DNA damage induced by staurosporine or calicheamicin γ 1 in H4 neuroglioma cells (*Deng et al., 2014*), another study demonstrated that FUS remained nuclear under the same treatment in the same cell type (*Rhoads et al., 2018*). Moreover, FUS was reported to translocate to the cytoplasm under oxidative stress caused by prolonged treatment with H₂O₂ (90 min) (*Singatulina et al., 2019*), but not by the treatment (1-2 h) with sodium arsenite (*Sama et al., 2013*). As it was discussed above, FUS shuttles to the cytoplasm due to the treatment with the inhibitors of transcription (DRB, α -amanitin and ActD) according to the early FET proteins studies (*Zinszner et al., 1994; Zinszner et al., 1997*). However, in more recent studies, FUS remained mostly nuclear after ActD treatment in HeLa cells and human neurons (*Hock et al., 2018; Ederle et al., 2018*).

One of the initially proposed mechanisms for the shuttling of FET proteins to the cytoplasm is through passive diffusion. This hypothesis was supported by an experiment

utilizing a protein enlargement assay, which quantifies the cytoplasmic concentration of FUS proteins fused with varying quantities of GFP tags. The findings of the experiment indicate that FUS proteins with a greater number of GFP tags required more time to relocate to the cytoplasm, consistent with a diffusion-based model (*Hock et al., 2018; Ederle et al., 2018*). The main flaw of this model is that it does not take into account numerous interactions of FET proteins with their binding targets (RNAs, proteins), which may affect their cellular distribution. One of the most recent studies of FUS translocation suggests that RNA, serving as a binding platform for FUS, retains it in the nucleus (*Tsai et al., 2022*). However, when the inhibition of transcription is taking place, FUS moves to the cytoplasm due to the lack of binding partners. The authors examined FUS localization in human U87 glioblastoma cells by immunofluorescence following exposure to different stresses, specifically doxorubicin (DNA double-strand breaks), sodium arsenite (oxidative stress), sorbitol (hypertonic stress) and flavopiridol or ActD (transcriptional inhibition). The striking FUS nuclear export was observed following transcriptional inhibition using either inhibitor. Moreover, the knockdown of the nuclear mRNA export factor NXF1 or RNA exosome cofactor MTR4, inducing the accumulation of RNA in the nucleus, suppressed FUS cytoplasmic translocation. In summary, reduced levels of nuclear RNA, which can reflect reduced transcription by RNAP II, result in increased accumulation of cytoplasmic FUS (*Tsai et al., 2022*).

FET proteins, when present in the cytoplasm, have been observed to accumulate in stress granules. These granules contain mRNA that has been silenced for translation, as well as certain RNA-binding proteins and translation initiation factors. The accumulation of FET proteins in stress granules depends on their concentration in the cytoplasm and the presence of stress, which induces the formation of stress granules by inhibiting translation. The overexpression of FUS and TAF15 can lead to the spontaneous formation of stress granules (*Andersson et al., 2008*). However, endogenous FUS protein accumulates in stress granules only during osmotic stress and remains in the nucleus during other types of stress, such as oxidative stress, heat shock, or endoplasmic reticulum stress (*Sama et al., 2013*). Additionally, mutations in the PY-NLS of FUS can increase the concentration

of FUS in the cytoplasm, leading to its accumulation in stress granules when stress is applied (Vance *et al.*, 2013; Bosco *et al.*, 2010; Sama *et al.*, 2013).

3.2.4 mRNA transport

The shuttling of FET proteins between the nucleus and cytoplasm and the dependence of this process on RNAs as their main binding partners implies a putative role of FET proteins in mRNA transport. The majority of published data refer to the transport of mRNA in neurons. Neurons are specialized cells that comprise a cell body (soma), dendrites, which possess small protrusions called spines, and an axon. According to reports, FUS localizes in the dendrites of mouse hippocampal neurons and moves to the spines in an activation-dependent manner through metabotropic glutamate receptor 5 (mGluR5) (Fujii *et al.*, 2005). The abnormal spine morphology observed in hippocampal neurons of FUS-null mice suggests that FUS may play a crucial role in transporting mRNA to maintain the spine shape during remodeling triggered by synaptic signals. FUS was reported to associate with mRNA encoding an actin-related protein Nd1-L and participate in actin reorganization in spines (Fujii & Takumi *et al.*, 2005). Additionally, FUS was found to associate with multiple motor proteins, including ATP-dependent actin-binding motors Myo5A (Yoshimura *et al.*, 2006) and Myo6 (Takarada *et al.*, 2009), and isolated as part of the large granule associated with the microtubule-dependent kinesin motor protein KIF5B (Kanai *et al.*, 2004). Notably, Myo5A has been shown to transport FUS-bound mRNAs, such as Nd1-L, into dendritic spines. After reaching the spines, Myo5A releases FUS and its associated mRNAs for local translation (Yoshimura *et al.*, 2006).

3.2.5 mRNA stability

The interaction of FUS with the 3'UTR sequence of particular target mRNAs suggests that it could regulate multiple facets of mRNA function, including stability/decay, translation, and transport (Hoell *et al.*, 2011). To investigate the cytoplasmic functions of FET proteins more thoroughly, RNA immunoprecipitation and chip analysis were utilized to identify mRNAs associated with FUS in ribonucleoprotein complexes from motoneuronal NSC-34 cells. While FUS was found to bind to certain 3'-UTRs of target genes, such as *Vps54*, *Nvl*,

and *Taf15*, its knockdown did not appear to affect the stability or translation of these targets (*Colombrita et al., 2012*). However, in primary cortical neurons, depletion of FUS resulted in the downregulation of the GluA1 protein subunit of the α -amino-3-hydroxy-5-methylisoxazole-4-propionate (AMPA) receptor, which is involved in synaptic transmission (*Udagawa et al., 2015*).

Moreover, FUS was found to interact with proteins involved in mRNA 3'-end processing and polyadenylation, such as PAN2, PABPC1, and CPSF6. Upon depletion of FUS, disruption of these interactions decreased the polyA tail length of GluA1 mRNA, and reduced mRNA stability was observed specifically in the cytoplasm, resulting in a decrease in GluA1 protein content (*Udagawa et al., 2015*).

3.2.6 MicroRNA processing

MicroRNAs (miRNAs) are small non-coding RNA molecules that play important roles in regulating gene expression by binding to messenger RNAs (mRNAs) and causing their degradation or inhibition of translation. They are involved in a variety of cellular processes, such as development, differentiation, proliferation, and apoptosis. MiRNAs are transcribed from DNA and are processed in the nucleus by several proteins, including Drosha and DGCR8, before being exported to the cytoplasm. Once in the cytoplasm, they are further processed by the RNAase III enzyme Dicer to form a mature miRNA duplex. The mature miRNA is then incorporated into the RNA-induced silencing complex (RISC), which binds to target mRNAs and represses their translation or promotes their degradation.

The FET proteins have been shown to play a role in the processing of miRNAs in the nucleus. EWSR1 and FUS were initially reported to be the components of the Drosha-containing complex (*Gregory et al., 2004*). Subsequent studies have revealed that by binding to nascent pri-miRNAs FUS is able to recruit Drosha at chromatin sites of active transcription to promote pri-miRNA processing (*Morlando et al., 2012*). As a consequence, in human neuroblastoma cells, FUS depletion altered the expression of a consistent number of analyzed miRNAs (44%) by mostly down-regulating their level, including miR-

9, miR-125b, and miR-132, which have important roles in neuronal metabolism and differentiation (Morlando et al., 2012; Ratti et al., 2016).

Additionally, FUS was shown to be involved in miRNA-induced gene silencing by binding to both miRNA and mRNA targets and interacting with the core RISC component AGO2 (Argonaute 2) (Zhang et al., 2018). This function of FUS was illustrated in the context of miR-200c and its target *ZEB1*. *C. elegans* homolog *fust-1* also regulated the gene silencing pathways (Zhang et al., 2018).

To summarize, FET proteins play a role in miRNA processing by:

- Interacting with two essential proteins, Drosha and AGO2, which are crucial for miRNA functions;
- Binding to nascent pri-miRNAs.

3.2.7 Long non-coding RNA processing

Long non-coding RNAs (lncRNAs) are RNA molecules that are more than 200 nucleotides in length and do not code for proteins. Despite lacking protein-coding ability, lncRNAs play crucial roles in various cellular processes, including gene regulation, chromatin remodeling, and epigenetic modification. Recent studies have shown that the RNA-binding protein FUS is involved in the processing of lncRNAs.

Through CLIP-seq analysis, FUS was identified to bind to 71 out of 234 literature-annotated lncRNAs, including NEAT1 and MALAT1, which make up a consistent fraction of 30% (Lagier-Tourenne et al., 2012; Lourenco et al., 2015). NEAT1 is a lncRNA that plays a role in the formation of nuclear paraspeckles, while MALAT1 is involved in regulating alternative splicing and gene expression. Studies have shown that FUS binds directly to NEAT1 lncRNA and is enriched in paraspeckles (Nishimoto et al., 2013; Nishimoto et al., 2021). Mutant FUS proteins are able to sequester paraspeckle components in the cytoplasm, leading to dysregulation of paraspeckle function and structure, which may contribute to the induction of neurodegeneration in ALS/FTLD (Shelkovernikova et al., 2013).

As lncRNAs are a relatively new topic in RNA biology and gene regulation, the precise role of FUS in lncRNA-regulated processes is still under investigation. However, the identified interaction between FUS and specific lncRNAs highlights the importance of understanding the role of RNA-binding proteins in regulating non-coding RNA species.

3.3 FET proteins - driven liquid-liquid phase separation and the formation of aggregates

3.3.1 Liquid-liquid phase separation

Eukaryotic cells are made up of organelles that serve specific functions and offer spatial and temporal regulation of cellular materials, metabolic processes, and signaling pathways. The nucleus, for instance, separates transcription from translation, allowing eukaryotes to develop a posttranscriptional control system absent in prokaryotes. In addition to membrane-bound organelles like lysosomes, the endoplasmic reticulum, and synaptic vesicles, cells also have membraneless organelles (*Boeynaems et al., 2018*). These supramolecular assemblies are found in the nucleus (nucleolus, nuclear speckles) and cytoplasm (stress granules, processing bodies, and the centriole). Though discovered decades ago, the formation and function of these organelles remained unclear until recent interdisciplinary advances shed light on their molecular properties, regulation, and physicochemical forces that drive their formation (*Uversky et al., 2016; Mitrea et al., 2016*). These membraneless organelles contribute to various cellular processes, such as stress response, gene expression regulation, and signal transduction (*Wheeler et al., 2016; Su et al., 2016*).

Recent proposals suggest that these compartments assemble through a physicochemical process called liquid-liquid phase separation (LLPS) (*Uversky et al., 2016; Mitrea et al., 2016*). LLPS is the demixing of a homogeneous polymer solution into two separate phases: polymer-rich condensates and a dilute aqueous phase. The process is described by the Gibbs equation, $\Delta G = \Delta H - T\Delta S$, where ΔG is the Gibbs free energy change, ΔH is the enthalpy change, ΔS is the entropy change, and T is temperature. LLPS occurs when ΔG decreases, which can happen when the ΔH component decreases and/or the ΔS

component increases (Alemasova *et al.*, 2022). This process can be achieved through the formation of energetically favorable intermolecular interactions (Banani *et al.*, 2017; Posey *et al.*, 2018) and/or the release of water molecules from an entropically unfavorable preorganized hydration shell into the bulk (Ahlers *et al.*, 2021). However, the formation of structured condensates is itself entropy-disadvantageous, which makes the enthalpic component more important for LLPS. Therefore, molecules' ability to engage in multiple interactions (also called multivalent interactions) is a key property that determines their susceptibility to LLPS.

Molecules capable of forming multivalent interactions include various polymers that possess multiple sites for specific and non-specific binding. These molecules encompass nucleic acids such as DNA, RNA, and PAR, as well as certain disordered proteins that feature degenerate regions of low complexity. In the following sections, we will explore the properties of RNA, PAR, and disordered proteins that render them prone to engage in LLPS. Additionally, we will examine the structure of FET proteins and the condensates they form both *in vitro* and *in vivo*.

3.3.1.1 Nucleic-acids-driven LLPS: DNA and RNA

The susceptibility of nucleic acids to phase separation and the ultimate structure of the resulting condensate depends on several key characteristics, including their charge, length, sequence, structure, and rigidity (Alemasova *et al.*, 2022).

Nucleic acids possess a highly negative charge due to the presence of phosphate moieties in their backbone. As a result, they can form multiple electrostatic interactions, leading to their phase separation, regardless of their sequence (Dutagaci *et al.*, 2021).

The length of the nucleic acid plays a crucial role in determining the fluidity of the resulting condensate. Studies have shown that shorter DNA molecules are more likely to form liquid-like condensates, while longer DNAs tend to form solid-like structures (Muzzopappa *et al.*, 2021).

Furthermore, the rigidity or flexibility of the nucleic acid is also a significant factor affecting the resulting condensate. Less flexible DNA molecules form weaker condensates that are more likely to dissolve in solutions with lower ion concentrations than those formed by more flexible DNAs of the same length and charge (*Shakya et al., 2018*).

The structure of nucleic acid, depending on whether it is single-stranded or double-stranded, also influences the structure of a condensate. Unlike double-stranded nucleic acids, exposed nucleobases in single-stranded nucleic acids can form pi-pi or cation-pi interactions. Base-paired double-stranded DNA has higher charge density allowing it to bind more strongly to polycations. This feature makes it more prone to form solid-like condensates or liquid-crystalline phases (*Mimura et al., 2021*).

Although several disordered proteins have been shown to phase-separate in the absence of nucleic acids, RNA plays a critical role in determining the size and composition of phase-separated condensates (*Alemasova et al., 2022, Navarro et al., 2019*). In a recent study, the ArtiGranule (ArtiG) bottom-up approach was used to form RNA-protein assemblies in living cells and investigate the role of RNA in their nucleation and composition (*Navarro et al., 2019*). This method involved expressing a genetically engineered prone-to-aggregation protein in HeLa cells, which formed biochemically neutral, liquid-like condensates. An RNA-binding domain was then inserted into the protein, leading to the recruitment of RNA to the condensates. The study revealed that different types of RNA contributed differently to the generation of artificial condensates, impacting their morphology in distinct ways.

One of the mechanisms describing the co-condensation of proteins with nucleic acids is monolayer protein recruitment (*Alemasova et al., 2022*). This mechanism was proposed by Renger et al. in a recent study describing the formation of FUS condensates driven by single- and double-stranded DNA (*Renger et al., 2022*). By using *in vitro* assay based on optical tweezers combined with confocal microscopy, the authors were tracking the association of FUS with DNA molecules. They observed that FUS adsorption along DNA promoted the interaction between the low-complexity domains of FUS proteins, resulting

in the formation of FUS-DNA condensates (Figure 13A). A similar condensation mechanism was also described for the formation of RNA-driven condensates using single-molecule Förster Resonance Energy Transfer (smFRET) and Electrophoretic Mobility Shift Assay (EMSA) (Niaki *et al.*, 2020). RNA molecule served as a binding platform for FUS facilitating protein-protein interactions between LC domains of several FUS proteins.

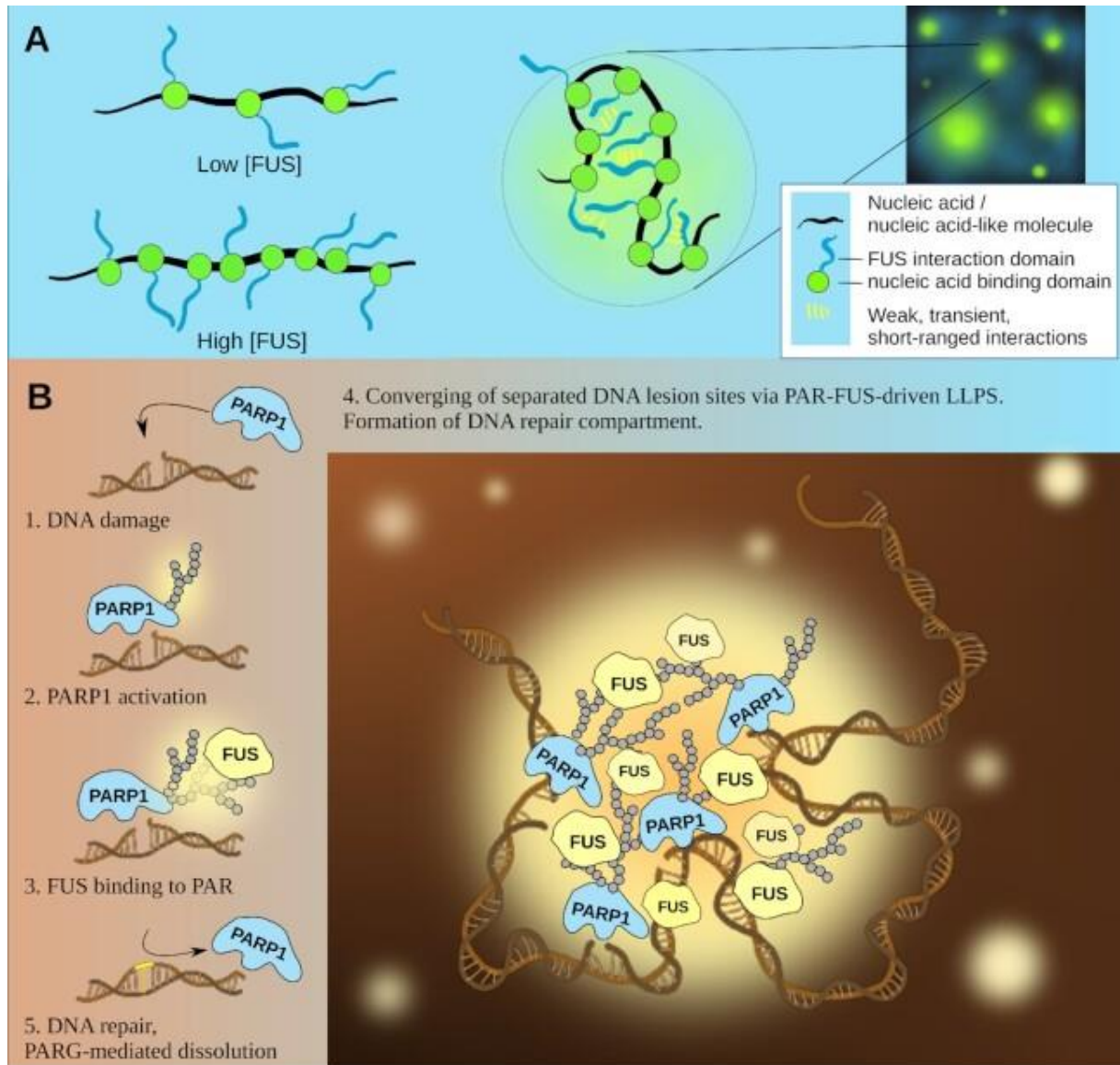


Figure 13: A monolayer protein recruitment mechanism of nucleic-acid-mediated FUS condensation
 A. A monolayer protein recruitment mechanism: nucleic acid serves as a binding platform for FUS facilitating protein-protein interactions between LC domains of several FUS proteins. B. The formation of large compartments at the sites of DNA damage occurring through the interaction of FUS with PAR synthesized by PARP-1, as well as multiple interactions occurring between LC domains of FUS (from Aemasova & Lavrik, 2022).

3.3.1.2 PAR-driven LLPS

The same characteristics that define the propensity of nucleic acids to phase separate are also applicable to poly(ADP-ribose) molecules, including their large negative charge, low complexity, flexibility, and chain length. However, there are characteristics of PAR, such as branching, that are unique (*Alemasova et al., 2022*).

Firstly, PAR's doubled negative charge and increased spacing between ribose moieties compared to DNA and RNA enable it to form more electrostatic interactions and bind more tightly to its partners (*Leung et al., 2020*).

Previous studies have shown that low-complexity RNA, such as polyU, can form liquid-like coacervates when combined with short polyamines, such as spermine and spermidine. These coacervates are similar to those formed by intrinsically disordered proteins and can compartmentalize peptides and oligonucleotides in a sequence- and length-dependent manner (*Aumiller et al., 2016*). Similarly, the low complexity of PAR may contribute to its predisposition to undergo LLPS.

A study investigating the structural flexibility of PAR in solutions demonstrated that it is more flexible than single-stranded DNA, likely due to the longer linkers between ribose moieties consisting of two phosphates instead of one. Molecular dynamics simulations have shown that PAR does not have a defined structure in solution but instead exists as a dynamic polymer, adopting numerous different conformations (*D'Annessa et al., 2014*). This dynamic nature allows it to form multiple interactions with proteins, regardless of their three-dimensional structure.

The length and branching of PAR chains dictate the quantity of PAR-binding proteins that interact with each PAR chain and, consequently, the local concentration of these proteins. For example, a high degree of branching may decrease the number of proteins that selectively recognize linear PAR and bind to the polymer (*Reber et al., 2021*). A recent study examined the relationship between PAR length and its effectiveness in driving the formation of FUS-containing condensates (*Rhine et al., 2022*). The study found that FUS

condensation requires PAR chains that are at least eight units in length, whereas PAR monomers, dimers, and tetramers are insufficient to drive FUS phase separation.

Similarly to RNA-driven LLPS, PAR-driven condensates can be generated by monolayer protein recruitment. The use of atomic force microscopy demonstrated the formation of compartments comprised of PAR and FUS, which concentrate damaged DNA (*Singatulina et al., 2019*). The formation of large compartments at the sites of DNA damage occurs through the interaction of FUS with PAR synthesized by PARP-1, as well as multiple interactions occurring between LC domains of FUS (Figure 13B). The importance of LC domains of FUS was demonstrated through their deletion, resulting in the impaired formation of FUS Δ LC: PAR compartments.

Interestingly, PAR was recently proposed to mediate FUS condensation via a catalyst-like mechanism (*Alemasova et al., 2022; Rhine et al., 2022*). According to this hypothesis, PAR forms transient interactions with FUS triggering its ability to undergo LLPS and generate condensates with liquid-like properties (Figure 14). Moreover, these condensates do not further require PAR to sustain as the treatment of FUS: PAR condensates with PAR-degrading enzyme PARG did not lead to their dissociation. Strikingly, the concentration of PAR (1 nM) required for the formation of FUS: PAR droplets was three orders of magnitude lower than the concentration of RNA (polyU, 1 μ M) required for the formation of FUS: RNA condensates. At the same time, the authors point out that FUS binds RNA with higher affinity than PAR ($K_d \sim 5$ nM for RNA vs. $K_d > 200$ nM for PAR), forming long-lived interactions with RNA contrary to transient interactions formed between FUS and PAR. Consistently with these data, RNA is necessary for the maintenance of FUS: RNA condensates as their treatment with RNase leads to their dissociation. Overall, the authors suggest that PAR, like RNA, can drive the formation of FUS liquid-like condensates but through a unique catalyst-like mechanism (*Rhine et al., 2022*).

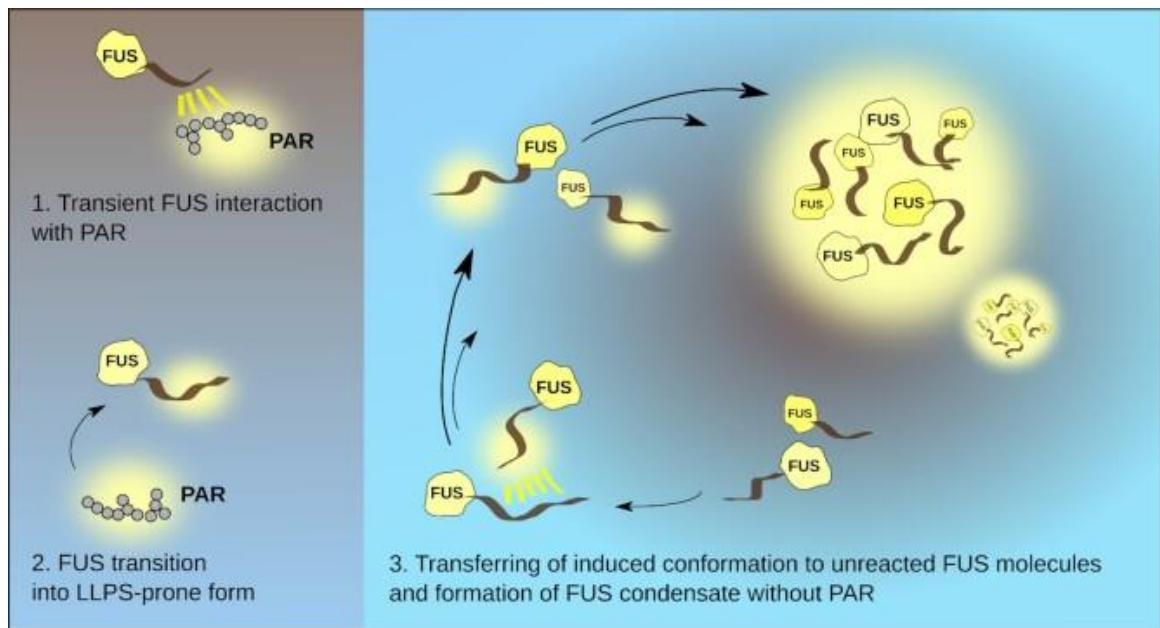


Figure 14: A catalyst-like mechanism of PAR-mediated FUS condensation. PAR forms transient interactions with FUS triggering its ability to undergo LLPS and generate condensates with liquid-like properties (from Alemasova & Lavrik, 2022).

3.3.1.3 Intrinsically disordered proteins in LLPS

Proteins that contain large intrinsically disordered regions (IDRs) have been observed to undergo phase separation under physiological conditions. IDRs are highly dynamic and lack a stable three-dimensional folded structure, often with a biased amino acid composition (low amino acid complexity). They are enriched with specific types of amino acids, primarily non-charged, such as glycine, serine, glutamine, asparagine, phenylalanine, and tyrosine, but occasionally charged, including lysine, arginine, glutamate, and aspartate. The limited sequence diversity generates multiple Gly/Ser-Phe/Tyr-Gly/Ser sequences and/or poly-Gln and poly-Asn tracts, as well as blocks of positive or negative charge (*Banani et al., 2017; Nott et al., 2015*). These repeats are often critical for IDR-containing proteins' interaction with nucleic acids, particularly RNA and PAR, for their direction to RNA granules, and for LLPS both *in vitro* and *in vivo* (*Kato et al., 2012; Burke et al., 2015; Molliex et al., 2015*).

Recent research has highlighted the significance of aromatic residues in promoting phase separation. Repeats containing multiple aromatic residues have the ability to form cation- π interactions with positively charged amino acids, as well as π -stacking interactions (*Nott et al., 2015*). Additionally, sequences rich in polar uncharged side chains, such as

Gln, Asn, or Ser, also contribute to phase separation via dipolar interactions (*Crick et al., 2013*). Blocks of oppositely charged residues can also drive phase separation, either between different molecular types or as alternating blocks within the same molecular type (*Patel et al., 2015; Altmeyer et al., 2015*). Overall, the most influential interactions in phase separation are charge-charge, polar, and aromatic. However, it's worth noting that these interactions do not provide significant structure to the peptide chain and can be easily disrupted, resulting in highly dynamic structures formed via LLPS.

In addition to these amino acid sidechain interactions, interactions involving the polypeptide backbone also likely play an important role in the LLPS of IDR-containing proteins. For example, hydrogels formed by RNA-binding proteins, such as FET family members, nhRNAP2, and CIBP, were reported to contain long filaments formed by interactions between backbone amino acid atoms in β -strands, similar to those observed in amyloid fibers (*Kato et al., 2012*). Additionally, the α -helical structure in TDP-43 was shown to be important for its phase separation (*Conicella et al., 2016*). It is worth noting that the contribution of sidechain and backbone interactions to phase separation may vary in different IDRs, depending on the protein's amino acid composition and overall sequence patterns. Although there is progress in developing predictive rules for protein sequence and its propensity for phase separation, this area of research remains important for future study.

3.3.1.4 FET proteins drive LLPS *in vitro* and *in vivo*

The capacity of FET proteins to undergo phase separation relies on two specific domains: the LC domain located at the N-terminal and the positively charged RGG domain (Figure 8). In light of recent research on the participation of FET family members in the formation of liquid-like condensates, we will further explore the function of each of these domains in LLPS.

The initial studies investigating the contribution of FET proteins in the assembly of condensates were focused on comprehending the dynamic formation of membraneless organelles in cells, such as stress granules, nucleoli, germ granules, or Cajal bodies. As

more evidence emerged, it became increasingly clear that these compartments exhibit liquid-like properties and are formed by the LLPS process. It was further demonstrated that LC domains are implicated in the formation of membraneless organelles. All three FET proteins, FUS, EWSR1, and TAF15, possess low-complexity regions, which hints at their possible ability to form liquid-like condensates such as membraneless organelles.

Indeed, two early studies on the topic demonstrated that FUS could form hydrogel droplets *in vitro* (Han *et al.*, 2012; Kato *et al.*, 2012). X-ray diffractions and electronic microscopy showed that these droplets were composed of amyloid-like fibers. Although these fibers had a morphology similar to pathogenic amyloid fibers, the condensates formed by FUS were shown to be dynamical and reversible. (Kato *et al.*, 2012). Interestingly, the N-terminal LC domain alone appeared to be sufficient to drive their formation. Moreover, tyrosine residues of the SYGQ motif located in the N-terminal LC domain play an important role in FUS LCD phase separation as their mutations to serine residues lead to the impaired ability of FUS LCD to form hydrogel droplets (Kato *et al.*, 2012). The importance of the LC domain was further strengthened by the fact that its phosphorylation was reported to impede FUS retention in FUS-formed hydrogels. FUS is phosphorylated by DNA-dependent protein kinase (DNA-PK) at the C-terminal [G/S]Y[G/S] motifs of its LC domain (Gardiner *et al.*, 2008). Incubation of phosphorylated FUS with FUS hydrogel droplets revealed its impaired ability to bind to FUS hydrogel, indicating that this posttranslational modification (PTM) may regulate FUS capacity to undergo phase separation (Han *et al.*, 2012). The role of PTMs in the regulation of FET proteins' functions will be discussed in detail in the following section.

Another study further confirmed these results (Patel *et al.*, 2015). FUS was reported to phase separate into dynamic liquid droplets *in vitro*. Again, the LC domain appeared to be essential for FUS-driven LLPS: a deletion mutant of FUS lacking the N-terminal domain, FUS Δ LC, failed to form liquid droplets *in vitro*, remaining homogeneously distributed. The same authors investigated the formation of various stress-induced compartments formed by FUS *in vivo* and demonstrated that FUS assemblies have the hallmarks of liquid-like compartments. There are three characteristics of liquid-like compartments: their

components undergo internal rearrangement, they have a spherical shape, and they can fuse, forming one spherical droplet. Both FUS-GFP cytoplasmic stress granules and FUS-GFP nuclear granules meet all three of these criteria (*Patel et al., 2015*).

Several studies indicate that FUS assembly is required for the recruitment of RNA Pol II through binding to its C-terminal domain (CTD) and, subsequently, for transcriptional activation (*Kwon et al., 2013; Schwartz et al., 2014; Thompson et al., 2018*). As earlier mentioned, the LC domain of FUS was shown to interact with the CTD of RNA Pol II and regulate its phosphorylation at Ser2 (*Schwartz et al., 2012*). It appeared that the RNA Pol II CTD did not bind to monomers of the LC domain of FET proteins but to the fibrous polymers organized by LC domains of FUS or TAF15, and the extent of binding between the CTD of RNA Pol II and FET LCD related to the potency of transcriptional activation. Interestingly, following phosphorylation of Ser2 at the CTD was shown to block RNA Pol II binding to hydrogel droplets formed by FET proteins (*Kwon et al., 2013*). These findings suggest that the LLPS driven by FET proteins could regulate transcription by influencing RNA Pol II recruitment and post-translational modifications.

The formation of liquid-like compartments by FET proteins at DNA damage sites, which are initiated by the seeding effect of PAR, is an interesting phenomenon highlighting the role of LLPS in the cellular stress response. An increasing number of studies reveal the formation of FUS compartments driven by poly(ADP-ribose) both *in vitro* and *in vivo* (*Patel et al., 2015; Altmeyer et al., 2015; Singatulina et al., 2019; Rhine et al., 2022*). The addition of PAR lowers the concentration threshold required for the formation of liquid-like droplets by FUS proteins, thereby promoting their LLPS. (*Patel et al., 2015*). Moreover, as was shown by atomic force microscopy (AFM) experiments, the synthesis of PAR catalyzed by PARP-1 in the presence of NAD⁺ stimulates the formation of FUS compartments at DNA damage sites where damaged DNA is accumulated (*Singatulina et al., 2019*). The assembly of compartments depends on the LC domain of FUS. All three studies investigated FUS mutants, the truncated mutant FUS Δ LC and FUS mutants containing six or twelve mutations of serine or threonine in LC domain to glutamic acid, mimicking its phosphorylation, showed the impaired capacity to form FUS: PAR compartments than the

wild-type protein. In summary, all the above-mentioned data prove the importance of the N-terminal low-complexity domain of FET proteins for their phase separation and the formation of liquid-like compartments.

Recently, RGG domains were also proposed to be involved in the formation of compartments by FET family members. For example, in the previously discussed study of Sungatulina et al., the deletion of two C-terminal RGG repeats in FUS resulted in inhibition of the formation of FUS: PAR compartments, while the deletion of just RGG3 led to impaired ability of FUS to phase separate (*Singatulina et al., 2019*). Mutations of arginine residues to glycine (R>G) in RGG1-RGG3 of FUS resulted in the incapacity of FUS to form condensates alone and very minimal capacity to compartmentalize in the presence of PAR (at the concentration of $>4 \mu\text{M}$ contrary to $>1 \mu\text{M}$ for the wild-type protein) (*Rhine et al., 2022*). Consistently with previous data, the mutations of tyrosine residues to serines (Y>S), described in the same study, also impaired the FUS condensation (*Rhine et al., 2022*). The ability of FUS to undergo LLPS was proposed to be regulated by cation- π interactions between tyrosine residues of the LCD and arginine residues of C-terminal RGG domains and the degree of methylation of arginine in the C-terminus (*Qamar et al., 2018*). Methylation of arginines in RGG domains of FUS can modulate phase separation in a salt-dependent manner, implying the possible electrostatic interactions these positively charged arginines may form with negatively charged residues located in LCD. FUS LCD contains only 5 negatively charged residues, however, it possesses 27 tyrosines capable of forming cation- π interactions with arginines of the C-terminal domain. Mutation of six arginines (showed to be methylated) or seven tyrosines in LCD abrogated the FUS-driven phase separation. Additionally, the authors investigated the phase separation of the LC domain and the arginine-rich CTD alone and mixed together. Both LCD and CTD alone showed minimal phase separation and only at high concentrations ($>50 \mu\text{M}$), while the mixture of two domains led to the formation of condensates at lower concentrations (*Qamar et al., 2018*). In summary, these data support the idea of the importance of both the N-terminal LC domain and C-terminal RGG domains for phase separation and formation of liquid-like compartments.

3.3.2 Stress granules and cytoplasmic inclusions as an intersection between pathological and physiological phase transition: role of FET proteins in the development of ALS and FTLD

FET proteins have received a lot of attention due to their involvement in such neurodegenerative diseases as amyotrophic lateral sclerosis (ALS) and frontotemporal lobar degeneration (FTLD). ALS is a progressive disease that affects the motor neurons in the brain and spinal cord, causing muscle weakness and difficulty in speaking, swallowing, and breathing. It is characterized by the degeneration of both upper and lower motor neurons, leading to muscle atrophy and, eventually, paralysis. FTLD is a disorder that affects the frontal and temporal lobes of the brain, leading to personality changes, language difficulties, and behavioral impairments. All three FET proteins primarily localize to the nucleus, however, they have been found in cytoplasmic aggregates in affected brain regions of ALS and FTLD patients, suggesting a role of the proteins in disease pathogenesis (*Mackenzie et al., 2011; Neumann et al., 2009; Rademakers et al., 2012; Kwiatkowski et al., 2009*). Mutations that cause FET protein mislocalization are typically found in the C-terminal domain of the proteins, with mutations in the PY-NLS region resulting in the most severe ALS cases. In the following chapter (Chapter 3.4.1) of this literature review, we will explore the specific pathological mutations linked to FET proteins in ALS and FTLD. In this chapter, we focus on the connection between the aggregation of FET proteins in the cytoplasm and the development of ALS/FTLD pathologies.

Neurodegenerative disorders are characterized by several hallmarks, including pathological protein aggregation, synaptic and neuronal network dysfunction, aberrant proteostasis, cytoskeletal abnormalities, altered energy homeostasis, DNA and RNA defects, inflammation, and neuronal cell death (*Wilson et al., 2023*). Among these hallmarks, two have garnered particular interest in the context of this research: *pathological protein aggregation* and *DNA and RNA defects*.

Neurodegenerative disorders, such as ALS and FTLD, are often characterized by the presence of *protein aggregates* in cells of specific regions of the brain, which are thought

to play a pathogenic role in disease development (*Mackenzie et al., 2011; Neumann et al., 2009; Rademarkers et al., 2012; Kwiatkowski et al., 2009*). In FTLD patients, for instance, EWSR1 and TAF15 co-accumulate with FUS in cytoplasmic inclusions found in neurons and glial cells (*Mackenzie et al., 2011*). Interestingly, the presence of cytoplasmic inclusions coincides with reduced nuclear staining of all FET proteins (*Mackenzie et al., 2011*). Both the accumulation of FET proteins in cytoplasmic inclusions and their reduced nuclear localization led to a two-hit model of pathology development: the gain-of-function and the loss-of-function model (*Schwartz, 2015*). The gain-of-function model suggests that the toxicity of neurodegenerative diseases such as ALS and FTLD is due to the accumulation of abnormal proteins with toxic properties. In the context of FET proteins, mutations in FUS, EWSR1, and TAF15 genes result in the accumulation of FET proteins in cytoplasmic aggregates, leading to toxicity and neuronal dysfunction. In contrast, the loss-of-function model suggests that the dysfunction of FET proteins in the nucleus, such as their impaired ability to bind to RNA or to regulate gene expression, leads to neurodegeneration.

The lack of FET proteins in the nucleus may lead to *dysregulation of RNA metabolism*, including alterations in the transcription of certain genes and alternative splicing of pre-mRNA. For instance, the pathogenic mutation R521C in FUS, which leads to protein mislocalization, was shown to cause defects in RNA transcripts that encode proteins responsible for dendritic growth regulation and synaptic functions (*Qui et al., 2014*). Dysregulation of RNA metabolism may, in its turn, lead to defects in RNA-driven processes, such as the formation of stress granules (SGs) (*Wolozin et al., 2012; Wolozin et al., 2019*). SGs are membraneless structures that form in the cytoplasm of cells in response to various stressors, such as heat shock, oxidative stress, or viral infection. They are composed of RNA-binding proteins, messenger RNAs (mRNAs), small but not large ribosomal subunits, transcription initiation factors, and various other proteins involved in mRNA metabolism, such as RNA helicases and PABP1 (*Anderson et al., 2006*). Stress granules are thought to act as a protective mechanism that allows cells to temporarily halt translation and store mRNAs until the stress is resolved. SGs form through a complex

interplay of intermolecular RNA-RNA, protein-protein, and RNA-protein interactions (Dobra et al., 2018). There are several types of interactions driving RNA-RNA binding: Watson-Crick and non-Watson-Crick interactions between bases, base stacking of single-stranded regions, and coaxial stacking between helices (Dobra et al., 2018; Van Treeck et al., 2018). Protein-protein interactions are mainly mediated by low-complexity domains and occasionally structured domains. Together with RNA-proteins interactions, they can generate phase separation in SGs via a monolayer protein recruitment mechanism: RNA binding domains of RBPs form interactions with RNA facilitating the interactions between LCDs, like in the case of FUS. Many RBPs containing LCDs are the components of SGs, which underscores the importance of LCD-mediated multivalent weak interactions in their formation (Dobra et al., 2018).

The presence of LCD-containing RBPs in cytoplasmic aggregates in patients with ALS or FTLN and their appearance in cytoplasmic SGs suggest a possible connection between the two types of aggregates. This raises the question of whether SGs can serve as a pathway for the aggregation of proteins implicated in neurodegenerative diseases. Recent evidence suggests that this may indeed be the case (Dobra et al., 2018). First, the pathological mutations of these proteins enhance their association with SGs (Dobra et al., 2018). For example, ALS-associated mutations in FUS have been found to promote the recruitment of the protein to SGs in the cytoplasm. (Bosco et al., 2010). Secondly, SGs were shown to have a biphasic structure with a dense core and more diffused shell. Their assembly occurs via a multistep process: an initial nucleation event that may be influenced by the stress stimulus and growth of the dynamic shell around the core (Dobra et al., 2018; Wheeler et al., 2016). In the case of neurodegenerative diseases, the increase in the local concentration of the mutated proteins harboring LCDs may shift the equilibrium towards the assembly of dense SGs and facilitate the maturation of insoluble aggregates. Thirdly, RNA is involved in the formation of SGs, and the presence of RNA was shown to facilitate the aggregation of several FET proteins (Dobra et al., 2018; Schwartz et al., 2013). Thus, the increased concentration of RNA in SGs may promote their aggregation. Finally, the involvement of SGs in the process of neurodegeneration is supported by the fact that

neurons are particularly susceptible to cellular stress due to their high energy demands and long lifespan, which leads to constant cycles of SG assembly-disassembly. The gelation-dissolution cycles *in vitro* were shown to trigger the formation of insoluble structures from liquid droplets formed by RBPs with IDRs. Similar insoluble structures may form in neurons, further evolving into solid pathological aggregates (*Dobra et al., 2018; Molliex et al., 2015; Patel et al., 2015; Murakami et al., 2015*).

In summary, the role of SGs formation in the development of ALS/FTLD pathology can also be described through the lens of gain-of-function loss-of-function models (*Li et al., 2013*). In accordance with the gain-of-function model, pathological mutations of FET proteins lead to their excessive accumulation in the cytoplasm and SGs during the episodes of stress, which drives the aggregation of these proteins in SGs. The presence of insoluble FET proteins' aggregates inhibits the cleaning mechanism of SGs and their dissolution when stress is resolved, trapping RNPs required for RNA processing and RNAs essential for neuronal viability. The loss-of-function model posits that the nuclear depletion of FET proteins disrupts their diverse nuclear functions, such as regulation of transcription, pre-mRNA splicing, and RNA stability, as well as affects RNA transport and shuttling. Finally, FET proteins have been recently reported to be involved in DNA damage response and DNA repair (Chapter 4). The dysregulation in the maintenance of genome stability, which requires FET proteins, due to their abnormal cytoplasmic localization may lead to the accumulation of *DNA damage* (*Madabhushi et al., 2014*). Notably, mutations in the C-terminal domain of FUS, linked to ALS, impair DNA repair (*Wang et al., 2013*), and motor complex samples from ALS patients show higher levels of DNA damage than normal brain tissues (*Wang et al., 2013*).

Overall, the study of ALS and FTLN is a rapidly evolving field, and new discoveries will likely continue to unveil the underlying mechanisms of these diseases. Such findings may pave the way for the development of more effective treatments for ALS and FTLN, which presently have limited therapeutic options.

3.4 FET proteins mutations and post-translational modifications and their role in the development of amyotrophic lateral sclerosis and frontotemporal lobar degeneration

3.4.1 Mutations of FET proteins

There are two main types of ALS: familial and sporadic.

Familial ALS (fALS) is a rare form of disease that is caused by genetic mutations inherited from one or both parents. Approximately 5-10% of all ALS cases are familial. fALS can be caused by mutations in more than 30 different genes, including SOD1, C9orf72, TARDBP, and FUS. In most cases, the inheritance pattern of fALS is autosomal dominant, which means that a child has a 50% chance of inheriting the mutated gene from an affected parent. fALS usually has an earlier age of onset and a slower progression rate compared to sporadic ALS (*Deng et al., 2014*).

Sporadic ALS (sALS) is the most common form of the disease, accounting for approximately 90-95% of all ALS cases. sALS occurs without any known genetic cause, and the underlying mechanisms that lead to the disease are not fully understood. Risk factors for sALS include age, gender, smoking, environmental toxins, and occupational exposure to certain chemicals. sALS usually has a later age of onset and a faster progression rate compared to fALS (*Deng et al., 2014*).

Mutations in the FUS gene are present in approximately 5% of familial ALS cases and 1% of sporadic ALS cases (*Deng et al., 2014*).

The hypothesis for the development of ALS suggests that mutations in the FUS gene disrupt its nuclear localization, causing an accumulation of the protein in the cytoplasm and the formation of persistent stress granules under stress conditions. The aberrant phase separation of FUS within these stress granules can ultimately lead to the formation of insoluble aggregates. Consistent with this hypothesis, the majority of FUS mutations identified in ALS patients cluster in two regions: the C-terminal RGG2-ZnF-RGG3-NLS domains (with NLS domain mutations resulting in the most severe ALS cases) and the N-

terminal prion-like domain (QGSY-rich region and RGG1 domain) (Figure 15) (*Deng et al., 2014*). Thus, these mutations can either disrupt the cellular localization of the protein by affecting the NLS domain or interfere with the low-complexity domains required for proper phase separation.

In 2009, the first 13 FUS mutations were identified in patients with familial ALS, all of which were localized in the C-terminus of the protein and specifically in the PY-NLS region. These mutations led to cytoplasmic retention and aggregation of FUS (*Kwiatkowski et al., 2009; Vance et al., 2009*). Later research further supported the link between mutations in the PY-NLS region and ALS development. The C-terminal PY-NLS of FUS is a non-classical PY-NLS that interacts with the nuclear import receptor Karyopherin $\beta 2$ (Kap $\beta 2$), which mediates the translocation of PY-NLS proteins across the nuclear pore complex (Chapter 3.1). The residues in the very C-terminus of FUS, such as R522, P525, and Y526, as well as residues in the C-terminal part of FUS NLS, R514, and R518, are required for this interaction and for subsequent FUS nuclear import. Accordingly, mutations in these key amino acids, as well as truncation mutations of the PY-NLS (e.g., due to the R495X mutation), cause severe impairment of nuclear import and lead to the most aggressive forms of ALS. In summary, mutations in the PY-NLS of FUS associated with ALS disrupt Kap $\beta 2$ -mediated nuclear import, leading to an increase in cytoplasmic FUS concentration and playing a role in the development of ALS pathogenesis. (*Bosco et al., 2010; Dormann et al., 2010; Dormann et al., 2011; Ito et al., 2011; Kino et al., 2011; Niu et al., 2012; Zhang et al., 2012*).

The mutations in the N-terminal region of FUS associated with ALS do not appear to impact nuclear transport, suggesting an alternative mechanism for their pathogenicity. However, given the crucial role of this region in FUS function in transcription and LLPS, it is plausible that mutations in this area could affect FUS-mediated transcription and/or its aggregation properties (*Deng et al., 2014*). Indeed, research has shown that the pathogenic mutation G156E in the QGSY-rich region of FUS substantially increases its aggregation propensity both *in vitro* and *in vivo* (*Nomura et al., 2014*). In the same study, the effects of three additional mutations (G225V, M254V, and P525L) on FUS's

aggregation properties were investigated. Unlike the G156E mutation, two mutations located in the RGG1 domain (G225V and M254V) had no effect on FUS solubility (Figure 15). The mutation P525L, examined in the same study, also did not alter FUS's tendency to aggregate. These findings suggest that mutations in the N-terminal low-complexity domain of FUS can lead to an increased propensity for protein aggregation, providing an alternative pathomechanism for ALS disease (Nomura et al., 2014).

Although initially identified in ALS patients, some mutations in the FUS gene have also been found in patients with FTLD. Our understanding of FUS mutations in FTLD remains limited, with only four mutations identified to date. Among these mutations, M254V and P106L have been found in patients with both FTLD and ALS. Moreover, the mutation of the R521 residue in the NLS of FUS has also been implicated in the development of FTLD pathology (Broustal et al., 2010; Van Langenhove et al., 2010; Huey et al., 2011).

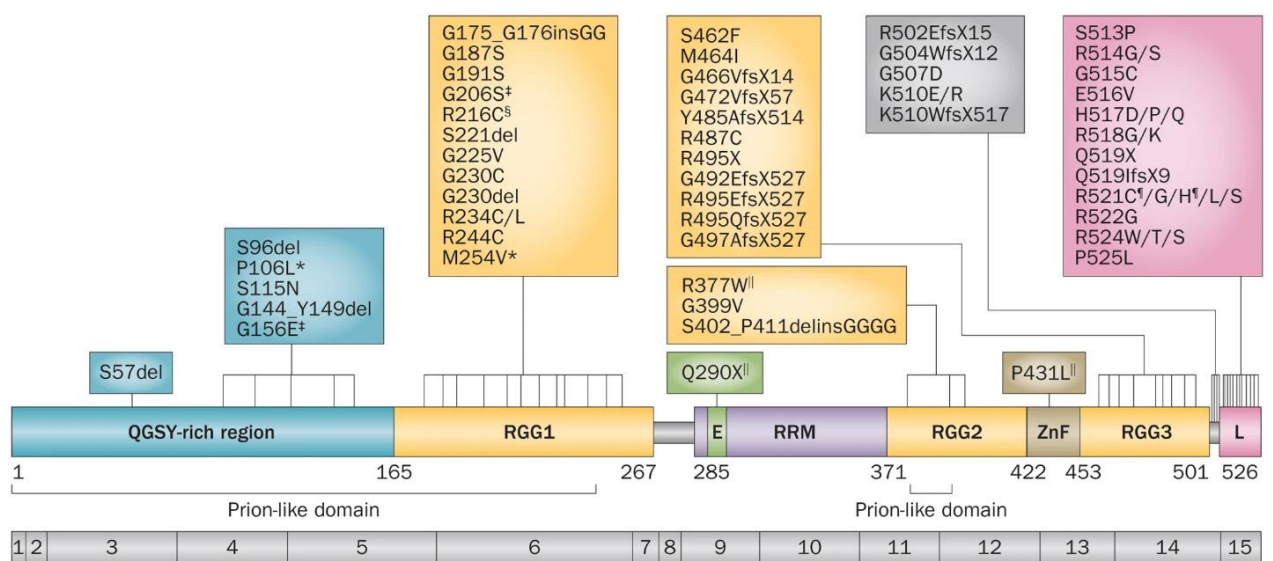


Figure 15: Schematic representation of the FUS transcript, and functional domains of the FUS protein with gene mutations identified in patients with neurodegenerative diseases. * The pathogenicity of many mutations identified in patients with FTLD still needs to be validated. ‡ Mutations identified in patients with ALS and FTLD, or in their families. § Mutations identified in patients with ALS, and in those with essential tremor. || Mutations identified in patients with essential tremor. ¶ Mutations identified in patients with ALS, and in those with both ALS and FTLD (from Deng et al., 2014).

Recent findings have revealed the potential role of EWSR1 and TAF15, members of the FET protein family like FUS, in the pathogenesis of ALS and FTLD. In cases of FUS-positive pathology (FTLD-FUS), EWSR1, and TAF15 are shown to co-accumulate in FUS-positive

cytoplasmic inclusions, which results in decreased nuclear staining for all three FET proteins (Neumann *et al.*, 2011). Conversely, in ALS-FUS, TAF15 and EWSR1 remain restricted to the nucleus and do not co-deposit with FUS-positive inclusions (Neumann *et al.*, 2011; Mackenzie *et al.*, 2012). It was demonstrated that FUS, EWSR1, and TAF15 can form homomultimeric and heteromultimeric complexes through interactions between their N-terminal domains (Tomsen *et al.*, 2013). The ability of FET proteins to form such complexes may explain why EWSR1 and TAF15 are present in FUS-containing condensates. Furthermore, a functional screen was conducted to identify proteins similar to FUS and TDP-43, which may contribute to the development of ALS/FTLD. The results identified EWSR1 and TAF15 as potential candidates. Although there is limited knowledge about the mutations in TAF15 and EWSR1 that are associated with ALS, some of these mutations have been observed in ALS patients, suggesting a potential contribution of these proteins to neurodegeneration (Couthouis *et al.*, 2011; Couthouis *et al.*, 2012; Ticozzi *et al.*, 2011).

3.4.2 Post-translational modifications of FET proteins

Post-translational modifications (PTMs) play an important role in regulating the function, stability, and localization of RBPs, including FET family members. PTMs in RBPs mostly occur in intrinsically disordered regions (IDRs) due to their accessibility. Given that IDRs are involved in liquid-liquid phase separation and the formation of membraneless compartments (Chapter 3.3.1.3), PTMs can also affect these processes. The altered phase separation of FET proteins due to specific PTMs may play a critical role in the formation of pathological RBP inclusions in diseases such as ALS and FTLD. It's important to note that disease-linked PTMs may also arise as compensatory mechanisms or "brakes" to counteract or slow down certain pathological processes. Currently, several PTMs have been described for FET proteins, including phosphorylation, methylation, acetylation, ubiquitination, and poly(ADP-ribosyl)ation (Figure 16) (Sternburg *et al.*, 2022).

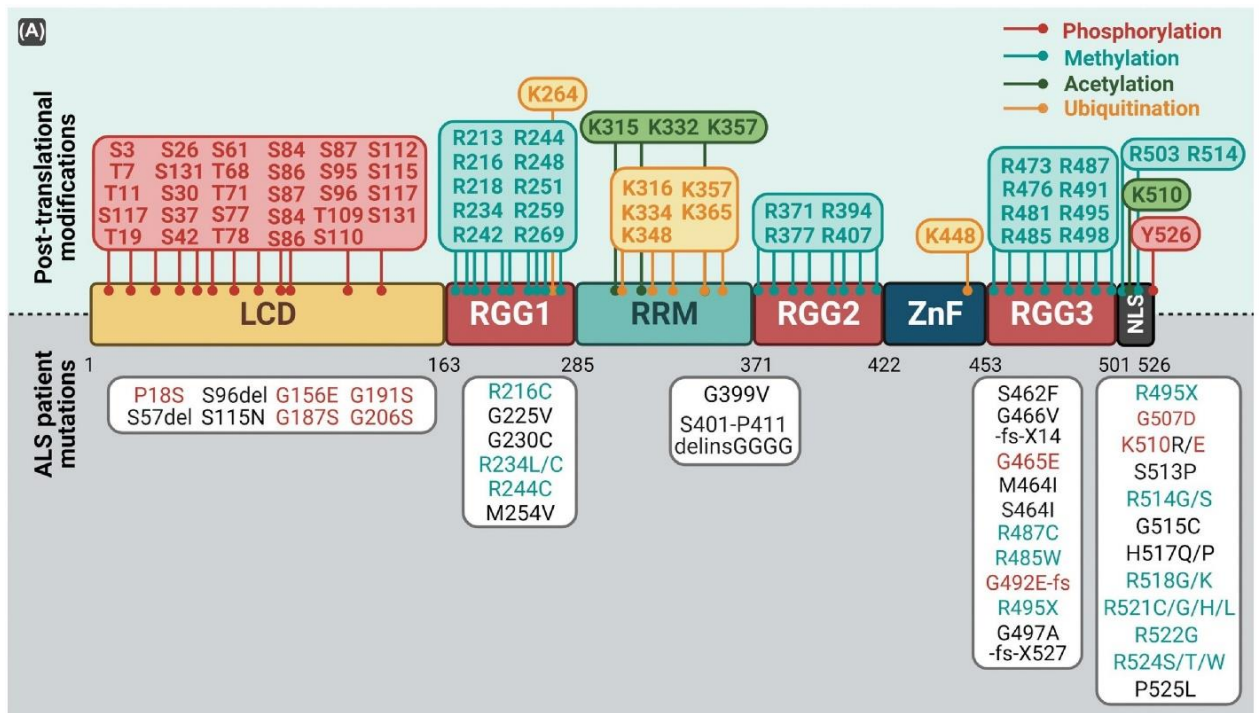


Figure 16: Post-translational modifications (PTMs) of FUS and disease-associated mutations that alter PTM sites. Above: FUS residues that undergo post-translational modifications: phosphorylations (red), methylation (blue), acetylation (green) and ubiquitination (yellow). Below: mutations found in ALS cases (with modifications from Sternburg et al., 2022).

Phosphorylation

Phosphorylation is a post-translational modification (PTM) that has been found to play an important role in regulating the localization and aggregation propensity of FET proteins. In 2008, the first FUS residue S42 was identified as the phosphorylation site both *in vitro* and *in vivo*. It was demonstrated that the phosphorylation of S42 occurs in response to DNA double-strand breaks and requires two kinases, ATM (ataxia-telangiectasia mutated) and DNA-PK (DNA-dependent protein kinase) (Gardiner et al., 2008). Further studies confirmed these data, as well as identified other phosphorylation sites in the FUS N-terminal domain (Deng et al., 2014; Han et al., 2012; Monahan et al., 2017; Murray et al., 2017; Rhoads et al., 2018). FUS has 12 S/T-Q sites on the N-terminal domain, which are specifically recognized by DNA-PK or ATM resulting in serine or threonine phosphorylation *in vitro*. Only three of these consensus sites (S26, S30, and S42) have been confirmed to be phosphorylated in cells (Rhoads et al., 2018). It is possible, however, that other predicted sites may be also phosphorylated. Interestingly, the phosphorylation of the LC domain of FUS was reported to reduce the protein LLPS and aggregation *in vitro*

(Han et al., 2012; Murray et al., 2017). Moreover, the use of phosphomimetic mutants of FUS was also shown to disrupt LCD self-interaction and LLPS (Monahan et al., 2017; Singatulina et al., 2019). These data suggest that the phosphorylation of the FUS LC domain in response to cellular stress works as a “switch-off” for phase separation. Unlike some low-complexity domains, the N-terminal domain of FUS is not charged containing only two charged amino acids among 163 residues. As the mechanism behind FUS LCD-driven LLPS is not based on electrostatic interactions, the introduction of multiple negative charges due to phosphorylation may disrupt protein-protein interactions through electrostatic repulsion (Rhoads et al., 2018). Besides its role in regulating the ability of FUS to undergo LLPS, phosphorylation of the LCD domain was suggested to mediate FUS translocation to the cytoplasm under cellular stress. (Deng et al., 2014). However, a recent study challenges this idea, as new data shows that phosphorylation of the LCD by DNA-PK alone is not enough to cause FUS translocation to the cytoplasm (Rhoads et al., 2018).

Although the majority of FUS phosphorylation takes place in its N-terminal LC domain (Figure 16), studies have demonstrated that several residues in the C-terminal PY-NLS of FUS are also phosphorylated (Kino et al., 2011; Darovic et al., 2015). As previously mentioned, the integrity of FUS NLS plays a critical role in the protein's appropriate cellular localization, and mutations in this domain have been linked to ALS and can result in FUS cytoplasmic accumulation (Chapter 3.4.1). Consistent with these findings, it has been demonstrated that phosphorylation of the C-terminal Y526 residue disrupts the interaction between FUS and Kap β 2, thereby inhibiting the transport of FUS into the nucleus (Darovic et al., 2015). This post-translational modification could serve as an additional mechanism for regulating FUS localization. Like FUS, phosphorylation of the C-terminal tyrosine of EWSR1 Y656 has been demonstrated to obstruct its binding to Kap β 2 and disrupt its nuclear import (Leeman-Zakaryan et al., 2011).

Methylation

Methylation is a widespread post-translational modification of proteins that involves the addition of a methyl group to certain amino acid residues in the protein. The two most commonly modified residues are lysine and arginine. Arginine methylation is catalyzed by N-arginine methyltransferases (PRMTs) and involves the transfer of a methyl group from S-adenosyl-L-methionine (SAM) onto one or both of the guanidinium nitrogens of the arginine side chain, resulting in monomethylated or dimethylated (symmetric or asymmetric) arginine residues. Certain proteins are more likely to be methylated due to the presence of specific domains. For instance, the presence of three arginine-rich domains (RGG domains) in FET proteins makes them highly probable targets for methylation. Indeed, FUS protein was shown to be asymmetrically dimethylated in all three RGG domains (Figure 16). This methylation has a crucial role in regulating the nuclear import of FUS protein, affecting its propensity to form aggregates and its involvement in the development of neurodegenerative diseases (*Sternburg et al., 2022*).

Nuclear import of FET proteins occurs through the interaction of PY-NLS with the nuclear import receptor Kap β 2 (Chapter 3.1). Interestingly, this process is regulated by arginine methylation of RGG3, located adjacent to the C-terminal nuclear localization signal. Studies have shown that hypomethylated RGG3 facilitates interaction with Kap β 2, while methylation of RGG3 reduces binding to Kap β 2 (*Dormann et al., 2012; Suárez-Calvet et al., 2016; Hofweber et al., 2018*). This regulatory mechanism is significant in understanding the pathology of FTLD. Normally, FUS protein is methylated in all three RGG domains, which is also observed in FUS protein of ALS patients. However, in FTLD-FUS patients, pathological inclusions in the cortex contain monomethylated and unmethylated forms of FUS, as well as other two FET proteins (EWSR1 and TAF15) and Kap β 2. These findings suggest that different mechanisms of FUS-Kap β 2 interaction exist in ALS and FTLD cases. In FTLD-FUS, hypomethylation of FET proteins leads to increased binding to Kap β 2, resulting in their joint accumulation in cytoplasmic aggregates. In contrast, the cytoplasmic inclusions of ALS-FUS patients contain only methylated FUS, indicating a more complex mechanism of pathology development (*Dormann et al., 2012*).

Moreover, studies have demonstrated that arginine methylation plays a significant role in the LLPS of FUS protein. Unmethylated FUS has been shown to have an increased propensity to undergo LLPS and aggregation *in vitro*, on the other hand FUS RGG methylation reduces its nuclear aggregation in cells (Qamar *et al.*, 2018; Hofweber *et al.*, 2018). Additionally, FUS arginine methylation was shown to reduce association of FUS with stress granules (Hofweber *et al.*, 2018). In summary, these findings suggest that this PTM may be a contributing factor to the aberrant LLPS and FUS aggregation observed in FTLD patients with reduced FUS methylation.

Acetylation

Acetylation is a PTM of proteins that involves the addition of an acetyl group (-COCH₃) to either the N-terminal amino group of the protein or the ϵ -amino group of lysine residues. N-terminal acetylation is the most common form of protein acetylation, and it occurs when the acetyl group is added to the N-terminal amino group of the protein. This modification is catalyzed by a family of enzymes called N-terminal acetyltransferases (NATs), which transfer the acetyl group from acetyl-CoA to the amino group of the protein's N-terminus. An example of the effect of N-terminal acetylation on protein function can be seen with the protein FUS. When co-expressed with the NatA complex in *Escherichia coli*, FUS was shown to be N-terminally acetylated. This post-translational modification has been found to slightly enhance the propensity of FUS to undergo LLPS (Bock *et al.*, 2021).

Lysine acetylation is another form of protein acetylation that involves the addition of an acetyl group to the ϵ -amino group of lysine residues. Enzymes known as lysine acetyltransferases (KATs) catalyze this modification, and it can be reversed by lysine deacetylases (KDACs). In the case of the protein FUS, lysine acetylation has been observed within its RRM domain and PY-NLS (Figure 16), catalyzed by CREB-binding protein/p300. Lysine acetylation within FUS RRM is performed on K315/K316 residues (Figure 16), which according to our NMR spectroscopy data are involved in the interaction of FUS RRM with RNA (Chapter 4 of the Results). Consistent with our findings, acetylation of these two residues was shown to impact FUS-RNA interaction by reducing binding of the protein to

RNA (Arenas *et al.*, 2020). Acetylation of K510 residue, located in PY-NLS, disrupts the interaction of FUS PY-NLS with Kap β 2, leading to mislocalization of FUS in the cytoplasm and the formation of cytoplasmic aggregates (Chapter 3.1). Deacetylation of FUS was shown to be performed by both sirtuins and histone deacetylases families of lysine deacetylases (Arenas *et al.*, 2020). These data suggest that dysregulation of acetylation-deacetylation process may be implicated in the pathology development in ALS and FTLD cases.

Ubiquitination

Ubiquitination is a post-translational modification process that tags proteins with ubiquitin, targeting them for degradation by the proteasome. Although FUS has been found to co-localize with UBQLN2 (ubiquitin-like protein ubiquilin 2), TDP43, and other RBPs in the cytoplasmic inclusions of ALS and FTLD patients, it is unclear whether FUS itself is ubiquitinated in this context, despite the high levels of ubiquitin found in these inclusions (Neumann *et al.*, 2009; Deng *et al.*, 2011; Williams *et al.*, 2012). Two independent mass-spectrometry proteomic analyses of post-translational modifications have demonstrated that FUS can be ubiquitinated in RRM and ZnF domains (Figure 16) (Mertins *et al.*, 2013; Akimov *et al.*, 2018). The ubiquitination of C-terminal domain of FUS is also predicted by another mass-spectrometry study (Radivojac *et al.*, 2010). However, there is limited information about FET protein ubiquitination, and the mass-spectrometry predictions of FUS ubiquitination have not been confirmed *in vivo*.

Poly(ADP-ribosyl)ation

Poly(ADP-ribosyl)ation, also known as PARylation, is a post-translational modification of proteins that is catalyzed by members of the PARP family (Chapter 2.1).

Recent large-scale analyses of PARylated proteins have demonstrated that FET proteins are extensively PARylated in response to various genotoxic stress agents, such as hydrogen peroxide, methyl methane sulfonate, UV radiation, and ionizing radiation (Gagné *et al.*, 2012; Jungmichel *et al.*, 2013; Zhang *et al.*, 2013; Martello *et al.*, 2016). Furthermore, FET proteins are among the most heavily PARylated RNA-binding proteins,

indicating an important role for PARylation in regulating their function. Previously, FUS was demonstrated to be PARylated *in vitro*, which has been further confirmed in the current study (Singatulina et al., 2019). Based on *in vitro* data, FUS appears to be heavily PARylated even when its N-terminal LC domain is deleted. Additionally, the truncated protein, which includes only the C-terminal part (RRM-RGG2-ZnF-RGG3-NLS), is also subject to PARylation (Singatulina et al., 2019; Singatulina, not published data). These findings, combined with the observation that most of the potentially PARylated residues (glutamate and aspartate) are located in the C-terminal region, suggest that PARylation of FUS likely occurs in its RGG, RRM, or ZnF domains. Such PTM as PARylation could potentially serve as an additional regulatory mechanism affecting protein functions. Our present study delves into the investigation of PARylation's role on two specific residues located in the RRM domain of FUS.

4. The role of FUS proteins in DNA damage response

FUS is a multifunctional RNA binding protein that is involved in a variety of cellular processes, including DNA repair.

One of the first results, supporting the role of FUS in DNA damage response and maintenance of genome stability were obtained in 2000, when two independent research groups obtained FUS-deficient mice. FUS deficiency led to male sterility in mice, mild defects in somatic growth, increased sensitivity to ionizing irradiation and perturbations in meiotic processes (*Kuroda et al., 2000*). Another study demonstrated that FUS is essential for the viability of neonatal animals and influences lymphocyte development in a non-cell-intrinsic manner. FUS also plays an intrinsic role in the proliferative responses of B cells to specific mitogenic stimuli and is required for maintaining genomic stability (*Hicks et al., 2000*).

FUS was reported to play a role in DNA double-strand break repair by mediating an essential step in homologous recombination, DNA annealing and D-loop formation (*Baechtold et al., 1999; Bertrand et al., 1999*). FUS depletion was shown to lead to a dampening of DNA damage response reflected by decreased phosphorylation of H2AX and increased amount of DNA damage (*Wang et al., 2013*). FUS interacts with a chromatin-modifying enzyme HDAC1 and regulates DDR signaling and DNA repair of DSB. In particular, FUS has been shown to promote homologous DNA pairing, a key step in homologous recombination (*Wang et al., 2013*).

Several studies demonstrated that FUS, as well as two other FET proteins, is recruited to DNA damage sites after laser microirradiation (*Altmeyer et al., 2015; Mastrocola et al., 2013; Rulten et al., 2014*). Interestingly, this recruitment is dependent on PARP-1 activity and PAR synthesis, as the cell pretreatment with PARP inhibitor completely blocked FUS accumulation in response to DNA damage (*Mastrocola et al., 2013; Rulten et al., 2014*). In addition, the ALS associated mutation R521G in FUS PY-NLS was shown to disrupt the recruitment of FUS to DNA damage sites (*Rulten et al., 2014*). The binding of FUS to PAR is mediated mostly by RGG domains with RGG2 playing a particular role in FUS-PAR interaction (*Altmeyer et al., 2015; Mastrocola et al., 2013*). The structural similarity between

RNA and PAR suggest a possible role of other RNA-binding domains, such as RRM, in the interaction with PAR, however this topic has not been investigated yet. FUS binds directly to PAR, as it was shown in slot blot experiments *in vitro* (Rulten *et al.*, 2014). In relation to FUS ability to bind to PAR, it should be noted that FUS was identified in several independent large scale mass spectrometry analyses as PAR reader and highly PARylated protein (Kliza *et al.*, 2021; Jungmichel *et al.*, 2013; Martello *et al.*, 2016; Zhang *et al.*, 2013; Gagne *et al.*, 2012).

Recently, FUS was demonstrated to form liquid-like compartments through interactions occurring between its low-complexity domains (Altmeyer *et al.*, 2015; Patel *et al.*, 2015; Schwartz *et al.*, 2013; Rhine *et al.*, 2022; Sukhanova *et al.*, 2022). As it was described in detail in the Chapter 3.3.1, FUS can undergo LLPS in the presence of RNA and PAR. FUS was recently shown to form dynamic and PARG-reversible compartments at DNA damage sites (Singatulina *et al.*, 2019). It was suggested that the formation of such compartments may help to concentrate DNA repair factors in the proximity to DNA damage sites, thus facilitating DNA repair. After DNA repair process is done the hydrolysis of PAR by PARG result is the dissociation of FUS-rich compartments (Singatulina *et al.*, 2019).

FUS was shown to be phosphorylated by ATM and DNA-PK at its N-terminal low-complexity domain (Gardiner *et al.*, 2008; Deng *et al.*, 2014; Monahan *et al.*, 2017; Rhoads *et al.*, 2018). Both kinases are activated in response to DNA double-strand breaks. The FUS phosphorylation following DNA damage was reported to reduce the protein LLPS and aggregation *in vitro* (Han *et al.*, 2012; Murray *et al.*, 2017). In addition, phosphomimetic FUS mutants showed decreased propensity to undergo LLPS (Monahan *et al.*, 2017; Singatulina *et al.*, 2019; Sukhanova *et al.*, 2022). This data suggests that this PTM in response to cellular stress may modulate FUS ability to form higher-order assemblies.

Finally, FUS is known to play a role in regulating the DDR via transcriptional mechanisms (Chapter 3.2.1). In a study by Wang *et al.*, it was demonstrated that FUS is recruited to the promoter of cyclin D1 (CCND1) through interactions with both sense and antisense noncoding CCND1 RNAs. By inhibiting CREB-binding protein, FUS is able to suppress CCND1 expression in response to DNA damage (Wang *et al.*, 2008).

In conclusion, FUS is a multifunctional RNA binding protein that plays a critical role in DNA damage response and maintenance of genome stability. FUS is involved in various aspects of the DDR, including DNA repair and transcriptional regulation of DDR genes. FUS interacts with chromatin-modifying enzymes and forms dynamic compartments at DNA damage sites, which may facilitate the recruitment and concentration of DNA repair factors. PTMs of FUS, such as phosphorylation, can modulate its ability to undergo phase separation and regulate its functions in the DDR. Further studies are needed to fully understand the molecular mechanisms underlying the diverse functions of FUS in the DDR and its potential implications in human diseases, including cancer and neurodegenerative disorders.

OBJECTIVES OF WORK

Recent studies have highlighted the crucial role of multivalent interactions between low complexity domains of RNA-binding proteins, such as FUS, in the formation of membraneless compartments (*Rhine et al., 2022; Teloni et al., 2015; Patel et al., 2015; Schwartz et al., 2013*). Previous research conducted by A. Singatulina, a PhD student in the laboratories of David Pastré and Olga Lavrik, revealed that FUS, in the presence of PAR, can generate dynamic compartments at DNA damage sites (*Singatulina et al., 2019*). We speculate that these compartments may aid in concentrating DNA repair factors at the sites of DNA damage. Although the regulation of DNA break repair was formerly attributed to PARP-1 and synthesized PAR (Literature review, Chapter 2.3), the findings suggest that the presence of RNA-binding proteins could be necessary to boost the capacity of PAR to recruit DNA repair factors and displace nucleosomes, thus promoting DNA repair. *In vitro* assays have consistently shown that PAR promotes liquid-liquid phase separation of FUS (Literature review, Chapter 3.3.1.2). Therefore, we were intrigued to investigate which RNA-binding proteins could colocalize and form compartments with PARP-1. Is FUS a primary partner of PARP-1 among RNA-binding proteins? And does the interaction between PARP-1 and FUS depends on PARP-1 activity and PAR synthesis? In addition, the DNA repair factors that can be recruited to FUS-rich membraneless compartments are mostly unknown. Therefore, an additional question we aimed to answer in this study is which DNA repair factors can be recruited to FUS-rich membraneless compartments? (Chapter1)

Despite multiple recent works describing FUS recruitment to the sites of DNA damage in a PARP-1 activity dependent manner, the biological functions of FUS in DNA repair mechanisms related to PARP-1 activation were still unclear (*Rulten et al., 2014; Izhar et al., 2015*). Given that FUS is not only a PAR reader but also one of the effective acceptors of PAR in cells, we asked whether FUS may regulate PARP-1 activity and PAR levels in cells as a PAR acceptor protein. To investigate this, we examined how changes in FUS and other RNA-binding proteins (HuR, TDP-43) expression levels affect PARP-1 activity and PAR synthesis under genotoxic stress. Specifically, we silenced or overexpressed FUS in HeLa

cells exposed to mild concentrations of hydrogen peroxide, a known oxidative stress agent that generates rapidly repairable DNA breaks and strongly activates PARP-1. (Chapters 2 and 3)

FUS is known to play a role in transcription by interacting with the C-terminal domain of RNA Pol II and binding to nascent mRNA. This suggests that FUS activity may be regulated by transcription status (*Schwartz et al., 2012; Burke et al., 2015*). Moreover, since DNA damage frequently occurs in open, transcriptionally-active chromatin, FUS is found in close proximity to DNA damage sites and can quickly relocate to them (*Pankotai et al., 2013; Dinant et al., 2008; Van Attikum & Gasser, 2009*). Given this, we were interested in whether inhibiting transcription might cause FUS to dissociate from mRNA and instead bind to PAR under genotoxic stress, potentially intensifying its role in DNA repair. To investigate this question, we treated HeLa cells with different transcription inhibitors (ActD, DRB, and oxaliplatin) prior to exposing them to hydrogen peroxide (Chapter 2). Both mRNA and PAR can act as binding platforms for FUS. Previous study has shown that nuclear RNA is a major factor to limit the aberrant formation of liquid phases of FUS in the nucleus. In this regard, we wondered how the simultaneous inhibition of transcription by ActD treatment and PARylation by olaparib treatment influence FUS nuclear distribution. (Chapter 1)

A number of RNA-binding proteins have been identified in large scale mass spectrometry analyses as PAR readers harboring PAR-binding domains, such as RRM domain, RGG repeats, SR-rich and KR-rich domains (Literature review, Table 1) (*Jungmichel et al., 2013; Martello et al., 2016; Zhang et al., 2013; Gagne et al., 2012; Teloni et al., 2015*). It was demonstrated that the interaction between FUS and PAR is mainly orchestrated by the unstructured RGG domains of FUS (*Rhine et al., 2022; Altmeyer et al., 2015*). It is not however clear why FUS appears as a protein particularly prone to bind to PAR and to be PARylated, while several other RNA-binding proteins bear RGG domains or SR-rich or KR-rich repeats that may also form electrostatic interactions with PAR. We suggest that the structured RRM domain of FUS may be the key to this puzzle. The RRM domain of FET proteins has distinct features that distinguish it from RRM domains of other RBPs (Literature review, Chapter 3). Therefore, in this work, we aimed to investigate the

structural basis of the recognition of PAR by FUS RRM and compare it with its binding to RNA using NMR spectroscopy analysis. To further investigated whether the RRM domain of FUS plays a role in the regulation of PARP-1 activity and affects PAR level in cells we expressed chimeric form of FUS in which RRM domain of FUS was replaced by the RRM1 of TDP-43. (Chapter 4 and 5)

Moreover, in order to delve deeper into the influence of FUS RRM on the control of PARP-1 activity, we made point mutations of the amino acid residues within the RRM domain (K315A/K316A, N284A, D342A, and D343A). Our objective was to examine the effect of certain residues situated in FUS RRM on its binding to PAR and the ensuing regulation of PARP-1 activity. During *in vivo* experiments, we found that the mutation in amino acid residue D343 has significant functional implications. (Chapter 6)

To sum up, the objective of this research is to investigate the interaction of FUS with PAR after DNA damage-induced PARP-1 activation and the regulation of PARP-1 activity by FUS. This study will therefore address the following questions:

- 1) Which RNA-binding proteins could colocalize and form compartments with PARP-1? Does the interaction between PARP-1 and FUS depends on PARP-1 activity and PAR synthesis? Which DNA repair factors can interact and form compartments with FUS?
- 2) Can FUS as a PAR acceptor protein regulate PARP-1 activity and levels of PAR in cells? How does the inhibition of transcription affect the influence of FUS on PARP-1-mediated PAR synthesis? How do the simultaneous inhibition of transcription and PAR synthesis influence FUS nuclear distribution?
- 3) What is the role of the RRM domain of FUS in PAR binding and regulation of PARP-1 activity? What is the role of certain residues within FUS RRM on its binding to PAR and the regulation of PARP-1 activity?

RESULTS

Chapter 1: FUS interacts with poly(ADP-ribosyl)ated PARP-1 under oxidative stress conditions that prevents aberrant FUS self-assemblies after transcription inhibition

During genotoxic stress, PARylation can take place on many residues such charged residues, Glu, Asp, Lys or Ser residues whose PARylation is promoted in the presence of histone PARylation factor 1 (HPF1) (*Jungmichel et al., 2013; Zhang et al., 2013; Bonfiglio et al., 2017*). FUS has been identified as being PARylated following oxidative stress in numerous large-scale studies obtained by mass spectroscopy in mammalian cells (*Martello et al., 2016; Zhang et al., 2013*). We consider two unbiased studies using hydrogen peroxide to generate DNA damages in human cells that activate PARP-1 and are rapidly repaired in contrast with dimethyl sulfate, an alkylating agent, also used to activate PARP-1 in cells (*Ström et al., 2011*). Among the 1,542 proteins previously identified as partners of RNA in human cells, only 17 of them were detected to be PARylated in the two large scale studies considered here (Figure 1) (*Gerstberger et al., Martello et al., 2016; Zhang et al., 2013*).

Out of these 17 proteins, there are two FET proteins, TAF15 and FUS. Since many PARylated proteins are themselves PAR readers, it is not surprising that a large majority of the 17 PARylated RNA-binding proteins are considered as PAR readers (13 out of 17), including TAF15 and FUS. In addition to their presence in this short list of RNA-binding proteins interacting with PARP-1, FUS is one of the first proteins to be recruited via PARP-1 activation at DNA damage sites under laser micro-irradiation of cells (*Levone et al., 2021; Rulten et al., 2014; Altmeyer et al., 2015*).

In view of all these convergent data, we decided to further investigate this special link between FUS and PARP-1. First, we explored the probability of formation of compartments in which PARP-1 and FUS would be mixed. For this, we used the microtubule bench assay, that was recently developed in the laboratory of David Pastré (*Maucuer et al., 2018; Renfigo-Gonzalez et al., 2021*). Briefly, two different RFP- or GFP-labelled proteins are brought onto microtubules thanks to a fusion with a microtubule-

binding domain (MBP). Their mixing/demixing score is then measured by automatically recording the relative fluorescence of the two proteins along the microtubules with an automatic HCS imager operating in confocal mode at high resolution to obtain robust data (Figure 2A, see Materials and Methods for details). When RNA-binding proteins are confined along microtubules, they can form compartments through their self-adhesive low-complexity domains but also through mRNAs which can be used as scaffolds for higher order assemblies of RBPs (*Maucuer et al., 2018*).

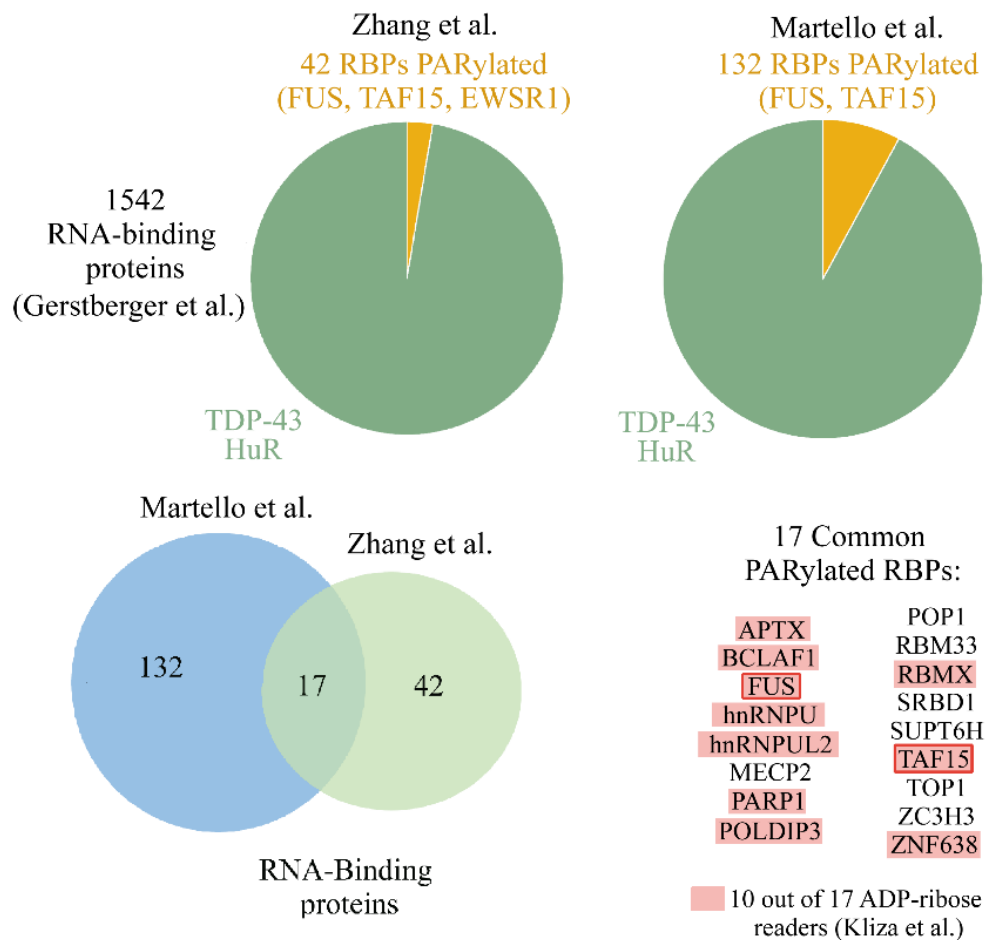


Figure 1: FET proteins have been identified to be PARylated in two large scale analyses. Analysis of protein PARylation among the 1542 known RNA-binding proteins after cell exposure to hydrogen peroxide from two independent large-scale analyses. Upper panel: Fraction of RBPs PARylated. Lower panel: Overlap between the RBPs identified as PARylated from the two indicated independent studies. List of PARylated RBPs in common and among them those that have been identified as PAR readers.

Our results obtained by confining PARP-1 and different RNA-binding proteins (FUS, TAF15, EWSR1, SAM68, TDP-43, HuR, G3BP1) on microtubules show that PARP-1 mixes much better with FUS than with TDP-43 and HuR, two other RNA-binding proteins which are not listed as particularly PARylated proteins (Figure 2B, Supplementary Figures S1 and S2). In fact, all the three FET proteins mix pretty well with PARP-1 compared to non-FET

RBPs, most probably because PARP-1 is activated on microtubules. It has already been shown that PARP-1 can be activated by nuclear snoRNA *in vivo* and RNA oligonucleotides *in vitro* (Kim *et al.*, 2019; Alemasova *et al.*, 2016). We then devised that it may also be the case with cytoplasmic RNA. In agreement with this hypothesis, we detected the presence of PAR on microtubules when PARP-1 is brought onto microtubules but not in control cells (Figure 3).

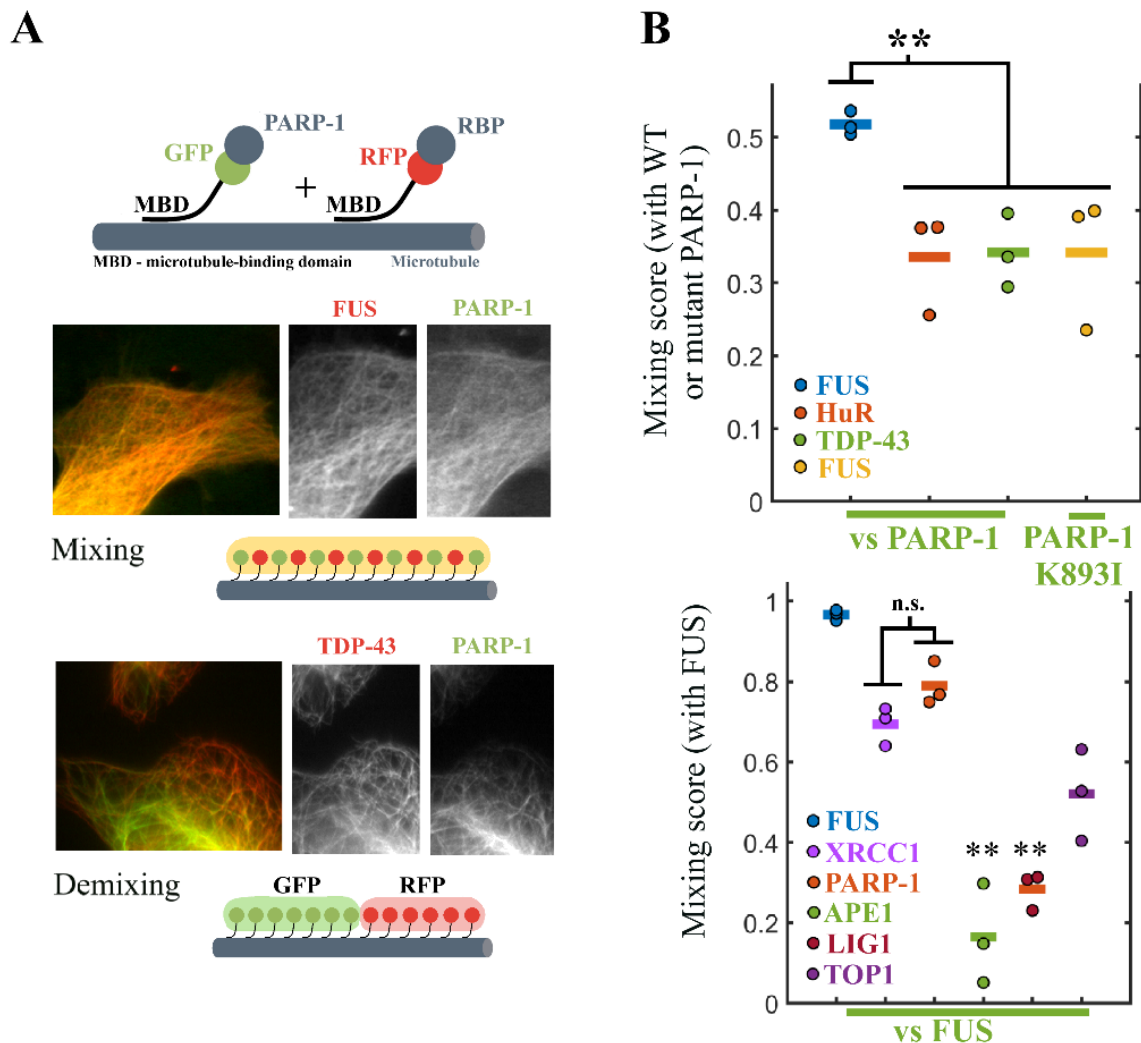


Figure 2: FUS mixes well along microtubules with PARP-1, as well as XRCC1. A. Principle of the microtubule bench assay used to measure the mixing/demixing score of two different proteins brought onto microtubules in HeLa cells. The two proteins under scrutiny were RFP- and GFP-labeled to automatically measure their mixing along microtubules in HeLa cells. Their respective fluorescence shows a mixing of PARP-1 with FUS, but not with TDP-43. MBD: Microtubule Binding Domain. B. Mixing scores were measured for different pairs of proteins with a HCS imager and automated pipeline. Upper panel: Mixing score of different RBPs versus wild-type PARP-1 or PARP-1 K893I, a PARylation-defective mutant. Lower panel: Mixing score of FUS versus different DNA repair factors. Each condition is presented in triplicate. **p < 0.01, paired t-test; n.s., non-significant. Each dot is the result of single cell analysis in a single well (see Materials and Methods and Supplementary Figure S1 for details).

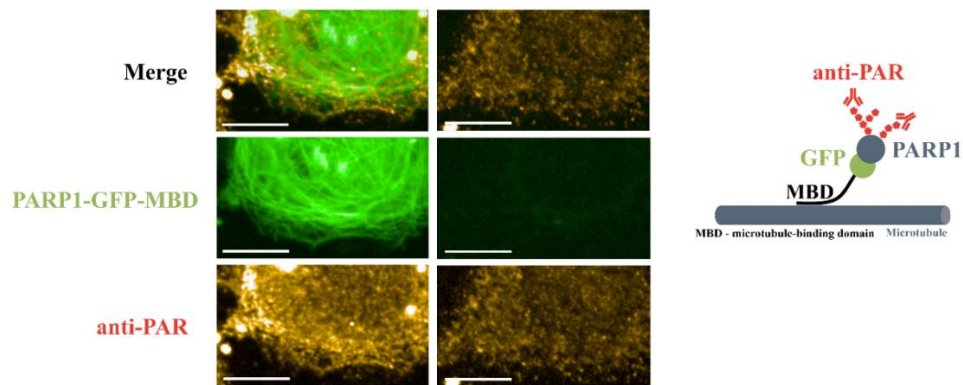


Figure 3: PAR can be detected on microtubule when PARP-1 is fused to a microtubule binding domain. Right panel: Scheme representing the assay used to detect the presence of PAR on microtubules when PARP-1 is brought onto microtubules. Left Panel: Representative pictures of HeLa cells expressing PARP-1-GFP-MBD encoding vector showing the distribution of PAR (anti-PAR antibody) along the microtubules. Scale bar: 10 μ m.

To understand whether the mixing between FUS and PARP-1 is dependent on PARP-1 activity and PAR synthesis we performed the mutation of the residue K893 located in the catalytic domain of PARP-1 which leads to the disruption of PARP-1 catalytic activity. The PARylation-defective PARP-1 mutant (K893I) poorly mixes with FUS in contrast with wild type PARP-1, suggesting the role of PAR in the mixing of two proteins (Figure 2B). To further probe the relevance of our results and investigate which DNA repair proteins can be potentially recruited to FUS-rich compartments, we also measured the mixing of FUS with itself, PARP-1 and other DNA repair factors including apurinic/apyrimidinic endonuclease 1 (APE1), DNA ligase 1 (LIG1), X-Ray Repair Cross Complementing 1 (XRCC1) and DNA Topoisomerase I (TOP1). The results of the microtubule bench assay show a strong mixing between FUS with itself which was expected but also with PARP-1 and XRCC1 (Figure 2B, Supplementary Figures S1 and S3). On the other hand, a marked demixing with 3 other DNA repair factors was observed with APE1, LIG1 and TOP1. FUS therefore seems to have a particular miscibility for PARP-1 but also XRCC1, in keeping with the reported interaction between XRCC1 and FUS (Wang *et al.*, 2018).

To obtain cellular data independently of the microtubule bench assay in cytoplasm, we tested PARP-1-FUS interaction measuring the colocalization between endogenous PARP-1 and FUS in nucleus using a PLA assay (Proximity Ligation Assay, Figure 4). Our results, in agreement with those of the MT bench Assay, confirm that FUS and PARP-1 are close to each other in the nucleus. The occurrence of this spatial proximity is however more

pronounced when cells are treated with H₂O₂ to activate PARP-1. As cell pretreatment with olaparib, a PARP-1 inhibitor, together with H₂O₂ (Figure 4) significantly decreases the colocalization between PARP-1 and FUS, we infer that PARP-1 and FUS are in close proximity thanks to PAR synthesized by PARP-1. We also noticed that PARP-1 interacts with FUS even in the absence of oxidative stress, which could be due to basal PARylation of PARP-1 under physiological conditions (Martello et al., 2013).

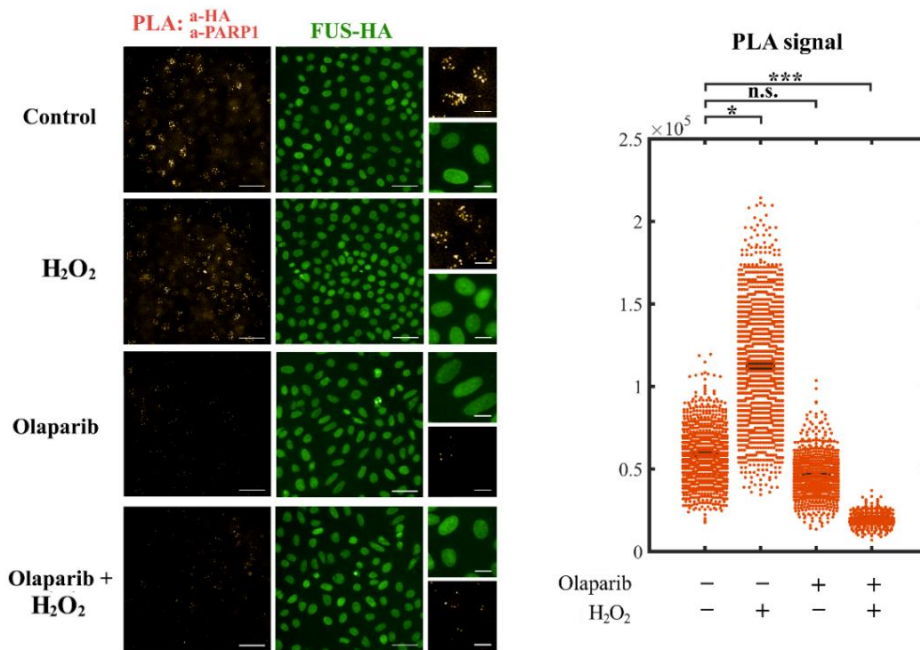


Figure 4: PLA assay shows the interaction between FUS and PARP-1 whose occurrence increase upon PARP-1 activation with H₂O₂. Left panel: Representative images showing PLA signal in HeLa cells expressing HA-tagged FUS exposed to H₂O₂ (150 μM, 25 min), PARylation inhibitor olaparib (2 μM, 2 h) or a combination of H₂O₂ and olaparib. Scale bar: 50 μm and 15 μm (higher magnification, right panel). Right panel: univariate scatter plots for PLA signal calculated as a PLA spot area multiplied by the number of spots in the nucleus of a single cell. *p < 0.05, ***p < 0.001, paired t-test; n.s., non-significant.

A previous study has shown that nuclear RNA is a major factor to limit the aberrant formation of liquid phases of FUS in the nucleus (Mahara et al., 2018). To investigate how the presence of RNA affects FUS nuclear distribution we inhibited transcription with Actinomycin D (ActD) for 1 h to prevent the binding of FUS to nascent mRNA but observed no visible changes. Endogenous FUS remained homogeneously distributed (Figure 5). As FUS is considered to be a PAR reader we suggested that PAR may also affect the distribution of FUS. We then inhibited the synthesis of PAR by PARP-1 with olaparib. While olaparib alone does not generate any change on the spatial distribution of FUS, the

simultaneous inhibition of PARylation and transcription generates the appearance of FUS-rich nuclear granules that were detected with two different antibodies (Figure 5).

The same type of granules is not observed with TDP-43 and HuR. In addition, mRNA is not present in the FUS granules, in agreement with the dissociation of FUS from nascent mRNA after transcription inhibition (Figure 6). In summary, the formation of FUS nuclear granules could therefore result from the presence of mRNA- and PAR-free FUS which would then tend to form nuclear granules via FUS self-adhesive domains. The results also demonstrate that PAR alone with RNA regulates the spatial distribution of FUS in the nucleus cells.

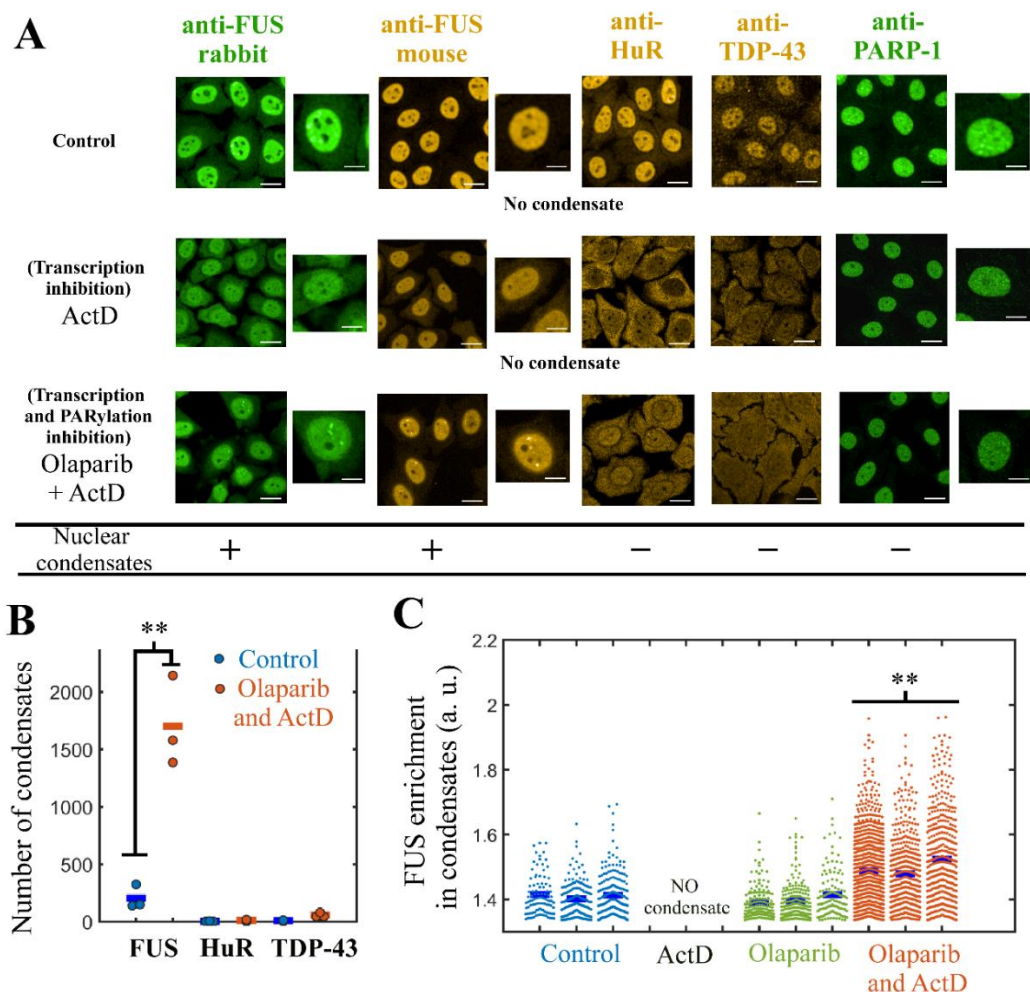


Figure 5. The interaction of FUS with PARylated PARP-1 prevents aberrant FUS self-assemblies after transcription inhibition. A. Nuclear distribution of FUS, TDP-43, HuR, and PARP-1 in HeLa cells after transcription inhibition (ActD, 5 μ g/ml, 1 h) and/or PARylation inhibition (olaparib, 2 μ M, 1 h). Zoom in on the nucleus shows the presence of FUS condensates in the nucleus after simultaneous transcription and PARylation inhibitions. Scale bars: 20 μ m and 8 μ m. B. Quantification of the number of condensates automatically detected with antibodies raised against indicated proteins and under indicated conditions (see Materials and Methods). Each condition is presented in triplicate. **p < 0.01, paired t-test. C. Quantification of the FUS enrichment in condensates under indicated conditions. Each condition is presented in triplicate. **p < 0.01, paired t-test.

FUS-containing nuclear condensates formed after ActD and olaparib treatment do not include mRNA

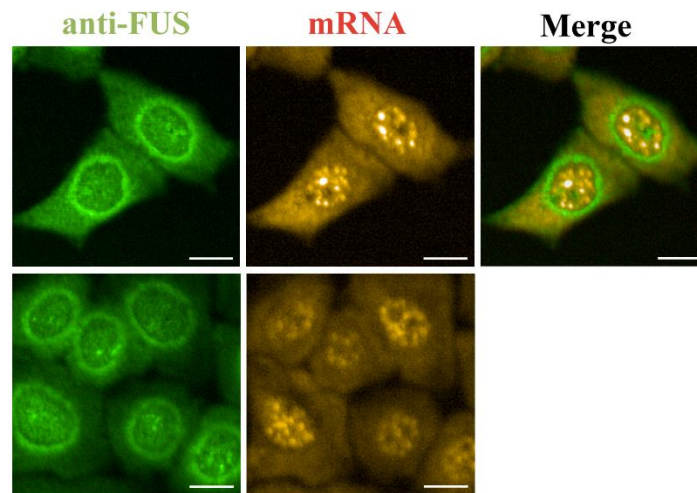


Figure 6: No enrichment in Poly(A) mRNAs inside nuclear FUS granules appearing after ActD and olaparib treatment. Representative images of HeLa cells treated with transcription inhibitor (ActD, 5 μ g/ml, 1 h) and PARylation inhibitor (Olaparib, 2 μ M, 1 h), fixed and stained to observe colocalization of FUS (anti-FUS antibody) and Poly(A) mRNA (in situ hybridization to detect mRNA). Poly(A) mRNA was not detected in FUS-containing nuclear condensates. Scale bar: 15 μ m.

Chapter 2: FUS increases the poly(ADP-ribose) level in H₂O₂-treated cells in a transcription-dependent manner

Having shown the specific link between FUS and PARP-1 by comparison with other non FET RNA-binding proteins (Chapter 1; Figures 2 and 5), we then asked whether FUS may regulate PARP-1 activity in response to genotoxic stress. The point is that PAR readers are also potent acceptor proteins themselves. We devised that the presence of acceptor proteins may control the PAR level in cells (Alemasova *et al.*, 2018). To address this point, HeLa cells treated with siNeg or siRNA to decrease FUS level were exposed to H₂O₂ for 15 min. This short time of exposure is sufficient to generate a significant increase of PAR level in cells (Figure 7). Using an HCS imager to perform a single cell analysis, we indeed detected a significant increase of PAR levels in the nuclei of H₂O₂-treated cell (Figure 7). In addition, nuclear PAR synthesis no longer increased when HeLa cells were treated with a PARP inhibitor, olaparib. These controls comfort the validity of our assay (see Materials and Methods for details, 2 different antibodies were also used to further validate our assays).

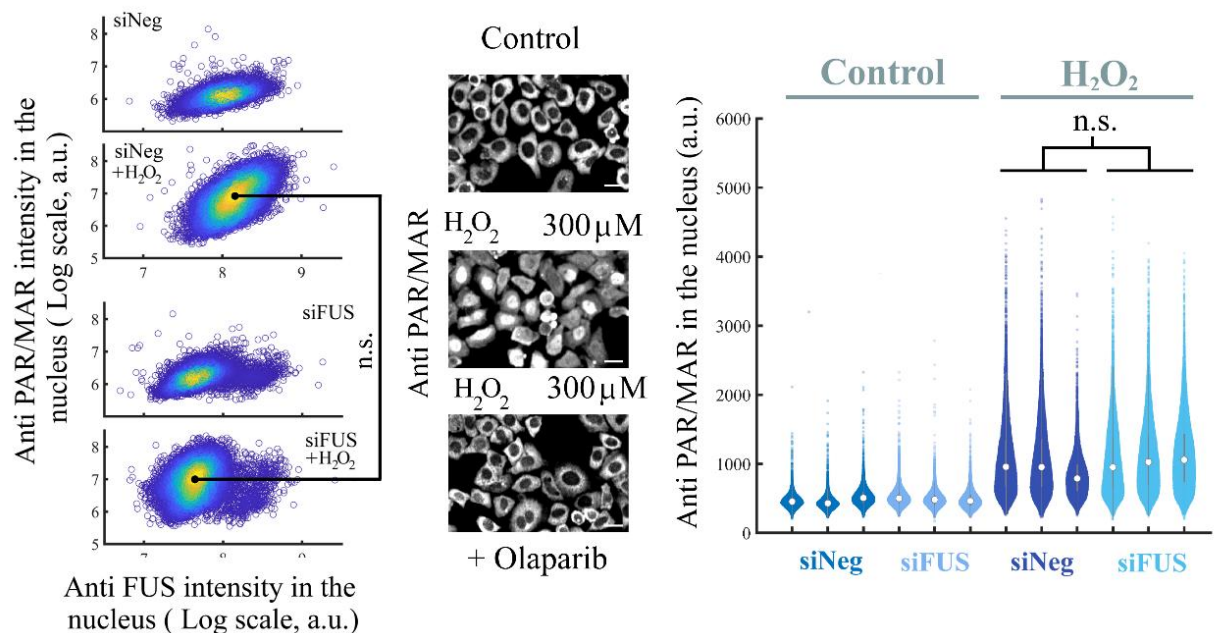


Figure 7: No difference in the global PAR level was detected by comparing siRNA- with siNeg-treated in cells exposed to H₂O₂. Left panel: Scatter plot showing nuclear PAR synthesis versus FUS level at the single cell level in control HeLa cells and in HeLa cells transfected with siFUS without any treatment or treated with H₂O₂ (300 μM, 15 min). Middle panel: Representative images showing the nuclear PAR in control cells under indicated conditions. Scale bar: 25 μm. Right panel: Violin plots representing the nuclear PAR synthesis in control HeLa cells and in HeLa cells transfected with siFUS without any treatment or treated with H₂O₂ as indicated. Each condition is presented in triplicate. n.s., non-significant.

However, no difference in the global PAR level was detected by comparing siRNA- with siNeg-treated in cells exposed to H₂O₂ (Figure 7). We devised that compensatory mechanisms may hinder the putative role of FUS in regulating PARP-1 activity. Indeed, reducing the expression of FUS changes the expression of other RBPs notably TAF15 which can substitute FUS in the network of protein interacting with PARP-1 (Kapeli *et al.*, 2016; Sun *et al.*, 2015). As we cannot silence the expression of all FET proteins without dramatically interfering with cellular functions, we decided to express HA-FUS in HeLa cells. Overexpression should be more difficult to compensate for the cells. Interestingly a significant increase in nuclear PAR level was detected in HA-FUS-expressing cells treated with H₂O₂ (Figure 8B).

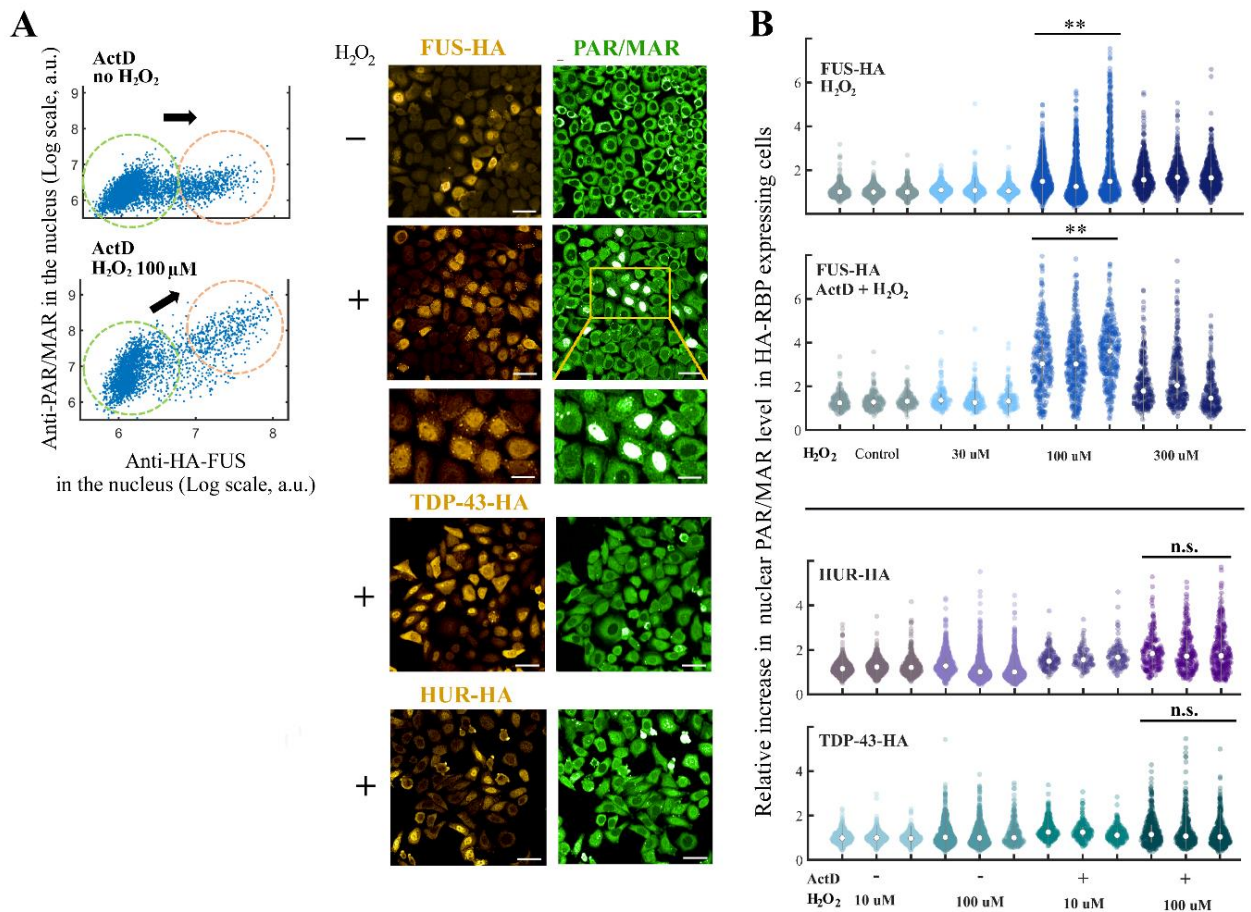


Figure 8: Overexpression of FUS increases PARP-1 mediated PAR synthesis in cells. A. Left panel: Nuclear PAR level in cells expressing HA-FUS treated with Actinomycin D (ActD, 5 μg/ml, 1 h) or ActD (ActD, 5 μg/ml, 1 h) and then H₂O₂ (100 μM, 30 min). Right panel: Representative images showing the nuclear PAR level in cells expressing HA-tagged FUS, TDP-43 or HuR exposed to ActD and H₂O₂. Scale bars: 25 μm or 50 μm. B. Measurement of the relative increase in nuclear PAR level in HA-RBP expressing HeLa cells versus control cells under indicated conditions. See Materials and methods for details about the automated single cell analysis. Each condition is presented in triplicate. **p < 0.01, paired t-test; n.s., non-significant.

This pattern was not detected when similar experiments were performed in HA-HuR or HA-TDP-43 expressing cells and with the same window of nuclear HA expression at the single cell level (Figure 8B), the nuclear overexpression of HA-RBP corresponds in average to that of endogenous FUS in the cell selected for the analysis (see Materials and Methods for details). Importantly, when transcription is blocked with ActD, the level of nuclear PAR increases significantly in HeLa cells expressing HA-FUS but not HA-HuR or HA-TDP-43 (Figures 8A and B).

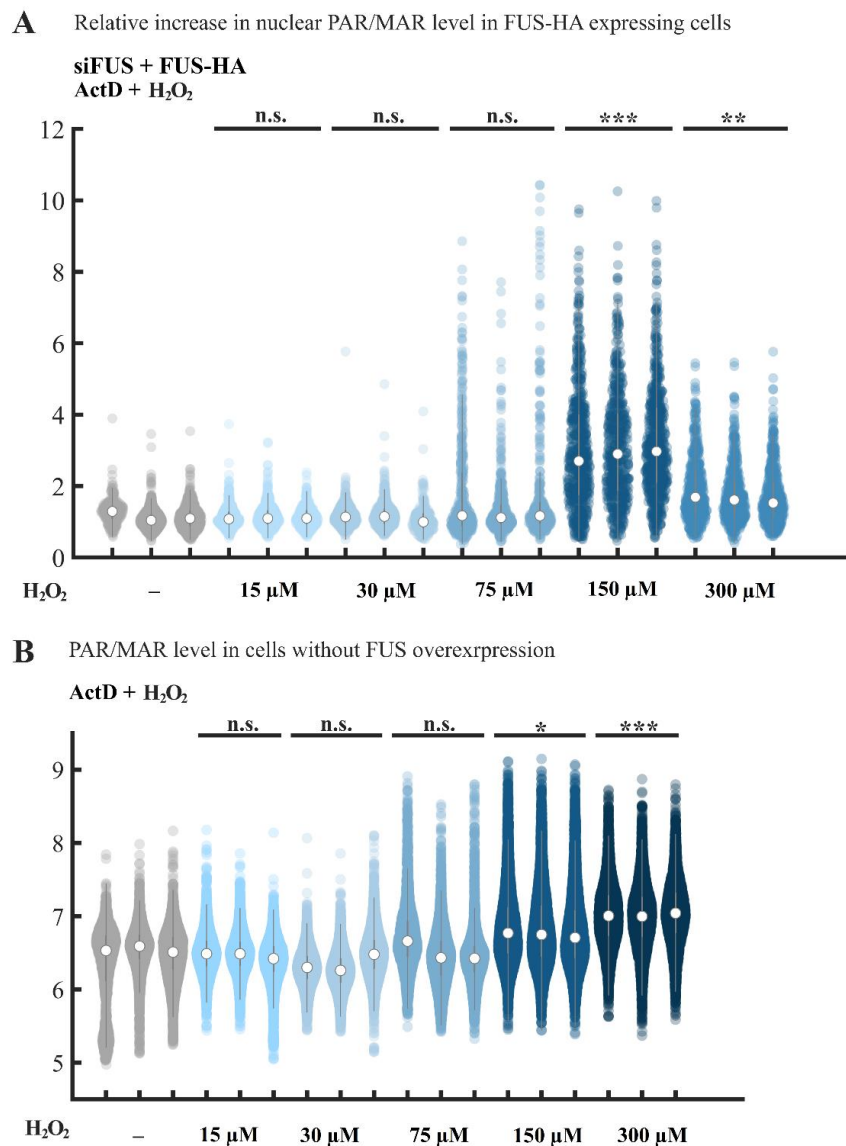


Figure 9: Relative increase in nuclear PAR/MAR level in HeLa cells expressing FUS-HA at various H₂O₂ concentrations. A. Violin plots representing the relative increase of nuclear PARylation in HeLa cells treated with siRNA targeting FUS mRNA and expressing HA-FUS versus control HeLa cells. Cells were treated with transcription inhibitor (ActD, 5 μg/ml, 1 h) and H₂O₂ (30 min) in indicated concentrations. Each condition is presented in triplicate. The relative increase is the most significant at 150 μM of H₂O₂. **p < 0.01, ***p < 0.001, paired t-test; n.s., non-significant. B. Violin plots representing the nuclear PARylation in control HeLa cells (without FUS overexpression).

In addition, the relative increase of PAR level in HA-FUS expressing cells is more significant at 100 μM than at 300 μM of H_2O_2 (Figure 8B and Figure 9). FUS thus better contributes to the increase of PAR levels when cells are not too extensively experiencing DNA damages. Finally, we controlled that cells expressing HA-FUS compared to control cells do not display increased levels of DNA damages measured as the level of phosphorylation of γH2AX at the single cell level under our experiment conditions (Figure 10).

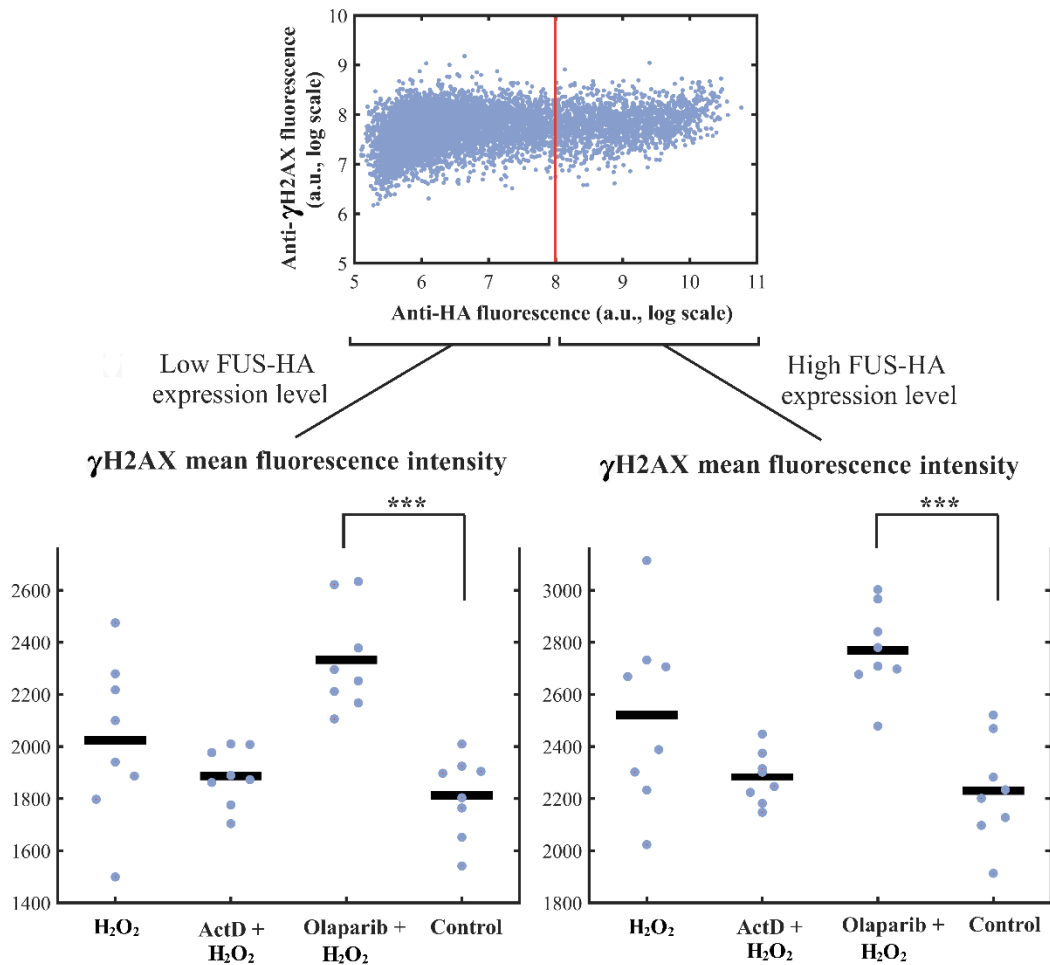


Figure 10: FUS expression does not significantly change γH2AX fluorescence level. Upper panel: Analysis at the single cell level of anti- γH2AX fluorescence versus HA-FUS expression level in HeLa cells transfected with HA-FUS expressing plasmid. Lower panel: mean anti- γH2AX fluorescence intensity in low (left panel, $\ln(\text{anti-HA fluorescence}) < 8$) and high (right panel, $\ln(\text{anti-HA fluorescence}) > 8$) HA-FUS expressing HeLa cells treated with H_2O_2 (250 μM , 30 min), ActD (5 $\mu\text{g}/\text{ml}$, 1 h) and H_2O_2 or Olaparib (2 μM , 1 h) and H_2O_2 . Each condition is presented in octuplicate. γH2AX fluorescence intensity increases after the treatment with H_2O_2 or Olaparib and H_2O_2 and does not depend on HA-FUS expression level. *** $p < 0.001$, paired t-test.

To better understand the mechanism behind the dramatic increase of nuclear PAR level in HA-FUS expressing cells under ActD/ H_2O_2 treatment (Figure 8), we performed another

series of experiments with measurements of the PAR level after different time of ActD pretreatments (Figure 11).

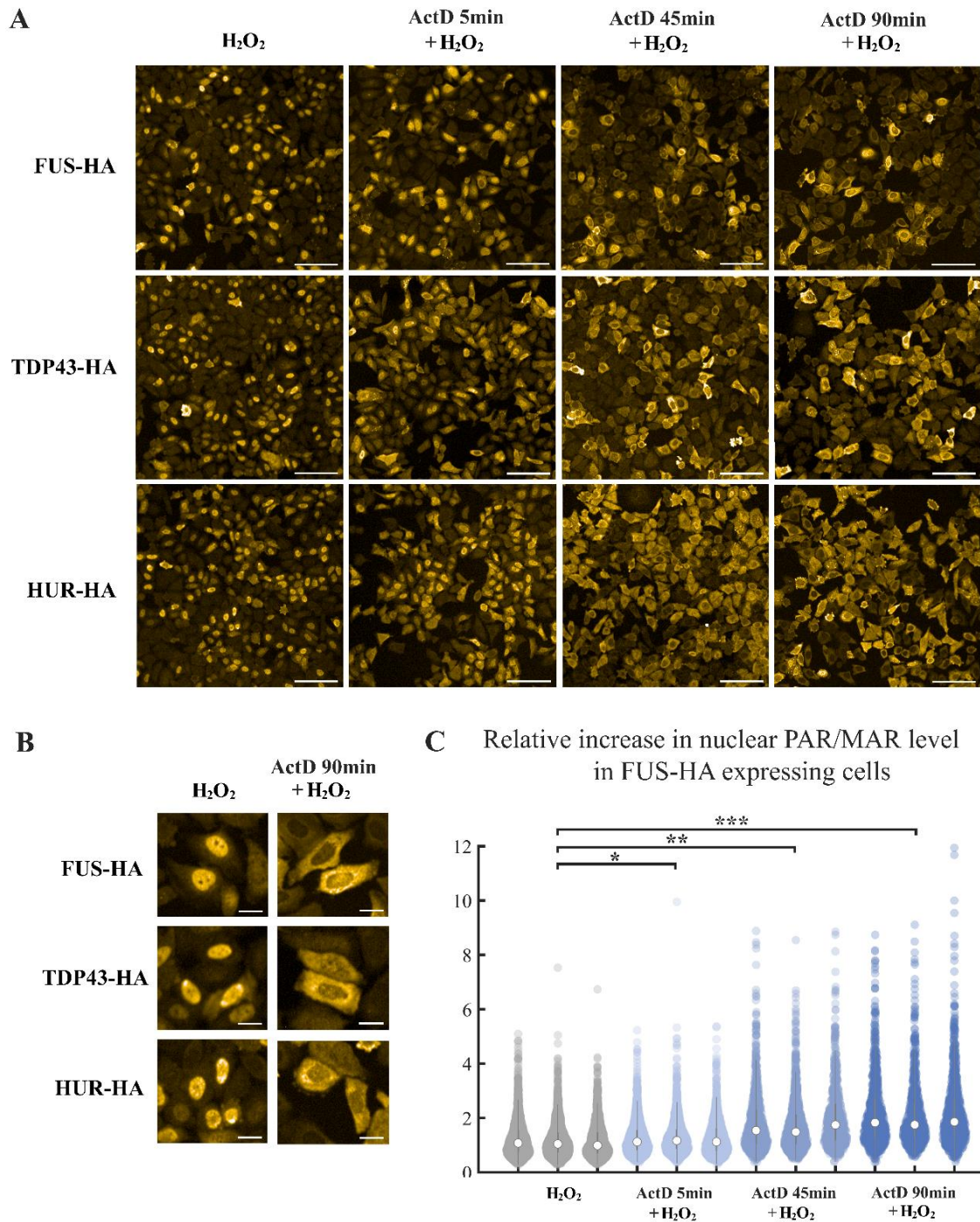


Figure 11: Only long ActD treatments (≥ 45 min) lead to an increased PARylation in the nuclei after H₂O₂ treatments. A. Representative images of HeLa cells expressing indicated HA-RBP and treated with the transcription inhibitor ActD (5 μ g/ml) for 5, 45 and 90 min or/and H₂O₂ (300 μ M, 30 min). Scale bar: 100 μ m. B. All three RBPs translocate to the cytoplasm over time following the treatment with ActD and H₂O₂, as indicated. Scale bar: 20 μ m (higher magnification of A). C. Violin plots representing the relative increase of nuclear PAR/MAR level in HeLa cells expressing HA-FUS versus control HeLa cells. Cells were treated with a transcription inhibitor (ActD, 5 μ g/ml) during indicated time and/or H₂O₂ (300 μ M, 30 min). Each condition is presented in triplicate. The PAR/MAR level is more pronounced when HA-FUS expressing cells were treated with ActD for at least 30 min. * $p < 0.05$, ** $p < 0.01$, *** $p < 0.001$, paired t-test.

The increase of PAR level is more pronounced when HA-FUS expressing cells were treated for at least 30 min with ActD before H₂O₂, which may correspond to the time required for releasing FUS from its mRNA targets after transcription inhibition (Figure 11A and C). Consistently, the nucleocytoplasmic shuttling of mRNA-binding proteins such as FUS, TDP-43 and HuR which relies on their binding to nuclear mRNAs also occurs after ActD treatment within the same frame of time (Figure 11B).

To explore whether the inhibition of RNA transcription is a prerequisite to detect an increase of PAR synthesis in HA-FUS expressing cells under our experimental conditions, we detected the global transcript level upon H₂O₂ exposure through the incorporation into RNA of 5-bromouridine (BrU) at the single cell level. We found that the concentrations of H₂O₂ used in this study (100-300 μ M) indeed progressively decrease but not totally suppress transcription in cells (Figure 12).

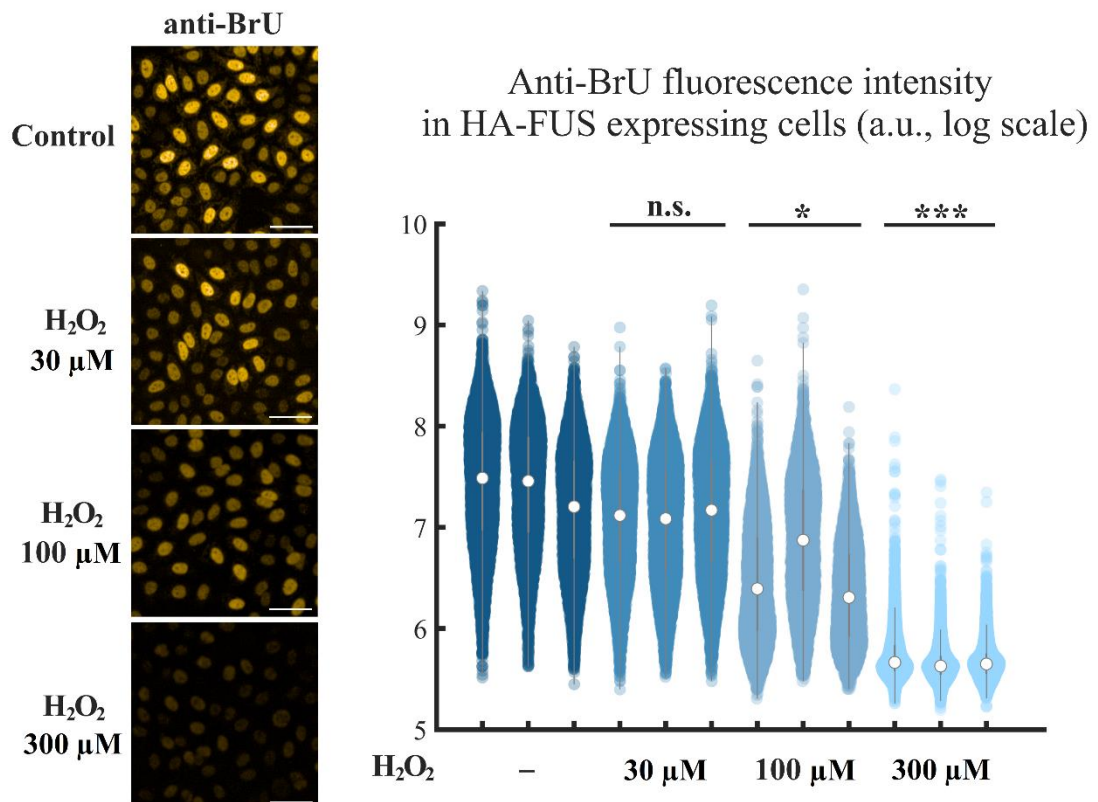


Figure 12: Global transcription significantly decreases after H₂O₂ treatment at higher concentrations than 100 μ M. Left panel: Representative pictures of anti-BrU fluorescence in HA-FUS expressing HeLa cells treated with H₂O₂ (30 min) and exposed to BrU for the last 5 min in indicated concentrations. Scale bar: 50 μ m. Right panel: Violin plots representing anti-BrU fluorescence intensity in HA-FUS expressing HeLa cells treated with H₂O₂ (30 min) in indicated concentrations and exposed to BrU for the last 5 min. Anti-BrU signal indicating transcription level is decreased but not totally suppressed for the concentration of H₂O₂ used in this study (150 μ M). Each condition is presented in triplicate. **p < 0.01, ***p < 0.001, paired t-test; n.s., non-significant.

Finally, as ActD blocks both RNA polymerase I and II at the concentrations used in our experiments, we repeated the same experiments with 5,6-dichloro-1-beta-D-ribofuranosylbenzimidazole (DRB), an inhibitor of the phosphorylation of P-TEFb which promotes mRNA transcription elongation, and oxaliplatin, an inhibitor rRNA transcription. DRB but not Oxaliplatin successfully increased the level of PAR in HA-FUS expressing cells (Figure 13) (Baumli *et al.*, 2010). We therefore conclude that expressing HA-FUS and inhibiting mRNA transcription significantly increase nuclear PAR level upon PARP-1 activation in H₂O₂ treated-cells.

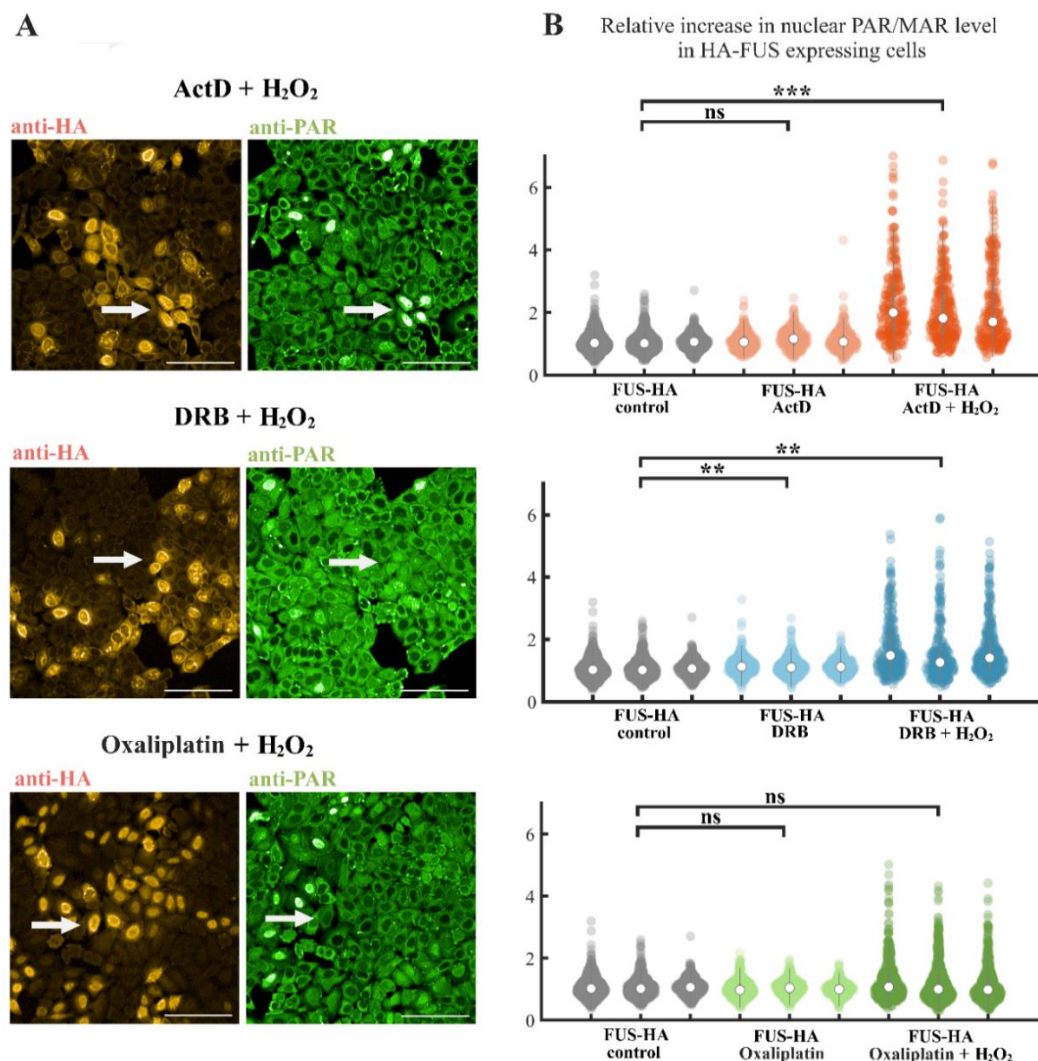


Figure 13: DRB but not Oxaliplatin increase the PARylation level in HeLa cells exposed to ActD and H₂O₂. A. Representative images of HA-FUS expressing HeLa cells treated with H₂O₂ (100 μ M, 30 min) and ActD (5 μ g/ml, 1 h), DRB (100 μ M, 1 h) or Oxaliplatin (10 μ M, 1 h). Arrows point to high PAR/MAR levels in HA-FUS expressing HeLa cells treated with ActD or DRB contrary to the cells treated with Oxaliplatin. Scale bar: 100 μ m. B. Violin plots indicating a relative increase in nuclear PAR/MAR level in HA-FUS expressing HeLa cells versus control HeLa cells (without HA-FUS expression) treated with H₂O₂ (100 μ M, 30 min) and ActD (5 μ g/ml, 1 h), DRB (100 μ M, 1 h) or Oxaliplatin (10 μ M, 1 h). Each condition is shown in triplicate. ActD and DRB but not Oxaliplatin treatment increases the level of PARylation in HA-FUS expressing cells. **p < 0.01, ***p < 0.001, paired t-test; n.s., non-significant.

Chapter 3: FUS is significantly PARylated and also increases total protein PARylation level *in vitro* and in cells

Given the significant increase in PAR level observed in HA-FUS expressing cells, we asked whether FUS is PARylated and alter the level of PAR synthesis in cells. To this end, we detected the PARylation of proteins using extracts of HEK293 cells exposed to H₂O₂ in the presence or absence of olaparib to prevent PARP-1 activation (Figure 14A and B).

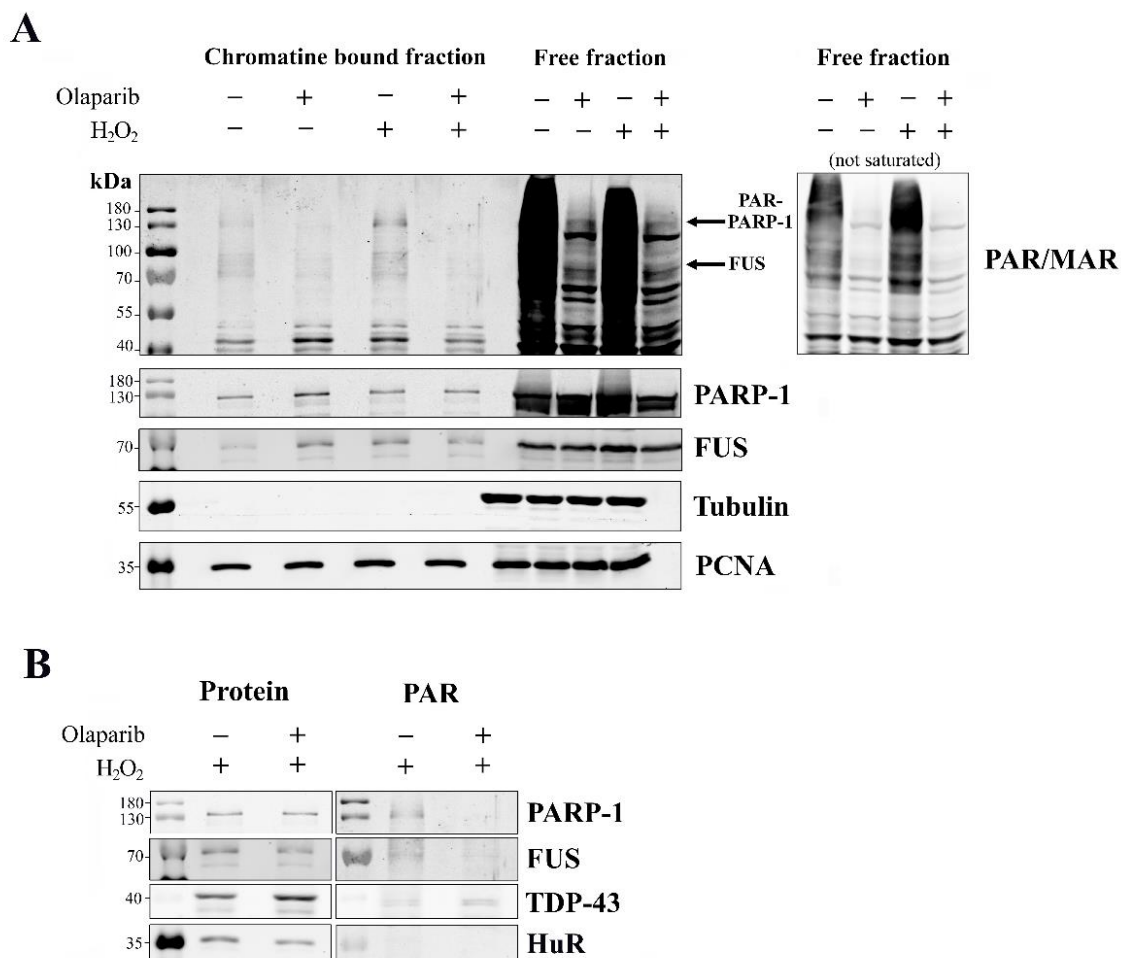


Figure 14: FUS is PARylated in cells-treated with H₂O₂ but not HuR and TDP-43 under our experimental conditions. A. The chromatin bound and free fractions of HEK293 cells treated with olaparib (2 μ M, 1 h), H₂O₂ (200 μ M, 30 min) or olaparib and H₂O₂ were subjected to SDS/PAGE and Western blot with PAR/MAR, PARP-1, FUS, tubulin and PCNA antibodies. The PARylation of PARP-1 and FUS is highest when cells are treated with H₂O₂ but not pretreated with olaparib. The fraction of FUS in the chromatin bound fraction is higher in the absence of olaparib than in the presence. B. The chromatin bound fractions of HEK293 cells treated with H₂O₂ (200 μ M, 30 min) or olaparib (2 μ M, 1 h) and H₂O₂ were subjected to SDS/PAGE and Western blot with antibodies to PARP-1, FUS, TDP-43 and HuR. PARP-1 and FUS are PARylated under genotoxic stress and their PARylation is dependent on olaparib treatment contrary to TDP-43 and HuR. The experiment was performed in two repeats.

In agreement with the recruitment and activation of PARP-1 at DNA damage sites, using an anti-PAR/MAR antibody, we observed in the chromatin bound fraction a band that

corresponds to PARylated PARP-1. In addition, we also noticed a band that could correspond to endogenous FUS in its PARylated form because of its increased intensity in the absence of olaparib. A similar band was not observed for TDP-43 and HuR (Figure 14B). To ensure that this band corresponds to PARylated FUS, we expressed HA-FUS or silenced the expression of endogenous FUS to induce a measurable difference on FUS expression level. Even from total nuclear cell extracts, we noticed an increased intensity of the band corresponding to PARylated FUS in HA-FUS expressing cells compared to siRNA treated cells (Figure 15). Thus, FUS PARylation level correlates with FUS expression level. The ease with which we detected FUS PARylation from cell extracts may indicate that FUS PARylation is significant. However, FUS PARylation only represents a small fraction of the overall protein PARylation level, which also increases in HEK293 cells expressing HA-FUS (Figure 15). Of note, we also noticed a slightly larger fraction of FUS detected in the chromatin bound fraction in the absence than in the presence of olaparib, which indicates that PARP-1 activation may at least partly direct FUS onto chromatin (Figure 14A).

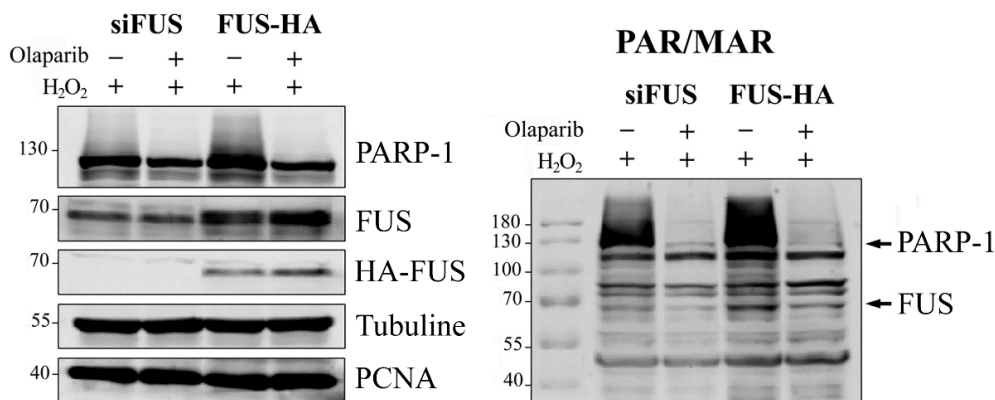


Figure 15: The increase in PAR level in HA-FUS-expressing HEK293 cells demonstrated by Western blot analysis. Western blot analyses of protein PARylation of free fractions obtained from HEK293 cells transfected with siFUS or FUS-HA and exposed to H₂O₂ (200 μM, 30 min) or olaparib (2 μM, 1 h) and H₂O₂. Left gel: antibodies for indicated proteins were used. Right gel: antibodies to PAR/MAR were used. Note the overall increase in PAR level in HA-FUS-expressing cells. The experiment was performed in two repeats.

We then considered whether FUS can be PARylated and whether FUS can also stimulate PARylation in a reconstituted system. Using recombinant PARP-1 and damaged DNA, we first controlled that PARP-1 autoPARylation increased with time in the absence of FUS (Figure 16). In the presence of FUS up to a FUS:PARP-1 molar ratio of 8:1, the overall

PARylation rate steadily increases, then decreases for the highest ratio of 30:1 (Figure 16). Importantly, FUS is itself significantly PARylated by PARP-1 which accounts for most of the increase of PAR level. Therefore, FUS is an acceptor protein, which increases the number of additional targets on which PAR can be attached but it does not increase significantly PARP-1 autoPARylation.

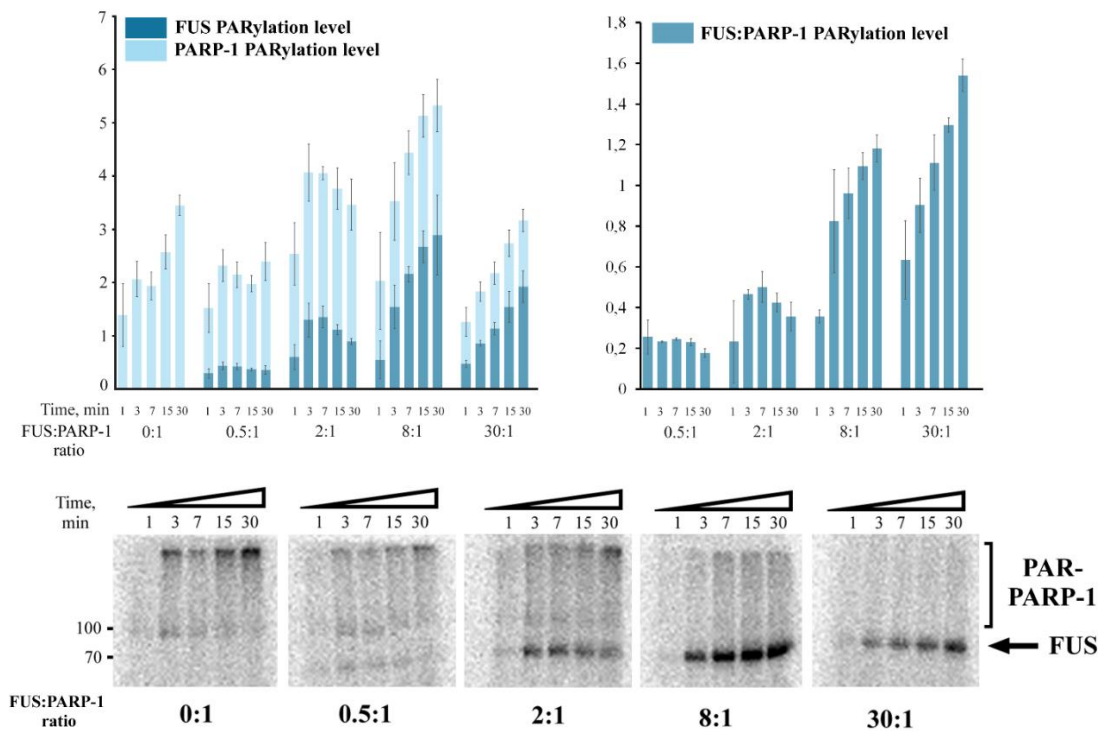


Figure 16: Serving as an acceptor protein, FUS increases significantly the level of PAR, synthesized by PARP-1 in a reconstituted system. Upper panels: Kinetics of *in vitro* PARylation of FUS and autoPARylation of PARP-1 in the presence of DNaseI-activated DNA, [³²P]-NAD⁺ (0.4 mCi) and indicated FUS:PARP-1 concentration ratios (see Materials and Methods for details). Both the overall PARylation level of PARP-1 and FUS (left) and FUS/PARP-1 PARylation ratio (right) were measured as the mean ± SD of three independent experiments and individual data points. Lower panel: SDS-PAGE analysis with subsequent phosphorimaging for indicated times after PARP-1 activation in the presence of DNase-activated DNA and [³²P]-NAD⁺ (0.4 mCi) and indicated FUS:PARP-1 concentration ratios (see Supplementary Figure S4A and Figure S5 for details).

PARP-1 is an unusual enzyme which attaches covalently PAR product to itself which may impair of the overall rate of PAR synthesis (notably by promoting the release of PARP-1 from DNA). The cooperation of PAR acceptor proteins with PARP-1 might be important to remove PAR product from catalytic subunits of PARP-1 which should result in increase of the turnover of PARP-1 activity and consequently in stimulation of PAR synthesis (Alemasova *et al.*, 2019; Naumenko *et al.*, 2020). This can be one of the reasons of the increase of PARP-1 activity and the overall level of PAR synthesis in the presence of FUS.

Chapter 4: Structural basis of the recognition of PAR by FUS RRM

Since FUS promotes PAR synthesis upon PARP-1 activation in cells (Figure 8), we focus our attention on the molecular basis of the interplay between PARP-1 and FUS. Most previous studies indicate that FUS RGG domains, notably those located in the C-terminus domain of protein, are responsible for the high affinity of FUS for PAR (Rhine *et al.*, 2022; Altmeyer *et al.*, 2015). PAR is long chain resembling RNA but with two phosphate groups in between consecutive bases instead of one for RNA. PAR is thus highly negatively charged which may explain the affinity of arginine-rich domains for PAR. However, repeats of RG, RGG or SR domains that all should interact with PAR or RNA electrostatically are quite abundant in many different RBPs (Chong *et al.*, 2018; Ozdilek *et al.*, 2017). We therefore wondered whether a structured domain may secure the specificity to FUS toward PAR in cells. RNA-binding domains and notably RRM1s have already been proposed as PAR readers in several RBPs such as NONO but no in-depth structural analyses are available to ascertain the proposed role of RRM1s as PAR readers (Literature Review, Table 1) (Krietsch *et al.*, 2012; Kliza *et al.*, 2021).

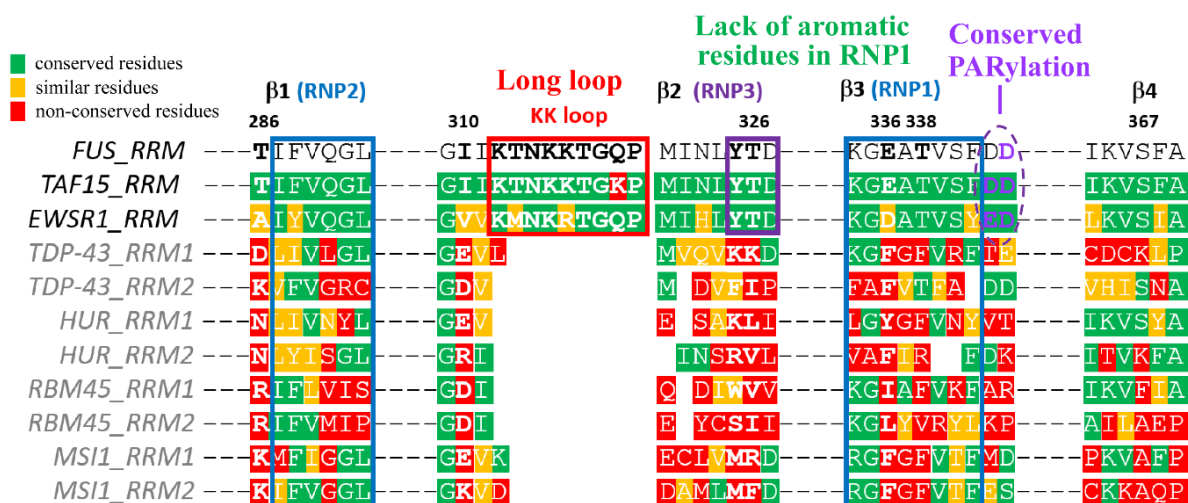
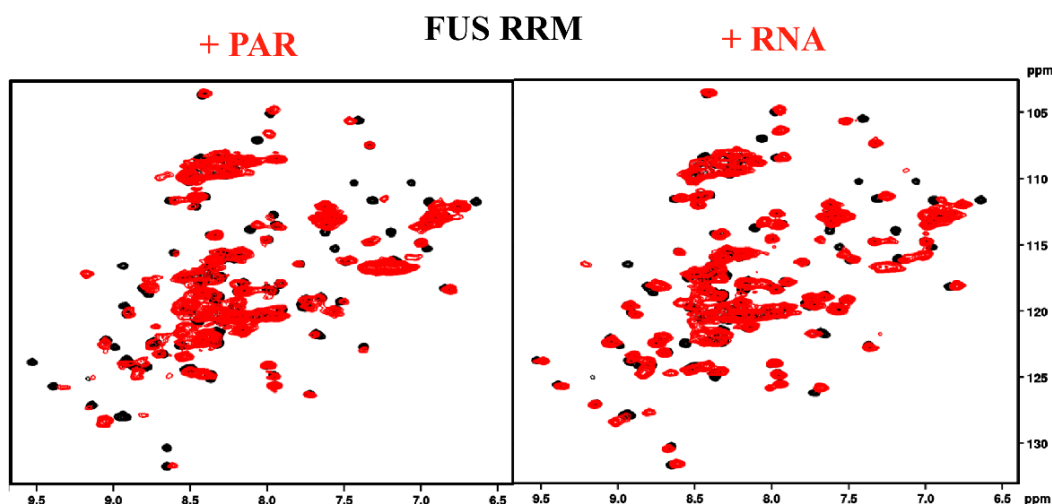


Figure 17: Sequence alignment of different RRM1s of human RBPs. RNP1-3 motifs in which most of the RRM1 residues interact with RNA are not conserved in FET protein, notably with a lack of aromatic residues in RNP1. FET proteins also have a long KK-loop. The colors indicate a decreasing degree of conservation from green to red.

If RRM1s are indeed PAR readers in cells, we may have a chance to detect PARylation in residues located in RBP RRM1s. Interestingly, among the 17 RBPs that we previously identified as PARylated in two independent studies (Figure 1), only FUS and TAF15 have

at least one PARylated residues located in their RRM (*Martello et al., 2016; Zhang et al., 2013*). In addition, in the study of Zhang et al., the three FET proteins RRMs, TAF15, EWSR1 and FUS were PARylated in two conserved negative residues, Asp-Asp or Asp-Glu, located in the short loop connecting $\beta 3$ and $\beta 4$ sheets (Figure 17) (*Zhang et al., 2013*). This analysis thus also points toward a specific cooperation between FET's RRM and PARylation process. To directly probe whether FUS RRM may specifically interact with PAR, we first compared the primary amino acid sequences of FET protein RRMs with sequences of canonical RRMs of non FET proteins like HuR, TDP-43, RMB-45 and MSI-1 (Figure 17). The most prominent discrepancies are the presence of a long Lys-Lys loop (KK-loop) in between $\beta 1$ and $\beta 2$ sheets and the lack of some aromatic residues generally present in the conserved RNP1 motif, which form stacking interactions with RNA bases. Then, using NMR spectroscopy in liquid, we observed the chemical shift perturbations (CSPs) occurring in 2D ^1H - ^{15}N SOFAST-HMQC spectra for the FUS RRM domain in the presence of protein-free PAR. Chemical shift perturbation is an NMR technique that measures changes in the chemical shifts of a protein when a ligand is added, which are then used to locate the binding site of the protein. In the presence of PAR, we noticed significant CSPs in the 3 RNP motifs (in particular in three threonine residues T286, T326 and T338) and in the KK-loop of FUS RRM (two lysines K314 and K315). Under the same condition, PAR interacts with HuR RRM1 weakly and induces limited CSPs with TDP-43 RRM2 (Figures 18 and 19, we had solubility issues with TDP-43 RRM1). Therefore, FUS RRM interacts more strongly with PAR than TDP-43 and HuR RRM. The binding of PAR to FUS RRM is very similar to that of a structured RNA loop (hnRNAP RNA loop) known to bind to FUS with a high affinity, as most of the CSPs occurred in the very same residues (Figures 18 and 19) (*Loughlin et al., 2019*). In summary, the results indicate a similar mode of binding of FUS RRM to PAR and RNA, which is not the case for canonical RRMs such as TDP-43 RRM2 and HuR RRM1 (Figure 20).



CSPs of RRM domains of FUS, TDP43 and HuR with oligonucleotides

	+ PAR	+ A20r	+ A20d	+ RNA loop	+ T10
FUS RRM	0.048	0.027	0.043	0.065	0.034
TDP-43 RRM2	0.022	0.036	0.006	0.062	0.047
HuR RRM1	0.002	0.005	0.002	0.002	nd

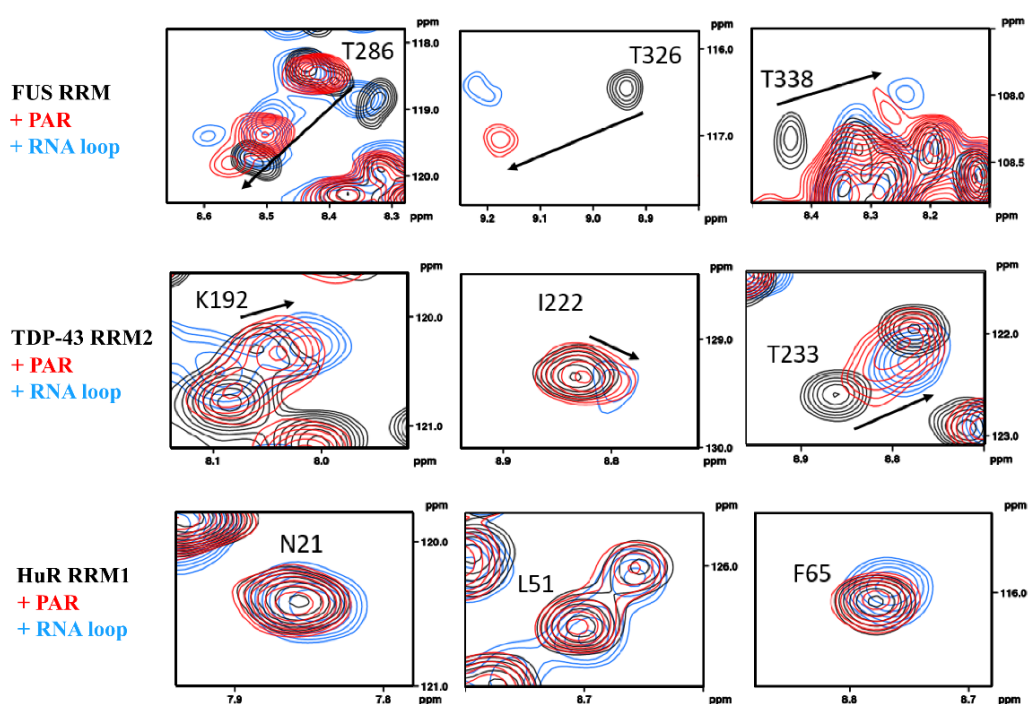


Figure 18: Structural basis of the interaction of FUS RRM, TDP-43 RRM2 and HuR RRM1 with PAR.

Upper panel: two-dimensional ^1H - ^{15}N SOFAST-HMQC NMR spectra of the ^{15}N -labelled FUS RRM residues in the apo state (black) and in the presence of PAR or RNA loop (hnRNP RNA loop) with a FUS:RNA or DNA molar ratio of 1:1.8. Abscissa and ordinate: ^1H and ^{15}N chemical shift (in ppm), respectively. Middle panel: Standard deviation of the CSP values of FUS RRM residues in the presence of indicated ligands (see also Supplementary Figure S6). A20r and A20d correspond to 20 nt-long poly(A) RNA and DNA, respectively. Lower panel: Zoom in on CSPs of selected FUS RRM residues to show the similar mode of interaction of FUS RRM with PAR and RNA.

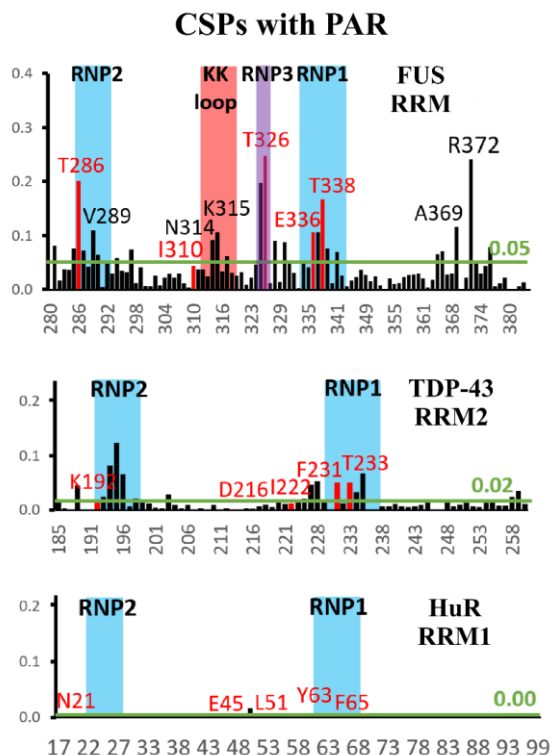


Figure 19: Structural basis of the interaction of FUS RRM, TDP-43 RRM2 and HuR RRM1 with PAR: CSP values. Histograms displaying the CSPs of the indicated RRM residues for FUS RRM, HuR RRM1 and TDP-43 RRM2 in the presence of PAR compared to FUS RRM, HuR RRM1, and TDP-43 RRM2 alone. Note the significant CSPs observed with FUS RRM. A20r and A20d: 10-nt long poly(A) RNA and DNA. T10: 10-nt long poly(T) DNA.

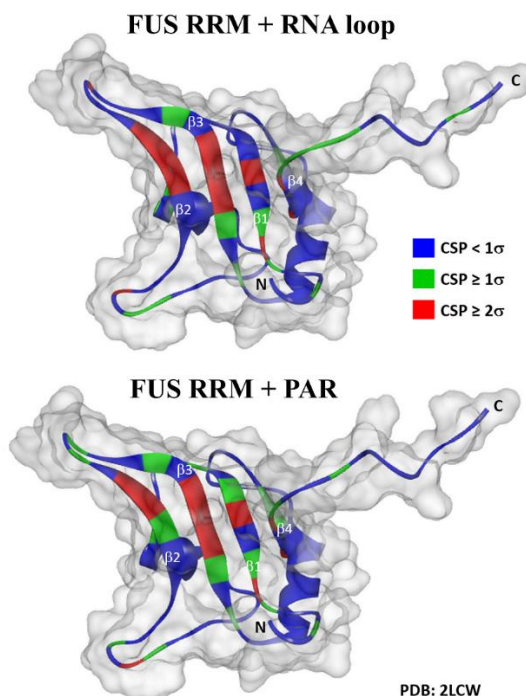


Figure 20: FUS RRM structure (PDB DOI: 10.2210/pdb2LCW/pdb) **in which the CSPs in presence of hnRNP RNA loop and PAR are indicated by colors according to their amplitude (σ of the CSP values).** A similar CSP pattern are observed when FUS RRM interacts with RNA or PAR. Note the same CSP signatures when FUS RRM interacts with RNA or PAR.

To gain further insights into the specific characteristics of FUS RRM that drives its binding to PAR, we compared the binding of FUS RRM, TDP-43 RRM2 and HuR RRM1 to unstructured 20-nt-long poly(A) RNA (A20r) or poly(dA) DNA (A20d), 10-nt-long poly(T) DNA (T10), and the structured RNA (hnRNAP RNA loop). Poly(A) nucleotides are structurally closer to linear poly(ADP-ribose) than structured RNA (Figure 18, Supplementary Figure S6). Again, in average, PAR induces stronger CSPs in the RRM of FUS than of TDP-43 and HuR. In contrast, TDP-43 RRM2 interacts more with A20r and T10 than the other RRMs tested. HuR RRM1 barely interacts with A20r, A20d and PAR. Limited CSPs were also observed for HuR RRM1 with the structured RNA whereas FUS RRM and TDP-43 RRM2 present strong CSPs with this RNA (Figure 21). These results indicate that FUS RRM does not display a marked affinity for linear polymer compared with TDP-43 RRM2 that would have explained its high affinity for PAR.

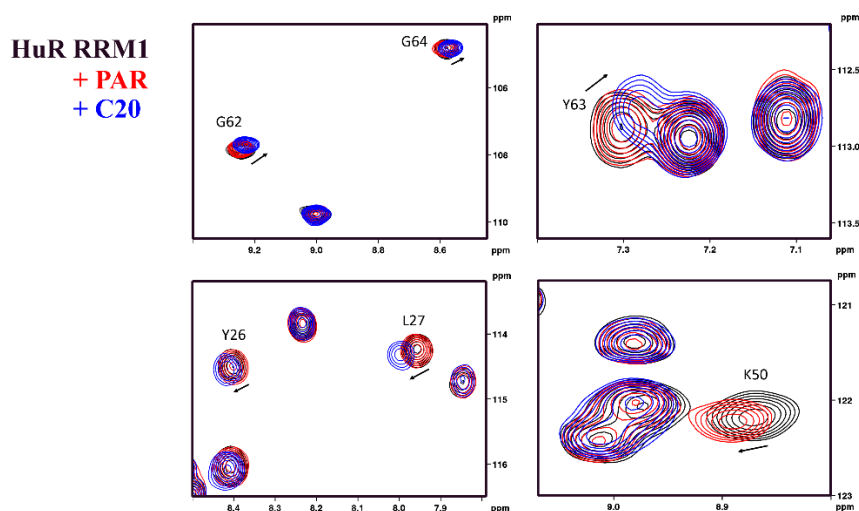


Figure 21: HuR RRM1 binds to C20 but to a very low extent to PAR. Zoom on CSPs of selected HuR RRM1 residues on the 1H-15N HSQC spectra of 15N-labeled HuR RRM1 in the apo state (black) and in the presence of PAR (red) and C-rich sequence (C20, blue). Note the significant CSPs in the presence of C20.

We then probed with point mutations into alanine residues the contribution of two residues in the KK-loop previously shown to reduce the affinity of FUS for RNA (K315A/K316A), one residue (N284A) in the C-terminus of the RRM which displays significant CSPs with PAR and the two Asp residues that are PARylated in cells (D342A and D343A). None of the mutations change the overall RRM structures except some CSPs in region around the mutations (Supplementary Figure S7). Based on the analysis of the CSPs (Supplementary Figure S17A and B), the results also indicate a significant decrease

of the binding affinity of K315A/K316A to PAR, a slight decrease for N284A and no effect for D342A/D343A RRM mutants (Figure 22, Supplementary Figure S8). Therefore, the KK-loop, which is only found in FET proteins, is most likely partly responsible for the strong interaction of FUS RRM with PAR and may explain, together with the lack of aromatic residues in RNP1 motif, the similar electrostatic binding of FUS RRM to PAR and RNA.

CSPs of FUS mutants with PAR

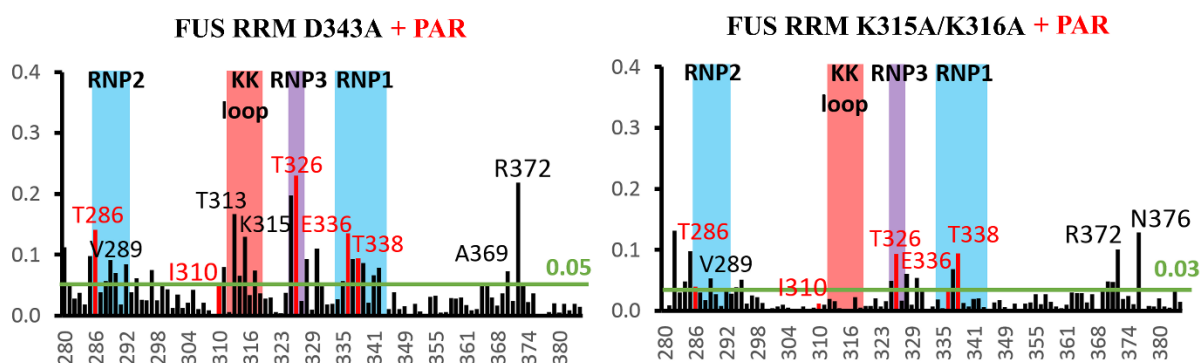


Figure 22: K315A/K316A mutations decrease FUS RRM binding to PAR. A. CSPs from NMR spectra of two FUS RRM mutants, D343A, K315A/K316A, in the presence of PAR. The FUS RRM non-conserved residues are depicted in red. Lines and numbers in green correspond to σ (standard deviation) of the CSP values.

Pronounced PAR-induced CSPs in FUS RRM residues may enable PAR to compete with nucleic acids for the binding to FUS RRM. To test this hypothesis, we chose to use a 10-nt-long poly(T) DNA (T10) because T10 induces similar CSPs in TDP-43- and FUS- RRM residues (Figure 23A).

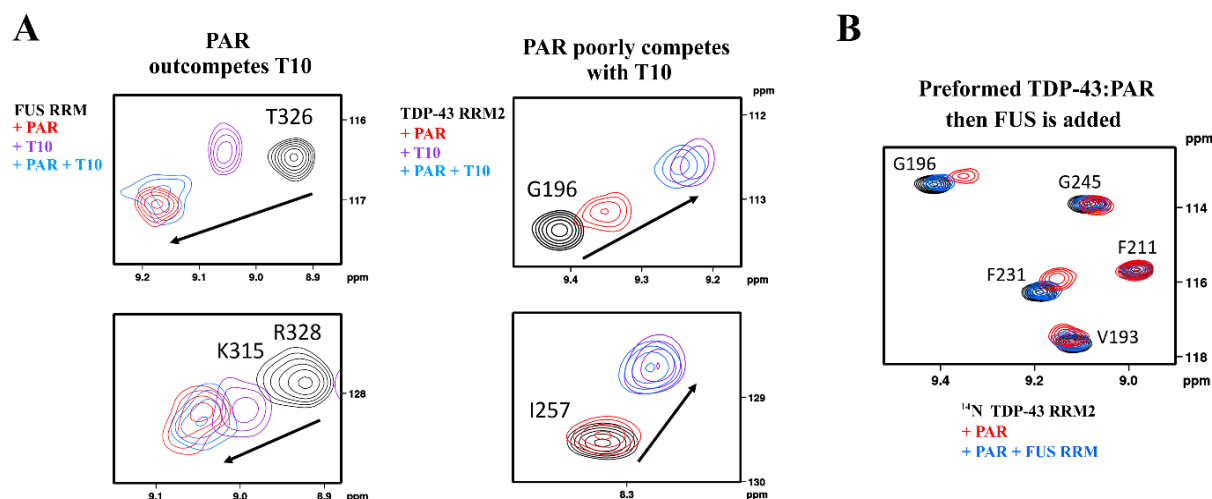


Figure 23: PAR interacts with FUS RRM and can outcompete DNA T10. A. NMR competition assays in the presence of PAR and/or T10 DNA for FUS RRM or TDP-43 RRM2. In specific residues, the direction or amplitudes of the CSPs varies for T10 and PAR. Zoom in on these residues indicates the preference for T10 (TDP-43 RRM2) or PAR (FUS RRM). B. TDP-43 RRM2 and PAR were left to interact before the addition of FUS RRM. The CSPs are displayed for representative residues.

However, with an equimolar mixture of PAR and T10, we noticed that the CSPs of some FUS RRM residues (T326 and K315) were very similar to those observed with PAR alone, as if PAR outcompetes T10 for the binding to FUS. On the other hand, TDP-43 RRM2 CSPs rather correspond to those observed with T10 alone in the presence of a mixture of T10 and PAR. To have a more precise view of the effectiveness of PAR to dislodge T10 from FUS RRM, we performed a WaterLOGSY assay which is a sensitive NMR method for the detection ligand:protein interaction from the analysis of 1D spectra from the ligand's side.

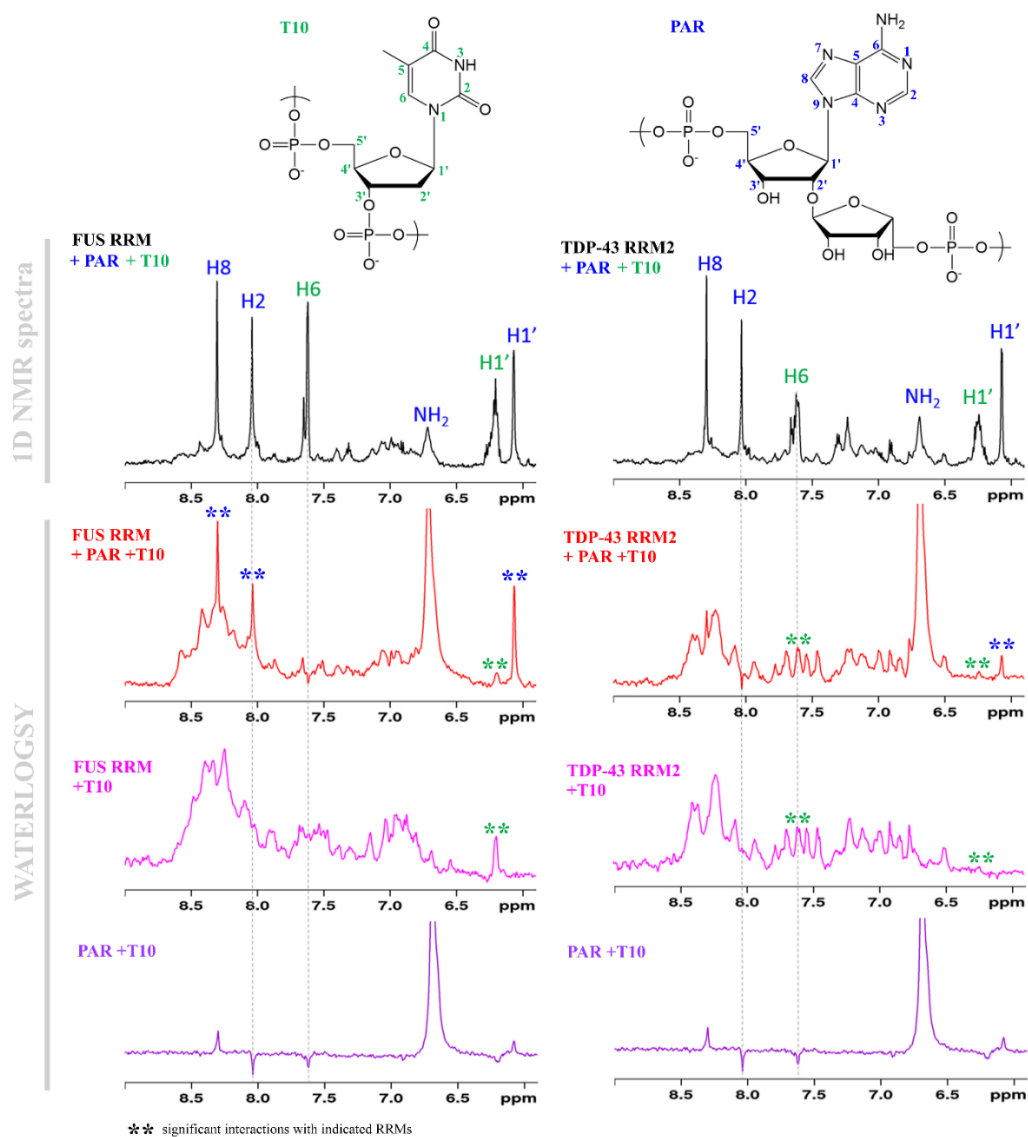


Figure: 24. WaterLOGSY analysis of the interaction of FUS RRM with PAR and T10. Upper panel: structural unit of PAR and T10. Lower panels: WaterLOGSY analyses of the interaction of PAR and T10, separately or in an equimolar mixture, with FUS RRM and TDP-43 RRM2. In the 1D NMR spectra. An interaction with RRM is detected when more positive ligand resonance peaks are observed in WaterLOGSY spectra in presence of RRMs compared to the spectra recorded with PAR and T10 alone. **): interactions with indicated RRMs with PAR (blue) and T10 (green). Note that PAR H8 and H2 atoms interact with FUS, but not TDP-43 RRM2.

In a mixture of PAR and T10 at equimolar concentration, we clearly detected a preferential binding of FUS RRM to PAR while TDP-43 RRM2 mostly interacts with T10 (Figure 24). In addition, WaterLOGSY analyses indicate a specific binding of FUS RRM to H8 and H2 atoms of ADP-ribose which is not the case for TDP-43 RRM2. The binding of FUS to H8 and H2 atoms is an additional evidence of the higher specificity of the binding of PAR to FUS RRM than to TDP-43 RRM2. To further explore the ability of FUS to bind to PAR, we probe whether FUS prevents PAR from interacting with TDP-43 RRM2. PAR induces some CSPs in TDP-43 RRM2 residues in the absence of FUS RRM. However, the addition of an equimolar concentration of non labelled FUS RRM dramatically reduced the CSPs induced by PAR in TDP-43 RRM2 residues (Figure 23B).

Altogether, our NMR data indicate that, even in the presence of oligonucleotides, FUS RRM is more likely to be directed to PAR compared to canonical RRM such as TDP-43 RRM2 and HuR RRM1, which most likely originates from the specific features of FET RRMs, namely a long positively charged KK-loop, absence of some aromatic residues in RNP1 motif).

Chapter 5: FUS RRM is important to increase the PARylation level in cells

To explore whether the RRM of FUS plays a specific role in the increase of PAR level in cells exposed to H_2O_2 , we replaced FUS RRM with the RRM1 of TDP-43. We preferred to use RRM1 rather than RRM2 because RRM2 has two Asp residues located in the short loop in between $\beta 3$ and $\beta 4$ sheets like in FUS and TAF15 proteins whose role in the binding of FUS to PAR will be investigated latter on in this paragraph. TDP-43 RRM1, like RRM2, has also the typical features of a canonical RRM with many aromatic residues in RNP1 motifs and no KK-loop like FET proteins (Figure 17). Endogenous FUS levels were decreased to better capture the impact of the FUS mutation in HeLa cells. HA-tagged wild-type and mutant FUS were then expressed in HeLa cells pretreated with siRNA targeting the 5'UTR of endogenous FUS transcripts. Importantly, our single cell analysis measured the overall PAR level in the nucleus with two different PAR antibodies that we validated under our experimental conditions (Figure 25).

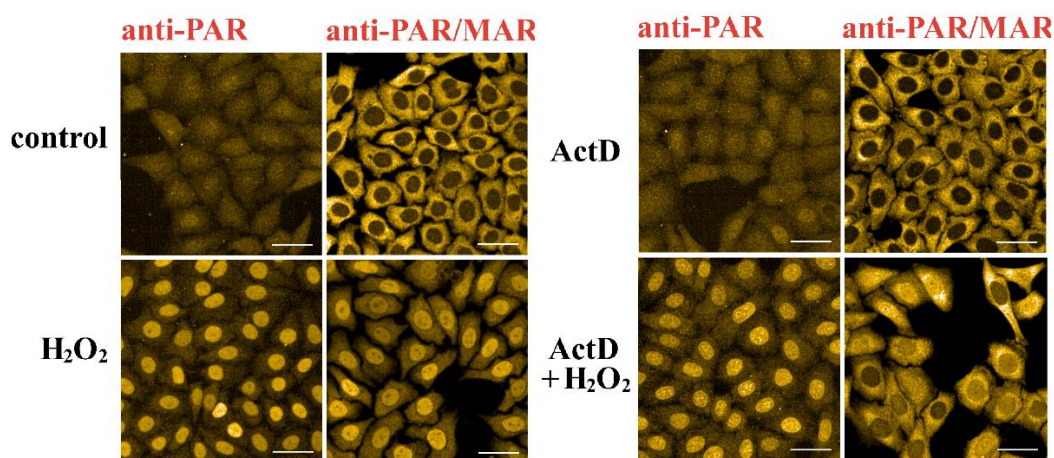


Figure 25: Cell pretreatment with ActD does not affect PAR level in control cells. A. Images of HeLa cells pre-treated or not with ActD (5 $\mu\text{g}/\text{ml}$, 1 h) prior to the activation of PARP-1 for 30 min with 100 μM H_2O_2 . The nuclear PAR was detected with two different antibodies. Scale bar: 50 μm .

In addition, we compared the PAR signal in nucleus expressing the same level of nuclear HA-tagged RBPs whatever their capacity to translocate in the cytoplasm under our experimental conditions. The level of PAR again strongly increases in HeLa cells expressing wild type HA-FUS when treated with H_2O_2 (Figure 26). The replacement of FUS RRM with the RRM-1 of TDP-43 completely alleviates the increase of PAR level (Figure 26). The RRM

of FUS may direct FUS to nascent mRNA in transcription active cells which provides an optimal protein location to increase PAR level when DNA damages occur. In addition, unlike non-FET RRM, FUS RRM has a comparable affinity for PAR and RNA (Figure 18). When TDP-43 RRM1 replaces FUS RRM in full length FUS, FUS may be routed on other RNA than nascent mRNA and/or lose its ability to quickly bind to PAR.

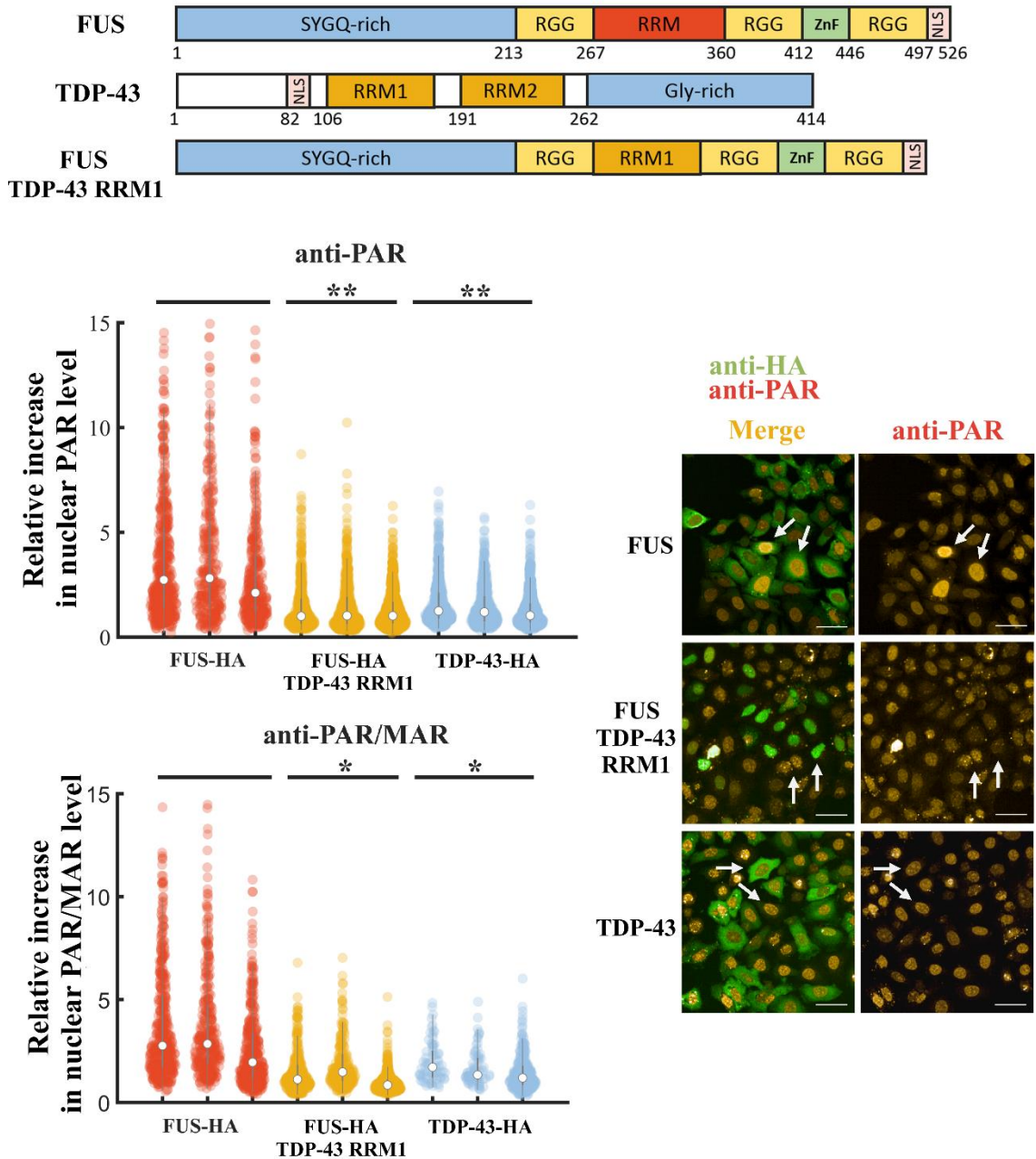


Figure 26: Exchanging FUS RRM with the RRM1 of TDP-43 completely alleviates the increase of PAR level observed in HA-FUS-expressing cells. Upper panel: the domain structures of FUS, TDP-43 and FUS with the substitution of its RRM domain to the RRM1 domain of TDP-43. Lower panels: Violin plots representing the relative increase of nuclear PAR in HeLa cells expressing indicated HA-tagged RBP versus control HeLa cells (left) and corresponding representative cell images (right). The quantitative results are shown for the two different antibodies. Each condition is shown in triplicate. n.s., non-significant, * $p < 0.05$; ** $p < 0.01$; t-test versus FUS-HA expressing cells. Note the high PAR level in cells expressing FUS-HA (shown by white arrows). Scale bar: 50 μm .

To further confirm our results and scrutinize how FUS RRM may control PARP-1 activity, we tested whether specific residues located in the FUS RRM increase PAR level in ActD and H₂O₂-treated HeLa cells (Figure 27). We considered the mutations whose impact on FUS RRM interaction with PAR were already assessed by NMR spectroscopy (Supplementary Figure S8), K315A/K316A, N284A, D342A, or D343A. To this end, we performed addback experiments in which endogenous FUS expression is reduced before expressing FUS mutants in HeLa cells (Figure 27). Even if K315A/K316A and N284A mutants of FUS RRM have a decreased CSPs in the presence of PAR compared to wild type RRM (Supplementary Figure S6 and S8), adding back the expression of these FUS mutants (K315A/K316A or N284A) in siFUS-pretreated cells did not affect the PAR level. In contrast, compared to wild type FUS, adding back FUS D343A or D342A significantly lower PAR levels in ActD and H₂O₂-treated cells (Figure 27). The PARylation level of FUS D343A is also slightly lower than that of WT FUS (Chapter 6), but this could not account for the global decrease in total PAR synthesis in cells expressing FUS D343A because FUS represents only a small fraction of PAR acceptors in cells.

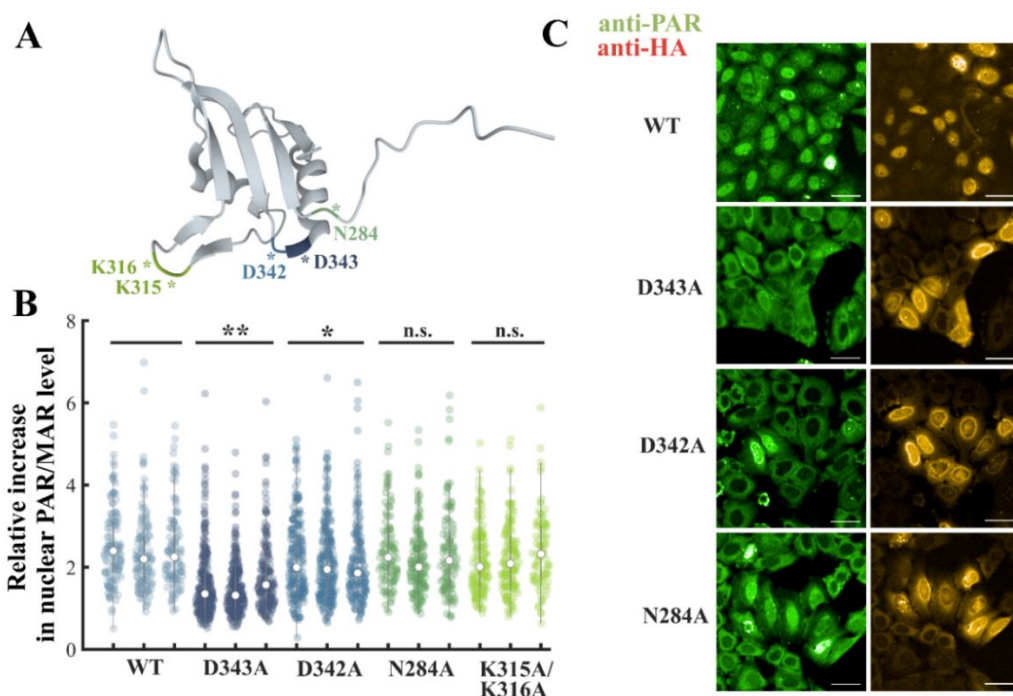


Figure 27: D343A mutation of FUS significantly decreases PAR level in ActD and H₂O₂-treated cells. A. FUS RRM structure (PDB DOI: [10.2210/pdb2LCW/pdb](https://doi.org/10.2210/pdb2LCW/pdb)) in which the positions of N284, K315, K316, D342 and D343 residues are indicated. B. Violin plots representing the relative increase of nuclear PAR in HeLa cells treated with siRNA to reduce FUS endogenous expression and expressing indicated FUS-HA mutants versus control HeLa cells. Each condition is shown in triplicate. n.s., non-significant, *p < 0.05; **p < 0.01; t-test versus WT FUS-HA expressing cells. C. Representative cell images corresponding to violin plot data. Scale bar: 30 μ m.

Chapter 6: D343A mutation interferes with the interaction of FUS RRM with activated PARP-1

The data obtained in cells with the FUS D343A mutant cannot show whether D343A directly impaired the interaction between activated PARP-1 and FUS, though D343A and wild type FUS has similar affinity for PAR and RNA (Supplementary Figure S6 and S8). A doubt remains since D343A RRM interaction with purified PAR and RNA is very similar to that of wild-type FUS RRM as evidenced by NMR spectroscopy (Supplementary Figure S6 and S8). We then devised to perform a unique assay in which the interaction of FUS RRM with PARP-1 activated by damaged DNA can be captured by NMR spectroscopy. To this end, we first controlled that PARP-1 consumption of NAD^+ upon its activation by damaged DNA can be followed by NMR spectroscopy using recombinant PARP-1 and DNA duplexes (30 bp) containing one nucleotide gap. After the addition of DNA duplex, the synthesis of poly(ADP-ribose) was clearly evidenced in 1D NMR spectra through the progressive decrease in NAD^+ proton intensities and the increase of those of nicotinamide with time (Figure 28).

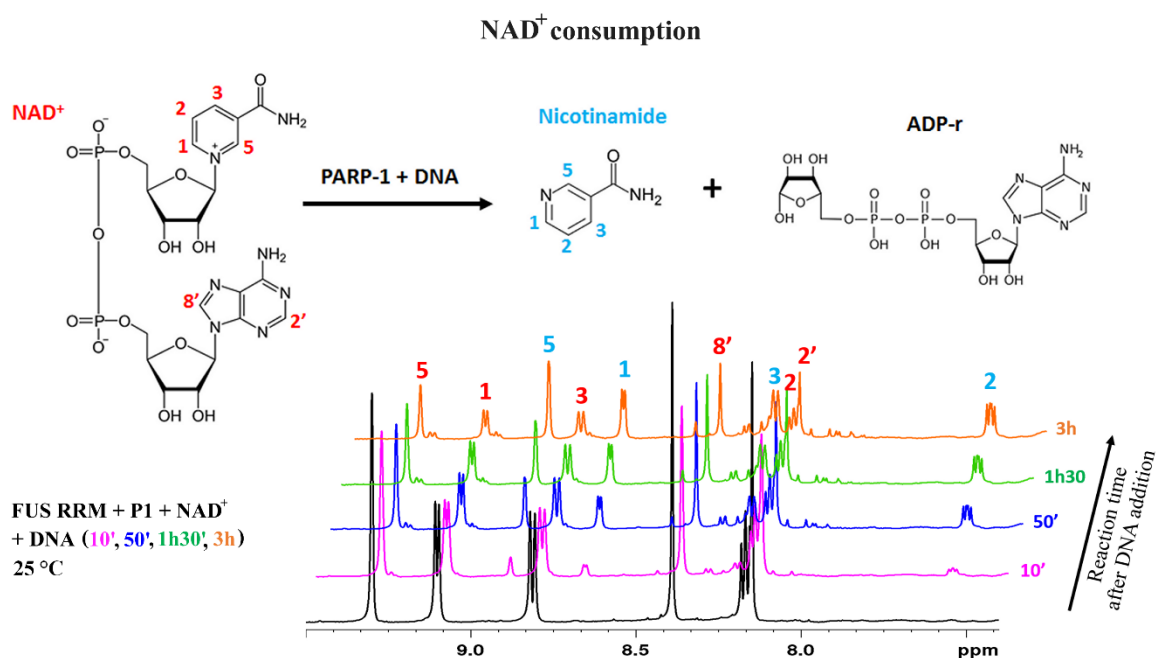


Figure 28: 1D NMR spectra showing the gradual consumption of NAD^+ upon the activation of PARP-1 in the presence of damaged DNA. Upper schema: schematic PARP-1 catalyzed reaction which leads to hydrolysis of NAD^+ to nicotinamide and ADP-ribose. P1 is PARP-1. NAD^+ and nicotinamide signals are labeled with red and blue numbers, respectively.

Then, we analyzed 2D SOFAST-HSQC spectra of wild-type FUS RRM and D343A RRM residues after PARP-1 activation by DNA duplex. Unexpectedly, we found a significant difference in the spectra. D343A RRM mutant interacted strongly with activated PARP-1 with the appearance of double peaks or their disappearance for some residues, which was not observed in the same conditions with wild-type FUS RRM (Figure 29). The disappearance of residues may be consecutive to changes in the exchange dynamics between free and bound states. The presence of double peaks is rather related to a slow exchange between two different states. As the residues with double peaks displayed no or limited CSPs in the presence of PAR, the presence of doubled peaks may result in the PARylation of a fraction of these RRM residues.

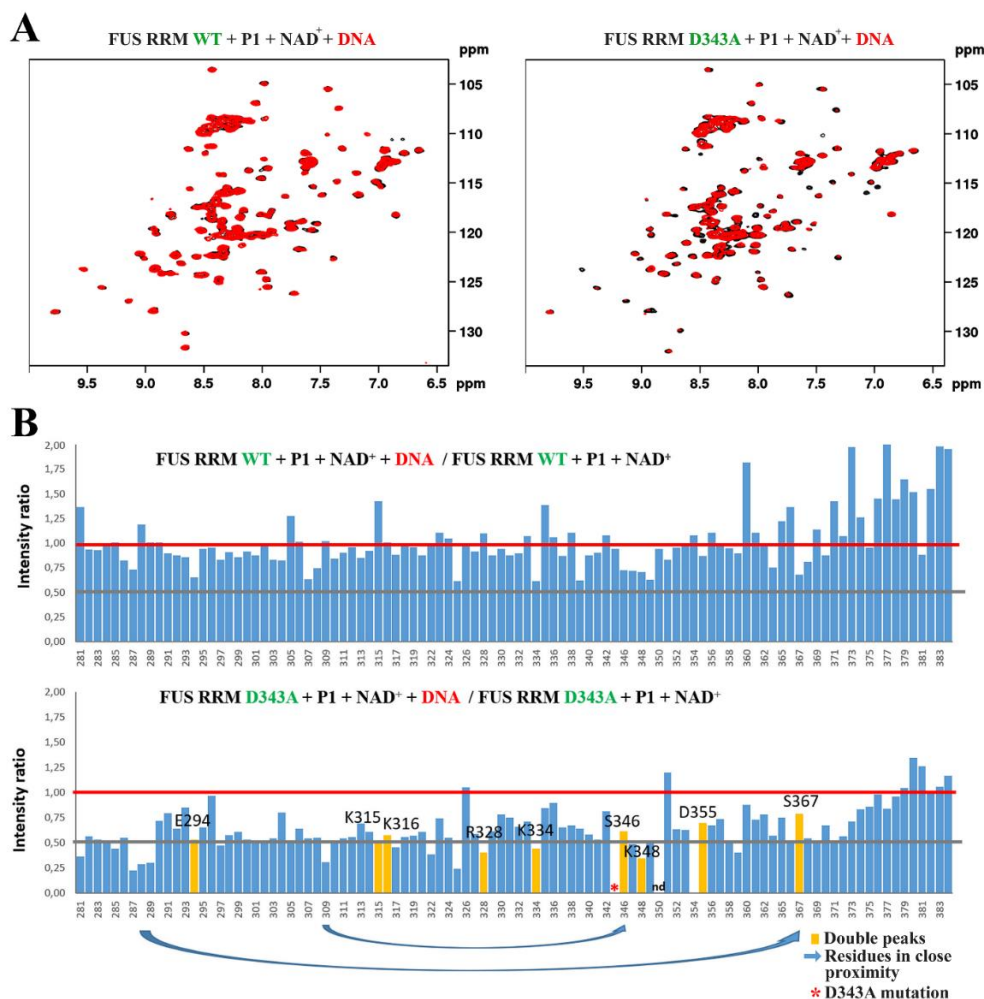


Figure 29: A significant difference in the interaction of D343A FUS RRM mutant and wild-type FUS RRM with activated PARP-1. A. ¹H-¹⁵N HSQC spectra of wild type and D343A FUS RRM in the presence (red) or absence (black) of damaged DNA to activate PARP-1. Note in the inset the broadening of some D343A RRM residues after the activation of PARP-1 but not for wild-type FUS RRM. B. Histograms showing the intensity ratio of the resonance peaks of RRM residues for wild type and D343A FUS RRM before and after PARP-1 activation. In yellow, residues having doubling peaks. Blue arrows: residues in close proximity to disappearing/doubling peak residues. Red asterisk: Mutated residue, D343.

Further analysis of the CSPs reveals the presence of many double peak residues, notably from charged residues that can be potentially PARylated, E294, K315, K316, R328, K334, and D355 (Figure 29 and 30).

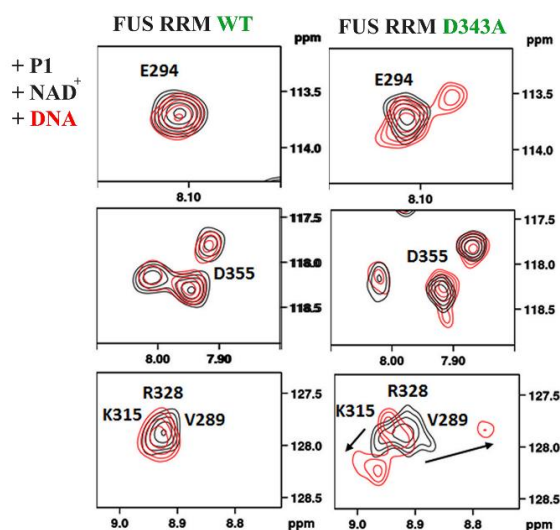


Figure 30: Zoom in on several residues experiencing doubling peaks in D343A FUS RRM after PARP-1 activation.

As NMR data reveal an increased interaction of D343ARRM with activated PARP-1, we then directly measured whether D343A FUS RRM is hyperPARylated *in vitro*. We first remarked the similarity in the low PARylation level of the FUS RRM and TDP-43 RRM2 *in vitro* (Figure 31).

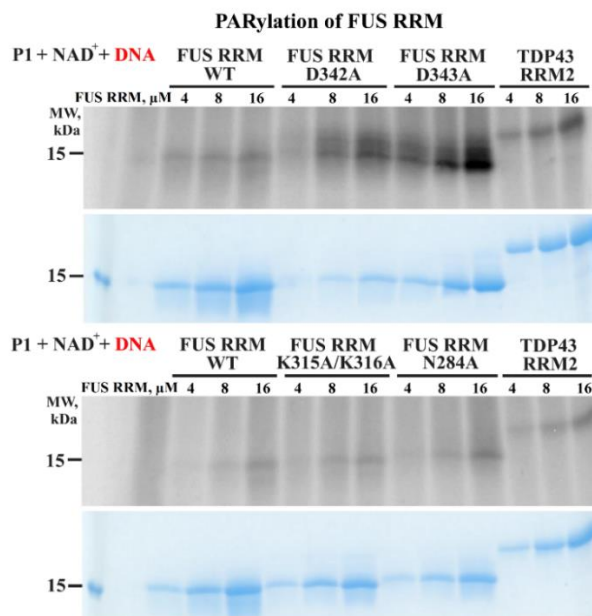


Figure 31: D343A FUS RRM is hyperPARylated *in vitro* compared to wild-type FUS RRM. SDS-PAGE followed by phosphorimage analysis of protein PARylation after PARP-1 activation in the presence of DNase-activated DNA and [³²P]-NAD⁺ (0.4 mCi) for indicated concentrations of different RRM fragments. Note the increase in the level of RRM PARylation in the case of D343A mutant and, to a lesser extent, in the case of D342A mutant. The experiment was performed in two repeats.

In contrast, the PARylation of full-length FUS is very significant but not that of full-length TDP-43 (Figure 32).

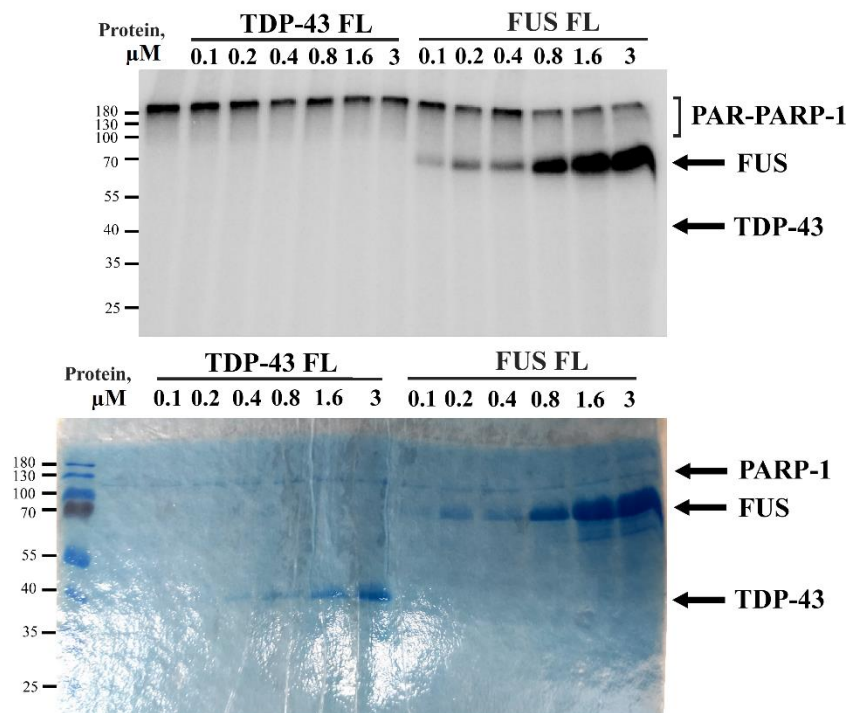


Figure 32: Full length FUS but not TDP-43 is highly PARylated by PARP-1 *in vitro*. Analysis of the PARylation of RNA-binding proteins TDP-43 and FUS (from 0.1 μM to 3 μM) by PARP-1 (100 nM) in the presence of DNase-activated DNA and [^{32}P]-NAD $^{+}$ (0.4 μCi). The reaction mixtures were analyzed by SDS-PAGE with subsequent phosphorimaging (upper panel) and Coomassie blue staining (lower panel). Note the PARylation of FUS compared to the PARylation of TDP-43.

Therefore, RRM fragments could not capture the significant PARylation of full-length FUS *in vitro*, which may mostly rely on the presence of other FUS domains such as the RGG domains. However, D343A RRM, but not wild-type FUS RRM or TDP-43 RRM2, is strongly PARylated (Figure 32). We also note that none of the other mutations (K315A/K316A, N284A) affect the PARylation of FUS RRM except D342A which increases the PARylation to a lesser extent than D343A.

As FUS D343A expressing cells display a reduced nuclear PAR level compared with wild-type FUS-expressing cells (Chapter 5, Figure 27), we also analyzed the PARylation of full-length wild-type and D343A FUS *in vitro* (Figure 33, Supplementary Figure S4 and S5). Wild-type FUS is strongly PARylated but also slightly reduces PARP-1 autoPARylation (Supplementary Figures S4 and S5). Compared to wild-type FUS, full length mutant D343A significantly increases PARP-1 autoPARylation level (Figure 33 and Supplementary Figures S4 and S5). Altogether, these results indicate that D343A mutation can influence PARP-1

activity by increasing PARP-1 autoPARylation and/or reducing the PARylation of acceptor proteins like FUS. Interestingly, both an increased autoPARylation of PARP-1, which in turn increases PARP-1 dissociation rate from damaged DNA, and a reduction of acceptor protein PARylation can lead to the overall decrease in PAR level as observed in cells expressing FUS D343A instead of wild-type FUS upon H₂O₂ and ActD exposure (Figure 27).

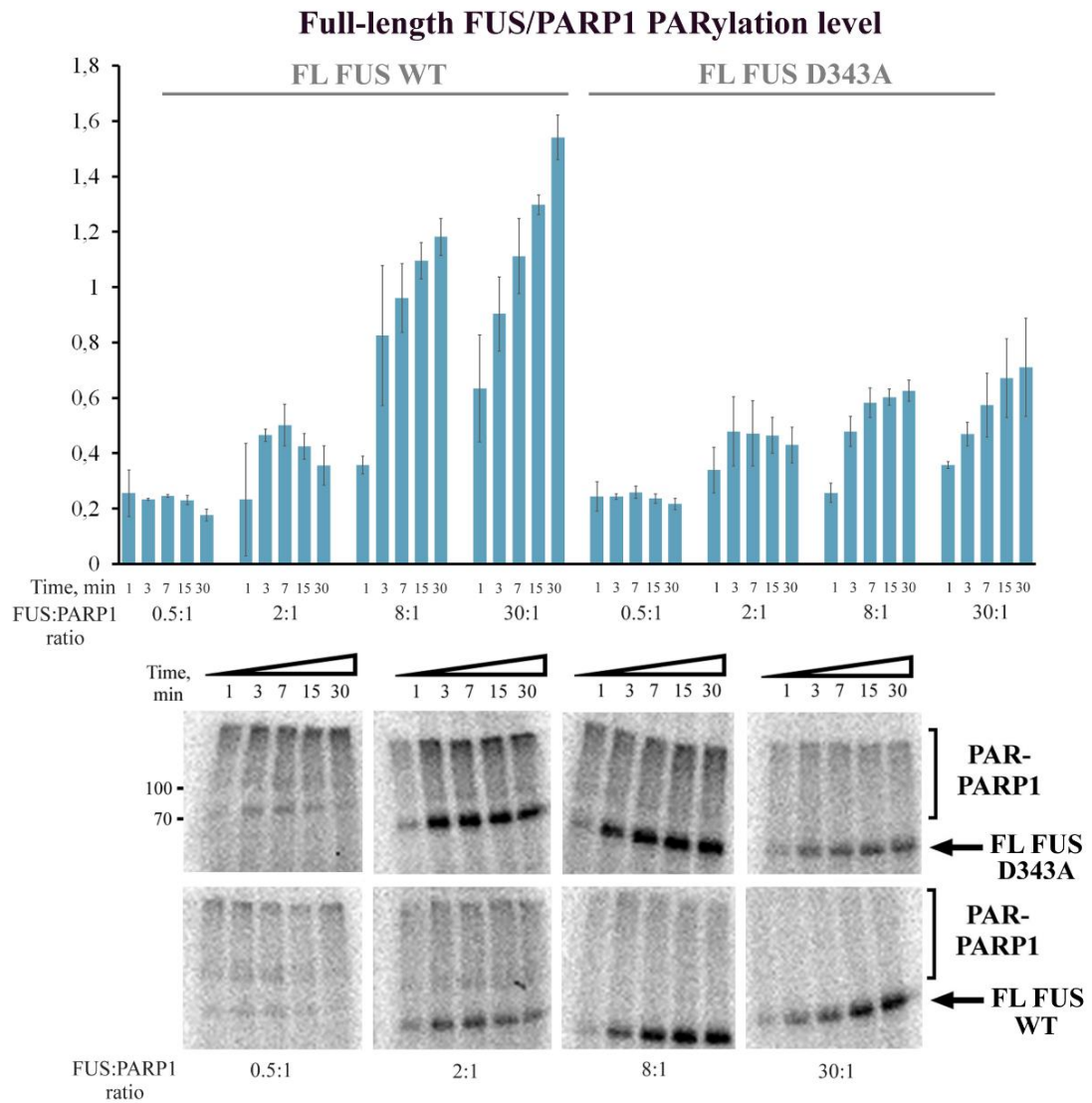


Figure 33: D343A mutation in full length FUS protein increases PARP-1 autoPARylation *in vitro*. Upper panel: Analysis of FUS/PARP-1 PARylation ratio for WT FUS or FUS D343A. PARylation took place in the presence of DNaseI-activated DNA, [³²P]-NAD⁺ (0.4 mCi) and indicated FUS:PARP-1 molar ratios. PARP-1 :100 nM. (see Materials and Methods for details). FUS/PARP-1 PARylation ratio was measured as the mean ± SD of three independent experiments. Lower panel: SDS-PAGE analysis with subsequent phosphorimaging for indicated times after PARP-1 activation in the presence of DNase-activated DNA and [³²P]-NAD⁺ (0.4 mCi) and indicated FUS:PARP-1 molar ratios (see Supplementary Figures S4 and S5 for details).

Supplementary information

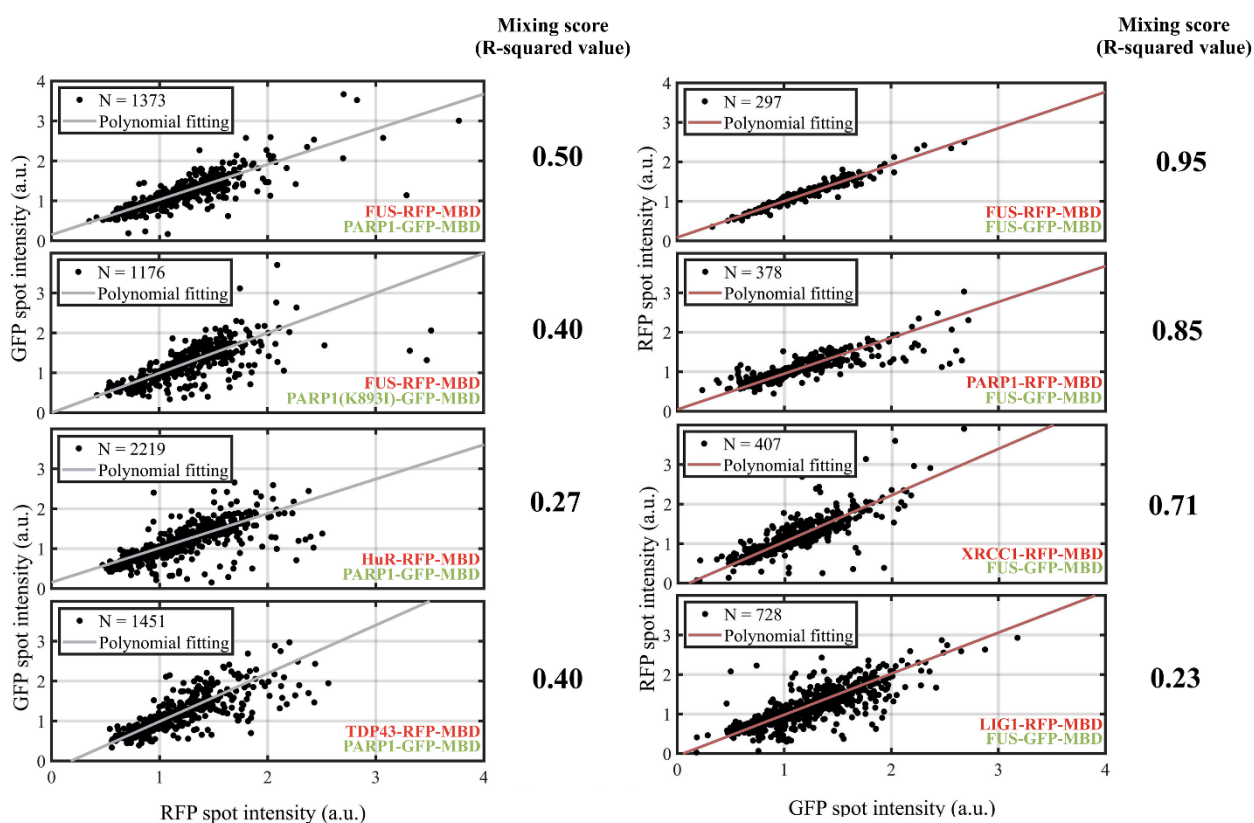


Figure S1: Representative scatter plots of relative GFP and RFP fluorescence intensity in each spot on the microtubules of HeLa cells co-transfected with indicated plasmids. N is a number of analyzed spots. The mixing score indicated on the figure 2 (Results, Chapter 1) is calculated as the coefficient of determination (R-squared value), showing how well the regression model (polynomial fitting shown in gray) fits the observed data. MBD: Microtubule Binding Domain.

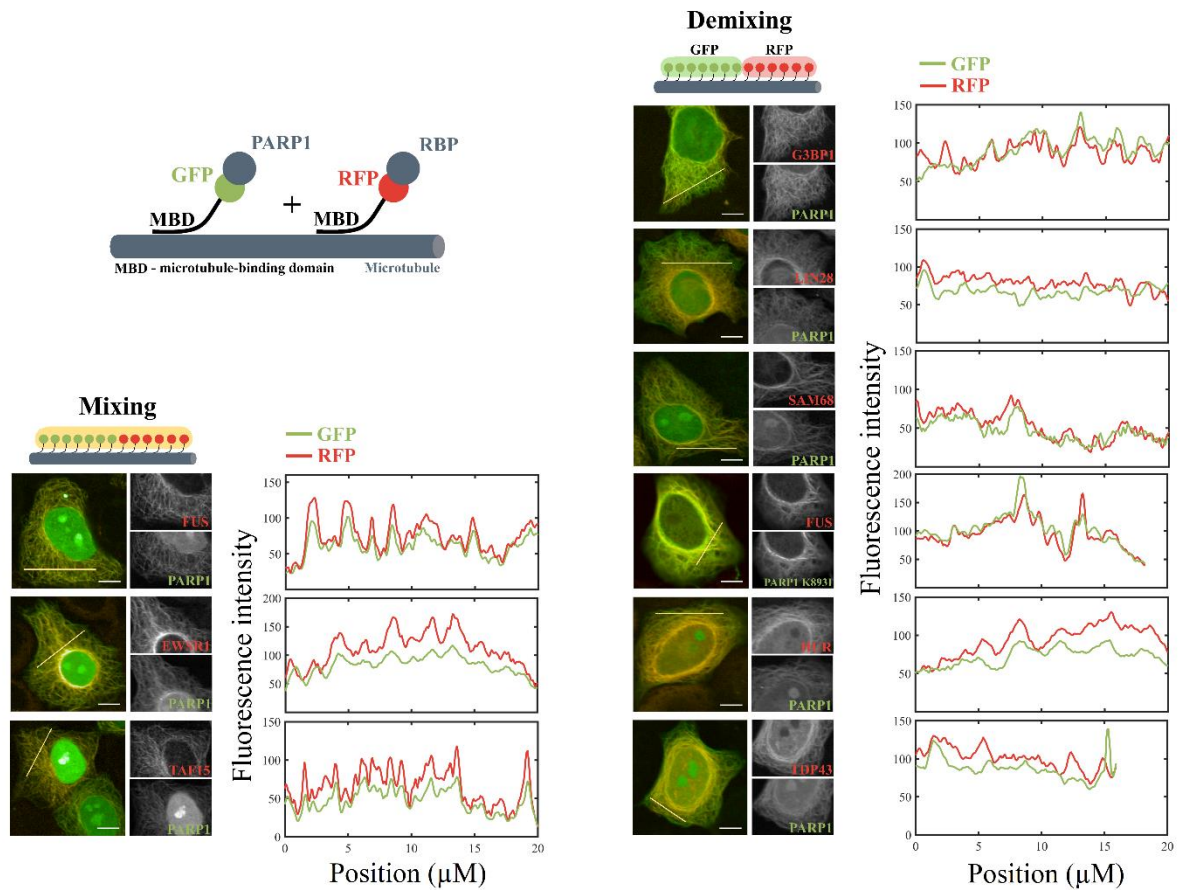


Figure S2: PARP-1 mixes well along microtubules with FET proteins but less so with the other RBPs tested. Scheme representing the microtubule bench assay used to probe interactions between PARP-1 and RNA-binding proteins (above). Images of HeLa cells co-expressing GFP-labeled PARP-1 and indicated RFP-labeled RNA-binding protein and representative line profiles of the fluorescence intensity along the yellow line. The line profiles show the mixing of FET proteins (FUS, EWSR1 and TAF15) or the other RBPs with PARP-1. Scale bar: 8 μm .

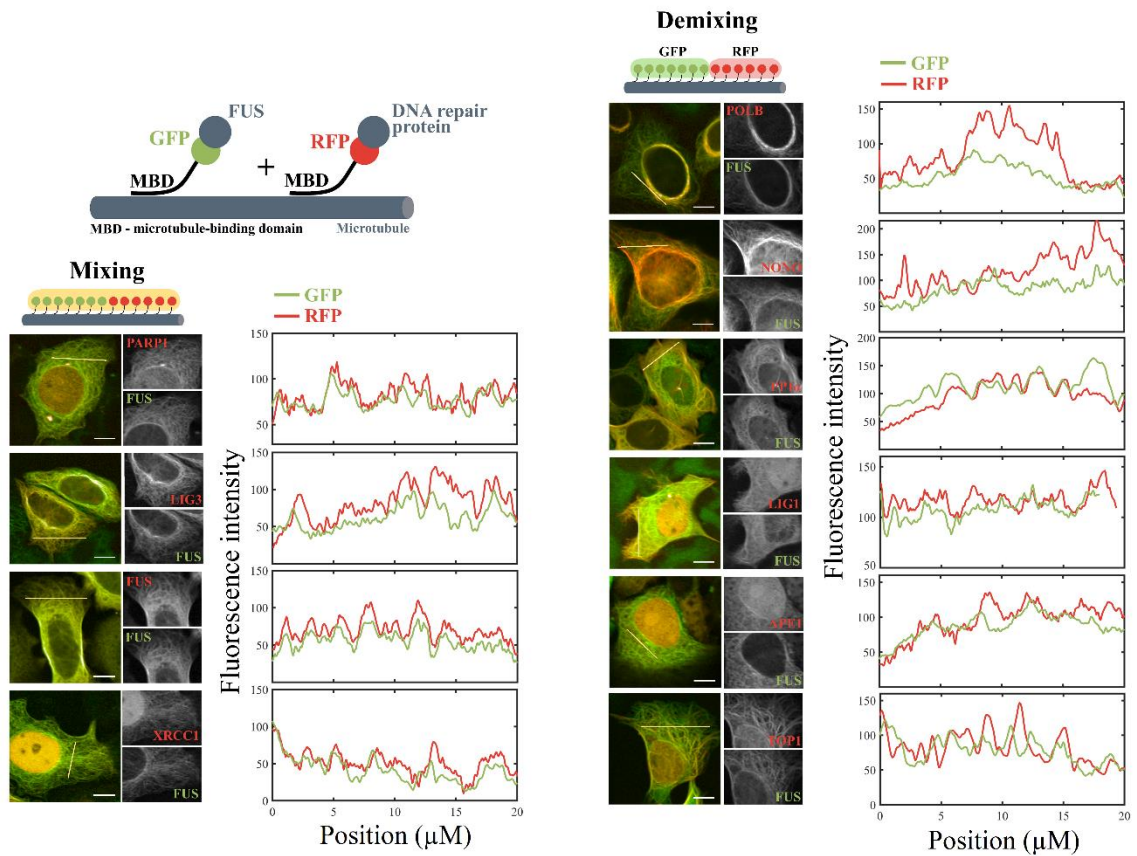


Figure S3: FUS mixes well along microtubules with PARP-1, XRCC1 and LIG3 but less with other DNA repair proteins tested. Scheme representing the microtubule bench assay used to probe interactions between FUS and DNA repair proteins (above). Images of HeLa cells co-expressing GFP-labeled FUS and indicated RFP-labeled DNA repair protein and representative line profiles of the fluorescence intensity along the yellow line. Note the alignment of RFP and GFP line profiles when tested proteins are mixing along microtubules. MBD: Microtubule Binding Domain. Scale bar: 8 μm .

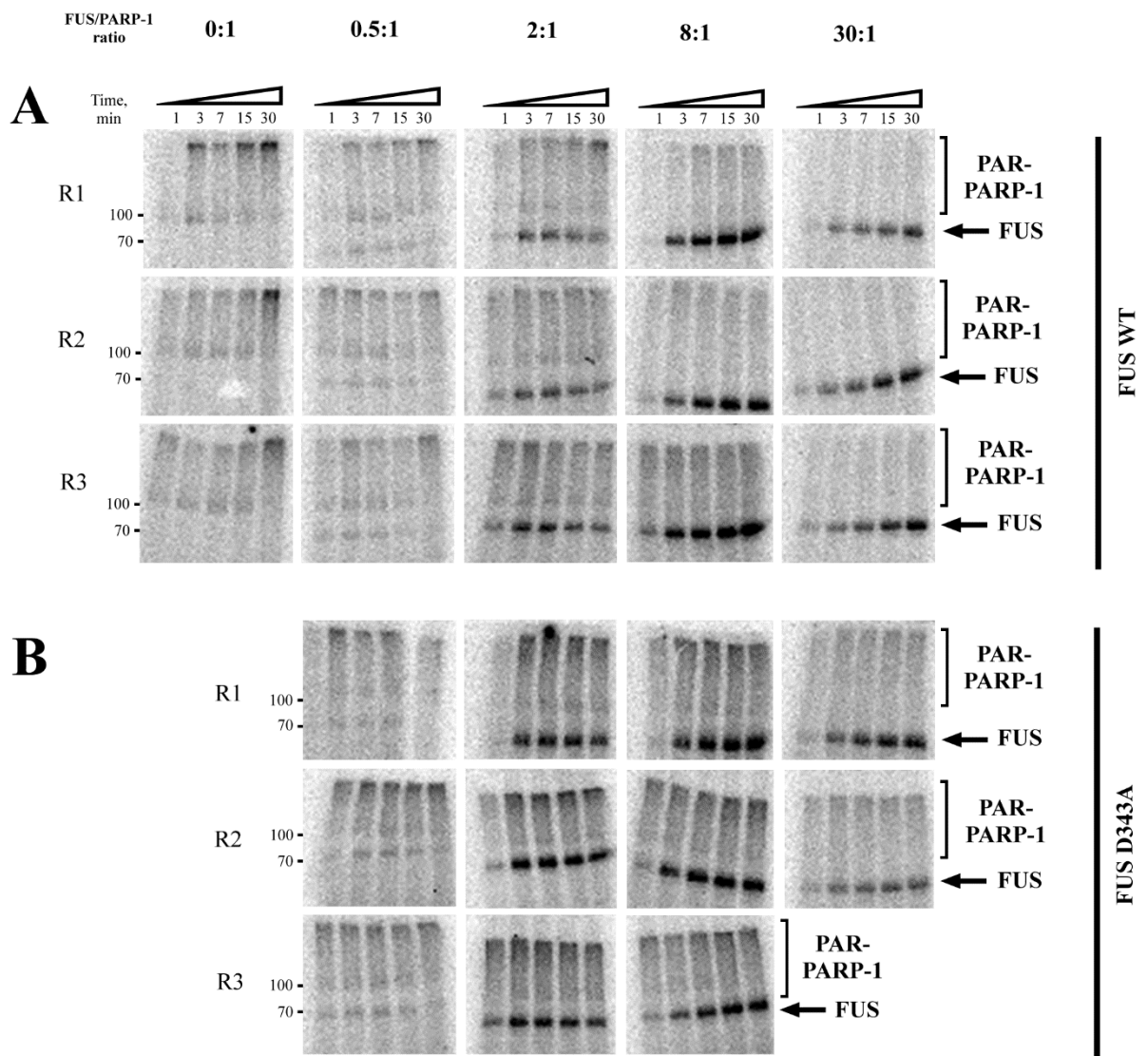


Figure S4: D343A changes the balance between PARP-1 and acceptor protein PARylation (A. FUS WT, B. FUS D343A). Analysis of the PARylation of FUS WT or FUS D343A (0.05, 0.2, 0.8 and 3 μ M) by PARP-1 (100 nM) in the presence of DNase-activated DNA and [32 P]-NAD $^{+}$ (0.4 μ Ci) after 1, 3, 7, 15 and 30 min of reaction. The reaction mixtures were analyzed by SDS-PAGE. The experiment was performed in three repeats (R1-R3).

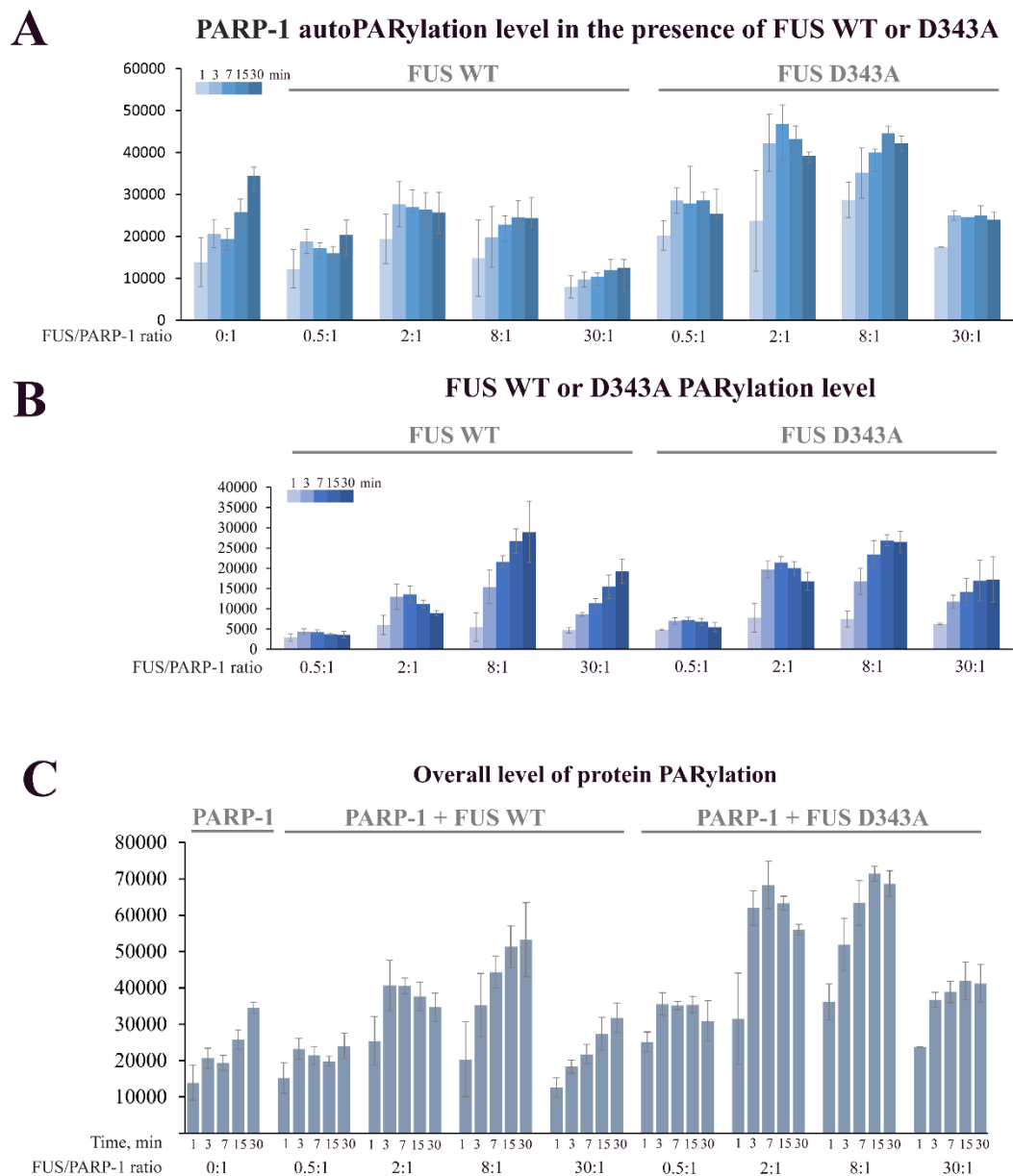


Figure S5: D343A favors PARP-1 autoPARylation at the expense of FUS PARylation. Analysis of the PARylation of FUS WT or FUS D343A (0.05, 0.2, 0.8 and 3 μ M) by PARP-1 (100 nM) in the presence of DNase-activated DNA and [32 P]-NAD $^{+}$ (0.4 μ Ci) after 1, 3, 7, 15 and 30 min of reaction. The reaction mixtures were analyzed by SDS-PAGE (Supplementary Figure S4). PARP-1 autoPARylation level (A), FUS PARylation level (B) and overall protein PARylation level (C) were calculated (the mean \pm SD of three independent experiments and individual data points). Note the increased level of PARP-1 autoPARylation in the presence of FUS D343A mutant compared to FUS WT (A).

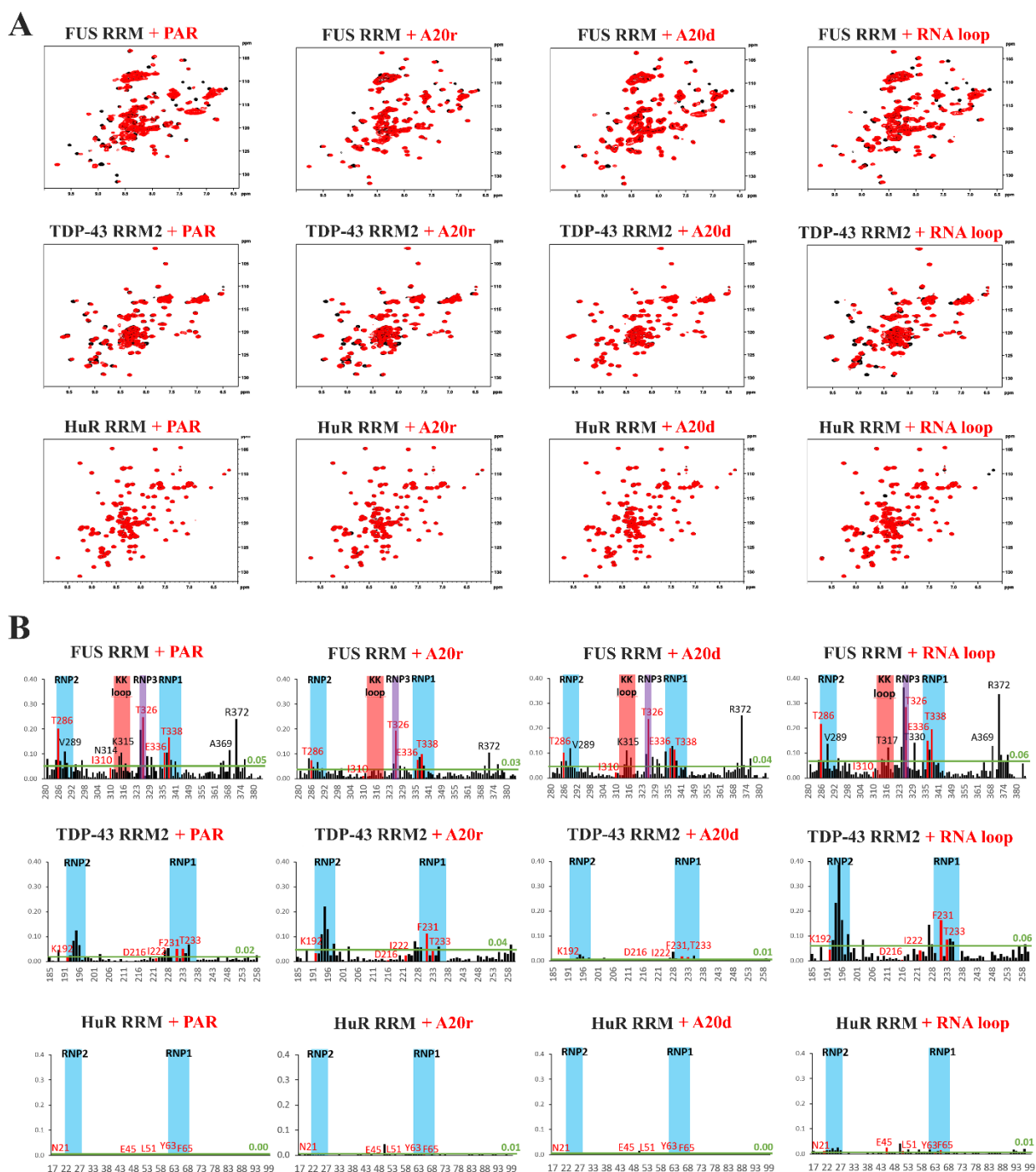


Figure S6: NMR analysis of the binding of FUS , TDP and HuR RRMs to various nucleic acids (RNA and ssDNA). A. Two-dimensional ^1H - ^{15}N HSQC spectra of ^{15}N -labeled FUS RRM, TDP43 RRM2 or HuR RRM residues in the apo state (black) and in the presence of PAR, A20r, A20d or hnRNP2/B1 RNA loop (red). B. Histograms displaying the CSPs of indicated RRM residues for FUS RRM, TDP43 RRM2 and HuR RRM in the presence of PAR, A20r, A20d or RNA loop compared to RRM of FUS, TDP43 or HuR alone. Note the significant CSPs observed for FUS RRM in the presence of PAR and RNA loop.

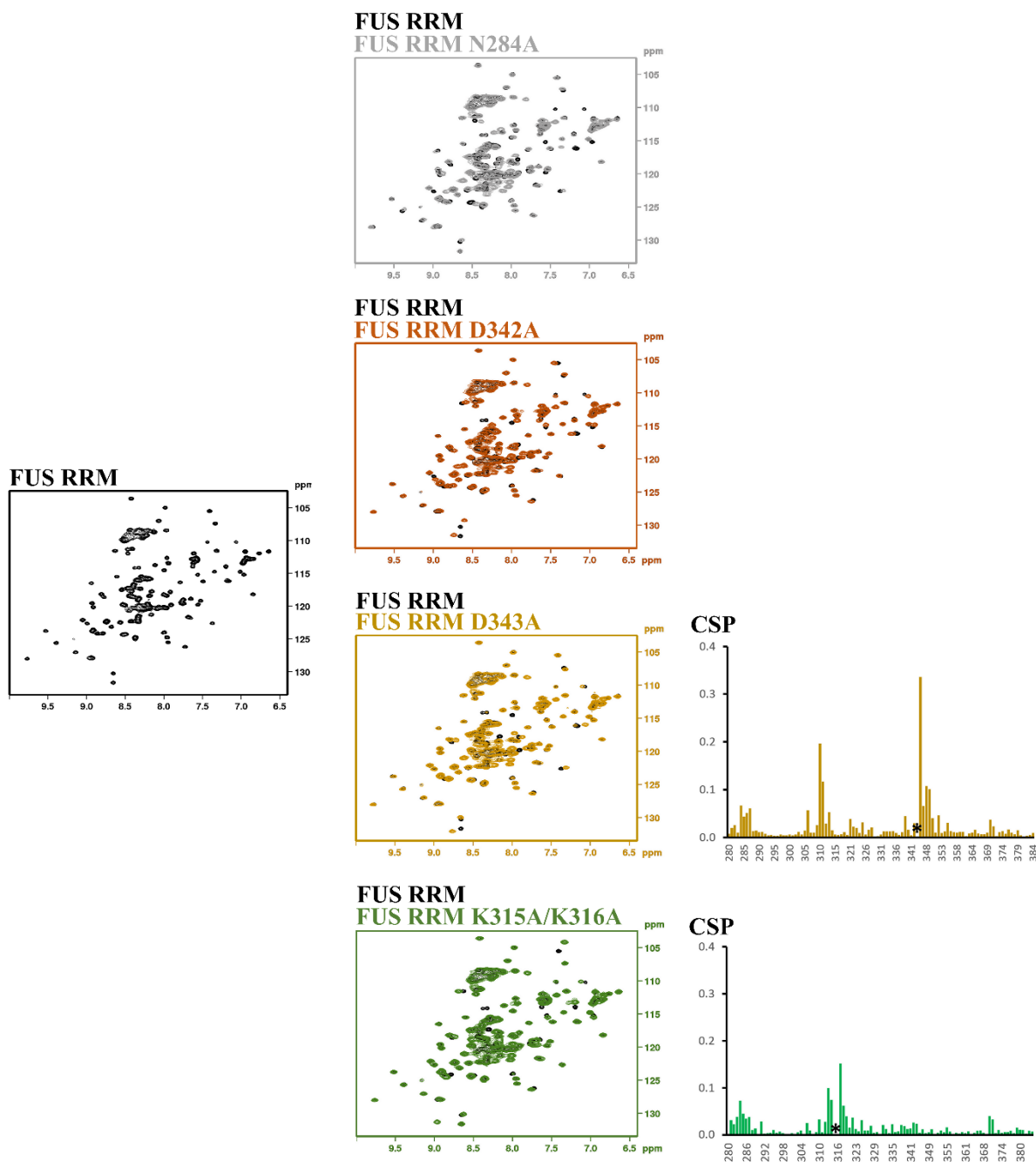


Figure S7: Varying CSPs induced by point mutation in the RRM of FUS (N284A, D342A, D343A and K315A/K316A). Left panel: two-dimensional ^1H - ^{15}N HSQC spectrum of ^{15}N -labeled FUS RRM. Middle panel: two-dimensional ^1H - ^{15}N HSQC spectra of ^{15}N -labeled FUS RRM (black) and FUS RRM N284A (gray), FUS RRM D342A (orange), FUS RRM D343A (yellow) or FUS RRM K315A/K316A (green). Right panel: histograms displaying the CSPs of indicated RRM residues for FUS RRM compared to FUS RRM D343A (yellow) or FUS RRM K315A/K316A (green). None of the mutations change the overall RRM structures besides some CSPs in a region around the mutation. *: position of the mutated residues in the histogram.

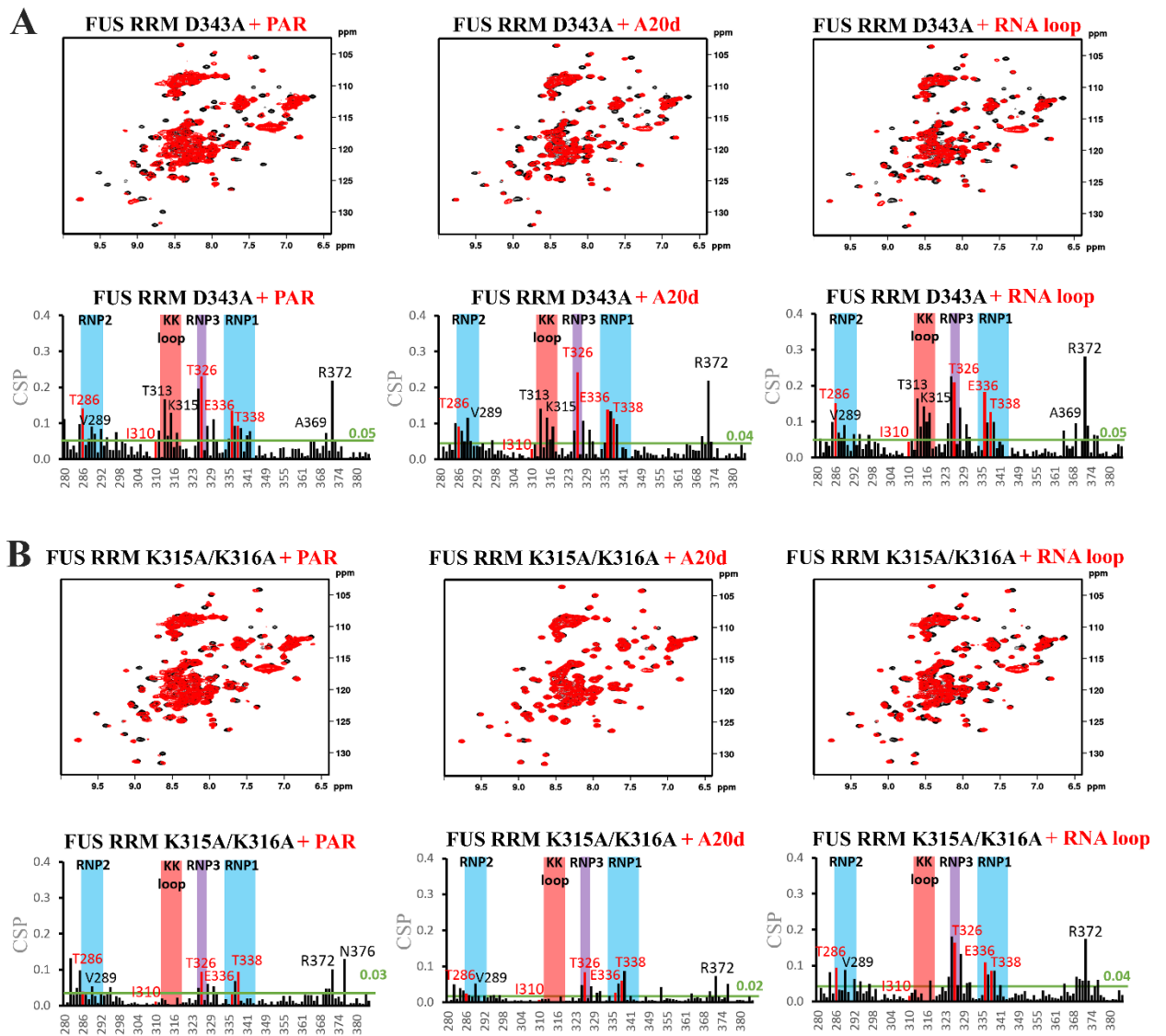


Figure S8: D343A RRM still binds to PAR while K315A/316A RRM displays a reduced affinity for PAR, RNA and ssDNA. A. Upper panel: two-dimensional ^1H - ^{15}N HSQC spectra of ^{15}N -labeled FUS RRM D343A residues in the apo state (black) and in the presence of PAR, A20d or nhRNP2/B1 RNA loop (red). Lower panel: histograms displaying the CSPs of indicated RRM residues for FUS RRM D343A in the presence of PAR, A20d or RNA loop compared to FUS RRM D343A alone. B. Upper panel: two-dimensional ^1H - ^{15}N HSQC spectra of ^{15}N -labeled FUS RRM K315A/K316A residues in the apo state (black) and in the presence of PAR, A20d or nhRNP2/B1 RNA loop (red). Lower panel: histograms displaying the CSPs of indicated RRM residues for FUS RRM K315A/K316A in the presence of PAR, A20d or RNA loop compared to FUS RRM K315A/K316A alone. Note the decrease of FUS RRM K315A/K316A binding to PAR compared to FUS RRM WT (Supplementary Figure S6).

Discussion

FUS is a protein which was first associated with cancers and for which, like the other FET family proteins, TAF15 and EWSR1, fusions with transcription factors are known to drive cancers (Literature review, Chapter 3) (Kovar *et al.*, 2010; Abraham *et al.*, 2015). More recently, the identification of pathological mutations and the presence of FUS in cytoplasmic inclusions in several neurodegenerative diseases including ALS have highlighted the role of FUS in neurodegenerative diseases (Literature review, Chapter 3.4.1) (Vance *et al.*, 2009). In addition, a link between the progression of neurodegenerative diseases and the deregulation of DNA repair has made its way (Maynard *et al.*, 2015). FUS in its wild form seems to be particularly involved in DNA repair mechanisms. In addition, pathological mutations may alter the ability of FUS to participate in these mechanisms (Naumann *et al.*, 2018; Wang *et al.*, 2018). However, the pathway by which FUS, a nuclear mRNA-binding protein, participates in DNA repair has not yet been clearly established. FUS interacts with PAR, the polymer produced by PARP-1 after the recognition of DNA breaks (Altmeyer *et al.*, 2015; Rulten *et al.*, 2014; Mastrocola *et al.*, 2013). The interaction of FUS with protein-free PAR, mostly with its RGG domains, promotes the formation of compartments behaving like liquid phases (Literature review, Chapter 3.3.1) (Patel *et al.*, 2015). FUS can also form dynamic and PARG-reversible compartments in the presence of damaged DNA following PARP-1 activation, bringing this model even closer to physiological conditions (Singatulina *et al.*, 2019). Here, using NMR spectroscopy analysis, we show that FUS interacts in a specific way with PAR thanks to its RRM domain which shares specific characteristics with other FET proteins, TAF15 and EWSR1, but a similar interaction cannot take place with other RRM harboring proteins in mammalian cells. First of all, some aromatic residues which are generally present on the RNP motifs are absent in FUS RRM (Chapter 4; Figure 17) (Loughlin *et al.*, 2019). The absence of these residues that interact with RNA bases through hydrophobic interactions explains the low binding specificities of FUS to mRNA that has been observed in genome-wide CLIP data (Rogelj *et al.*, 2012). PAR resembles RNA from a structural point of view but the bases are separated by two phosphate groups instead of one for RNA. The lack of aromatic residues of the RNP motifs could therefore explain the similar interaction of

FUS with PAR and mRNA while canonical RRM proteins which have all their aromatic residues prefer to bind to RNA. Finally, to compensate for the loss of interaction due to the missing aromatic residues, FUS like other FET proteins harbors a long positively charged loop, the KK-loop (*Liu et al., 2013*), which interacts electrostatically with both RNA and PAR (Chapter 4; Figure 18 and 19). FUS RRM thus has a similar electrostatic interaction with PAR and RNA which, based on our model and our results obtained with the RRM of HuR and TDP-43 (Chapter 4; Figures 18 and 19), should not be found in other RNA-binding proteins possessing canonical RRMs. By promoting the recruitment to PARylated PARP-1, the dual and competitive interaction of PAR and RNA with FUS RRM explains the high occurrence of FET proteins in proteomic data generated to identify PARylated proteins following oxidative stress, while the presence of arginine-rich low complexity domain is quite common among RNA-binding proteins (*Jungmichel et al., 2013; Zhang et al., 2013; Thandapani et al., 2013*).

Reducing the expression of FUS has no effect on PAR level in HeLa cells after H₂O₂ treatment (Chapter 2; Figure 7), which we attributed to compensatory expression of other FET proteins. However, the overexpression of HA-FUS, but not HA-HuR or HA-TDP-43, increases the level of PAR synthesis in cells subjected to oxidative stress (Chapter 2; Figure 8). The most significant increase in the level of PAR is observed when transcription is stalled and when oxidative stress does not exceed a certain level (H₂O₂ < 300 μM). These last two points are important. The need to stop transcription reflects a competition between the binding of FUS to nascent mRNA and PAR. However, the binding of FUS to nascent mRNA may turn into an advantage to direct FUS to PARP-1 at DNA damages which more likely occurred in transcription-active open chromatin (*Takata et al., 2013; Amouroux et al., 2010*). Consistently, a global transcription inhibition increases the sensitivity of our cell assays. However, when few DNA damages take place, transcription is locally stalled which may release protein factors, such as FUS, associated to nascent mRNA nearby the site of DNA damages. While a higher concentration of H₂O₂ (> 300 μM) allows more DNA damages and an increase in overall PAR level (Chapter 2; Figure 9), the capacity of FUS to increase PAR level is altered significantly. Under these conditions, many PARP-1 molecules are activated in the nucleus, which could disperse FUS proteins over a

large number of DNA damage sites and prevent several FUS from being directed to the same DNA damage site. Consistently with this model, we show that FUS has the ability to significantly increase the level of PARylation *in vitro* at elevated FUS:PARP-1 ratios by serving as a PAR acceptor (Chapter 3; Figure 16). In cells, it is also not excluded that additional protein partners are recruited in a compartment formed by FUS following the activation of PARP-1 to be themselves PARylated such as XRCC1. All these results lead us to propose the following scheme (Figure 34).

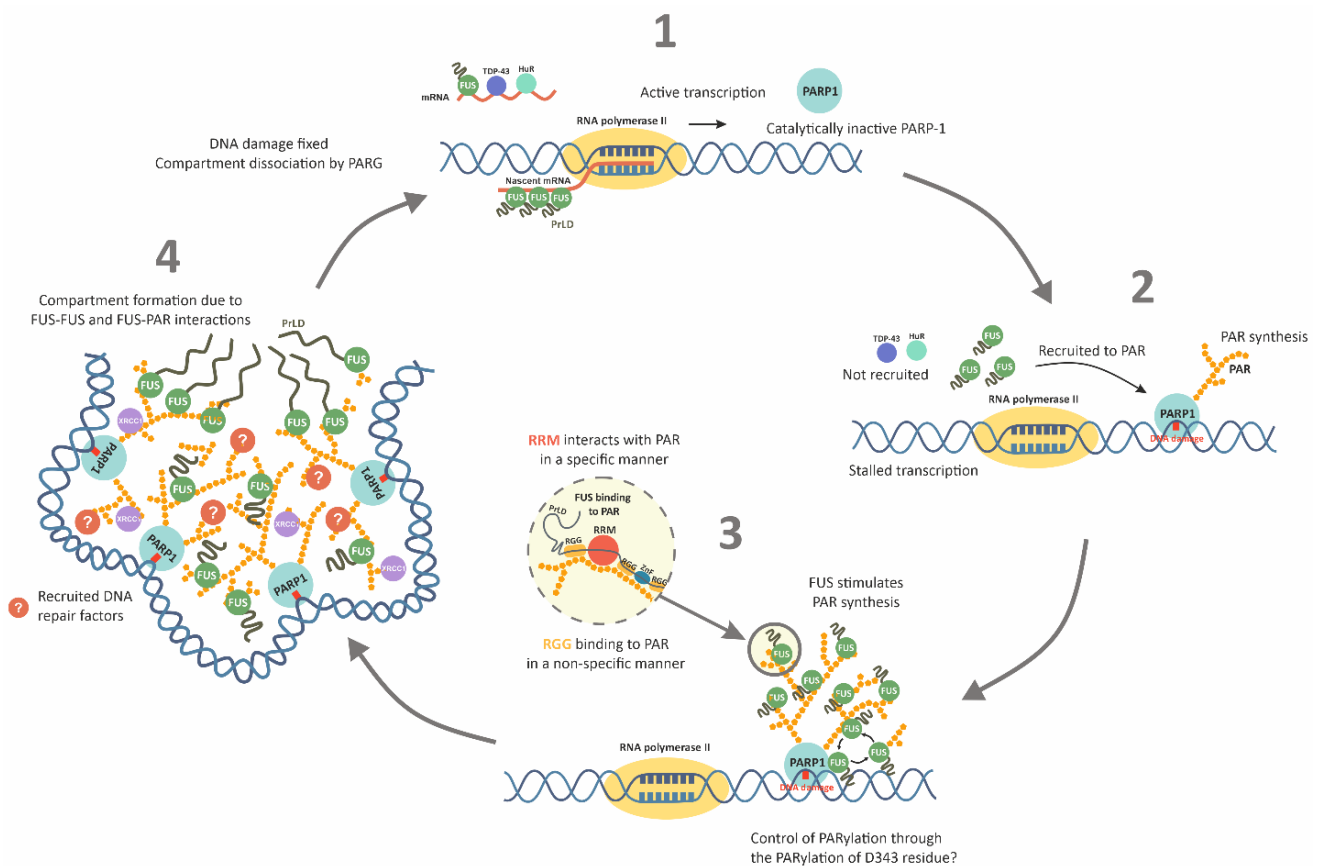


Figure 34: Schematic view of the role of FUS in PARP-1-mediated DNA repair. When RNA polymerase II transcription is taking place, FUS is bound to nascent mRNA (1). After genotoxic stress, PARP-1 recognizes DNA damage which leads to its activation and local PAR synthesis. If transcription is also stalled it will release FUS from nascent mRNA. PAR binding by RRM and RGG domains will contribute to FUS recruitment to PARylated PARP-1 (2). FUS stimulates PAR synthesis acting as PAR acceptor protein (3) and facilitates the formation of FUS-rich compartments due to FUS-FUS and FUS-PAR interactions (4). Other DNA repair factors such as XRCC1 can be recruited in these compartments. (4). After DNA repair process is done the compartments are dissociated due to PAR degradation catalyzed by PARG.

After genotoxic stress, PARP-1 recognizes DNA damage sites which leads to its activation and autoPARylation. Transcription is also stalled, which releases FUS from nascent mRNA in the vicinity of autoPARylated PARP-1. FUS is then becoming of PAR acceptor and stimulate the overall rate of PARylation process. According to our results, the recruitment

of FUS in the vicinity of activated PARP-1 bound to DNA damage stimulates PARP-1 activity and leads to the increase in PAR level. At the same time, the recruitment of FUS by PARylated PARP-1 may facilitate the formation of FUS-rich compartments (Figure 34) (Altmeyer *et al.*, 2015; Singatulina *et al.*, 2019).

In this study, we also identified the role of a residue, D343, previously identified as potentially PARylatable in the RRM of FET proteins (Zhang *et al.*, 2013). D343A mutation does not change the FUS RRM structure (Supplementary Figure S7). The interaction of FUS RRM with nucleic acids and protein-free PAR is also not altered (Supplementary Figure S8). However, D343A mutation drastically modifies the interactions of FUS with PARP-1 following its activation by damaged DNA *in vitro* (Chapter 6; Figure 29A and B). Importantly, the D343A mutation reduces the PAR level in cells overexpressing HA-FUS and exposed to ActD and H₂O₂ (Chapter 5; Figure 27). These results open up the possibility that PARylation of FUS RRM may be used as another regulation layer to control PARP-1 activation in cells. The RRM PARylation level increases in the case of RRM D343A (Chapter 6; Figure 31), which may, in turn, reduce the PARylation level of acceptor protein in full length FUS as observed in the test tube and/or promote the release of activated PARP-1 from DNA by increasing PARP-1 autoPARylation (Chapter 6; Figure 33).

In summary, we have found that FUS and probably the other FET proteins are key players in the cell response to genotoxic stresses that activate PARP-1 (Lee *et al.*, 2020). While RGG domains are common among RBPs and known to interact PAR, the RRM of FUS and most likely TAF15 and EWSR1 appear to specifically interact with PAR (Ozdilek *et al.*, 2017; Altmeyer *et al.*, 2015; Singatulina *et al.*, 2019). Through its specific interaction with PARylated PARP-1, FUS increases PAR levels, which may regulate the formation of compartments at DNA damage sites (Singatulina *et al.*, 2019). In these compartments, other DNA repair factors, such as XRCC1, can be potentially recruited (Wang *et al.*, 2018), which may also increase the availability of PAR acceptor proteins to facilitate overall synthesis of PAR (Wang *et al.*, 2018). Interestingly, DNA repair factors preferentially interact with phase separated FUS. However, further data should be produced to understand the functions behind the recruitment of DNA repair factors in FUS/PAR

compartments (*Abraham et al., 2015*). We anticipate that the result presented here will provide the basis for understanding the role of FUS in regulation of PARP-1 activity, notably in cancers for which PARP-1 is an important target, with several FDA-approved drugs being already available for different indications (*Slade et al., 2020*). Other perspectives of this work are obviously associated with neurodegenerative diseases such as ALS in which pathological FET protein mutation have been identified (*Harrison et al., 2017*). We did not investigate whether pathological FUS mutations or posttranslational modifications (phosphorylation or methylation) may interfere with the capacity of FUS to regulate PARylation, which may be interesting to address in the future (*Amouroux et al., 2010; Qamar et al., 2018; Hofweber et al., 2018*). In addition, the C-terminal RGG domains are known to interact with PAR and to be the recipient of many pathological mutations in ALS as well as posttranslational modifications (Literature review, Figures 15 and 16), whose roles within the frame of our model also deserve to be explored (*Deng et al., 2014; Slade et al., 2020*).

MATERIALS AND METHODS

1. Cell culture experiments

Preparation of plasmids for microtubule bench experiments and high-content screening experiments

Plasmids harboring cDNA of the full length FUS, TDP43, HuR, G3BP1, Lin28a, SAM68 genes fused with RFP-MBD (Microtubule-Binding Domain of Tau) and/ or GFP-MBD were obtained previously (*Maucuer et al., 2018*). The constructs with C-terminal RFP-MBD fusion harboring cDNA of the full length PARP-1, Lig3, XRCC1, POL β , NONO, PP1 α , Lig1, APE1, TOP1, EWSR1 or TAF15 genes were engineered using the gateway strategy as previously described (*Maucuer et al., 2018*). In brief, cDNAs encoding the proteins of interest were amplified using primers containing PaeI and AseI restriction sites and inserted into the backbone entry plasmid RFP-MBD-pCR8/GW/TOPO previously digested with the corresponding restriction enzymes (Figure 35A). Sequences encoding gene of interest fused with RFP-MBD were cloned from pCR8/GW/TOPO plasmids into the Gateway® pEF-Dest51 plasmid (Invitrogen™) using LR recombination reactions (Invitrogen™) according to the manufacturer's protocol (Figure 35B). Mutations K893I within the PARP-1 coding sequence was carried out by site-directed mutagenesis directly on the PARP1-RFP-MBD-PEF-DEST51 expression plasmid by using the "Quikchange II XL site-directed mutagenesis kit" (Stratagene) and appropriate oligonucleotides (Eurofins Genomics). The sequence of mutant PARP-1 gene was confirmed by DNA sequencing (Eurofins Genomics).

To produce the plasmids encoding the full length FUS, TDP43 or HuR fused to HA-tag, the corresponding cDNAs were amplified by PCR using primers containing NdeI and XhoI restriction sites and inserted into HA-pcDNA3.1 vector. For the preparation of K315A/K316A, N284A, D342A and D343A FUS mutants site-directed mutagenesis of FUS coding gene was performed directly on the HA-FUS-pcDNA3.1 expression vector by using the "Quikchange II XL site-directed mutagenesis kit" from Stratagene and appropriate oligonucleotides (Eurofins Genomics). The introduced mutations were verified by DNA sequencing (Eurofins Genomics).

For the preparation of HA-FUS Δ RRMTDP43-pcDNA3.1 plasmid, first, the cDNAs encoding amino acids 1-275 and 385-526 were amplified by PCR using primers containing NdeI, EcoRV and EcoRV, XhoI restriction sites respectively and inserted into HA-pcDNA3.1 vector previously digested with the NdeI and XhoI restriction enzymes. Then the cDNA encoding RRM1 domain of TDP43 was amplified by PCR using primers containing EcoRV restriction sites and inserted into HA-FUS-pcDNA3.1 plasmid with insertions encoding amino acids 1-275 and 385-526. The inserted cDNAs and reading frames for all prepared plasmids were verified by DNA sequencing (Eurofins Genomics).

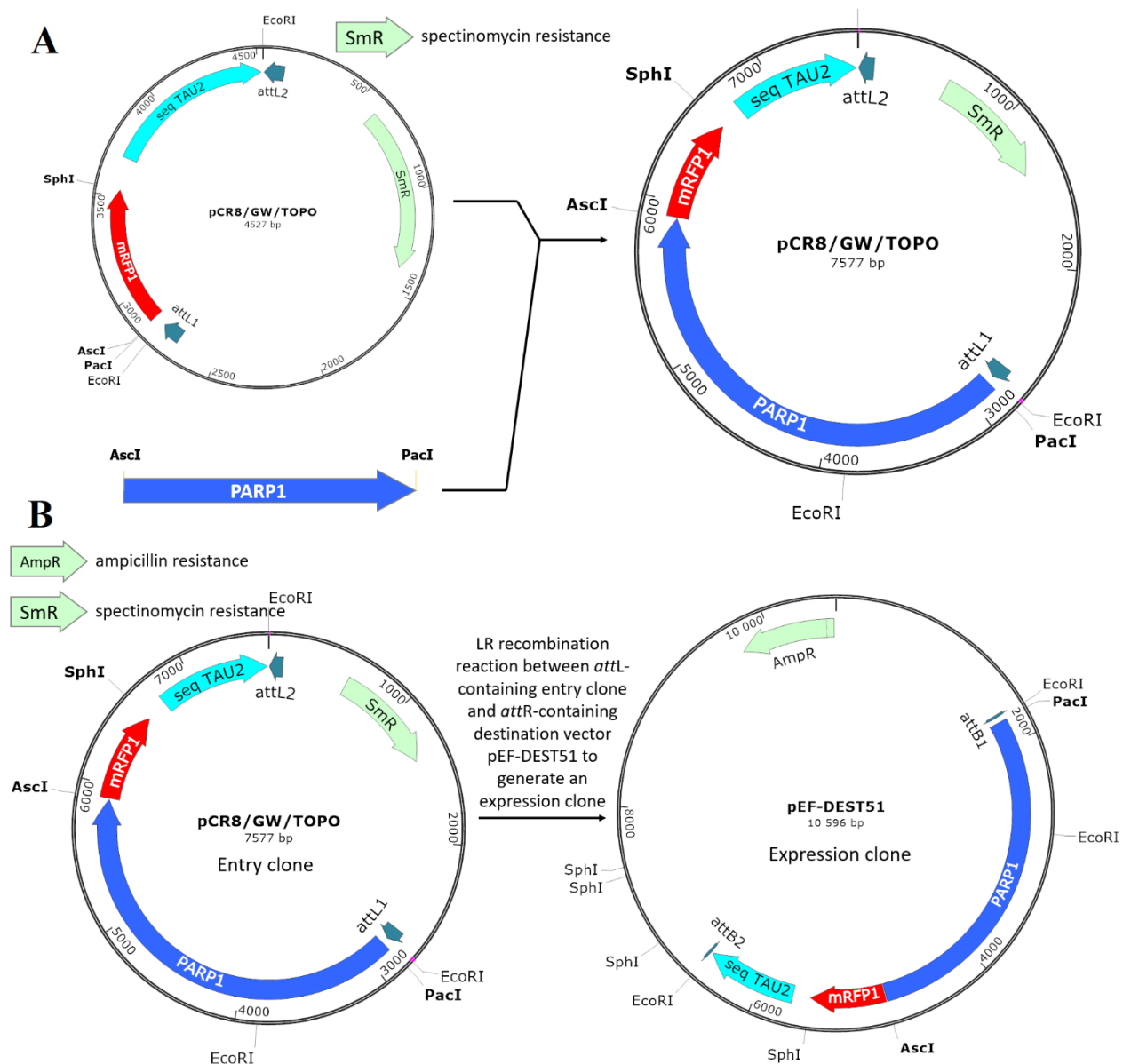


Figure 35: Steps of the preparation of RFP-MBD expression vectors using the gateway strategy. A. Insertion of the cDNA of PARP-1 into the backbone entry plasmid RFP-MBD-pCR8/GW/TOPO. B. Preparation of PARP-1-RFP-MBD-harboring Gateway® pEF-Dest51 plasmid (Invitrogen™) using LR recombination reactions.

Table 1: List of the primers used for PCR amplification of cDNAs

PCR primers	Sequence 5' -> 3'
PARP1-Pac1-For	GCGTTAATTAAGCCACCATGGCGGAGTCTTCGGATAAGCTC
PARP1-Asc1-Rev	GCGGGCGCGCCGCCACAGGGAGGTCTTAAAATTGAATTTAG
XRCC1-Pac1-For	GCGTTAATTAAGCCACCATGCCGGAGATCCGCCTCCGC
XRCC1-Asc1-Rev	GCGGGCGCGCCGCCGCTTGCGGCACCACCCCATAGAG
Lig3-Pac1-For	GCGTTAATTAAGCCACCCTTATGGCTGAGCAACGG
Lig3-Asc1-Rev	GCGGGCGCGCCGCCAGGGAGCTACCACTCTCCG
Lig1-Pac1-For	GCGTTAATTAAGCCACCATGCAGCGAAGTATCATG
Lig1-Asc1-Rev	GCGGGCGCGCCGCGTAGGTATCTTCAGGGTCAGAGCC
APE1-Pac1-For	GCGTTAATTAAGCCACCATGCCGAAGCGTGGGAAAAGGGA
APE1-Asc1-Rev	GCGGGCGCGCCGCCAGTGCTAGGTATAGGGTGATAGG
TOP1-Pac1-For	GCGTTAATTAAGCCACCATGAGTGGGGACCACCTCC
TOP1-Asc1-Rev	GCGGGCGCGCCGCAAACTCATAGTCTTCATCAGC
POLB-Pac1-For	GCGTTAATTAAGCCACCACTCTCAACGGGGGAATCACC
POLB-Asc1-Rev	GCGGGCGCGCCGCTTCGCTCAGGTCCTTGGGTTCC
PP1 α -Pac1-For	GCGTTAATTAAGCCACCATGTCCGACAGCGAGAAGCTC
PP1 α -Asc1-Rev	GCGGGCGCGCCGCTCCGGTGGATCCTTTCTTGGCTTTGGC
NONO-Pac1-For	GCGTTAATTAAGCCACCATGCAGAGTAATAAACTTTTAAAC
NONO-Asc1-Rev	GCGGGCGCGCCGCGTATCGGCGACGTTTGTGGG
EWSR1-Pac1-For	GCGTTAATTAAGCCACCATGGCGTCCACGGATTACAGTAC
EWSR1-Asc1-Rev	CGCGGCGCGCCTGGTAGGGCCGATCTCTGCGCTCCTGAC
TAF15-Pac1-For	GCGTTAATTAAGCCACCATGTCGGATTCTGGAAGTTACG
TAF15-Asc1-Rev	CGCGGCGCGCCTGGTATGGTCCGTTGCGCTGATC
PARP1-K893I-For	GGCTACATGTTTGGTATAGGGATCTATTTTCGC
PARP1-K893I-Rev	CGCATGTACAAACCATATCCCTAGATAAAGCG
FUS-NdeI-For	GCGCATATGATGGCCTCAAACGATTATACCC
FUS-XhoI-Rev	CGCCTCGAGTTAATACGGCCTCTCCCTGCGATCCTG
HuR-NdeI-For	GCGCATATGATGTCTAATGGTTATGAAGACCACATGG
HuR-XhoI-Rev	CGCCTCGAGTTTGTGGGACTTGTGGTTTTG
FUS-K315A-For	GTATTATTAAGACAAACGCGAAAACGGGACAGCCC
FUS-K315A-Rev	GGGCTGTCCCGTTTTTCGCGTTTGTCTTAATAATAC
FUS-K316A-For	GTATTATTAAGACAAACGCGGCAACGGGACAGCCCATG
FUS-K316A-Rev	CATGGGCTGTCCCGTTGCCGCGTTTGTCTTAATAATAC
FUS-N284A-For	CAGGATAATTCAGACGCCAACACATCTTTGTG
FUS-N284A-Rev	CACAAAGATGGTGTGGCGTCTGAATTATCCTG
FUS-D342A-For	GCAACGGTCTCTTTTGCTGACCCACCTTCAGC
FUS-D342A-Rev	GCTGAAGGTGGGTCAGCAAAAGAGACCGTTGC
FUS-D343A-For	GCAACGGTCTCTTTTGATGCCACCTTCAGCTAAAG
FUS-D343A-Rev	CTTTAGCTGAAGGTGGGGCATCAAAGAGACCGTTGC
FUS-NdeI-For	GCGCATATGATGGCCTCAAACGATTATACCC
FUS275-EcoRV-Rev	CGCGATATCACGTGATCCTTGGTCCCGAG
FUS365-EcoRV-For	GCGGATATCCGAGGGCGAGGAGGCCCATG
FUS-XhoI-Rev	CGCCTCGAGTTAATACGGCCTCTCCCTGCGATCCTG
TDP43-EcoRv-For	CGCGATATCAAACATCCGATTTAATAGTG
TDP43-EcoRv-Rev	CGCGATATCTCTGCTTCTCAAAGGCTC

Table 2: Recombinant DNAs

Reagent	Source	Identifier
pEGFP(C1)-PP1alpha	Addgene	Cat#44224
pCDNA3-HA-PSPC1	Addgene	Cat#101764
pcDNA3.1-HA-NONO	Addgene	Cat#127655
pGEX4T-hLIG3	Addgene	Cat#81055
pQE30-hPolB	Addgene	Cat#70761
pET16b -XRCC1	Dr. Pablo J. Radicella	N/A
pET15b-hLigI		N/A
pET32a-PARP1	Dr. M. Satoh	N/A
pXC53-hAPE1	Dr. S.H. Wilson	N/A

Table 3: Mammalian expression vectors

Name of plasmid	Expression vector	Accession numbers
PARP1-RFP-MBD	PEF-DEST51	NP_001609.2
LIG3-RFP-MBD	PEF-DEST51	NP_002302.2
XRCC1-RFP-MBD	PEF-DEST51	NP_006288.2
POLB-RFP-MBD	PEF-DEST51	NP_002681.1
NONO-RFP-MBD	PEF-DEST51	NP_001138881.1
PP1 α -RFP-MBD	PEF-DEST51	NP_002699.1
LIG1-RFP-MBD	PEF-DEST51	NP_000225.1
APE1-RFP-MBD	PEF-DEST51	NP_001231178.1
TOP1-RFP-MBD	PEF-DEST51	NP_003277.1
FUS-RFP-MBD	PEF-DEST51	NP_004951.1
EWSR1-RFP-MBD	PEF-DEST51	NP_053733.2
TAF15-RFP-MBD	PEF-DEST51	NP_631961.1
G3BP1-RFP-MBD	PEF-DEST51	NP_005745.1
LIN28-RFP-MBD	PEF-DEST51	NP_078950.1
SAM68-RFP-MBD	PEF-DEST51	NP_006550.1
HuR-RFP-MBD	PEF-DEST51	NP_001410
TDP43-RFP-MBD	PEF-DEST51	NP_031401.1
PARP1-GFP-MBD	PEF-DEST51	NP_001609.2
PARP1(K893I)-GFP-MBD	PEF-DEST51	
FUS-GFP-MBD	PEF-DEST51	NP_004951.1
FUS-HA	pcDNA3.1	NP_004951.1
FUS Δ RRMTDP43-HA	pcDNA3.1	
FUS(K315A/K316A)-HA	pcDNA3.1	
FUS(N284A)-HA	pcDNA3.1	
FUS(D342A)-HA	pcDNA3.1	
FUS(D343A)-HA	pcDNA3.1	
TDP43-HA	pcDNA3.1	NP_031401.1
HuR-HA	pcDNA3.1	NP_001410

Cell culture conditions

In this work we used two cell lines: HEK293 (Human Embryonic Kidney 293 cell line), which was used for cell extract preparation and Western blot analyses and HeLa (American Type Collection, USA), which was used for all immunofluorescence experiments. Cells were cultivated at 37°C in high glucose Dulbecco's Modified Eagle Medium (DMEM, Life Technologies) with an addition of two antibiotics (100U/ml of penicillin G and 100 µg/ml of streptomycin) and 10% fetal bovine serum (FBS, Thermofisher). The cells were plated in 96-well plates (PhenoPlate™-96, PerkinElmer) at a density of 1.3×10^4 for immunofluorescence or in 10-cm Petri dishes for the cell extract preparation.

Microtubule bench assay

HeLa cells were grown in 96-well plates and were co-transfected with the indicated plasmids at the final concentration of 0.4 µg (GFP expressing plasmid) or 0.2 µg (RFP expressing plasmid) using lipofectamine 2000 (Thermofisher) transfection reagent for 24 h according to the manufacturer's instructions. After 24 h of transfection and before the fixation procedure cells were washed once with PBS. The fixation was performed in two steps: first, cells were incubated with ice-cold methanol for 10 min at -20°C, second, 4% paraformaldehyde (PFA) in PBS was used to fix the cells for 10 min at 37 °C. The staining of the cells with 300 nM of 4',6-diamidino-2-phenylindole (DAPI) was performed to visualize the nuclei. The cell images were obtained with the Opera Phenix® Plus High Content Screening System (PerkinElmer) on 40x magnification (Figure 37).

To measure sub-compartmentalization in the system with both proteins fused to GFP/RFP-MBD, the cell image analysis was carried out using the PerkinElmer Harmony v4.8 software. First, nuclei, cytoplasm and spots of proteins fused to GFP/RFP-MBD along the microtubule network were automatically detected. Then, the following parameters defining spatial segregation of two proteins were quantified: RFP/GFP fluorescence intensity in the spot, number of spots, width to length ratio of the spot, RFP/GFP fluorescence intensity in the cytoplasm. Fluorescence analysis included processing of signal by filtering out cells with low co-transfection level (RFP/GFP fluorescence intensity

in the cytoplasm > 5.8 in log scale) and spots with high width to length ratio (> 0.22). The RFP/GFP fluorescence intensity of each spot was normalized to the RFP/GFP intensity in the cytoplasm and presented in the scatter plots as it is shown on the supplementary figure S1.

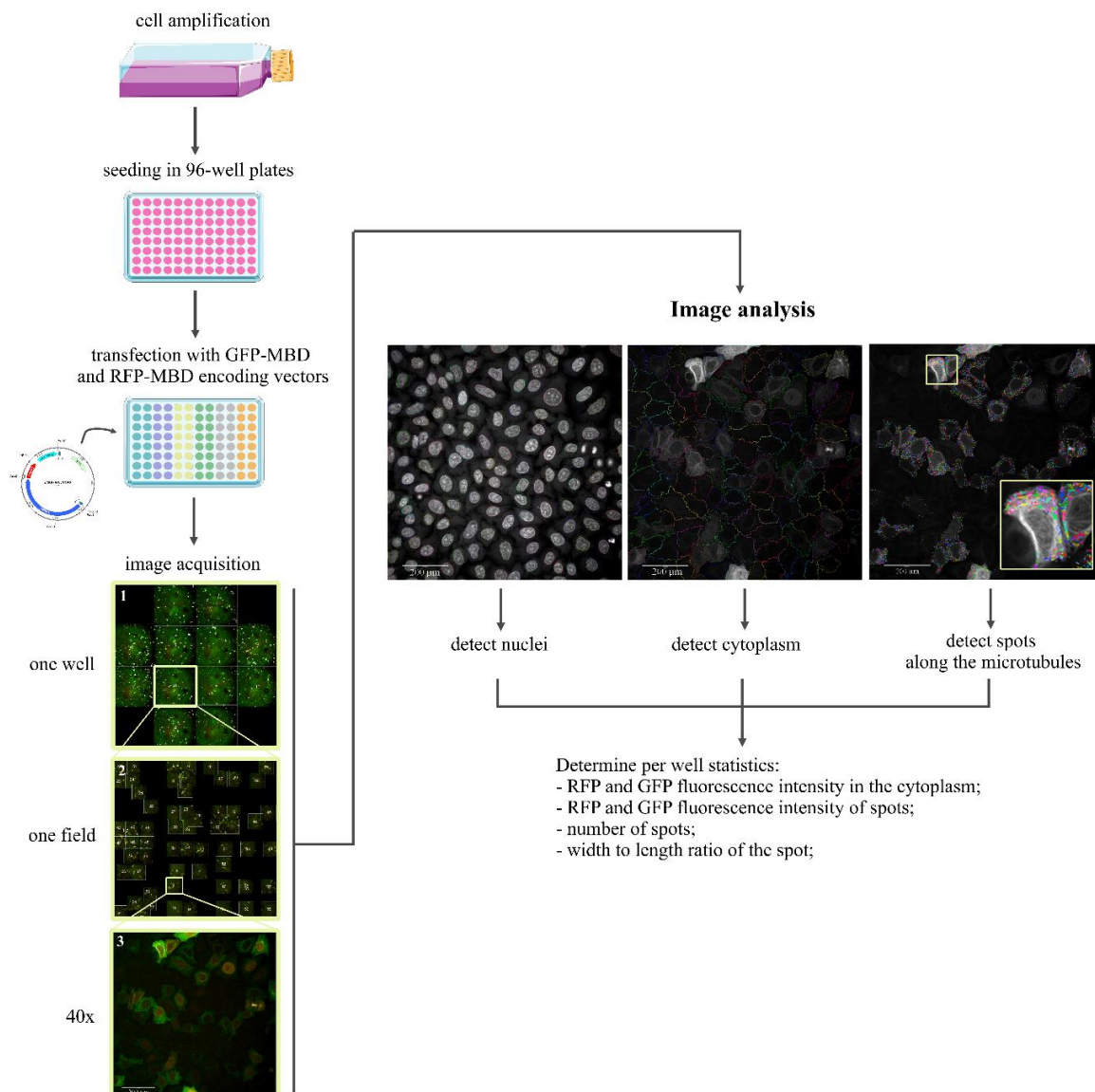


Figure 37: Detection scheme allowing to score the mixing between two proteins. Scheme of the cellular assay. HeLa cells were plated in 96-well plates (13000 cells per well) and co-transfected with the GFP-MBD or RFP-MBD encoding plasmids, using lipofectamine 2000 reagent (Invitrogen). Co-transfected cells were incubated for 24 hrs, fixed with ice-cold methanol and then with 4% paraformaldehyde (PFA) (see Materials and Methods for details). Image acquisition was performed with the Opera Phenix® Plus High Content Screening System (PerkinElmer) at 40x magnification. Images 1 is an overview of one well in a 96-well plate, image 2 - is a zoom to one of 12 fields of the well and image 3 - 40x magnification image of co-transfected HeLa cells. MBD: Microtubule Binding Domain. Automated detections of nuclei, cytoplasm, and spots of GFP-MBD and RFP-MBD expression along the microtubules were performed with Harmony v4.8 software. The various parameters defining spatial segregation of two proteins along the microtubule network were then quantified (RFP and GFP fluorescence intensity in the spot, number of spots, width to length ratio of the spot, RFP and GFP fluorescence intensity in the cytoplasm). Scale bar: 200 μm . Parts of the figure were drawn by using pictures from Servier Medical Art (<http://smart.servier.com/>).

The mixing scores presented on the figure 2 and supplementary figure S1 were calculated based on these plots as the coefficient of determination (R-squared value) showing how well the observed data fit the regression model (polynomial fitting shown on the supplementary figure S1). The scatter plots were created using MATLAB R2022a software.

Overexpression and silencing experiments: transfection with plasmids and siRNAs

For overexpression experiments HeLa cells, growing in 96-well plates, were transiently transfected with plasmids, carrying the studied protein gene, at a final concentration of 0,2 µg using lipofectamine 2000 (Thermofisher) transfection reagent for 24-48 h according to the manufacturer's instructions.

For the silencing of FUS, TDP-43 or HuR HeLa cells were transfected the corresponding small interfering RNA (siRNA) at a final concentration of 0,15 µg using lipofectamine 2000 for 24 h. To distinguish non-specific effects a negative control siRNA (AllStars Negative Control siRNA) was used.

Add-back experiments

For the add-back experiments, firstly, HeLa cells were transfected with siRNA targeting endogenous FUS for 24 h and, secondly, the cells were transfected with the plasmid encoding wild type or mutant FUS, as indicated. The efficiency of transfection with HA-FUS overexpressing plasmid was measured at the single cell level using antibodies to FUS and HA-tag and was calculated as the increase of total FUS expression for the HA-FUS overexpressing cells compared to the cells with endogenous FUS expression level (Figure 36B). The efficiency of transfection with siRNA was calculated as the difference in FUS expression for the cells treated with a non-targeting sequence siRNA and siRNA targeting FUS (Figure 36C).

Treatment conditions

For overexpression and silencing experiments described in the Chapter 2 (Figures 7, 8, 9, 11), HeLa cells were treated with indicated concentration of hydrogen peroxide (H₂O₂) to induce oxidative stress and incubated for 30 min at 37°C. For inhibition of transcription, cells were pre-treated with actinomycin D (ActD, 5 µg/ml) for 30 min prior to H₂O₂

treatment. To calculate γ H2AX fluorescence level (Figure 10), HeLa cells were treated with H_2O_2 (250 μM , 30 min), ActD (5 $\mu\text{g}/\text{ml}$, 1 h) and H_2O_2 or Olaparib (2 μM , 1 h) and H_2O_2 . To compare different transcription inhibitors (Figure 13), the treatment with 5 $\mu\text{g}/\text{ml}$ of ActD, 100 μM of DRB or 10 μM of oxaliplatin was performed for 1 h.

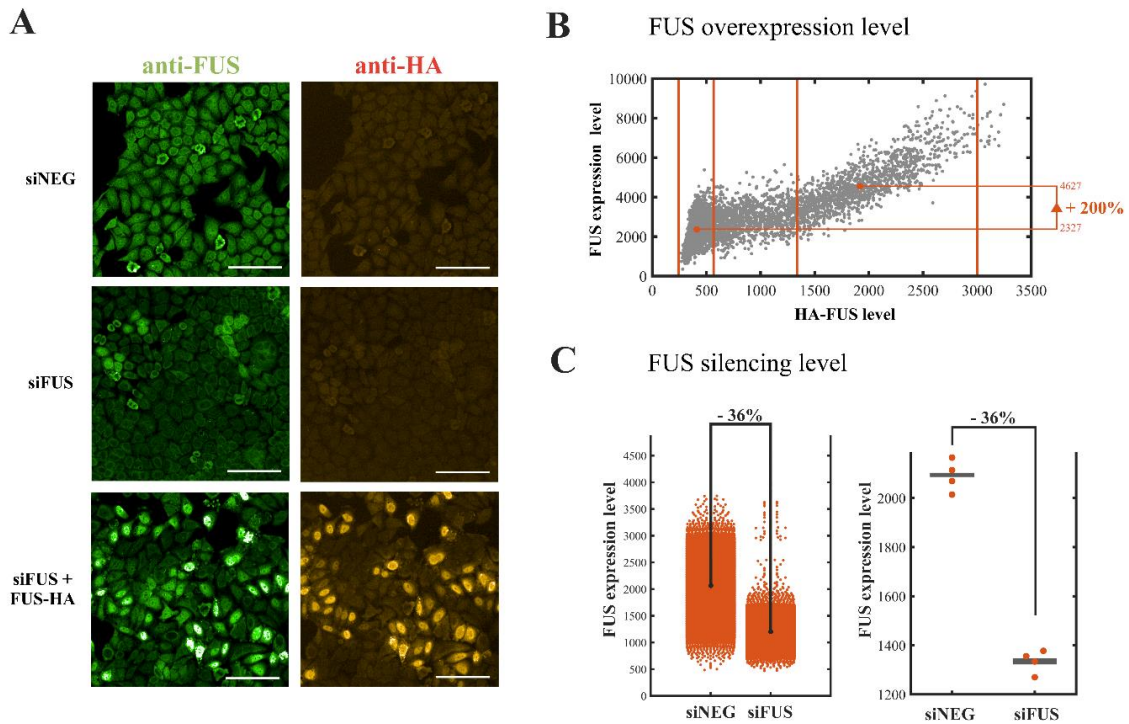


Figure 36: Quantification of FUS silencing and overexpression levels in HeLa cells. A. Representative images of HeLa cells treated with control siRNA (siNEG), siRNA targeting FUS mRNA or treated with siFUS and transfected with the plasmid encoding HA-tagged FUS. Anti-FUS and anti-HA antibodies were used to quantify the expression level of total FUS and HA-tagged FUS. Scale bar: 100 μM . B. Analysis of the expression of total FUS and HA-tagged FUS at the single cell level. The scatter plot shows the increase of total FUS expression versus the expression of HA-tagged FUS. FUS overexpression level was calculated as the increase of total FUS expression for a window of HA-tagged FUS expression (HA-FUS level: 1340-3000) compared to the background (cells not transfected with FUS-HA expressing plasmid, HA-FUS level: 250-550). Nuclear overexpression of HA-FUS corresponds to about 100% of that of endogenous FUS. C. Left panel: Single-cell analysis of FUS expression level per cell located in a single well for two conditions: control siRNA (siNEG) treatment and treatment with siRNA targeting FUS mRNA. Right panel: Decrease in FUS expression level was calculated for four independent wells and amounted to 36% in average.

Table 4: siRNA oligonucleotides

Reagent	Source	Identifier	Sequence
AllStar Negative Control siRNA	QIAGEN	Cat#1027281	
siRNA-FUS-3'	Eurofins Genomics		Sense 5'-(AAUAACGAGGGUAACACUGGG)dTdT-3' Antisense 5'-(CCCAGUGUUACCCUCGUUAAU)dTdT-3'
siRNA-HuR	QIAGEN	Cat#SI00300139	
siRNA-TDP43	Eurofins Genomics		Sense 5'-(GCUCUAAUUCUGGUGGAGCAA)dTdT-3' Antisense 5'-(UUGCUCACCAGAAUAGAGC)dTdT-3'

Fixation of the cells and high-content imaging assay and analysis

Before the fixation procedure cells were washed once with PBS. The fixation was performed in two steps: first, cells were incubated with ice-cold methanol for 10 min at -20°C, second, 4% paraformaldehyde (PFA) in PBS was used to fix the cells for 10 min at 37 °C. Then, cells were rinsed with PBS and incubated in a blocking buffer (50 mM Tris pH 7.5, 100 mM NaCl, BSA 2%, 0.15% Triton X-100) for 30 min at 37 °C. After washing with PBS, cells were kept with blocking buffer (50 mM Tris pH 7.5, 100 mM NaCl, BSA 2%, 0.15% Triton X-100) for 30 min at 37 °C to permeabilize the cells and to reduce background interference. Blocking buffer was removed and cells were washed and then incubated with mentioned primary antibodies overnight at 4 °C.

The wash with PBS was repeated thrice, after this the fluorochrome (Alexa Fluor®488 and -594)-coupled secondary antibodies in blocking buffer were added to the cells for 1 h, followed by the final wash with PBS. The staining of the cells with 300 nM of 4',6-diamidino-2-phenylindole (DAPI) was performed to visualize the nuclei. The cell images were obtained with the Opera Phenix® Plus High Content Screening System (PerkinElmer) on 20x or 40x magnification. Image capture was performed using three channels:

- a. DAPI (excitation 345 nm; emission 455 nm);
- b. Alexa 488 (excitation 494 nm; emission 517 nm);
- c. Alexa 594 (excitation 590 nm; emission 617 nm).

Images were analyzed using the PerkinElmer Harmony v4.8 software. DAPI signal was used for nuclei detection. The signal intensity of silenced/overexpressed proteins or PAR was measured in the nucleus. The relative increase in nuclear PAR level in protein overexpressing cells was calculated as the ratio of the nuclear PAR level in protein overexpressing cells (protein expression signal > 6.8 and < 9 in log scale) to the nuclear PAR level in cells with low protein expression (protein expression signal < 6.5 in log scale). The corresponding scatter plots and violin plots were created using MATLAB R2022a software (Figure 5, 7-13, 26, 27).

***In situ* hybridization to visualize RNA**

To visualize poly(A) mRNA the hybridization *in situ* was performed. For this, fixated cells were incubated with oligo-dT-[Cy3] for 2 h at 37°C in 2×SSC buffer, containing 1 mg/ml yeast tRNA, 0.005% BSA, 10% dextran sulfate, and 25% formamide. After incubation, cells were washed with 4× and then 2× SSC buffer (0.88% sodium citrate, 1.75% NaCl, pH 7.0).

5-Bromouridin (BrU) incorporation analysis

After 24 h of transfection with FUS-HA expressing plasmid HeLa cells were incubated with 5mM BrU for 35 min at 37°C and with H₂O₂ (30, 100 or 300 μM) for 30 min. The fixation procedure described above was performed. The primary anti-BrdU monoclonal rat antibodies (ab6326, Abcam) recognizing both BrdU and BrU were diluted 1:1000 in blocking buffer and applied to cells for incubation overnight at 4 °C. After PBS washings, the secondary goat anti-rat antibody (Alexa 594, Invitrogen) were diluted 1:1000 in blocking buffer and added to cells for 1 h at RT. The staining of the cells with 300 nM of 4',6-diamidino-2-phenylindole (DAPI) was performed to visualize the nuclei. The anti-BrdU fluorescence was detected and measured automatically using Opera Phenix® Plus High Content Screening System (PerkinElmer) and the Harmony v4.8 software (Figure 12).

Proximity ligation assay (PLA)

The principle of proximity ligation assay (PLA) is based on the ability of two DNA probes to recognize and bind to adjacent target molecules, resulting in their close proximity. This close proximity enables the ligation of the two probes, which generates a unique circular DNA molecule that can be amplified and detected using various techniques such as PCR, sequencing or microscopy (Figure 38). PLA involves the use of two primary antibodies, each conjugated to a short DNA probe, that recognize and bind to specific target molecules on the sample (Figure 38A and B). If the two target molecules are in close proximity (e.g., within 40 nm), the DNA probes will also come into close proximity and can be ligated by a DNA ligase enzyme to form a circular DNA molecule (Figure 38C). The circular DNA molecule serves as a template for amplification, and detection of the amplified product provides a readout of the presence and location of the target molecules in the sample (Figure 38E and F).

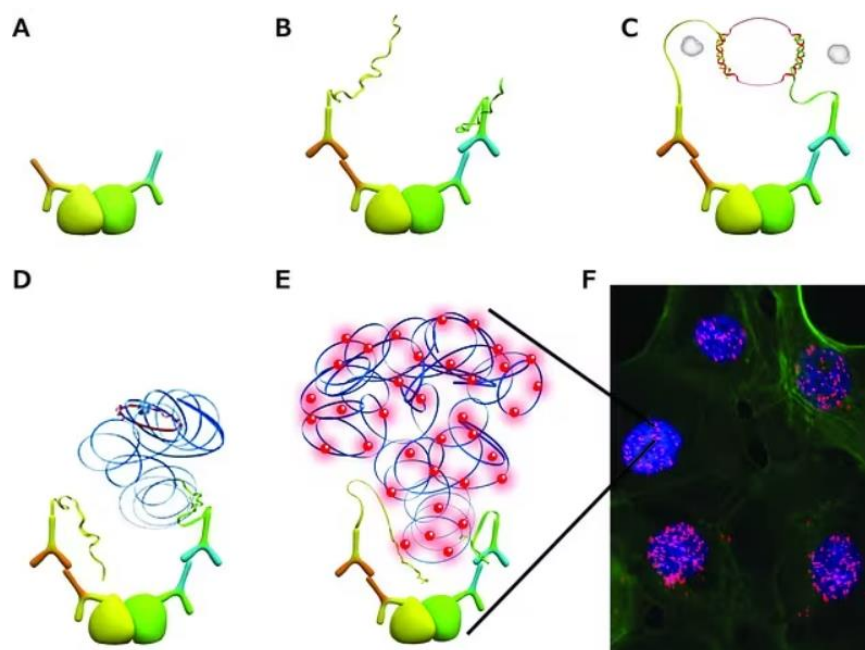


Figure 38: Schematic of Duolink® PLA reaction. (from Duolink® PLA technology Kit (Sigma) product information <https://www.sigmaaldrich.com/FR/en/products/protein-biology/duolink-proximity-ligation-assay>)

Proximity ligation assay was performed using Duolink® PLA technology Kit (Sigma) according to the manufacturer's recommendations. HeLa cells were grown in a 96-well plate (13000 cells per well) and transfected with corresponding plasmids for 24 h. The cells were washed with PBS for 5 min, then fixed with 4% PFA for 30 min at 37 °C and washed with PBS. The cells were permeabilized using 0.2% Triton in PBS for 10 min and blocked using blocking solution for 60 min at 37 °C. The samples were incubated with anti-HA and anti-PARP-1 primary antibodies in the supplied buffer at 4 °C overnight, then washed thrice with PBS, 0.2% Triton. The PLUS and MINUS PLA probes were diluted 1:5 in corresponding buffers, provided by manufacturer, and incubated with cells for 60 min at 37 °C, then the samples were washed thrice with PBS. The DNA ligase was diluted 1:40 in the ligation buffer (diluted 1:5) and added to the samples for 30 min at 37 °C, then the samples were washed twice with PBS. The samples were incubated in the amplification solution (1:80 DNA polymerase in the amplification solution diluted 1:5) for 100 min at 37°C and washed twice with PBS for 10 min. The samples were stained with DAPI. The cell images were obtained with the Opera Phenix® Plus High Content Screening System (PerkinElmer) and analyzed with Harmony v4.8 software.

2. *In vitro* methods

Isolation of Chromatin-bound proteins and Western blot analysis

HEK293 cells were grown on 10 cm Petri dishes, transfected and treated with the indicated plasmids and reagents. The preparation of chromatin bound fraction and soluble fraction was performed as described previously (Groth *et al.*, 2007). Briefly, soluble proteins of HEK293 cells were isolated by extracted with Triton, namely, 3 volumes of 0.5% Triton X-100 in CSK buffer were added to the cells for 20 min on ice, then the cells were centrifuged for 5 min at 1500 g and the supernatant was used for WB as a free fraction. The pellet was rinsed in 0.1% Triton CSK buffer, then rinsed in DNase I digest buffer (10 mM Tris-HCl pH 7.8, 10 mM NaCl, 5 mM MgCl₂, protease inhibitors) and treated 20 min at 37°C with DNase I (35U in 50 µl of DNase I digest buffer). Cell extracts were centrifuged for 10 min at 16000 g and the supernatant was used for WB as a chromatin bound fraction.

For Western blot analysis, first, proteins were separated on 10 % SDS-PAGE and transferred onto a PVDF membrane. After that, the membrane was stained with ponceau S red 0,2% solution to detect proteins on membrane. The stained membrane was washed with 1% CH₃COOH for fixation, then washed with TBS-Tween buffer (20 mM Trizma Base, 143 mM NaCl, pH 7.6, 1% Tween 20) and blocked with non-fat dry milk 5% for 1 h at room temperature. Then, the membrane was washed again with TBS-Tween buffer and incubated overnight at 4 °C with indicated primary antibodies. After a wash step, the secondary antibody (LI-COR IRDye, IRDye 800CW goat-anti-rabbit 1:5000, IRDye 680RD goat-anti-mouse 1:5000) was added to the membrane in TBS-Tween buffer for 45 min at RT. The membrane was washed with TBS-Tween buffer, bound antibodies were detected with Amersham Typhoon Bioimager.

Table 5: List of antibodies.

Reagent or resource	Source	Identifier
Rabbit polyclonal anti-PARP1	Abcam	Cat#ab227244
Rabbit polyclonal anti-gamma H2A.X (phosphor S139)	Abcam	Cat#ab11174
Rabbit polyclonal anti-FUS	Novus Biologicals	Cat#NB100-565
Mouse monoclonal anti-Histone H3	Santa Cruz Biotechnology	Cat#sc-517576

Mouse monoclonal anti-HA-Tag (F-7)	Santa Cruz Biotechnology	Cat#sc-7392
Rabbit polyclonal anti-TDP43 (C-terminal)	Proteintech	Cat#12892-1-AP
Mouse monoclonal anti-PCNA (PC10)	Novus Biologicals	Cat#NB500-106SS
Rat monoclonal anti-BrdU [BU1/75 (ICR1)]	Abcam	Cat#ab6326
Mouse monoclonal anti-TARDBP	Abnova	Cat#H00023435-M01
Mouse monoclonal anti-HuR (3A2)	Invitrogen	Cat#39-0600
Rabbit monoclonal anti-HuR (D9W7E)	Cell Signaling Technology	Cat#12582
Mouse monoclonal anti-FUS (CL0190)	Novus Biologicals	Cat#NBP2-52874
Rabbit monoclonal anti-Poly/Mono-ADP Ribose (E6F6A)	Cell Signaling Technology	Cat#83732
Rabbit polyclonal anti-PAR	R&D Systems	Cat#4336-BPC-100
Anti-tubuline		

Recombinant protein production and purification

Recombinant PARP-1 was overexpressed in *E. coli* Rosetta (DE3) pLysS (Novogen, catalog # 70956-3) and purified by Ni-NTA agarose (GE Healthcare United States, catalog # GE17-5255-01) affinity chromatography, HiTrap Heparin High Performance (GE Healthcare, United States, catalog # GE17-0407-01) affinity chromatography, and deoxyribonucleic acid–cellulose (single-stranded calf thymus DNA) (Sigma-Aldrich, United States, catalog #D8273) affinity chromatography as described previously (Naumenko *et al.*, 2022).

The recombinant His6-tagged FUS-RRM fragment (275His-385Gly) from the human full-length FUS was first cloned into the pET-28-a expression vector while the recombinant His6-tagged TDP-RRM2 fragment was cloned as previously described (Renfigo-Gonzalez *et al.*, 2021). BL21 (DE3) competent *E. coli* cells were transformed with the constructed plasmid pET-28-a-FUS_275-385 or pTDP-RRM2_176-277 and grown at 37 °C in minimal medium M9 supplemented with 15NH₄Cl and 50 µg/mL of kanamycin. The protein expression was induced by IPTG 1mM added at OD_{600nm} = 0.7. The culture was grown at 37 °C for 4 hr and cells were harvested and washed with 20 mL of cold 30 mM Tris-HCl buffer, pH 7.6, containing 100mM KCl. The cell pellet was resuspended in 20 mL of buffer A (20 mM Tris-HCl, pH 7.6, 1.5 M KCl, 1 mM TCEP, 1 mM PMSF, and EDTA-free protease inhibitor Cocktail (Roche)) and cells were disrupted by sonication on ice (Biolock Vibracell sonicator, model 72412). The cell lysate was centrifuged at 4 °C for 30 min at 150,000×g in a TL100 Beckman centrifuge.

The FUS and TDP-43 RRM protein fragments (WT and mutants) protein fragments were purified following the manufacturer's recommendations (Qiagen). Briefly, the supernatant was incubated for 2 h at 4 °C with Ni²⁺ - NTA-agarose (Qiagen) (20 mg of proteins/mL of resin) pre-equilibrated in buffer A. The resin was then washed extensively with buffer A containing 10 mM imidazole and then with buffer A containing 20 mM imidazole. The elution of the protein was performed by increasing progressively the imidazole concentrations (from 50 mM to 500 mM) in buffer A. Pure protein fractions were pooled and buffer-exchanged against NMR buffer (15 mM K₂HPO₄/KH₂PO₄, pH 6.8 containing 25 mM KCl and 1 mM TCEP by using a PD-10 column (GE Healthcare). The final preparations were snap-frozen and stored at -80 °C.

For the full-length forms of FUS WT and D343A mutant, BL21 (DE3) competent *E. coli* cells harboring the expression vector pET-22-b-FUS-FL or pET-22-b-FUS-FL-D343A were grown at 37 °C in 1L of 2xYT medium supplemented with 100 µg/mL of ampicillin. The protein expression was induced as described above and purification as previously described (*Singatulina et al., 2019*). Briefly, the cell pellet after disruption was resuspended in 10 mL of buffer A containing 8 M urea and 5 mM imidazole and incubated for 2 h at 4 °C. The resulting suspension was centrifuged at 4 °C for 30 min at 200,000× g in a TL100 Beckman centrifuge and the His₆-tagged proteins were purified as described above in presence of 8 M urea. The protein purity was monitored at all stages of the purification by SDS-PAGE.

Site-directed mutagenesis of the FUS RRM was carried out directly on the pET-28-a-FUS_275-385 or pET-22-b-FUS-FL expression plasmid by using the 'Quikchange II XL site-directed mutagenesis kit' from Stratagene and appropriate oligonucleotides (Eurofins Genomics). The introduced mutations (N284A, K315A/K316A, D342A, and D343A) were checked by DNA sequencing (Eurofins Genomics). Overexpression and purification of mutated forms were performed following the method described above.

Radioactive assay of protein PARylation *in vitro*

The preparation of [³²P]-NAD⁺ was performed as previously described (*Singatulina et al., 2019*). Briefly, [³²P]-NAD⁺ labeled on the adenylate phosphate was synthesized in a

reaction mixture (100 μ L) containing 2 mM β -Nicotinamide mononucleotide, 1 mM ATP and 0.25 mCi of [α - 32 P]-ATP (1000 Ci/mmol), 1.5 mg/mL nicotinamide mononucleotide adenylyl transferase (NMNAT), 25 mM Tris- HCl (pH 7.5), and 20 mM MgCl₂ was incubated for 1 h at 37°C. The enzyme was denatured at 65°C for 10 min and precipitated proteins were removed by centrifugation.

An *in vitro* poly(ADP-ribosyl)ation assay was performed in the reaction mixtures (12 μ L) containing 20 mM Tris-HCl, pH 7.5, 25 mM NaCl, 1 mM DTT, 400 mM Urea, 0.1 μ M A260/mL of DNase I-activated calf thymus DNA, 100 nM PARP-1, 0.3 mM NAD⁺, 0.4 μ Ci [32 P]-NAD⁺ and 50, 200, 800 or 3000 nM of FUS WT or FUS(D343A). The initiation of the reaction was performed by the addition of NAD⁺. The reaction mixtures were incubated at 37°C for 1, 3, 7, 15 or 30 min and inhibited by adding SDS-sample buffer and heating for 5 min at 90°C. The reaction mixtures were analyzed by 10% SDS-PAGE with subsequent phosphorimaging and/or colloidal Coomassie staining.

An *in vitro* poly(ADP-ribosyl)ation of RRM fragments was performed in the reaction mixture (15 μ L) containing 20 mM Tris-HCl, pH 7.5, 25 mM NaCl, 1 mM DTT, 0.1 μ M A260/mL of DNase I-activated calf thymus DNA, 100 nM PARP-1, 0.3 mM NAD⁺, 0.4 μ Ci [32 P]-NAD⁺ and 4, 8, or 16 μ M of indicated RRM fragment. The initiation of the reaction was performed by the addition of NAD⁺. The reaction mixtures were incubated at 37°C for 30 min and inhibited by adding SDS-sample buffer and heating for 5 min at 90°C. The reaction mixtures were analyzed by 10% SDS-PAGE with subsequent phosphorimaging and/or colloidal Coomassie staining.

3. NMR analysis

All NMR Experiments were performed on 60 μ L samples prepared in 25 mM potassium phosphate buffer pH 6.8, using 1.7 mm diameter capillary tubes. NMR spectra were acquired at 298K on a Bruker AVIII HD 600MHz spectrometer equipped with a triple-resonance cryoprobe.

Interactions of the purified 15 N protein fragments (FUS RRM, TDP-43 RRM2 and HuR RRM1) with PAR or synthetic DNA (*Eurofins*) or ARN (*Eurogentec*) oligonucleotides (A20r,

A20d, T10 and hnRNPA2/B1 RNA stem loop) were investigated using 2D ^1H - ^{15}N SOFAST-HMQC experiments. The spectra were recorded on 50 μM protein samples alone and in presence of 90 μM ligand. Data were acquired with 16 dummy scans, 256 scans, 2048 points along the direct dimension, 128 t_1 increments and a relaxation delay of 0.2 s. Shaped pulse length and power were calculated by considering an amide ^1H bandwidth of 4.5 ppm and a chemical shift offset of 8.25 ppm. The same experimental conditions were used for studying the interaction of the FUS RRM mutants (N284A, K315/216A, D342A and D343A) with PAR. From the 2D ^1H - ^{15}N SOFAST-HMQC spectra, chemical shift perturbations (CSPs) were calculated as $\Delta\delta = \sqrt{0.5(0.14 \cdot \Delta\delta^{15}\text{N})^2 + (\Delta\delta^1\text{H})^2}$. The overall binding efficiency between the protein fragments and the different ligands is evaluated by calculating the standard deviation (σ) of the CSPs.

In order to analyze the binding specificity of FUS RRM:PAR interaction, NMR competition assays were performed using 2D ^1H - ^{15}N SOFAST-HMQC experiments recorded on equimolar samples (50 μM) of ^{15}N FUS RRM or TDP-43 RRM2 in presence of PAR, T10 or a mixture of both ligands. These same samples have been used to record WaterLOGSY experiments (1024 scans). Control experiments were carried out without PAR and with the ligands alone. The binding is evaluated by the modification of ligand peak intensities (more positive or less negative) upon protein binding. A last NMR competition assay has been performed by recording 2D ^1H - ^{15}N SOFAST-HMQC experiment on a sample containing preformed TDP-43:PAR complex on which FUS RRM has been added.

NMR experiments have been also designed to analysis the PARylation effect on FUS RRM and its D343 mutant. 1D (64 scans) and 2D ^1H - ^{15}N SOFAST-HMQC (32 scans) spectra has been recorded at different times (0, 10', 50', 1h30 and 3h) on a sample containing 50 μM ^{15}N FUS RRM or D343, 1 μM PARP-1, 3 mM NAD^+ and 25 mM MgCl_2 in HEPES buffer (20 mM, pH 7.5). The PARP-1 activation was initiated by the addition of 1 μM DNA duplex (30 bp) and it could be easily followed on the 1D spectra by the observation of NAD^+ consumption and nicotinamide appearance over time.

PAR used for NMR analysis was synthesized in the reaction mixture (3 ml) consisting of 50 mM Tris- HCl (pH 7.5), 2 mM DTT, 4 mM MgCl_2 , 1 μM DNA duplex (30 bp), 0.35 μM

PARP-1 and 0.5 mM NAD⁺ + 0.05 μCi [³²P]-NAD⁺ (was added for the visualization). The mixture was incubated at 37°C for 1 hour. After that, the purification of PAR was processed as described previously (*Amé et al., 2017*). The bulk PAR was analyzed by gel electrophoresis using modified DNA sequencing gels as described (*Panzeter et al., 1990*). PAR concentration was estimated by measurement of absorbance at 258 nm (A₂₅₈) and application of an extinction coefficient of 13.5 mM⁻¹cm⁻¹ for ADP-ribose (ADPr).

CONCLUSIONS AND PERSPECTIVES

The goal of this research is to explore the relationship between FUS and PAR in response to the oxidative stress-induced PARP-1 activation. The study can be divided into three main parts.

In the first part (Chapter 1), we examine the interaction between FUS and PARylated PARP-1, along with other RNA-binding proteins, including FET family members EWSR1 and TAF15, and DNA repair factors that are involved in single-strand DNA break repair. The second part (Chapter 2 and 3) focuses on the interplay between transcription and the DNA damage response. Our findings demonstrate that FUS enhances PAR levels in cells exposed to oxidative stress in a transcription-dependent manner. In the final part (Chapter 4-6), we investigate the structure-function relationship of FUS and PARP-1, with a particular focus on the interaction of the structured RRM domain of FUS with PAR and its role in the regulation of PARP-1 activity.

Numerous RNA-binding proteins, including TDP-43, HuR, and NONO, have been studied for their involvement in DNA repair (*Mitra et al., 2019; Gorospe, 2003; Krietsch et al., 2012*). However, for DNA repair mechanisms that rely on PARP-1 activation, members of the FET family, namely FUS, TAF15, and EWSR1, seem to be crucial. By using a new “microtubule bench” method recently developed in the laboratory of Pr. David Pastré, we demonstrated that PARP-1 mixes much better with FET family members, particularly with FUS, than with other RNA-binding proteins, including TDP-43, HuR, SAM68, G3BP1 and LIN28. We suggested that the interaction and mixing between PARP-1 and FUS is mediated by PAR, which is present in the cytoplasm due to basal PARylation of PARP-1 tagged with the microtubule binding domain. Our hypothesis was supported by the detection of PAR along the microtubule network when PARP-1 is brought to microtubules. Moreover, our experiments demonstrated that the PARP-1 mutant K893I, which lacks the ability to catalyze PAR synthesis, shows a weaker interaction with FUS than the wild-type PARP-1. Results of PLA (proximity ligation assay) further confirmed the colocalization of PARP-1 and FUS in the nucleus after oxidative DNA damage, which was significantly

reduced when cells were pre-treated with the PARP inhibitor olaparib, implying the PAR-mediated nature of their interaction.

Previous research has shown that FUS creates dynamic compartments where damaged DNA accumulates when PARylated PARP-1 is present (*Singatulina et al., 2019*). We postulated that such compartments might assist in concentrating DNA repair factors at sites of DNA damage, thereby facilitating DNA repair. However, it was unclear which DNA repair factors could be recruited to these FUS-rich compartments. In this study, we discovered that in addition to PARP-1, XRCC1 - another highly PARylated DNA repair protein - exhibits strong mixing with FUS. This finding is not unexpected, given that XRCC1 has been previously shown to interact with FUS and PARylated PARP-1 (*Wang et al., 2018*).

Despite multiple recent works describing FUS recruitment to the sites of DNA damage in a PARP-1 activity dependent manner, the biological functions of FUS in DNA repair mechanisms related to PARP-1 activation were still unclear (*Mastrocola et al., 2013; Altmeyer et al., 2015*). To investigate whether FUS expression level may impact PARP-1 activity and PAR level in cells, we, first, treated HeLa cells with siRNA targeting FUS in oxidative stress conditions. The reduction of FUS expression had no effect on PAR level, which can be explained by compensatory expression mechanisms of other FET proteins. Then we tried to overexpress HA-FUS, HA-HuR and HA-TDP-43. The overexpression of HA-FUS but not other RBPs followed by H₂O₂ treatment resulted in the significant increase in PAR level. As it was previously demonstrated that RNA and PAR compete for binding to FUS, we suggested that binding of the majority of FUS molecules to RNA may mask its functions in DNA damage response mediated by PARP-1. The treatment of HA-FUS expressing cells with the transcription inhibitor ActD followed by oxidative stress lead to a striking increase in PAR level. Given that, first, FUS is bound to nascent mRNA and, second, DNA damage more likely takes place in the transcriptionally active chromatin, FUS is found in close proximity to DNA damage sites and can quickly relocate to them. Consistently with the result obtained *in vivo*, FUS significantly increases the level of PARylation in reconstituted system *in vitro* by serving as a PAR acceptor. Based on these results we propose the following model: upon DNA breaks, mRNA transcription is locally

halted, which result in the release of FUS from nascent mRNA. FUS can be further recruited to PARylated PARP-1 located in DNA damage sites and stimulate PARP-1 activity leading to the formation of liquid-like compartments and the recruitment of additional DNA repair factors (Figure 39).

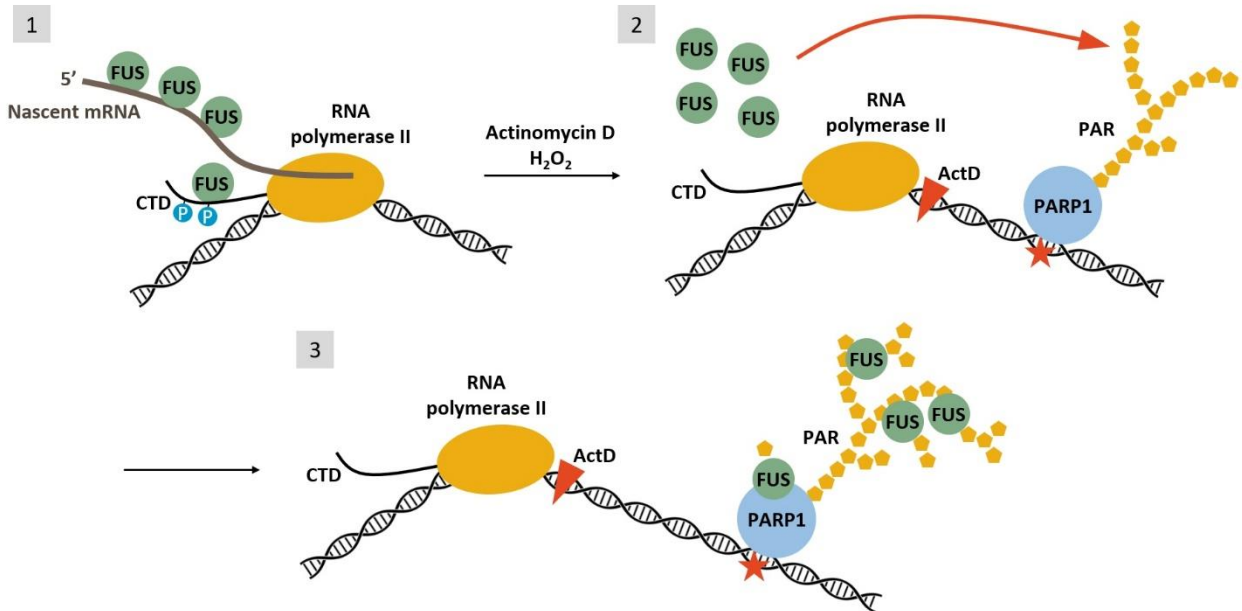


Figure 39: The model of FUS stimulation of PARP-1 activity in H₂O₂-treated cells in a transcription-dependent manner.

Interestingly, we have also demonstrated that the simultaneous treatment of HeLa cells with transcription inhibitor ActD and PARylation inhibitor olaparib affect drastically FUS nuclear distribution. Due to losing two binding platforms, mRNA and PAR, free FUS tend to form nuclear aggregates via its self-adhesive domains (Figure 40).

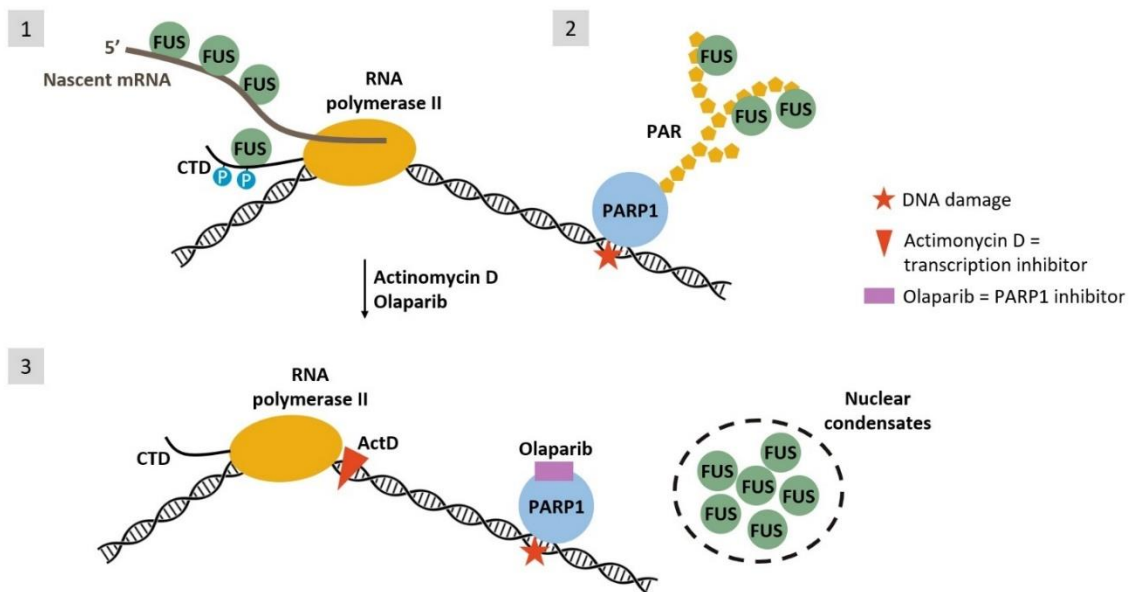


Figure 40: Schematic of FUS formation of nuclear condensates in the absence of PAR and mRNA.

Numerous RNA-binding proteins have been identified as PAR readers in large-scale mass spectrometry analyses, with some containing PAR-binding domains such as RGG domains or KR-rich domains (*Jungmichel et al., 2013; Martello et al., 2016; Zhang et al., 2013; Gagne et al., 2012; Teloni et al., 2015*). FUS, for example, interacts with PAR via electrostatic interactions between its positively charged RGG domains and negatively charged PAR polymer (*Rhine et al., 2022; Altmeyer et al., 2015*). However, the reason for FUS's particularly prominent role in PARP-1-mediated mechanisms compared to other RBPs with similar domains remains unclear. The answer may lie in the RRM domain of FET family members, which is distinct from canonical RRM domains. The RRM domain of FUS lacks several aromatic residues in the RNP1 motif, which are usually involved in the interaction of RBPs' RRM with RNA (*Liu et al., 2013*). This absence may explain the low specificity of FUS towards different mRNAs, as well as its similar interaction with mRNA and structurally resembling PAR. Additionally, the RRM domain of FET proteins contains a long positively charged Lys-Lys-containing loop (KK-loop), which can form electrostatic interactions with both RNA and PAR (*Van Attikum & Gasser, 2009*). In our study, we used a structural approach to demonstrate that the RRM domain of FUS specifically interacts with protein-free PAR. Importantly, the same residues in FUS RRM are involved in its interaction with both RNA and PAR. FUS RRM is also important for FUS-dependent increase of the PARylation level in cell. Thus, the replacement of FUS RRM domain to RRM1 domain of TDP-43 completely alleviated the increase of PAR level in cells after the chimeric protein overexpression and treatment with ActD and H₂O₂.

Finally, in this study we identified the role D343 residue in the RRM domain, that was previously showed to be PARylated in large-scale mass-spectrometry analysis (*Zhang et al., 2013*). We demonstrated that D343A mutation neither change FUS RRM structure, nor affect FUS RRM interaction with PAR or RNA. However, similar to the results obtained for FUS with RRM domain exchanged to RRM1 domain of TDP-43, this point D343A mutation led to the drastic decrease in PAR level in HeLa cells after transcription inhibition and exposure to oxidative stress. To better understand such effect of the point mutation, we performed an additional experiment of FUS D343A PARylation in the

reconstituted system *in vitro*. FUS D343A appeared to be slightly less PARylated compared to wild-type FUS, however the presence of FUS D343A significantly increased PARP-1 PARylation *in vitro*. The exact mechanism by which the point mutation in the FUS protein leads to a global decrease in PAR levels in HA-FUS expressing cells under oxidative stress and transcriptional inhibition remains to be determined. However, our results suggest that PARylation of the FUS RRM domain may serve as an additional mode of regulation and control of PARP-1 activation in cells.

Exploring this area further in the future may uncover insights into the following matters:

- The pathological mutations of FUS have been linked to several neurodegenerative diseases, such as ALS and FTL. It has been recently established that the deregulation of DNA repair is associated with the progression of these diseases. Therefore, understanding the functional role of FUS in PARP-1-dependent DNA repair is critical in understanding the development of the pathology. First of all, the pathological mutations in FUS often occur in its RGG domains (Literature review, Chapter 3.4.1, Figure 15), which are also involved in FUS binding to PAR. In this regard, it would be interesting to investigate how the ALS-associated mutations impact FUS binding to PAR and the capacity to control PARP-1 activity *in vitro* and *in vivo*. Secondly, the LC domain of FUS is also subjected to mutations or PTMs in ALS and FTL cases, with several of them impacting the ability of FUS to undergo LLPS. But how do these mutations or PTMs affect the role of FUS in PARP-1-dependent DNA damage response? If the formation of FUS-rich compartments in DNA damage sites indeed increases the efficiency of DNA repair we may speculate that the mutations or PTMs in IDRs of FUS may result in a decreased DNA repair rate or efficiency. It was previously demonstrated that the phosphomimetic mutant of FUS (with 12 mutations of serine to glutamic acid in the LC domain) totally loses the ability to compartmentalize in a reconstituted system *in vitro* containing activated PARP-1 (Singatulina *et al.*, 2019). However, the role of LC domain phosphorylation in FUS ability to regulate PARP-1 have not been investigated.

- The dysregulation of PARP-1 activity, leading to the accumulation of DNA damage and genomic instability, has been associated with the development of cancer (Wang L. *et al.*, 2017). The findings of this study shed new light on the molecular mechanisms underlying the role of FUS in the regulation of PARP-1 activity after genotoxic stress. In this regard, may the disruption of FUS normal functions play a role in the development of these pathologies?
- Several additional questions concerning the formation, function and dissociation of FUS-rich compartments at DNA damage sites arise. FUS is known to interact with non-coding RNAs (Literature review, Chapter 3.2.6 and 3.2.7), suggesting that they may be recruited to FUS-rich compartments formed at the sites of PARP-1 activation. Which non-coding RNAs can be recruited to FUS-rich compartments following PARP-1 activation and what is their role in DNA repair? It is known that damaged DNA-accumulating PAR-FUS compartments dissociate in the presence of PARG. Possibly, the additional control mechanisms of compartment dissociation exist in cells. For example, the phosphorylation of LC domain of FUS was shown to inhibit the capacity of FUS to form compartments *in vitro* (Singatulina *et al.*, 2019), suggesting that the phosphorylation of FUS LC domain in cells may also stimulate the dissociation of compartments, which would be interesting to investigate.
- PARP-1 plays an important role in the remodelling of chromatin, when DNA damage occurs, resulting in DNA more accessible for repair (Sinha *et al.*, 2021). The interplay between FUS function in the formation of compartments in DNA damage sites and PARP-1-modulated chromatin remodelling have never been investigated, leaving a room to maneuver for further studies. To start, the formation of FUS compartments in the presence of reconstituted nucleosomes can be investigated.
- Recently a new binding factor of PARP-1, known as HPF1, has been discovered (Leung, 2017), which targets the PARylation catalysed by PARP-1 to serine residues (Bonfiglio *et al.*, 2017). The PARylation of FUS by PARP-1 in the presence of HPF1 can be further investigated *in vitro*, thus working in more physiologically relevant conditions as HPF1 is present in a relatively high concentration in cells (Leung, 2017).

- Finally, in the long term perspective the understanding of the interplay between the functions of RNA-binding proteins and PARP-1-mediated DNA repair mechanisms can be used for the development of drugs for the treatment of neurodegenerative diseases, such as ALS and FTLN, as well as certain types of cancer.

SYNTHESE EN FRANÇAIS

INTRODUCTION

Les dommages causés à l'ADN sont une conséquence inévitable de la vie quotidienne, car notre matériel génétique est continuellement exposé à une variété d'agents dommageables tels que les radiations, les toxines et les sous-produits métaboliques. Ces agents peuvent provoquer des mutations génétiques et des anomalies chromosomiques, entraînant le développement de maladies graves telles que le cancer et les troubles neurologiques. Heureusement, nos cellules ont développé des mécanismes sophistiqués pour détecter et réparer les dommages causés à l'ADN, assurant ainsi la préservation de l'intégrité génomique et prévenant l'apparition de telles maladies (*Ciccia & Elledge, 2010*).

La réparation de l'ADN désigne l'ensemble des processus cellulaires qui reconnaissent et corrigent les dommages causés à l'ADN. Dans le cas des cassures simple brin (SSB), l'enzyme poly(ADP-ribose) polymérase 1 (PARP-1) joue un rôle clé dans la réparation de l'ADN des SSB. PARP-1 est un capteur de dommages à l'ADN qui est rapidement recruté sur les sites de dommages à l'ADN où il catalyse la synthèse du poly(ADP-ribose) en utilisant le NAD⁺ comme substrat. Ainsi, PARP-1 transfère des unités d'ADP-ribose du NAD⁺ à elle-même ou à d'autres protéines cibles, formant une chaîne de poly(ADP-ribose) (PAR) (*Schreiber et al., 2006 ; Alessova & Lavrik, 2019*). De nombreux rôles fonctionnels ont été attribués à la formation des chaînes PAR. L'un des principaux rôles de PAR est de recruter et d'activer d'autres facteurs de réparation de l'ADN sur les sites de dommages à l'ADN en leur servant de molécule d'échafaudage (*Haince et al., 2008 ; Hanzlikova et al., 2017*). PAR joue également un rôle essentiel dans la régulation de la condensation de la chromatine. La PARylation des histones et d'autres protéines associées à la chromatine peut modifier la structure de la chromatine et réguler l'expression des gènes (*Luo et al., 2012 ; Chaudhuri & Nussenzweig, 2017*). PAR participe à plusieurs autres processus cellulaires, tels que la régulation du cycle cellulaire, l'apoptose et l'inflammation. Les longues chaînes de PAR ont une durée de vie très courte, de quelques secondes à quelques minutes, grâce à l'action permanente de la poly(ADP-ribose) glycohydrolase

(PARG), une enzyme qui hydrolyse les polymères de poly(ADP-ribose) (*Illuzzi et al., 2014*). La nature réversible de la PARylation permet une régulation dynamique des processus cellulaires, l'équilibre entre la PARylation et la dégradation de la PAR étant étroitement contrôlé.

L'activation de PARP-1 recrute plusieurs facteurs protéiques, qui ont été identifiés grâce à des analyses à grande échelle par spectrométrie de masse. Ces facteurs ont une affinité pour PAR (lecteurs de PAR) ou sont eux-mêmes PARylés (*Kliza et al., 2021 ; Jungmichel et al., 2013 ; Martello et al., 2016 ; Zhang et al., 2013 ; Gagne et al., 2012*). Outre les facteurs de réparation de l'ADN tels que XRCC1 et l'ADN polymérase β , plusieurs autres protéines dont le lien avec la réparation de l'ADN est moins clair ont également été identifiées, suscitant un intérêt considérable. L'un de ces groupes est celui des protéines de liaison à l'ARN (RBP). Si l'on considère les mécanismes de réparation de l'ADN qui dépendent de l'activation de PARP-1, il apparaît que les membres de la famille FET des protéines de liaison à l'ARN, FUS, EWSR1 et TAF15, jouent un rôle central. Les trois membres de la famille FET sont recrutés sur les sites de lésions de l'ADN après une exposition à un faisceau laser, et ce recrutement dépend de l'activité de PARP-1 (*Izhar et al., 2015 ; Rulten et al., 2014*). Ils ont été identifiés dans des analyses de spectrométrie de masse des protéines PARylées après un stress génotoxique et, en outre, en tant que lecteurs PAR (*Jungmichel et al., 2013 ; Zhang et al., 2013 ; Rhine et al., 2022 ; Teloni & Altmeyer, 2015*). FUS, mais aussi certainement les autres membres de la famille FET, forment des compartiments sur les sites de dommages à l'ADN grâce à des interactions entre ses domaines peu complexes (*Rhine et al., 2022 ; Teloni et al., 2015 ; Patel et al., 2015 ; Schwartz et al., 2013*). La formation de tels compartiments sur les sites de dommages à l'ADN a été observée dans un système reconstitué suite à l'activation de PARP-1 (*Singatulina et al., 2019*). Par ailleurs, outre ses rôles dans la biogenèse de l'ARN et la réparation de l'ADN qui se chevauchent avec les rôles des deux autres protéines FET, la fonction cellulaire de FUS est associée au développement de troubles neurologiques tels que la sclérose latérale amyotrophique (SLA) et la dégénérescence lobaire frontotemporale (FTLD), ce qui en fait une cible originale pour des recherches plus approfondies (*Zhao et al., 2018 ; Van Langenhove et al., 2010*).

L'objectif de cette étude est d'étudier les fonctions biologiques de FUS dans la réponse aux dommages de l'ADN liée à l'activation de PARP-1. FUS est connu pour participer à la régulation de la transcription en interagissant avec le domaine C-terminal de l'ARN Pol II et en se liant à l'ARNm naissant (Schwartz *et al.*, 2012 ; Burke *et al.*, 2015). Étant donné que les dommages à l'ADN se produisent souvent dans une chromatine ouverte et transcriptionnellement active, FUS est situé à proximité des sites de dommages à l'ADN et peut être rapidement dirigé vers eux (Pankotai *et al.*, 2013 ; Dinant *et al.*, 2008 ; Van Attikum & Gasser ; 2009). A cet égard, la première question décrite dans cette étude était le lien entre la transcription et la réparation de l'ADN dans le contexte des fonctions de FUS dans le noyau. Deuxièmement, la fonction de FUS dans la réparation de l'ADN dépendante de PARP-1 est basée sur sa capacité à lier PAR. Alors que d'autres protéines liant l'ARN peuvent également se lier à PAR par le biais d'interactions électrostatiques, FUS a une propension unique à se lier à PAR et à être PARylée (Teloni & Altmeyer ; 2015). Par conséquent, la compréhension des caractéristiques structurales qui rendent FUS unique parmi les autres protéines de liaison à l'ARN et la nature des interactions FUS-PAR peuvent contribuer à éclairer son rôle dans la réparation de l'ADN dépendante de PAR.

OBJECTIFS DE LA THÈSE

Des études récentes ont mis en évidence le rôle crucial des interactions multivalentes entre des domaines peu complexes de protéines liant l'ARN, comme FUS, dans la formation de compartiments sans membrane (Rhine *et al.*, 2022 ; Teloni *et al.*, 2015 ; Patel *et al.*, 2015 ; Schwartz *et al.*, 2013). Des recherches antérieures menées par A. Singatulina, doctorante dans les laboratoires de David Pastré et Olga Lavrik, ont révélé que FUS, en présence de PAR, peut générer des compartiments dynamiques sur les sites de dommages à l'ADN (Singatulina *et al.*, 2019). Nous supposons que ces compartiments peuvent aider à concentrer les facteurs de réparation de l'ADN sur les sites de dommages à l'ADN. Bien que la régulation de la réparation des cassures de l'ADN ait été précédemment attribuée à PARP-1 et à PAR synthétisé (Revue de la littérature, chapitre 2.3), les résultats suggèrent que la présence de protéines de liaison à l'ARN pourrait être nécessaire pour stimuler la capacité de PAR à recruter des facteurs de réparation de l'ADN

et à déplacer les nucléosomes, favorisant ainsi la réparation de l'ADN. Des essais *in vitro* ont systématiquement montré que PAR favorise la séparation de la phase liquide-liquide des FUS (Revue de la littérature, chapitre 3.3.1.2). C'est pourquoi nous avons voulu savoir quelles protéines liant l'ARN pouvaient se colocaliser et former des compartiments avec PARP-1. Parmi les protéines liant l'ARN, FUS est-il le principal partenaire de PARP-1 ? L'interaction entre PARP-1 et FUS dépend-elle de l'activité de PARP-1 et de la synthèse de PAR ? En outre, les facteurs de réparation de l'ADN qui peuvent être recrutés dans les compartiments sans membrane riches en FUS sont pour la plupart inconnus. Par conséquent, une question supplémentaire à laquelle nous avons tenté de répondre dans cette étude est la suivante : quels facteurs de réparation de l'ADN peuvent être recrutés dans les compartiments sans membrane riches en FUS ? (Chapitre 1)

Malgré de nombreux travaux récents décrivant le recrutement de FUS sur les sites de dommages à l'ADN de manière dépendante de l'activité de PARP-1, les fonctions biologiques de FUS dans les mécanismes de réparation de l'ADN liés à l'activation de PARP-1 n'étaient toujours pas claires (*Rulten et al., 2014 ; Izhar et al., 2015*). Étant donné que FUS n'est pas seulement un lecteur de PAR mais aussi l'un des accepteurs efficaces de PAR dans les cellules, nous nous sommes demandé si FUS pouvait réguler l'activité de PARP-1 et les niveaux de PAR dans les cellules en tant que protéine acceptrice de PAR. Pour ce faire, nous avons examiné comment les modifications des niveaux d'expression de FUS et d'autres protéines de liaison à l'ARN (HuR, TDP-43) affectent l'activité de PARP-1 et la synthèse de PAR dans le cadre d'un stress génotoxique. Plus précisément, nous avons réduit l'expression ou surexprimé FUS dans des cellules HeLa exposées à de faibles concentrations de peroxyde d'hydrogène, un agent de stress oxydatif connu qui génère des cassures de l'ADN rapidement réparables et active fortement PARP-1 (chapitres 2 et 3).

On sait que FUS joue un rôle dans la transcription en interagissant avec le domaine C-terminal de l'ARN Pol II et en se liant à l'ARNm naissant. Cela suggère que l'activité de FUS peut être régulée par l'état de la transcription (*Schwartz et al., 2012 ; Burke et al., 2015*). De plus, comme les dommages à l'ADN se produisent fréquemment dans la

chromatine ouverte et transcriptionnellement active, FUS se trouve à proximité des sites de dommages à l'ADN et peut rapidement s'y déplacer (*Pankotai et al., 2013 ; Dinant et al., 2008 ; Van Attikum & Gasser, 2009*). Dans ce contexte, nous avons voulu savoir si l'inhibition de la transcription pouvait amener FUS à se dissocier de l'ARNm et à se lier à PAR en cas de stress génotoxique, ce qui pourrait intensifier son rôle dans la réparation de l'ADN. Pour répondre à cette question, nous avons traité des cellules HeLa avec différents inhibiteurs de la transcription (ActD, DRB et oxaliplatine) avant de les exposer au peroxyde d'hydrogène (chapitre 2). L'ARNm et le PAR peuvent tous deux servir de plateformes de liaison pour FUS. Une étude antérieure a montré que l'ARN nucléaire est un facteur majeur pour limiter la formation aberrante de phases liquides de FUS dans le noyau. À cet égard, nous nous sommes demandés comment l'inhibition simultanée de la transcription par le traitement ActD et de la PARylation par le traitement olaparib influençait la distribution nucléaire de FUS. (Chapitre 1)

Un certain nombre de protéines liant l'ARN ont été identifiées dans des analyses de spectrométrie de masse à grande échelle comme des lecteurs de PAR hébergeant des domaines de liaison PAR, tels que le domaine RRM, les répétitions RGG, les domaines riches en SR et en KR (revue de la littérature, tableau 1) (*Jungmichel et al., 2013 ; Martello et al., 2016 ; Zhang et al., 2013 ; Gagne et al., 2012 ; Teloni et al., 2015*). Il a été démontré que l'interaction entre FUS et PAR est principalement orchestrée par les domaines RGG non structurés de FUS (*Rhine et al., 2022 ; Altmeyer et al., 2015*). Il n'est cependant pas clair pourquoi FUS apparaît comme une protéine particulièrement encline à se lier à PAR et à être PARylée, alors que plusieurs autres protéines liant l'ARN portent des domaines RGG ou des répétitions riches en SR ou en KR qui peuvent également former des interactions électrostatiques avec PAR. Nous suggérons que le domaine RRM structuré de FUS pourrait être la clé de cette énigme. Le domaine RRM des protéines FET présente des caractéristiques distinctes qui le distinguent des domaines RRM d'autres RBP (Revue de la littérature, chapitre 3). Par conséquent, dans ce travail, nous avons cherché à étudier la base structurelle de la reconnaissance de PAR par le RRM de FUS et à la comparer avec sa liaison à l'ARN en utilisant une analyse par spectroscopie RMN. Pour étudier plus avant si le domaine RRM de FUS joue un rôle dans la régulation de l'activité de PARP-1 et affecte

le niveau de PAR dans les cellules, nous avons exprimé une forme chimérique de FUS dans laquelle le domaine RRM de FUS a été remplacé par le RRM1 de TDP-43 (chapitres 4 et 5). (Chapitres 4 et 5)

De plus, afin d'approfondir l'influence du RRM de FUS sur le contrôle de l'activité de PARP-1, nous avons procédé à des mutations ponctuelles des résidus d'acides aminés dans le domaine RRM (K315A/K316A, N284A, D342A et D343A). Notre objectif était d'examiner l'effet de certains résidus situés dans le RRM de FUS sur sa liaison à PAR et la régulation de l'activité de PARP-1 qui s'ensuit. Au cours d'expériences *in vivo*, nous avons constaté que la mutation du résidu d'acide aminé D343 a des implications fonctionnelles significatives. (Chapitre 6)

En résumé, l'objectif de cette recherche est d'étudier l'interaction de FUS avec PAR après l'activation de PARP-1 induite par les dommages à l'ADN et la régulation de l'activité de PARP-1 par FUS. Cette étude répondra donc aux questions suivantes :

- 1) Quelles protéines liant l'ARN pourraient se colocaliser et former des compartiments avec PARP-1 ? L'interaction entre PARP-1 et FUS dépend-elle de l'activité de PARP-1 et de la synthèse de PAR ? Quels facteurs de réparation de l'ADN peuvent interagir et former des compartiments avec FUS ?
- 2) FUS, en tant que protéine acceptrice de PAR, peut-il réguler l'activité de PARP-1 et les niveaux de PAR dans les cellules ? Comment l'inhibition de la transcription affecte-t-elle l'influence de FUS sur la synthèse PARP-1 ? Comment l'inhibition simultanée de la transcription et de la synthèse de PAR influence-t-elle la distribution nucléaire de FUS ?
- 3) Quel est le rôle du domaine RRM de FUS dans la liaison à PAR et la régulation de l'activité de PARP-1 ? Quel est le rôle de certains résidus du domaine RRM de FUS dans sa liaison à PAR et dans la régulation de l'activité de PARP-1 ?

CONCLUSIONS ET PERSPECTIVES

L'objectif de cette recherche est d'explorer la relation entre FUS et PAR en réponse à l'activation de PARP-1 induite par le stress oxydatif. L'étude peut être divisée en trois parties principales.

Dans la première partie (chapitre 1), nous examinons l'interaction entre FUS et PARP-1 PARylée, ainsi que d'autres protéines de liaison à l'ARN, notamment les membres de la famille FET EWSR1 et TAF15, et les facteurs de réparation de l'ADN qui sont impliqués dans la réparation des cassures simple brin de l'ADN. La deuxième partie (chapitres 2 et 3) se concentre sur l'interaction entre la transcription et la réponse aux dommages de l'ADN. Nos résultats démontrent que FUS augmente les niveaux de PAR dans les cellules exposées au stress oxydatif d'une manière dépendante de la transcription. Dans la dernière partie (chapitre 4-6), nous étudions la relation structure-fonction de FUS et de PARP-1, en nous concentrant particulièrement sur l'interaction du domaine RRM structuré de FUS avec PAR et sur son rôle dans la régulation de l'activité de PARP-1.

De nombreuses protéines liant l'ARN, dont TDP-43, HuR et NONO, ont été étudiées pour leur implication dans la réparation de l'ADN (*Mitra et al., 2019 ; Gorospe, 2003 ; Krietsch et al., 2012*). Cependant, pour les mécanismes de réparation de l'ADN qui reposent sur l'activation de PARP-1, les membres de la famille FET, à savoir FUS, TAF15 et EWSR1, semblent être cruciaux. En utilisant une nouvelle méthode de "microtubules bench" récemment développée dans le laboratoire SABNP, nous avons démontré que PARP-1 se mélange beaucoup mieux avec les membres de la famille FET, en particulier avec FUS, qu'avec d'autres protéines liant l'ARN, y compris TDP-43, HuR, SAM68, G3BP1 et LIN28. Nous avons suggéré que l'interaction et le mélange entre PARP-1 et FUS sont médiés par PAR, qui est présent dans le cytoplasme en raison de la PARylation basale de PARP-1 marqué avec le domaine de liaison aux microtubules. Notre hypothèse a été confirmée par la détection de PAR le long du réseau de microtubules lorsque PARP-1 est amené sur les microtubules. De plus, nos expériences ont démontré que le mutant PARP-1 K893I, qui n'a pas la capacité de catalyser la synthèse de PAR, présente une interaction plus faible avec FUS que le PARP-1 de type sauvage. Les résultats du PLA (proximity

ligation assay) ont confirmé la colocalisation de PARP-1 et de FUS dans le noyau après un dommage oxydatif de l'ADN, qui a été significativement réduite lorsque les cellules ont été prétraitées avec l'inhibiteur de PARP, l'olaparib, ce qui implique que PAR est essentielle à leur médiation.

Des recherches antérieures ont montré que FUS crée des compartiments dynamiques où l'ADN endommagé s'accumule en présence de PARP-1 PARylée (*Singatulina et al., 2019*). Nous avons postulé que ces compartiments pourraient aider à concentrer les facteurs de réparation de l'ADN sur les sites de dommages à l'ADN, facilitant ainsi la réparation de l'ADN. Cependant, nous ne savions pas exactement quels facteurs de réparation de l'ADN pouvaient être recrutés dans ces compartiments riches en FUS. Dans cette étude, nous avons découvert qu'en plus de PARP-1, XRCC1 - une autre protéine de réparation de l'ADN hautement PARylée - présente un fort mélange avec FUS. Ce résultat n'est pas inattendu, étant donné qu'il a été précédemment démontré que XRCC1 interagit avec FUS et PARP-1 PARylée (*Wang et al., 2018*).

Malgré de nombreux travaux récents décrivant le recrutement de FUS sur les sites de dommages à l'ADN de manière dépendante de l'activité de PARP-1, les fonctions biologiques de FUS dans les mécanismes de réparation de l'ADN liés à l'activation de PARP-1 n'étaient toujours pas claires (*Mastrocola et al., 2013 ; Altmeyer et al., 2015*). Afin d'étudier si le niveau d'expression de FUS peut avoir un impact sur l'activité de PARP-1 et le niveau de PAR dans les cellules, nous avons tout d'abord traité des cellules HeLa avec un siRNA ciblant FUS dans des conditions de stress oxydatif. La réduction de l'expression de FUS n'a pas eu d'effet sur le niveau de PAR, ce qui peut s'expliquer par des mécanismes d'expression compensatoires d'autres protéines FET. Nous avons ensuite essayé de surexprimer HA-FUS, HA-HuR et HA-TDP-43. La surexpression de HA-FUS, mais pas des autres RBP, suivie d'un traitement au H₂O₂ a entraîné une augmentation significative du niveau de PAR. Comme il a été démontré précédemment que l'ARN et la PAR sont en compétition pour la liaison à FUS, nous avons suggéré que la liaison de la majorité des molécules FUS à l'ARN pourrait masquer ses fonctions dans la réponse aux dommages de l'ADN médiée par la PARP-1. Le traitement des cellules exprimant HA-FUS avec l'inhibiteur

de transcription ActD suivi d'un stress oxydatif a conduit à une augmentation frappante du niveau de PAR. Étant donné que, premièrement, FUS est lié à l'ARNm naissant et que, deuxièmement, les lésions de l'ADN se produisent plus probablement dans la chromatine transcriptionnellement active, FUS se trouve à proximité des sites de lésions de l'ADN et peut rapidement s'y déplacer. Conformément aux résultats obtenus *in vivo*, FUS augmente de manière significative le niveau de PARylation dans le système reconstitué *in vitro* en servant d'accepteur de PAR. Sur la base de ces résultats, nous proposons le modèle suivant : lors des cassures de l'ADN, la transcription de l'ARNm est localement interrompue, ce qui entraîne la libération de FUS de l'ARNm naissant. FUS peut ensuite être recruté par la PARP-1 PARylée située dans les sites de dommages à l'ADN et stimuler l'activité de la PARP-1, ce qui entraîne la formation de compartiments liquides et le recrutement d'autres facteurs de réparation de l'ADN (Figure 39).

De manière intéressante, nous avons également démontré que le traitement simultané des cellules HeLa avec l'inhibiteur de transcription ActD et l'inhibiteur de PARylation olaparib affecte drastiquement la distribution nucléaire de FUS. En raison de la perte de deux plateformes de liaison, l'ARNm et PAR, FUS libre a tendance à former des agrégats nucléaires grâce à ses domaines auto-adhésifs (Figure 40).

De nombreuses protéines liant l'ARN ont été identifiées comme des lecteurs de PAR dans des analyses de spectrométrie de masse à grande échelle, certaines contenant des domaines de liaison à PAR tels que des domaines RGG ou des domaines riches en KR (Jungmichel et al., 2013 ; Martello et al., 2016 ; Zhang et al., 2013 ; Gagne et al., 2012 ; Teloni et al., 2015). FUS, par exemple, interagit avec PAR par le biais d'interactions électrostatiques entre ses domaines RGG chargés positivement et le polymère PAR chargé négativement (Rhine et al., 2022 ; Altmeyer et al., 2015). Cependant, la raison pour laquelle FUS joue un rôle particulièrement important dans les mécanismes régulés par PARP-1 par rapport à d'autres RBP ayant des domaines similaires n'est pas claire. La réponse pourrait se trouver dans le domaine RRM des membres de la famille FET, qui est distinct des domaines RRM canoniques. Le domaine RRM de FUS est dépourvu de plusieurs résidus aromatiques dans le motif RNP1, qui sont généralement impliqués dans l'interaction du

RRM des RBP avec l'ARN (Liu et al., 2013). Cette absence peut expliquer la faible spécificité de FUS vis-à-vis de différents ARNm, ainsi que son interaction similaire avec l'ARNm et sa ressemblance structurelle avec PAR. De plus, le domaine RRM des protéines FET contient une longue boucle Lys-Lys chargée positivement (boucle KK), qui peut former des interactions électrostatiques avec l'ARN et PAR (Van Attikum & Gasser, 2009). Dans notre étude, nous avons utilisé une approche structurale pour démontrer que le domaine RRM de FUS interagit spécifiquement avec PAR sans protéine. Il est important de noter que les mêmes résidus du RRM de FUS sont impliqués dans son interaction avec l'ARN et la PAR. Le RRM de FUS est également important pour l'augmentation dépendante de FUS du niveau de PARylation dans la cellule. Ainsi, le remplacement du domaine RRM de FUS par le domaine RRM1 de TDP-43 a complètement atténué l'augmentation du niveau de PAR dans les cellules après la surexpression de la protéine chimérique et le traitement avec ActD et H₂O₂.

Enfin, dans cette étude, nous avons identifié le rôle du résidu D343 dans le domaine RRM, qui a été précédemment décrit comme PARylée dans l'analyse de spectrométrie de masse à grande échelle (Zhang et al., 2013). Nous avons démontré que la mutation D343A ne modifie pas la structure du RRM de FUS, ni n'affecte l'interaction du RRM de FUS avec PAR ou RNA. Cependant, à l'instar des résultats obtenus pour FUS dont le domaine RRM a été échangé avec le domaine RRM1 de TDP-43, cette mutation ponctuelle D343A a conduit à une diminution drastique du niveau de PAR dans les cellules HeLa après inhibition de la transcription et exposition à un stress oxydatif. Pour mieux comprendre cet effet de la mutation ponctuelle, nous avons réalisé une expérience supplémentaire de PARylation de FUS D343A dans le système reconstitué *in vitro*. FUS D343A semble être légèrement moins PARylé que FUS de type sauvage, mais la présence du FUS D343A augmente significativement la PARylation de PARP-1 *in vitro*. Le mécanisme exact par lequel la mutation ponctuelle de la protéine FUS entraîne une diminution globale des niveaux de PAR dans les cellules exprimant HA-FUS en cas de stress oxydatif et d'inhibition de la transcription reste à déterminer. Cependant, nos résultats suggèrent que la PARylation du domaine RRM de FUS peut servir de mode supplémentaire de régulation et de contrôle de l'activation de PARP-1 dans les cellules.

L'exploration plus poussée de ce domaine à l'avenir pourrait permettre de mieux comprendre les questions suivantes :

- Les mutations pathologiques de FUS ont été associées à plusieurs maladies neurodégénératives, telles que la SLA et la FTLD. Il a été récemment établi que la dérégulation de la réparation de l'ADN est associée à la progression de ces maladies. Il est donc essentiel de comprendre le rôle fonctionnel des FUS dans la réparation de l'ADN dépendante de PARP-1 pour comprendre le développement de la pathologie. Tout d'abord, les mutations pathologiques de FUS se produisent souvent dans ses domaines RGG (Revue de la littérature, chapitre 3.4.1, figure 15), qui sont également impliqués dans la liaison de FUS à PAR. À cet égard, il serait intéressant d'étudier l'impact des mutations associées à la SLA sur la liaison de FUS à PAR et sur sa capacité à contrôler l'activité de PARP-1 *in vitro* et *in vivo*. Deuxièmement, le domaine LC de FUS est également soumis à des mutations ou à des PTM dans les cas de SLA et de FTLD, plusieurs d'entre elles ayant un impact sur la capacité de FUS à subir une LLPS. Mais comment ces mutations ou PTM affectent-elles le rôle de FUS dans la réponse aux dommages de l'ADN dépendant de PARP-1 ? Si la formation de compartiments riches en FUS dans les sites de dommages à l'ADN augmente effectivement l'efficacité de la réparation de l'ADN, on peut supposer que les mutations ou PTM dans les IDR de FUS peuvent entraîner une diminution du taux ou de l'efficacité de la réparation de l'ADN. Il a été démontré précédemment que le mutant phosphomimétique de FUS (avec 12 mutations de sérine en acide glutamique dans le domaine LC) perd totalement la capacité de se compartimenter dans un système reconstitué *in vitro* contenant PARP-1 activé (Singatulina et al., 2019). Cependant, le rôle de la phosphorylation du domaine LC dans la capacité de FUS à réguler PARP-1 n'a pas été étudié.

- La dysrégulation de l'activité de PARP-1, conduisant à l'accumulation de dommages à l'ADN et à l'instabilité génomique, a été associée au développement du cancer (Wang L. et al., 2017). Les résultats de cette étude apportent un nouvel éclairage sur les mécanismes moléculaires qui sous-tendent le rôle de FUS dans la régulation de l'activité de PARP-1

après un stress génotoxique. À cet égard, la perturbation des fonctions normales de FUS pourrait-elle jouer un rôle dans le développement de ces pathologies ?

- Plusieurs questions supplémentaires se posent concernant la formation, la fonction et la dissociation des compartiments riches en FUS sur les sites de lésions de l'ADN. On sait que FUS interagit avec des ARN non codants (Revue de la littérature, chapitres 3.2.6 et 3.2.7), ce qui suggère qu'ils peuvent être recrutés dans les compartiments riches en FUS formés sur les sites d'activation de PARP-1. Quels ARN non codants peuvent être recrutés dans les compartiments riches en FUS après l'activation de PARP-1 et quel est leur rôle dans la réparation de l'ADN ? On sait que les compartiments PAR-FUS accumulant l'ADN endommagé se dissocient en présence de PARG. Il est possible que d'autres mécanismes de contrôle de la dissociation des compartiments existent dans les cellules. Par exemple, il a été démontré que la phosphorylation du domaine LC de FUS inhibe la capacité de FUS à former des compartiments *in vitro* (Singatulina et al., 2019), ce qui suggère que la phosphorylation du domaine LC de FUS dans les cellules peut également stimuler la dissociation des compartiments, ce qu'il serait intéressant d'étudier.

- PARP-1 joue un rôle important dans le remodelage de la chromatine lorsque l'ADN est endommagé, ce qui rend l'ADN plus accessible pour la réparation (Sinha et al., 2021). L'interaction entre la fonction de FUS dans la formation de compartiments dans les sites de dommages à l'ADN et le remodelage de la chromatine modulé par PARP-1 n'a jamais été étudiée, ce qui laisse une marge de manœuvre pour d'autres études. Pour commencer, la formation de compartiments FUS en présence de nucléosomes reconstitués peut être étudiée.

- Récemment, un nouveau facteur de liaison de PARP-1, connu sous le nom de HPF1, a été découvert (Leung, 2017), qui cible la PARylation catalysée par PARP-1 sur des résidus sérine (Bonfiglio et al., 2017). La PARylation de FUS par PARP-1 en présence de HPF1 peut être étudiée plus avant *in vitro*, travaillant ainsi dans des conditions plus physiologiquement pertinentes puisque HPF1 est présent à une concentration relativement élevée dans les cellules (Leung, 2017).

- Enfin, dans une perspective à long terme, la compréhension de l'interaction entre les fonctions des protéines de liaison à l'ARN et les mécanismes de réparation de l'ADN régulés par PARP-1 peut être utile pour le développement de médicaments afin de traiter des maladies neurodégénératives, telles que la SLA et la FTLD, ainsi que de certains types de cancer.

BIBLIOGRAPHY

-A-

Abraham, M.J. et al. GROMACS: High performance molecular simulations through multi-level parallelism from laptops to supercomputers. *SoftwareX* **1**, 19–25 (2015).

Adamietz, P. & Hilz, H. Quantitative Erfassung von Poly(Adp-Ribose), Das über Zwei Verschiedene Bindungstypen an Nucleare Proteine Gebunden Ist. *Hoppe. Seylers. Z. Physiol. Chem.* **357**, 527–534 (1976).

Adamson, B., Smogorzewska, A., Sigoillot, F. D., King, R. W. & Elledge, S. J. A genome-wide homologous recombination screen identifies the RNA-binding protein RBMX as a component of the DNA-damage response. *Nat. Cell Biol.* **2012 143 14**, 318–328 (2012).

Aguiar, R. C. T., Takeyama, K., He, C., Kreinbrink, K. & Shipp, M. A. B-aggressive lymphoma family proteins have unique domains that modulate transcription and exhibit poly(ADP-ribose) polymerase activity. *J. Biol. Chem.* **280**, 33756–33765 (2005).

Ahel, I. et al. Poly(ADP-ribose)-binding zinc finger motifs in DNA repair/checkpoint proteins. *Nat.* **2007 4517174 451**, 81–85 (2008).

Ahlers, J. et al. The key role of solvent in condensation: Mapping water in liquid-liquid phase-separated FUS. *Biophys. J.* **120**, 1266–1275 (2021).

Akimov, V. et al. UbiSite approach for comprehensive mapping of lysine and N-terminal ubiquitination sites. *Nat. Struct. Mol. Biol.* **2018 257 25**, 631–640 (2018).

Alemasova, E. E. & Lavrik, O. I. A sePARate phase? Poly(ADP-ribose) versus RNA in the organization of biomolecular condensates. *Nucleic Acids Res.* **50**, 10817–10838 (2022).

Alemasova, E. E. & Lavrik, O. I. Poly(ADP-ribosyl)ation by PARP1: reaction mechanism and regulatory proteins. *Nucleic Acids Res.* **47**, 3811–3827 (2019).

Alemasova, E.E. et al. Y-box-binding protein 1 as a non-canonical factor of base excision repair. *Biochimica et Biophysica Acta (BBA)-Proteins and Proteomics* **1864**, 1631–1640 (2016).

Alemasova, E.E., Naumenko, K.N., Kurgina, T.A., Anarbaev, R.O. & Lavrik, O.I. The multifunctional protein YB-1 potentiates PARP1 activity and decreases the efficiency of PARP1 inhibitors. *Oncotarget* **9**, 23349 (2018).

Ali, A. A. E. et al. The zinc-finger domains of PARP1 cooperate to recognize DNA strand breaks. *Nat. Struct. Mol. Biol.* **2012 197 19**, 685–692 (2012).

Althaus F. R. *et al.* Poly ADP-ribosylation: a DNA break signal mechanism. *Mol. Cell Biochem.* **193**, 5-11 (1999).

Altmeyer, M. *et al.* Liquid demixing of intrinsically disordered proteins is seeded by poly(ADP-ribose). *Nat. Commun.* 2015 61 **6**, 1–12 (2015).

Altmeyer, M., Messner, S., Hassa, P. O., Fey, M. & Hottiger, M. O. Molecular mechanism of poly(ADP-ribosyl)ation by PARP1 and identification of lysine residues as ADP-ribose acceptor sites. *Nucleic Acids Res.* **37**, 3723–3738 (2009).

Amé, J. C., Spenlehauer, C. & De Murcia, G. The PARP superfamily. *BioEssays* **26**, 882–893 (2004).

Amouroux, R., Campalans, A., Epe, B. & Radicella, J.P. Oxidative stress triggers the preferential assembly of base excision repair complexes on open chromatin regions. *Nucleic acids research* **38**, 2878-2890 (2010).

Anderson, P. & Kedersha, N. RNA granules. *J. Cell Biol.* **172**, 803–808 (2006).

Andersson, M. K. *et al.* The multifunctional FUS, EWS and TAF15 proto-oncoproteins show cell type-specific expression patterns and involvement in cell spreading and stress response. *BMC Cell Biol.* **9**, 1–17 (2008).

Araya, N. *et al.* Cooperative interaction of EWS with CREB-binding protein selectively activates hepatocyte nuclear factor 4-mediated transcription. *J. Biol. Chem.* **278**, 5427–5432 (2003).

Arenas, A. *et al.* Lysine acetylation regulates the RNA binding, subcellular localization and inclusion formation of FUS. *Hum. Mol. Genet.* **29**, 2684–2697 (2020).

Aumiller, W. M., Pir Cakmak, F., Davis, B. W. & Keating, C. D. RNA-Based Coacervates as a Model for Membraneless Organelles: Formation, Properties, and Interfacial Liposome Assembly. *Langmuir* **32**, 10042–10053 (2016).

-B-

Baechtold, H. *et al.* Human 75-kDa DNA-pairing protein is identical to the pro-oncoprotein TLS/FUS and is able to promote D-loop formation. *J. Biol. Chem.* **274**, 34337–34342 (1999).

Bai, P. Biology of Poly(ADP-Ribose) Polymerases: The Factotums of Cell Maintenance. *Mol. Cell* **58**, 947–958 (2015).

Banani, S. F., Lee, H. O., Hyman, A. A. & Rosen, M. K. Biomolecular condensates: organizers of cellular biochemistry. *Nat. Rev. Mol. Cell Biol.* 2017 185 **18**, 285–298 (2017).

Barkauskaite, E., Jankevicius, G. & Ahel, I. Structures and Mechanisms of Enzymes Employed in the Synthesis and Degradation of PARP-Dependent Protein ADP-Ribosylation. *Mol. Cell* **58**, 935–946 (2015).

Baumli, S., Endicott, J.A. & Johnson, L.N. Halogen bonds form the basis for selective P-TEFb inhibition by DRB. *Chemistry & biology* **17**, 931–936 (2010).

Bentley, D. L. Coupling mRNA processing with transcription in time and space. *Nat. Rev. Genet.* 2014 153 **15**, 163–175 (2014).

Bertolotti, A. *et al.* EWS, but Not EWS-FLI-1, Is Associated with Both TFIID and RNA Polymerase II: Interactions between Two Members of the TET Family, EWS and hTAFII68, and Subunits of TFIID and RNA Polymerase II Complexes. <https://doi.org/10.1128/MCB.18.3.1489> **18**, 1489–1497 (2023).

Bertolotti, A., Bell, B. & Tora, L. The N-terminal domain of human TAFII68 displays transactivation and oncogenic properties. *Oncogene* 1999 1856 **18**, 8000–8010 (2000).

Bertolotti, A., Lutz, Y., Heard, D. J., Chambon, P. & Tora, L. hTAF(II)68, a novel RNA/ssDNA-binding protein with homology to the pro-oncoproteins TLS/FUS and EWS is associated with both TFIID and RNA polymerase II. *EMBO J.* **15**, 5022–5031 (1996).

Bertrand, P., Corteggiani, E., Dutreix, M., Coppey, J. & Lopez, B. S. Homologous pairing between single-stranded DNA immobilized on a nitrocellulose membrane and duplex DNA is specific for RecA activity in bacterial crude extract. *Nucleic Acids Res.* **21**, 3653–3657 (1993).

Bock, A. S. *et al.* N-terminal acetylation modestly enhances phase separation and reduces aggregation of the low-complexity domain of RNA-binding protein fused in sarcoma. *Protein Sci.* **30**, 1337–1349 (2021).

Boeynaems, S. *et al.* Protein Phase Separation: A New Phase in Cell Biology. *Trends Cell Biol.* **28**, 420–435 (2018).

Bonfiglio, J. J. *et al.* Serine ADP-Ribosylation Depends on HPF1. *Mol. Cell* **65**, 932–940.e6 (2017).

Bosco, D. A. *et al.* Mutant FUS proteins that cause amyotrophic lateral sclerosis incorporate into stress granules. *Hum. Mol. Genet.* **19**, 4160–4175 (2010).

Braun, S. A., Panzater, P. L., Collinge, M. A. & Althaus, F. R. Endoglycosidic cleavage of branched polymers by poly(ADP-ribose) glycohydrolase. *Eur. J. Biochem.* **220**, 369–375 (1994).

Bredehorst, R. *et al.* Two Different Types of Bonds Linking Single ADP-Ribose Residues Covalently to Proteins. *Eur. J. Biochem.* **92**, 129–135 (1978).

Brès, V., Yoh, S. M. & Jones, K. A. The multi-tasking P-TEFb complex. *Curr. Opin. Cell Biol.* **20**, 334–340 (2008).

Breslin, C. *et al.* The XRCC1 phosphate-binding pocket binds poly (ADP-ribose) and is required for XRCC1 function. *Nucleic Acids Res.* **43**, 6934–6944 (2015).

Broustal O. *et al.* FUS mutations in frontotemporal lobar degeneration with amyotrophic lateral sclerosis. *J. Alzheimers Dis.* **22**, 765–769 (2010).

Burke, K. A., Janke, A. M., Rhine, C. L. & Fawzi, N. L. Residue-by-Residue View of In Vitro FUS Granules that Bind the C-Terminal Domain of RNA Polymerase II. *Mol. Cell* **60**, 231–241 (2015).

-C-

Caldecott, K. W. Mammalian single-strand break repair: Mechanisms and links with chromatin. *DNA Repair (Amst)*. **6**, 443–453 (2007).

Caldecott, K. W. Single-strand break repair and genetic disease. *Nat. Rev. Genet.* 2008 **9**, 619–631 (2008).

Caldecott, K. W., McKeown, C. K., Tucker, J. D., Ljungquist, S. & Thompson, L. H. An interaction between the mammalian DNA repair protein XRCC1 and DNA ligase III. *Mol. and Cell. Biology* **14**, 68–76 (2023).

Calvio C., Neubauer G., Mann M., Lamond A. I. Identification of hnRNP P2 as TLS/FUS using electrospray mass spectrometry. *RNA* **1**, 724–733 (1995).

Chapman, J. R., Taylor, M. R. G. & Boulton, S. J. Playing the End Game: DNA Double-Strand Break Repair Pathway Choice. *Mol. Cell* **47**, 497–510 (2012).

Cheng, Q. *et al.* Ku counteracts mobilization of PARP1 and MRN in chromatin damaged with DNA double-strand breaks. *Nucleic Acids Res.* **39**, 9605–9619 (2011).

Chong, P.A., Vernon, R.M. & Forman-Kay, J.D. RGG/RG motif regions in RNA binding and phase separation. *Journal of molecular biology* **430**, 4650–4665 (2018).

Ciccia, A. & Elledge, S.J. The DNA damage response: making it safe to play with knives. *Mol Cell* **40**, 179–204 (2010).

Cléry, A., Blatter, M. & Allain, F. H. T. RNA recognition motifs: boring? Not quite. *Curr. Opin. Struct. Biol.* **18**, 290–298 (2008).

Colombrita, C. *et al.* TDP-43 and FUS RNA-binding proteins bind distinct sets of cytoplasmic messenger RNAs and differently regulate their post-transcriptional fate in motoneuron-like cells. *J. Biol. Chem.* **287**, 15635–15647 (2012).

Conicella, A. E., Zerze, G. H., Mittal, J. & Fawzi, N. L. ALS Mutations Disrupt Phase Separation Mediated by α -Helical Structure in the TDP-43 Low-Complexity C-Terminal Domain. *Structure* **24**, 1537–1549 (2016).

Cortes, U. *et al.* Depletion of the 110-Kilodalton Isoform of Poly(ADP-Ribose) Glycohydrolase Increases Sensitivity to Genotoxic and Endotoxic Stress in Mice. *Mol. and Cell. Biology* **24**, 7163–7178 (2023).

Couthouis, J. *et al.* Evaluating the role of the FUS/TLS-related gene EWSR1 in amyotrophic lateral sclerosis. *Hum. Mol. Genet.* **21**, 2899–2911 (2012).

Couthouisa, J. *et al.* A yeast functional screen predicts new candidate ALS disease genes. *Proc. Natl. Acad. Sci. U. S. A.* **108**, 20881–20890 (2011).

Crick, S. L., Ruff, K. M., Garai, K., Frieden, C. & Pappu, R. V. Unmasking the roles of N- and C-terminal flanking sequences from exon 1 of huntingtin as modulators of polyglutamine aggregation. *Proc. Natl. Acad. Sci. U. S. A.* **110**, 20075–20080 (2013).

Crozat, A., Åman, P., Mandahl, N. & Ron, D. Fusion of CHOP to a novel RNA-binding protein in human myxoid liposarcoma. *Nat. 1993 3636430* **363**, 640–644 (1993).

-D-

D'Amours D., Desnoyers S., D'Silva I., Poirier G. G. Poly(ADP-ribosyl)ation reactions in the regulation of nuclear functions. *Biochem. J.* **342**, 249–268 (1999).

D'Annessa, I., Coletta, A. & Desideri, A. Geometrical constraints limiting the poly(ADP-ribose) conformation investigated by molecular dynamics simulation. *Biopolymers* **101**, 78–86 (2014).

Dalvit, C., Fogliatto, G., Stewart, A., Veronesi, M. & Stockman, B. WaterLOGSY as a method for primary NMR screening: practical aspects and range of applicability. *Journal of biomolecular NMR* **21**, 349–359 (2001).

Daniels, C. M., Ong, S. E. & Leung, A. K. L. Phosphoproteomic approach to characterize protein mono- and poly(ADP-ribosyl)ation sites from cells. *J. Proteome Res.* **13**, 3510–3522 (2014).

Daniels, C. M., Thirawatananond, P., Ong, S. E., Gabelli, S. B. & Leung, A. K. L. Nudix hydrolases degrade protein-conjugated ADP-ribose. *Sci. Reports 2015 51* **5**, 1–12 (2015).

Dantzer, F. *et al.* Base Excision Repair Is Impaired in Mammalian Cells Lacking Poly(ADP-ribose) Polymerase-1. *Biochemistry* **39**, 7559–7569 (2000).

- Dantzer, F. *et al.* Involvement of poly(ADP-ribose) polymerase in base excision repair. *Biochimie* **81**, 69–75 (1999).
- Darovic, S. *et al.* Phosphorylation of C-terminal tyrosine residue 526 in FUS impairs its nuclear import. *J. Cell Sci.* **128**, 4151–4159 (2015).
- Das, R. *et al.* SR Proteins Function in Coupling RNAP II Transcription to Pre-mRNA Splicing. *Mol. Cell* **26**, 867–881 (2007).
- Davies, G. & Henrissat, B. Structures and mechanisms of glycosyl hydrolases. *Structure* **3**, 853–859 (1995).
- Dawicki-McKenna, J. M. *et al.* PARP-1 Activation Requires Local Unfolding of an Autoinhibitory Domain. *Mol. Cell* **60**, 755–768 (2015).
- De Bont, R. & van Larebeke, N. Endogenous DNA damage in humans: a review of quantitative data. *Mutagenesis* **19**, 169–185 (2004).
- de Murcia, G. *et al.* Structure and function of poly(ADP-ribose) polymerase. *Mol. Cell. Biochem.* **138**, 15–24 (1994).
- Déjardin, J. & Kingston, R. E. Purification of Proteins Associated with Specific Genomic Loci. *Cell* **136**, 175–186 (2009).
- Delattre, O. *et al.* Gene fusion with an ETS DNA-binding domain caused by chromosome translocation in human tumours. *Nat. 1992 3596391* **359**, 162–165 (1992).
- Demin, A. A. *et al.* XRCC1 prevents toxic PARP1 trapping during DNA base excision repair. *Mol. Cell* **81**, 3018-3030.e5 (2021).
- Deng, H. X. *et al.* Mutations in UBQLN2 cause dominant X-linked juvenile and adult-onset ALS and ALS/dementia. *Nat. 2011 4777363* **477**, 211–215 (2011).
- Deng, H., Gao, K. & Jankovic, J. The role of FUS gene variants in neurodegenerative diseases. *Nat. Rev. Neurol.* 2014 106 **10**, 337–348 (2014).
- Deng, Q. *et al.* FUS is Phosphorylated by DNA-PK and Accumulates in the Cytoplasm after DNA Damage. *J. Neurosci.* **34**, 7802–7813 (2014).
- Deriano, L. & Roth, D. B. Modernizing the Nonhomologous End-Joining Repertoire: Alternative and Classical NHEJ Share the Stage. *Annual Review of Genetics* **47**, 433–455 (2013).
- di Fagagna, F.d.A. A direct role for small non-coding RNAs in DNA damage response. *Trends in cell biology* **24**, 171-178 (2014).

Dinant, C., Houtsmuller, A.B. & Vermeulen, W. Chromatin structure and DNA damage repair. *Epigenetics & chromatin* **1**, 1-13 (2008).

Dobra, I., Pankivskiy, S., Samsonova, A., Pastre, D. & Hamon, L. Relation Between Stress Granules and Cytoplasmic Protein Aggregates Linked to Neurodegenerative Diseases. *Curr. Neurol. Neurosci. Rep.* **18**, 1–9 (2018).

Dormann, D. & Haass, C. TDP-43 and FUS: a nuclear affair. *Trends Neurosci.* **34**, 339–348 (2011).

Dormann, D. *et al.* ALS-associated fused in sarcoma (FUS) mutations disrupt Transportin-mediated nuclear import. *EMBO J.* **29**, 2841–2857 (2010).

Dormann, D. *et al.* Arginine methylation next to the PY-NLS modulates Transportin binding and nuclear import of FUS. *EMBO J.* **31**, 4258–4275 (2012).

Dreyfuss, G., Swanson, M. S. & Piñol-Roma, S. Heterogeneous nuclear ribonucleoprotein particles and the pathway of mRNA formation. *Trends Biochem. Sci.* **13**, 86–91 (1988).

Dutagaci, B. *et al.* Charge-driven condensation of RNA and proteins suggests broad role of phase separation in cytoplasmic environments. *Elife* **10**, 1–103 (2021).

-E-

Ederle, H. *et al.* Nuclear egress of TDP-43 and FUS occurs independently of Exportin-1/CRM1. *Sci. Reports 2018 81* **8**, 1–18 (2018).

El-Khamisy, S. F., Masutani, M., Suzuki, H. & Caldecott, K. W. A requirement for PARP-1 for the assembly or stability of XRCC1 nuclear foci at sites of oxidative DNA damage. *Nucleic Acids Res.* **31**, 5526–5533 (2003).

Erdélyi, K. *et al.* Dual role of poly(ADP-ribose) glycohydrolase in the regulation of cell death in oxidatively stressed A549 cells. *FASEB J.* **23**, 3553–3563 (2009).

Eustermann, S. *et al.* Solution structures of the two PBZ domains from human APLF and their interaction with poly(ADP-ribose). *Nat. Struct. Mol. Biol.* 2009 172 **17**, 241–243 (2010).

-F-

Fahrer, J., Kranaster, R., Altmeyer, M., Marx, A. & Bürkle, A. Quantitative analysis of the binding affinity of poly(ADP-ribose) to specific binding proteins as a function of chain length. *Nucleic Acids Res.* **35**, e143–e143 (2007).

Fattaha, F. *et al.* Ku Regulates the Non-Homologous End Joining Pathway Choice of DNA Double-Strand Break Repair in Human Somatic Cells. *PLoS Genet.* **6**, e1000855 (2010).

Fisher, A. E. O., Hochegger, H., Takeda, S. & Caldecott, K. W. Poly(ADP-Ribose) Polymerase 1 Accelerates Single-Strand Break Repair in Concert with Poly(ADP-Ribose) Glycohydrolase. *Mol. and Cell. Biology* **27**, 5597–5605 (2023).

Frouin, I. *et al.* Human Proliferating Cell Nuclear Antigen, Poly(ADP-ribose) Polymerase-1, and p21 /. *J. Biol. Chem.* **278**, 39265–39268 (2003).

Fu, H. *et al.* Poly (ADP-ribosylation) of P-TEFb by PARP1 disrupts phase separation to inhibit global transcription after DNA damage. *Nature cell biology* **24**, 513-525 (2022).

Fujii, R. & Takumi, T. TLS facilitates transport of mRNA encoding an actin-stabilizing protein to dendritic spines. *J. Cell Sci.* **118**, 5755–5765 (2005).

Fujii, R. *et al.* The RNA binding protein TLS is translocated to dendritic spines by mGluR5 activation and regulates spine morphology. *Curr. Biol.* **15**, 587–593 (2005).

-G-

Gagné, J. P. *et al.* Proteome-wide identification of poly(ADP-ribose) binding proteins and poly(ADP-ribose)-associated protein complexes. *Nucleic Acids Res.* **36**, 6959–6976 (2008).

Gagné, J. P. *et al.* Quantitative proteomics profiling of the poly(ADP-ribose)-related response to genotoxic stress. *Nucleic Acids Res.* **40**, 7788–7805 (2012).

Gagné, J. P., Haince, J. F., Pic, É. & Poirier, G. G. Affinity-Based Assays for the Identification and Quantitative Evaluation of Noncovalent Poly(ADP-Ribose)-Binding Proteins. *Methods Mol. Biol.* **780**, 93–115 (2011).

Gagné, J. P., Hunter, J. M., Labrecque, B., Chabot, B. & Poirier, G. G. A proteomic approach to the identification of heterogeneous nuclear ribonucleoproteins as a new family of poly(ADP-ribose)-binding proteins. *Biochem. J.* **371**, 331–340 (2003).

Garcia-Jove Navarro, M. *et al.* RNA is a critical element for the sizing and the composition of phase-separated RNA–protein condensates. *Nat. Commun.* **2019 101** **10**, 1–13 (2019).

Gardiner, M., Toth, R., Vandermoere, F., Morrice, N. A. & Rouse, J. Identification and characterization of FUS/TLS as a new target of ATM. *Biochem. J.* **415**, 297–307 (2008).

Gatti, M., Imhof, R., Huang, Q., Baudis, M. & Altmeyer, M. The Ubiquitin Ligase TRIP12 Limits PARP1 Trapping and Constrains PARP Inhibitor Efficiency. *Cell Rep.* **32**, 107985 (2020).

Gehring, H., Leemann-Zakaryan, R. P., Pahlich, S. & Grossenbacher, D. Tyrosine Phosphorylation in the C-Terminal Nuclear Localization and Retention Signal (C-NLS) of the EWS Protein. *Sarcoma* **2011**, (2011).

Gerstberger, S., Hafner, M. & Tuschl, T. A census of human RNA-binding proteins. *Nature Reviews Genetics* **15**, 829-845 (2014).

Gibbs-Seymour, I., Fontana, P., Rack, J. G. M. & Ahel, I. HPF1/C4orf27 Is a PARP-1-Interacting Protein that Regulates PARP-1 ADP-Ribosylation Activity. *Mol. Cell* **62**, 432–442 (2016).

Gilbertson, S., Federspiel, J.D., Hartenian, E., Cristea, I.M. & Glaunsinger, B. Changes in mRNA abundance drive shuttling of RNA binding proteins, linking cytoplasmic RNA degradation to transcription. *elife* **7**(2018).

Gorospe, M. HuR in the mammalian genotoxic response: post-transcriptional multitasking. *Cell Cycle* **2**, 411-413 (2003).

Gregory, R. I. *et al.* The Microprocessor complex mediates the genesis of microRNAs. *Nat. 2004 4327014* **432**, 235–240 (2004).

-H-

Hackl, W. & Lührmann, R. Molecular Cloning and Subcellular Localisation of the snRNP-associated Protein 69KD, a Structural Homologue of the Proto-oncoproteins TLS and EWS, with RNA and DNA-binding Properties. *J. Mol. Biol.* **264**, 843–851 (1996).

Haince, J. F. *et al.* Ataxia telangiectasia mutated (ATM) signaling network is modulated by a novel poly(ADP-ribose)-dependent pathway in the early response to DNA-damaging agents. *J. Biol. Chem.* **282**, 16441–16453 (2007).

Haince, J. F. *et al.* PARP1-dependent kinetics of recruitment of MRE11 and NBS1 proteins to multiple DNA damage sites. *J. Biol. Chem.* **283**, 1197–1208 (2008).

Haines, N.M., Kim, Y.-I.T., Smith, A.J. & Savery, N.J. Stalled transcription complexes promote DNA repair at a distance. *Proceedings of the National Academy of Sciences* **111**, 4037-4042 (2014).

Han, T. W. *et al.* Cell-free formation of RNA granules: Bound RNAs identify features and components of cellular assemblies. *Cell* **149**, 768–779 (2012).

Hanzlikova, H., Gittens, W., Krejcikova, K., Zeng, Z. & Caldecott, K. W. Overlapping roles for PARP1 and PARP2 in the recruitment of endogenous XRCC1 and PNKP into oxidized chromatin. *Nucleic Acids Res.* **45**, 2546–2557 (2017).

Harris, J. L. *et al.* Aprataxin, poly-ADP ribose polymerase 1 (PARP-1) and apurinic endonuclease 1 (APE1) function together to protect the genome against oxidative damage. *Hum. Mol. Genet.* **18**, 4102–4117 (2009).

Harrison, A.F. & Shorter, J. RNA-binding proteins with prion-like domains in health and disease. *Biochemical Journal* **474**, 1417–1438 (2017).

Hicks, G. G. *et al.* Fus deficiency in mice results in defective B-lymphocyte development and activation, high levels of chromosomal instability and perinatal death. *Nat. Genet.* **24**, 175–179 (2000).

Hoch, N. C. *et al.* XRCC1 mutation is associated with PARP1 hyperactivation and cerebellar ataxia. *Nat.* 2016 5417635 **541**, 87–91 (2016).

Hochegger, H. *et al.* Parp-1 protects homologous recombination from interference by Ku and Ligase IV in vertebrate cells. *EMBO J.* **25**, 1305–1314 (2006).

Hoell, J. I. *et al.* RNA targets of wild-type and mutant FET family proteins. *Nat. Struct. Mol. Biol.* 2011 1812 **18**, 1428–1431 (2011).

Hofweber, M. *et al.* Phase Separation of FUS Is Suppressed by Its Nuclear Import Receptor and Arginine Methylation. *Cell* **173**, 706–719.e13 (2018).

Hottiger, M. O. Nuclear ADP-Ribosylation and Its Role in Chromatin Plasticity, Cell Differentiation, and Epigenetics. *Annu. Rev. Biochem.* **84**, 227–263 (2015).

Hottiger, M. O., Hassa, P. O., Lüscher, B., Schüler, H. & Koch-Nolte, F. Toward a unified nomenclature for mammalian ADP-ribosyltransferases. *Trends Biochem. Sci.* **35**, 208–219 (2010).

Hu, Y. *et al.* PARP1-driven poly-ADP-ribosylation regulates BRCA1 function in homologous recombination-mediated DNA repair. *Cancer Discov.* **4**, 1430–1447 (2014).

Huambachano, O., Herrera, F., Rancourt, A. & Satoh, M. S. Double-stranded DNA binding domain of poly(ADP-ribose) polymerase-1 and molecular insight into the regulation of its activity. *J. Biol. Chem.* **286**, 7149–7160 (2011).

Huang, D. & Kraus, W. L. The expanding universe of PARP1-mediated molecular and therapeutic mechanisms. *Mol. Cell* **82**, 2315–2334 (2022).

Huey, E. D. *et al.* FUS and TDP43 genetic variability in FTD and CBS. *Neurobiol. Aging* **33**, 1016.e9–1016.e17 (2012).

-I-

Ichikawa H., Shimizu K., Hayashi Y., Ohki M. An RNA-binding protein gene, TLS/FUS, is fused to ERG in human myeloid leukemia with t(16;21) chromosomal translocation. *Cancer Res.* **54**, 2865-2868 (1994).

Iko, Y. *et al.* Domain architectures and characterization of an RNA-binding protein, TLS. *J. Biol. Chem.* **279**, 44834–44840 (2004).

Illuzzi, G. *et al.* PARG is dispensable for recovery from transient replicative stress but required to prevent detrimental accumulation of poly(ADP-ribose) upon prolonged replicative stress. *Nucleic Acids Res.* **42**, 7776–7792 (2014).

Immanuel, D., Zinszner, H. & Ron, D. Association of SARFH (Sarcoma-Associated RNA-Binding Fly Homolog) with Regions of Chromatin Transcribed by RNA Polymerase II. *Mol. And Cell. Biology* **15**, 4562–4571 (2023).

Isabelle, M., Gagné, J. P., Gallouzi, I. E. & Poirier, G. G. Quantitative proteomics and dynamic imaging reveal that G3BP-mediated stress granule assembly is poly(ADP-ribose)-dependent following exposure to MNNG-induced DNA alkylation. *J. Cell Sci.* **125**, 4555–4566 (2012).

Ishigaki, S. *et al.* Position-dependent FUS-RNA interactions regulate alternative splicing events and transcriptions. *Sci. Reports 2012 21* **2**, 1–9 (2012).

Isogai, S. *et al.* Solution structure of a zinc-finger domain that binds to poly-ADP-ribose. *Genes to Cells* **15**, 101–110 (2010).

Ito, D., Seki, M., Tsunoda, Y., Uchiyama, H. & Suzuki, N. Nuclear transport impairment of amyotrophic lateral sclerosis-linked mutations in FUS/TLS. *Ann. Neurol.* **69**, 152–162 (2011).

Izhar, L. *et al.* A Systematic Analysis of Factors Localized to Damaged Chromatin Reveals PARP-Dependent Recruitment of Transcription Factors. *Cell Rep.* **11**, 1486–1500 (2015).

-J-

Jacobson, M. K. & Alvarez-Gonzalez, R. Characterization of Polymers of Adenosine Diphosphate Ribose Generated in Vitro and in Vivo. *Biochemistry* **26**, 3218–3224 (1987).

Jankevicius, G. *et al.* A family of macrodomain proteins reverses cellular mono-ADP-ribosylation. *Nat. Struct. Mol. Biol.* 2013 204 **20**, 508–514 (2013).

Ji, Y. & Tulin, A. V. Poly(ADP-ribosylation) of heterogeneous nuclear ribonucleoproteins modulates splicing. *Nucleic Acids Res.* **37**, 3501–3513 (2009).

Jungmichel, S. *et al.* Proteome-wide identification of poly(ADP-Ribosylation) targets in different genotoxic stress responses. *Mol. Cell* **52**, 272–285 (2013).

-K-

Kalisch, T., Amé, J. C., Dantzer, F. & Schreiber, V. New readers and interpretations of poly(ADP-ribosylation). *Trends Biochem. Sci.* **37**, 381–390 (2012).

Kanai, Y., Dohmae, N. & Hirokawa, N. Kinesin transports RNA: Isolation and characterization of an RNA-transporting granule. *Neuron* **43**, 513–525 (2004).

Kang, H. C. *et al.* Iduna is a poly(ADP-ribose) (PAR)-dependent E3 ubiquitin ligase that regulates DNA damage. *Proc. Natl. Acad. Sci. U. S. A.* **108**, 14103–14108 (2011).

Kapeli, K. *et al.* Distinct and shared functions of ALS-associated proteins TDP-43, FUS and TAF15 revealed by multisystem analyses. *Nat. Commun.* **2016 71 7**, 1–14 (2016).

Kato, M. *et al.* Cell-free formation of RNA granules: Low complexity sequence domains form dynamic fibers within hydrogels. *Cell* **149**, 753–767 (2012).

Kent, T., Mateos-Gomez, P. A., Sfeir, A. & Pomerantz, R. T. Polymerase θ is a robust terminal transferase that oscillates between three different mechanisms during end-joining. *Elife* **5**, (2016).

Khodyreva, S. N. & Lavrik, O. I. Poly(ADP-Ribose) polymerase 1 as a key regulator of DNA repair. *Mol. Biol.* **2016 504 50**, 580–595 (2016).

Kim, D.-S. *et al.* Activation of PARP-1 by snoRNAs controls ribosome biogenesis and cell growth via the RNA helicase DDX21. *Molecular cell* **75**, 1270-1285. e14 (2019).

Kino, Y. *et al.* Intracellular localization and splicing regulation of FUS/TLS are variably affected by amyotrophic lateral sclerosis-linked mutations. *Nucleic Acids Res.* **39**, 2781–2798 (2011).

Kliza, K.W. *et al.* Reading ADP-ribosylation signaling using chemical biology and interaction proteomics. *Molecular Cell* **81**, 4552-4567. e8 (2021).

Koh, D. W. *et al.* Failure to degrade poly(ADP-ribose) causes increased sensitivity to cytotoxicity and early embryonic lethality. *Proc. Natl. Acad. Sci. U. S. A.* **101**, 17699–17704 (2004).

Kovar, H. Dr. Jekyll and Mr. Hyde: the two faces of the FUS/EWS/TAF15 protein family. *Sarcoma* **2011**(2010).

Krietsch, J. *et al.* PARP activation regulates the RNA-binding protein NONO in the DNA damage response to DNA double-strand breaks. *Nucleic Acids Res.* **40**, 10287–10301 (2012).

Krietsch, J. *et al.* Reprogramming cellular events by poly(ADP-ribose)-binding proteins. *Mol. Aspects Med.* **34**, 1066–1087 (2013).

Kurgina, T. A. *et al.* Dual function of HPF1 in the modulation of PARP1 and PARP2 activities. *Commun. Biol.* **2021 41 4**, 1–11 (2021).

Kuroda, M. *et al.* Male sterility and enhanced radiation sensitivity in TLS^{-/-} mice. *EMBO J.* **19**, 453–462 (2000).

Kwiatkowski, T. J. *et al.* Mutations in the FUS/TLS gene on chromosome 16 cause familial amyotrophic lateral sclerosis. *Science (80-.).* **323**, 1205–1208 (2009).

Kwon, I. *et al.* Phosphorylation-regulated binding of RNA polymerase II to fibrous polymers of low-complexity domains. *Cell* **155**, 1049 (2013).

-L-

Lagerwerf, S., Vrouwe, M.G., Overmeer, R.M., Fousteri, M.I. & Mullenders, L.H. DNA damage response and transcription. *DNA repair* **10**, 743–750 (2011).

Lagier-Tourenne, C. *et al.* Divergent roles of ALS-linked proteins FUS/TLS and TDP-43 intersect in processing long pre-mRNAs. *Nat. Neurosci.* **2012 1511 15**, 1488–1497 (2012).

Laing, S., Koch-Nolte, F., Haag, F. & Buck, F. Strategies for the identification of arginine ADP-ribosylation sites. *J. Proteomics* **75**, 169–176 (2011).

Laing, S., Unger, M., Koch-Nolte, F. & Haag, F. ADP-ribosylation of arginine. *Amino Acids* **41**, 257–269 (2011).

Langelier, M. F. & Pascal, J. M. PARP-1 mechanism for coupling DNA damage detection to poly(ADP-ribose) synthesis. *Curr. Opin. Struct. Biol.* **23**, 134–143 (2013).

Langelier, M. F., Zandarashvili, L., Aguiar, P. M., Black, B. E. & Pascal, J. M. NAD⁺ analog reveals PARP-1 substrate-blocking mechanism and allosteric communication from catalytic center to DNA-binding domains. *Nat. Commun.* **2018 91 9**, 1–13 (2018).

Lee, B. J. *et al.* Rules for Nuclear Localization Sequence Recognition by Karyopherin β 2. *Cell* **126**, 543–558 (2006).

Lee, J. *et al.* Stimulation of Oct-4 Activity by Ewing's Sarcoma Protein. *Stem Cells* **23**, 738–751 (2005).

- Lee, S.g. et al. Ewing sarcoma protein promotes dissociation of poly (ADP-ribose) polymerase 1 from chromatin. *EMBO reports* **21**, e48676 (2020).
- Leichter, M. et al. A fraction of the transcription factor TAF15 participates in interactions with a subset of the spliceosomal U1 snRNP complex. *Biochim. Biophys. Acta - Proteins Proteomics* **1814**, 1812–1824 (2011).
- Leung, A. K. L. Poly(ADP-ribose): A Dynamic Trigger for Biomolecular Condensate Formation. *Trends Cell Biol.* **30**, 370–383 (2020).
- Leung, A. K. L. Poly(ADP-ribose): An organizer of cellular architecture. *J. Cell Biol.* **205**, 613–619 (2014).
- Leung, A. K. L. SERious Surprises for ADP-Ribosylation Specificity: HPF1 Switches PARP1 Specificity to Ser Residues. *Mol. Cell* **65**, 777–778 (2017).
- Levone, B.R. et al. FUS-dependent liquid–liquid phase separation is important for DNA repair initiation. *Journal of cell biology* **220**(2021).
- Li, M. & Yu, X. Function of BRCA1 in the DNA Damage Response Is Mediated by ADP-Ribosylation. *Cancer Cell* **23**, 693–704 (2013).
- Li, Y. R., King, O. D., Shorter, J. & Gitler, A. D. Stress granules as crucibles of ALS pathogenesis. *J. Cell Biol.* **201**, 361–372 (2013).
- Lindahl, T., & Barnes, D. E. (2000). Repair of Endogenous DNA Damage. *Cold Spring Harbor Symposia on Quantitative Biology*, **65**, 127–134.
- Liu, X. et al. The RRM domain of human fused in sarcoma protein reveals a non-canonical nucleic acid binding site. *Biochim. Biophys. Acta - Mol. Basis Dis.* **1832**, 375–385 (2013).
- Loughlin, F. E. et al. The Solution Structure of FUS Bound to RNA Reveals a Bipartite Mode of RNA Recognition with Both Sequence and Shape Specificity. *Mol. Cell* **73**, 490-504.e6 (2019).
- Lourenco, G. F., Janitz, M., Huang, Y. & Halliday, G. M. Long noncoding RNAs in TDP-43 and FUS/TLS-related frontotemporal lobar degeneration (FTLD). *Neurobiol. Dis.* **82**, 445–454 (2015).
- Luijsterburg, M. S. et al. PARP1 Links CHD2-Mediated Chromatin Expansion and H3.3 Deposition to DNA Repair by Non-homologous End-Joining. *Mol. Cell* **61**, 547–562 (2016).
- Luo, X. & Kraus, W.L. On PAR with PARP: cellular stress signaling through poly (ADP-ribose) and PARP-1. *Genes & development* **26**, 417-432 (2012).

-M-

MacKenzie, I. R. A. & Neumann, M. FET proteins in frontotemporal dementia and amyotrophic lateral sclerosis. *Brain Res.* **1462**, 40–43 (2012).

Madabhushi, R., Pan, L. & Tsai, L. H. DNA damage and its links to neurodegeneration. *Neuron* **83**, 266–282 (2014).

Maharana, S. et al. RNA buffers the phase separation behavior of prion-like RNA binding proteins. *Science* **360**, 918–921 (2018).

Majidinia, M. & Yousefi, B. Long non-coding RNAs in cancer drug resistance development. *DNA repair* **45**, 25–33 (2016).

Malanga, M. & Althaus, F. R. Noncovalent protein interaction with poly(ADP-ribose). *Methods Mol. Biol.* **780**, 67–82 (2011).

Malanga, M., Czubyty, A., Girstun, A., Staron, K. & Althaus, F. R. Poly(ADP-ribose) binds to the splicing factor ASF/SF2 and regulates its phosphorylation by DNA topoisomerase I. *J. Biol. Chem.* **283**, 19991–19998 (2008).

Malanga, M., Pleschke, J. M., Kleczkowska, H. E. & Althaus, F. R. Poly(ADP-ribose) binds to specific domains of p53 and alters its DNA binding functions. *J. Biol. Chem.* **273**, 11839–11843 (1998).

Maniatis, T. & Reed, R. An extensive network of coupling among gene expression machines. *Nat. 2002 4166880* **416**, 499–506 (2002).

Manning, D. R., Fraser B. A., Kahn R. A., Gilman A. G. ADP-ribosylation of transducin by islet-activation protein. Identification of asparagine as the site of ADP-ribosylation. *J. Biol. Chem.* **259**, 749–756 (1984).

Mansour, W. Y., Rhein, T. & Dahm-Daphi, J. The alternative end-joining pathway for repair of DNA double-strand breaks requires PARP1 but is not dependent upon microhomologies. *Nucleic Acids Res.* **38**, 6065–6077 (2010).

Marintchev, A. et al. Domain specific interaction in the XRCC1–DNA polymerase β complex. *Nucleic Acids Res.* **28**, 2049–2059 (2000).

Marsischky, G. T., Wilson, B. A. & Collier, R. J. Role of Glutamic Acid 988 of Human Poly-ADP-ribose Polymerase in Polymer Formation. *J. Biol. Chem.* **270**, 3247–3254 (1995).

Marteijn, J. A., Lans, H., Vermeulen, W. & Hoeijmakers, J. H. J. Understanding nucleotide excision repair and its roles in cancer and ageing. *Nat. Rev. Mol. Cell Biol.* **2014 157** **15**, 465–481 (2014).

- Martello, R. *et al.* Proteome-wide identification of the endogenous ADP-ribosylome of mammalian cells and tissue. *Nat. Commun.* 2016 71 **7**, 1–13 (2016).
- Martello, R., Mangerich, A., Sass, S., Dedon, P.C. & Burkle, A. Quantification of cellular poly (ADP-ribosyl) ation by stable isotope dilution mass spectrometry reveals tissue- and drug-dependent stress response dynamics. *ACS chemical biology* **8**, 1567–1575 (2013).
- Mashimo, M., Kato, J. & Moss, J. Structure and function of the ARH family of ADP-ribosyl-acceptor hydrolases. *DNA Repair (Amst)*. **23**, 88–94 (2014).
- Mastrocola, A. S., Kim, S. H., Trinh, A. T., Rodenkirch, L. A. & Tibbetts, R. S. The RNA-binding protein fused in sarcoma (FUS) functions downstream of poly(ADP-ribose) polymerase (PARP) in response to DNA damage. *J. Biol. Chem.* **288**, 24731–24741 (2013).
- Mateos-Gomez, P. A. *et al.* Mammalian polymerase θ promotes alternative NHEJ and suppresses recombination. *Nat.* 2015 5187538 **518**, 254–257 (2015).
- Maynard, S., Fang, E.F., Scheibye-Knudsen, M., Croteau, D.L. & Bohr, V.A. DNA damage, DNA repair, aging, and neurodegeneration. *Cold Spring Harbor perspectives in medicine* **5**, a025130 (2015).
- McDonald, L. J. & Moss, J. Enzymatic and nonenzymatic ADP-ribosylation of cysteine. *Mol. Cell. Biochem.* **138**, 221–226 (1994).
- Mehta, A. & Haber, J. E. Sources of DNA Double-Strand Breaks and Models of Recombinational DNA Repair. *Cold Spring Harb. Perspect. Biol.* **6**, a016428 (2014).
- Mertins, P. *et al.* Integrated proteomic analysis of post-translational modifications by serial enrichment. *Nat. Methods* 2013 107 **10**, 634–637 (2013).
- Messner, S. & Hottiger, M. O. Histone ADP-ribosylation in DNA repair, replication and transcription. *Trends Cell Biol.* **21**, 534–542 (2011).
- Messner, S. *et al.* PARP1 ADP-ribosylates lysine residues of the core histone tails. *Nucleic Acids Res.* **38**, 6350–6362 (2010).
- Millevoi, S., Moine, H., & Vagner, S. G-quadruplexes in RNA biology. *Wiley Interdisciplinary Reviews. RNA*, **3(4)**, 495–507 (2012).
- Mimura, M. *et al.* Uncharged Components of Single-Stranded DNA Modulate Liquid-Liquid Phase Separation With Cationic Linker Histone H1. *Front. Cell Dev. Biol.* **9**, 2129 (2021).
- Min, W. *et al.* Poly(ADP-ribose) binding to Chk1 at stalled replication forks is required for S-phase checkpoint activation. *Nat. Commun.* 2013 41 **4**, 1–14 (2013).

- Min, W. K., Cortes, U., Herceg, Z., Tong, W. M. & Wang, Z. Q. Deletion of the nuclear isoform of poly(ADP-ribose) glycohydrolase (PARG) reveals its function in DNA repair, genomic stability and tumorigenesis. *Carcinogenesis* **31**, 2058–2065 (2010).
- Mitra, J. et al. Motor neuron disease-associated loss of nuclear TDP-43 is linked to DNA double-strand break repair defects. *Proceedings of the National Academy of Sciences* **116**, 4696–4705 (2019).
- Mitrea, D. M. & Kriwacki, R. W. Phase separation in biology; functional organization of a higher order. *Cell Commun. Signal.* 2016 141 **14**, 1–20 (2016).
- Molliex, A. et al. Phase Separation by Low Complexity Domains Promotes Stress Granule Assembly and Drives Pathological Fibrillization. *Cell* **163**, 123–133 (2015).
- Monahan, Z. et al. Phosphorylation of the FUS low-complexity domain disrupts phase separation, aggregation, and toxicity. *EMBO J.* **36**, 2951–2967 (2017).
- Moor, N. A., Vasil'eva, I. A., Anarbaev, R. O., Antson, A. A. & Lavrik, O. I. Quantitative characterization of protein–protein complexes involved in base excision DNA repair. *Nucleic Acids Res.* **43**, 6009–6022 (2015).
- Morlando, M. et al. FUS stimulates microRNA biogenesis by facilitating co-transcriptional Drosha recruitment. *EMBO J.* **31**, 4502–4510 (2012).
- Mortusewicz, O., Rothbauer, U., Cardoso, M. C. & Leonhardt, H. Differential recruitment of DNA Ligase I and III to DNA repair sites. *Nucleic Acids Res.* **34**, 3523–3532 (2006).
- Muñoz, M. J. et al. DNA Damage Regulates Alternative Splicing through Inhibition of RNA Polymerase II Elongation. *Cell* **137**, 708–720 (2009).
- Murakami, T. et al. ALS/FTD Mutation-Induced Phase Transition of FUS Liquid Droplets and Reversible Hydrogels into Irreversible Hydrogels Impairs RNP Granule Function. *Neuron* **88**, 678–690 (2015).
- Murawska, M., Hassler, M., Renkawitz-Pohl, R., Ladurner, A. & Brehm, A. Stress-Induced PARP Activation Mediates Recruitment of Drosophila Mi-2 to Promote Heat Shock Gene Expression. *PLOS Genet.* **7**, e1002206 (2011).
- Murray, D. T. et al. Structure of FUS Protein Fibrils and Its Relevance to Self-Assembly and Phase Separation of Low-Complexity Domains. *Cell* **171**, 615–627.e16 (2017).
- Muzzopappa, F., Hertzog, M. & Erdel, F. DNA length tunes the fluidity of DNA-based condensates. *Biophys. J.* **120**, 1288–1300 (2021).

-N-

Naumann, M. et al. Impaired DNA damage response signaling by FUS-NLS mutations leads to neurodegeneration and FUS aggregate formation. *Nature communications* **9**, 1-17 (2018).

Naumenko, K.N. et al. Regulation of poly (ADP-Ribose) polymerase 1 activity by Y-Box-Binding protein 1. *Biomolecules* **10**, 1325 (2020).

Neumann, M. et al. A new subtype of frontotemporal lobar degeneration with FUS pathology. *Brain* **132**, 2922–2931 (2009).

Neumann, M. et al. FET proteins TAF15 and EWS are selective markers that distinguish FTLD with FUS pathology from amyotrophic lateral sclerosis with FUS mutations. *Brain* **134**, 2595–2609 (2011).

Nguyen, C. D. et al. Characterization of a Family of RanBP2-Type Zinc Fingers that Can Recognize Single-Stranded RNA. *J. Mol. Biol.* **407**, 273–283 (2011).

Niaki, A. G. et al. Loss of Dynamic RNA Interaction and Aberrant Phase Separation Induced by Two Distinct Types of ALS/FTD-Linked FUS Mutations. *Mol. Cell* **77**, 82-94.e4 (2020).

Nickoloff, J. A., Sharma, N. & Taylor, L. Clustered DNA Double-Strand Breaks: Biological Effects and Relevance to Cancer Radiotherapy. *Genes (Basel)*. **11**, (2020).

Nishimoto, Y. et al. The long non-coding RNA nuclear-enriched abundant transcript 1-2 induces paraspeckle formation in the motor neuron during the early phase of amyotrophic lateral sclerosis. *Mol. Brain* **6**, 1–18 (2013).

Nishimoto, Y., Nakagawa, S. & Okano, H. NEAT1 lncRNA and amyotrophic lateral sclerosis. *Neurochem. Int.* **150**, 105175 (2021).

Niu, C. et al. FUS-NLS/Transportin 1 Complex Structure Provides Insights into the Nuclear Targeting Mechanism of FUS and the Implications in ALS. *PLoS One* **7**, e47056 (2012).

Nomura, T. et al. Intranuclear aggregation of mutant FUS/TLS as a molecular pathomechanism of amyotrophic lateral sclerosis. *J. Biol. Chem.* **289**, 1192–1202 (2014).

Noren Hooten, N., Kompaniez, K., Barnes, J., Lohani, A. & Evans, M. K. Poly(ADP-ribose) polymerase 1 (PARP-1) binds to 8-oxoguanine-DNA glycosylase (OGG1). *J. Biol. Chem.* **286**, 44679–44690 (2011).

Nott, T. J. *et al.* Phase Transition of a Disordered Nuage Protein Generates Environmentally Responsive Membraneless Organelles. *Mol. Cell* **57**, 936–947 (2015).

-O-

O'Sullivan, J. *et al.* Emerging roles of eraser enzymes in the dynamic control of protein ADP-ribosylation. *Nat. Commun.* 2019 101 **10**, 1–14 (2019).

Oberoi, J. *et al.* Structural basis of poly(ADP-ribose) recognition by the multizinc binding domain of Checkpoint with Forkhead-associated and RING domains (CHFR). *J. Biol. Chem.* **285**, 39348–39358 (2010).

Ohno T., Rao V. N., Reddy E. S. EWS/Fli-1 chimeric protein is a transcriptional activator. *Cancer Res.* **53**, 5859–5863 (1993).

Oka, S., Kato, J. & Moss, J. Identification and characterization of a mammalian 39-kDa poly(ADP-ribose) glycohydrolase. *J. Biol. Chem.* **281**, 705–713 (2006).

Okano, S., Lan, L., Caldecott, K. W., Mori, T. & Yasui, A. Spatial and Temporal Cellular Responses to Single-Strand Breaks in Human Cells. *Mol. and Cell. Biology* **23**, 3974–3981 (2023).

Ong, S. E., Mittler, G. & Mann, M. Identifying and quantifying in vivo methylation sites by heavy methyl SILAC. *Nat. Methods* 2004 12 **1**, 119–126 (2004).

Oppenheimer N. J. & Bodley J. W. Diphtheria toxin. Site and configuration of ADP-ribosylation of diphthamide in elongation factor 2. *J. Biol. Chem.* **256**, 8579–8581 (1981).

Ozdilek, B. A. *et al.* Intrinsically disordered RGG/RG domains mediate degenerate specificity in RNA binding. *Nucleic Acids Res.* **45**, 7984–7996 (2017).

-P-

Palazzo, L. *et al.* ENPP1 processes protein ADP-ribosylation in vitro. *FEBS J.* **283**, 3371–3388 (2016).

Palazzo, L. *et al.* Processing of protein ADP-ribosylation by Nudix hydrolases. *Biochem. J.* **468**, 293–301 (2015).

Palazzo, L., Mikoč, A. & Ahel, I. ADP-ribosylation: new facets of an ancient modification. *FEBS J.* **284**, 2932–2946 (2017).

Panagopoulos, I. *et al.* Fusion of the FUS gene with ERG in acute myeloid leukemia with t(16;21)(p11;q22). *Genes, Chromosom. Cancer* **11**, 256–262 (1994).

- Pankotai, T. & Soutoglou, E. Double strand breaks: hurdles for RNA polymerase II transcription? *Transcription* **4**, 34-38 (2013).
- Paronetto, M. P., Miñana, B. & Valcárcel, J. The Ewing Sarcoma Protein Regulates DNA Damage-Induced Alternative Splicing. *Mol. Cell* **43**, 353–368 (2011).
- Patel, A. *et al.* A Liquid-to-Solid Phase Transition of the ALS Protein FUS Accelerated by Disease Mutation. *Cell* **162**, 1066–1077 (2015).
- Perina, D. *et al.* Distribution of protein poly(ADP-ribosyl)ation systems across all domains of life. *DNA Repair (Amst)*. **23**, 4–16 (2014).
- Petermann, E., Ziegler, M. & Oei, S. L. ATP-dependent selection between single nucleotide and long patch base excision repair. *DNA Repair (Amst)*. **2**, 1101–1114 (2003).
- Pines, A. *et al.* PARP1 promotes nucleotide excision repair through DDB2 stabilization and recruitment of ALC1. *J. Cell Biol.* **199**, 235–249 (2012).
- Pleschke, J. M., Kleczkowska, H. E., Strohm, M. & Althaus, F. R. Poly(ADP-ribose) binds to specific domains in DNA damage checkpoint proteins. *J. Biol. Chem.* **275**, 40974–40980 (2000).
- Poirier, G. G., de Murcia, G., Jongstra-Bilen, J., Niedergang, C. & Mandel, P. Poly(ADP-ribosyl)ation of polynucleosomes causes relaxation of chromatin structure. *Proc. Natl. Acad. Sci.* **79**, 3423–3427 (1982).
- Polo, S. E. & Jackson, S. P. Dynamics of DNA damage response proteins at DNA breaks: a focus on protein modifications. *Genes Dev.* **25**, 409–433 (2011).
- Pommier, Y. Topoisomerase I inhibitors: camptothecins and beyond. *Nat. Rev. Cancer* **2006 610 6**, 789–802 (2006).
- Posey, A. E., Holehouse, A. S. & Pappu, R. V. Phase Separation of Intrinsically Disordered Proteins. *Methods Enzymol.* **611**, 1–30 (2018).
- Pouliot, J. J., Yao, K. C., Robertson, C. A. & Nash, H. A. Yeast Gene for a Tyr-DNA Phosphodiesterase that Repairs Topoisomerase I Complexes. *Science (80-.)*. **286**, 552–555 (1999).
- Prasad, R. *et al.* DNA polymerase β -mediated long patch base excision repair: Poly(ADP-ribose) polymerase-1 stimulates strand displacement DNA synthesis. *J. Biol. Chem.* **276**, 32411–32414 (2001).

-Q-

Qamar, S. *et al.* FUS Phase Separation Is Modulated by a Molecular Chaperone and Methylation of Arginine Cation- π Interactions. *Cell* **173**, 720-734.e15 (2018).

Qiu, H. *et al.* ALS-associated mutation FUS-R521C causes DNA damage and RNA splicing defects. *J. Clin. Invest.* **124**, 981–999 (2014).

-R-

Rabbits, T. H., Forster, A., Larson, R. & Nathan, P. Fusion of the dominant negative transcription regulator CHOP with a novel gene FUS by translocation t(12;16) in malignant liposarcoma. *Nat. Genet.* 1993 42 **4**, 175–180 (1993).

Rademakers, R., Neumann, M. & MacKenzie, I. R. Advances in understanding the molecular basis of frontotemporal dementia. *Nat. Rev. Neurol.* 2012 88 **8**, 423–434 (2012).

Radivojac, P. *et al.* Identification, analysis, and prediction of protein ubiquitination sites. *Proteins Struct. Funct. Bioinforma.* **78**, 365–380 (2010).

Ratti, A. & Buratti, E. Physiological functions and pathobiology of TDP-43 and FUS/TLS proteins. *J. Neurochem.* **138**, 95–111 (2016).

Ray Chaudhuri, A. & Nussenzweig, A. The multifaceted roles of PARP1 in DNA repair and chromatin remodelling. *Nat. Rev. Mol. Cell Biol.* 2017 1810 **18**, 610–621 (2017).

Reber, J. M. & Mangerich, A. Why structure and chain length matter: on the biological significance underlying the structural heterogeneity of poly(ADP-ribose). *Nucleic Acids Res.* **49**, 8432–8448 (2021).

Renger, R. *et al.* Co-condensation of proteins with single- and double-stranded DNA. *Proc. Natl. Acad. Sci. U. S. A.* **119**, e2107871119 (2022).

Rengifo-Gonzalez, J.C. *et al.* The cooperative binding of TDP-43 to GU-rich RNA repeats antagonizes TDP-43 aggregation. *Elife* **10**, e67605 (2021).

Rhine, K. *et al.* Poly(ADP-ribose) drives condensation of FUS via a transient interaction. *Mol. Cell* **82**, 969-985.e11 (2022).

Rhoads, S. N. *et al.* The prionlike domain of FUS is multiphosphorylated following DNA damage without altering nuclear localization. *Mol. Biol. Cell* **29**, 1786–1797 (2018).

Robu, M. *et al.* Role of poly(ADP-ribose) polymerase-1 in the removal of UV-induced DNA lesions by nucleotide excision repair. *Proc. Natl. Acad. Sci. U. S. A.* **110**, 1658–1663 (2013).

Rogelj, B. *et al.* Widespread binding of FUS along nascent RNA regulates alternative splicing in the brain. *Sci. Reports* 2012 21 **2**, 1–10 (2012).

Rolli, V., O'Farrell, M., Ménissier-de Murcia, J. & De Murcia, G. Random Mutagenesis of the Poly(ADP-ribose) Polymerase Catalytic Domain Reveals Amino Acids Involved in Polymer Branching†. *Biochemistry* **36**, 12147–12154 (1997).

Rosenthal, F. & Hottiger, M. O. Identification of ADP-ribosylated peptides and ADP-ribose acceptor sites. *Front. Biosci. - Landmark* **19**, 1041–1056 (2014).

Rosenthal, F. *et al.* Macrod domain-containing proteins are new mono-ADP-ribosylhydrolases. *Nat. Struct. Mol. Biol.* 2013 204 **20**, 502–507 (2013).

Ruf, A., Rolli, V., De Murcia, G. & Schulz, G. E. The mechanism of the elongation and branching reaction of Poly(ADP-ribose) polymerase as derived from crystal structures and mutagenesis. *J. Mol. Biol.* **278**, 57–65 (1998).

Rulten, S. L. *et al.* PARP-1 dependent recruitment of the amyotrophic lateral sclerosis-associated protein FUS/TLS to sites of oxidative DNA damage. *Nucleic Acids Res.* **42**, 307–314 (2014).

Rulten, S. L. *et al.* PARP-3 and APLF function together to accelerate nonhomologous end-joining. *Mol. Cell* **41**, 33–45 (2011).

Rulten, S. L., Cortes-Ledesma, F., Guo, L., Iles, N. J. & Caldecott, K. W. APLF (C2orf13) Is a Novel Component of Poly(ADP-Ribose) Signaling in Mammalian Cells. *Mol. and Cell. Biology* **28**, 4620–4628 (2023).

Ruscetti, T. *et al.* Stimulation of the DNA-dependent protein kinase by poly(ADP-ribose) polymerase. *J. Biol. Chem.* **273**, 14461–14467 (1998).

-S-

Sama, R. R. K. *et al.* FUS/TLS assembles into stress granules and is a prosurvival factor during hyperosmolar stress. *J. Cell. Physiol.* **228**, 2222–2231 (2013).

Satoh, M. S. & Lindahl, T. Role of poly(ADP-ribose) formation in DNA repair. *Nat.* 1992 3566367 **356**, 356–358 (1992).

Scaramuzzino, C. *et al.* Protein Arginine Methyltransferase 1 and 8 Interact with FUS to Modify Its Sub-Cellular Distribution and Toxicity In Vitro and In Vivo. *PLoS One* **8**, e61576 (2013).

- Schreiber, V., Dantzer, F., Ame, J.C. & de Murcia, G. Poly(ADP-ribose): novel functions for an old molecule. *Nat Rev Mol Cell Biol* **7**, 517-28 (2006).
- Schwartz, J. C. *et al.* FUS binds the CTD of RNA polymerase II and regulates its phosphorylation at Ser2. *Genes Dev.* **26**, 2690–2695 (2012).
- Schwartz, J. C. *et al.* FUS is sequestered in nuclear aggregates in ALS patient fibroblasts. *Mol. Biol. Cell* **25**, 2571–2578 (2014).
- Schwartz, J. C., Cech, T. R. & Parker, R. R. Biochemical Properties and Biological Functions of FET Proteins. *Annu. Rev. Biochem.* **84**, 355–379 (2015).
- Schwartz, J. C., Wang, X., Podell, E. R. & Cech, T. R. RNA Seeds Higher-Order Assembly of FUS Protein. *Cell Rep.* **5**, 918–925 (2013).
- Schwertman, P., Bekker-Jensen, S. & Mailand, N. Regulation of DNA double-strand break repair by ubiquitin and ubiquitin-like modifiers. *Nat. Rev. Mol. Cell Biol.* **17**, 379–394 (2016).
- Shakya, A. & King, J. T. DNA Local-Flexibility-Dependent Assembly of Phase-Separated Liquid Droplets. *Biophys. J.* **115**, 1840–1847 (2018).
- Shelkovanikova, T. A., Robinson, H. K., Connor-Robson, N. & Buchman, V. L. Recruitment into stress granules prevents irreversible aggregation of FUS protein mislocalized to the cytoplasm. *Cell Cycle* **12**, 3383–3391 (2013).
- Shiao Li Oei & Ziegler, M. ATP for the DNA ligation step in base excision repair is generated from poly(ADP-ribose). *J. Biol. Chem.* **275**, 23234–23239 (2000).
- Singatulina, A. S. *et al.* PARP-1 Activation Directs FUS to DNA Damage Sites to Form PARG-Reversible Compartments Enriched in Damaged DNA. *Cell Rep.* **27**, 1809-1821.e5 (2019).
- Sinha, S., Molla, S. & Kundu, C. N. PARP1-modulated chromatin remodeling is a new target for cancer treatment. *Med. Oncol.* **38**, (2021).
- Slade, D. PARP and PARG inhibitors in cancer treatment. *Genes & development* **34**, 360-394 (2020).
- Smith, J. A. & Stocken, L. A. Chemical and metabolic properties of adenosine diphosphate ribose derivatives of nuclear proteins. *Biochem. J.* **147**, 523–529 (1975).
- Spagnolo, L., Barbeau, J., Curtin, N. J., Morris, E. P. & Pearl, L. H. Visualization of a DNA-PK/PARP1 complex. *Nucleic Acids Res.* **40**, 4168–4177 (2012).

Steffen, J. D., Brody, J. R., Armen, R. S. & Pascal, J. M. Structural implications for selective targeting of PARPs. *Front. Oncol.* **3 DEC**, 301 (2013).

Sternburg, E. L., Gruijs da Silva, L. A. & Dormann, D. Post-translational modifications on RNA-binding proteins: accelerators, brakes, or passengers in neurodegeneration? *Trends Biochem. Sci.* **47**, 6–22 (2022).

Ström, C.E. et al. Poly (ADP-ribose) polymerase (PARP) is not involved in base excision repair but PARP inhibition traps a single-strand intermediate. *Nucleic acids research* **39**, 3166-3175 (2011).

Su, X. et al. Phase separation of signaling molecules promotes T cell receptor signal transduction. *Science (80-.)*. **352**, 595–599 (2016).

Suárez-Calvet, M. et al. Monomethylated and unmethylated FUS exhibit increased binding to Transportin and distinguish FTLD-FUS from ALS-FUS. *Acta Neuropathol.* **131**, 587–604 (2016).

Süel, K. E., Gu, H. & Chook, Y. M. Modular Organization and Combinatorial Energetics of Proline–Tyrosine Nuclear Localization Signals. *PLOS Biol.* **6**, e137 (2008).

Sukhanova, M. V. et al. Single molecule detection of PARP1 and PARP2 interaction with DNA strand breaks and their poly(ADP-ribosylation) using high-resolution AFM imaging. *Nucleic Acids Res.* **44**, e60–e60 (2016).

Sukhanova, M.V., Singatulina, A.S., Pastré, D. & Lavrik, O.I. Fused in sarcoma (FUS) in DNA Repair: Tango with poly (ADP-ribose) polymerase 1 and compartmentalisation of damaged DNA. *International Journal of Molecular Sciences* **21**, 7020 (2020).

Sun, S. et al. ALS-causative mutations in FUS/TLS confer gain and loss of function by altered association with SMN and U1-snRNP. *Nature communications* **6**, 1-14 (2015).

-T-

Takahama, K. & Oyoshi, T. Specific binding of modified rgg domain in tls/fus to g-quadruplex rna: Tyrosines in rgg domain recognize 2'-oh of the riboses of loops in g-quadruplex. *J. Am. Chem. Soc.* **135**, 18016–18019 (2013).

Takahama, K. et al. Regulation of Telomere Length by G-Quadruplex Telomere DNA- and TERRA-Binding Protein TLS/FUS. *Chem. Biol.* **20**, 341–350 (2013).

Takahama, K., Kino, K., Arai, S., Kurokawa, R. & Oyoshi, T. Identification of Ewing's sarcoma protein as a G-quadruplex DNA- and RNA-binding protein. *FEBS J.* **278**, 988–998 (2011).

- Takarada, T. *et al.* A protein–protein interaction of stress-responsive myosin VI endowed to inhibit neural progenitor self-replication with RNA binding protein, TLS, in murine hippocampus. *J. Neurochem.* **110**, 1457–1468 (2009).
- Takata, H. *et al.* Chromatin compaction protects genomic DNA from radiation damage. *PloS one* **8**, e75622 (2013).
- Tan, A. Y. & Manley, J. L. TLS Inhibits RNA Polymerase III Transcription. *Mol. Cell. Biol.* **30**, 186–196 (2010).
- Tan, A. Y., Riley, T. R., Coady, T., Bussemaker, H. J. & Manley, J. L. TLS/FUS (translocated in liposarcoma/fused in sarcoma) regulates target gene transcription via single-stranded DNA response elements. *Proc. Natl. Acad. Sci. U. S. A.* **109**, 6030–6035 (2012).
- Teloni, F. & Altmeyer, M. Readers of poly(ADP-ribose): designed to be fit for purpose. *Nucleic Acids Res.* **44**, 993–1006 (2016).
- Thandapani, P., O'Connor, T. R., Bailey, T. L. & Richard, S. Defining the RGG/RG Motif. *Mol. Cell* **50**, 613–623 (2013).
- Thompson, V. F. *et al.* Transcription-Dependent Formation of Nuclear Granules Containing FUS and RNA Pol II. *Biochemistry* **57**, 7021–7032 (2018).
- Thomsen, C., Grundevik, P., Elias, P., Ståhlberg, A. & Åman, P. A conserved N-terminal motif is required for complex formation between FUS, EWSR1, TAF15 and their oncogenic fusion proteins. *FASEB J.* **27**, 4965–4974 (2013).
- Ticozzi, N. *et al.* Mutational analysis reveals the FUS homolog TAF15 as a candidate gene for familial amyotrophic lateral sclerosis. *Am. J. Med. Genet. Part B Neuropsychiatr. Genet.* **156**, 285–290 (2011).
- Timinszky, G. *et al.* A macrodomain-containing histone rearranges chromatin upon sensing PARP1 activation. *Nat. Struct. Mol. Biol.* 2009 169 **16**, 923–929 (2009).
- Torgovnick, A., & Schumacher, B. (2015). DNA repair mechanisms in cancer development and therapy. *Frontiers in Genetics*, 6(APR).
- Tradewell, M. L. *et al.* Arginine methylation by PRMT1 regulates nuclear-cytoplasmic localization and toxicity of FUS/TLS harbouring ALS-linked mutations. *Hum. Mol. Genet.* **21**, 136–149 (2012).
- Truong, L. N. *et al.* Microhomology-mediated End Joining and Homologous Recombination share the initial end resection step to repair DNA double-strand breaks in mammalian cells. *Proc. Natl. Acad. Sci. U. S. A.* **110**, 7720–7725 (2013).

Tsai, Y. L., Mu, Y. C. & Manley, J. L. Nuclear RNA transcript levels modulate nucleocytoplasmic distribution of ALS/FTD-associated protein FUS. *Sci. Reports* 2022 **12**, 1–14 (2022).

Tsuiji, H. *et al.* Spliceosome integrity is defective in the motor neuron diseases ALS and SMA. *EMBO Mol. Med.* **5**, 221–234 (2013).

Tyzack, G. E. *et al.* Widespread FUS mislocalization is a molecular hallmark of amyotrophic lateral sclerosis. *Brain* **142**, 2572–2580 (2019).

-U-

Udagawa, T. *et al.* FUS regulates AMPA receptor function and FTLD/ALS-associated behaviour via GluA1 mRNA stabilization. *Nat. Commun.* 2015 **6**, 1–13 (2015).

Ummarino, S., Hausman, C. & Di Ruscio, A. The PARP Way to Epigenetic Changes. *Genes* 2021, Vol. 12, Page 446 **12**, 446 (2021).

Urwin, H. *et al.* FUS pathology defines the majority of tau-and TDP-43-negative frontotemporal lobar degeneration. *Acta Neuropathol.* **120**, 33–41 (2010).

Uversky, V. N. Intrinsically disordered proteins in overcrowded milieu: Membrane-less organelles, phase separation, and intrinsic disorder. *Curr. Opin. Struct. Biol.* **44**, 18–30 (2017).

-V-

Van Attikum, H. & Gasser, S.M. Crosstalk between histone modifications during the DNA damage response. *Trends in cell biology* **19**, 207–217 (2009).

Van Langenhove, T. *et al.* Genetic contribution of FUS to frontotemporal lobar degeneration. *Neurology* **74**, 366–371 (2010).

Van Treeck, B. & Parker, R. Emerging Roles for Intermolecular RNA-RNA Interactions in RNP Assemblies. *Cell* **174**, 791–802 (2018).

Vance, C. *et al.* ALS mutant FUS disrupts nuclear localization and sequesters wild-type FUS within cytoplasmic stress granules. *Hum. Mol. Genet.* **22**, 2676–2688 (2013).

Vance, C. *et al.* Mutations in FUS, an RNA processing protein, cause familial amyotrophic lateral sclerosis type 6. *Science* (80-.). **323**, 1208–1211 (2009).

Voigt, A. *et al.* TDP-43-Mediated Neuron Loss In Vivo Requires RNA-Binding Activity. *PLoS One* **5**, e12247 (2010).

-W-

- Wang, H. & Hegde, M.L. New mechanisms of dna repair defects in fused in sarcoma-associated neurodegeneration: Stage set for dna repair-based therapeutics? *Journal of Experimental Neuroscience* **13**, 1179069519856358 (2019).
- Wang, H. et al. Mutant FUS causes DNA ligation defects to inhibit oxidative damage repair in Amyotrophic Lateral Sclerosis. *Nature Communications* **9**, 1-18 (2018).
- Wang, J. et al. A molecular grammar governing the driving forces for phase separation of prion-like RNA binding proteins. *Cell* **174**, 688-699. e16 (2018).
- Wang, L. et al. PARP1 in Carcinomas and PARP1 Inhibitors as Antineoplastic Drugs. *Int. J. Mol. Sci.* **18**, (2017).
- Wang, M. et al. PARP-1 and Ku compete for repair of DNA double strand breaks by distinct NHEJ pathways. *Nucleic Acids Res.* **34**, 6170-6182 (2006).
- Wang, W. Y. et al. Interaction of FUS and HDAC1 regulates DNA damage response and repair in neurons. *Nat. Neurosci.* 2013 1610 **16**, 1383-1391 (2013).
- Wang, X., Schwartz, J. C. & Cech, T. R. Nucleic acid-binding specificity of human FUS protein. *Nucleic Acids Res.* **43**, 7535-7543 (2015).
- Wang, Z. et al. Recognition of the iso-ADP-ribose moiety in poly(ADP-ribose) by WWE domains suggests a general mechanism for poly(ADP-ribosyl)ation-dependent ubiquitination. *Genes Dev.* **26**, 235-240 (2012).
- Wheeler, J. R., Matheny, T., Jain, S., Abrisch, R. & Parker, R. Distinct stages in stress granule assembly and disassembly. *Elife* **5**, (2016).
- Whitehouse, C. J. et al. XRCC1 stimulates human polynucleotide kinase activity at damaged DNA termini and accelerates DNA single-strand break repair. *Cell* **104**, 107-117 (2001).
- Williams, K. L. et al. UBQLN2/ubiquilin 2 mutation and pathology in familial amyotrophic lateral sclerosis. *Neurobiol. Aging* **33**, 2527.e3-2527.e10 (2012).
- Wilson, D. M. et al. Hallmarks of neurodegenerative diseases. *Cell* **186**, 693-714 (2023).
- Winstall, E. et al. Preferential Perinuclear Localization of Poly(ADP-ribose) Glycohydrolase. *Exp. Cell Res.* **251**, 372-378 (1999).
- Wolozin, B. & Ivanov, P. Stress granules and neurodegeneration. *Nat. Rev. Neurosci.* 2019 2011 **20**, 649-666 (2019).

Wolozin, B. Regulated protein aggregation: Stress granules and neurodegeneration. *Mol. Neurodegener.* **7**, 1–12 (2012).

-Y-

Yamaguchi, A. & Kitajo, K. The Effect of PRMT1-Mediated Arginine Methylation on the Subcellular Localization, Stress Granules, and Detergent-Insoluble Aggregates of FUS/TLS. *PLoS One* **7**, e49267 (2012).

Yamazaki, T. *et al.* FUS-SMN Protein Interactions Link the Motor Neuron Diseases ALS and SMA. *Cell Rep.* **2**, 799–806 (2012).

Yang, L., Embree, L. J. & Hickstein, D. D. TLS-ERG Leukemia Fusion Protein Inhibits RNA Splicing Mediated by Serine-Arginine Proteins. *Mol. and Cell. Biology* **20**, 3345–3354 (2023).

Yang, L., Embree, L. J., Tsai, S. & Hickstein, D. D. Oncoprotein TLS interacts with serine-arginine proteins involved in RNA splicing. *J. Biol. Chem.* **273**, 27761–27764 (1998).

Yang, S. W. *et al.* A eukaryotic enzyme that can disjoin dead-end covalent complexes between DNA and type I topoisomerases. *Proc. Natl. Acad. Sci.* **93**, 11534–11539 (1996).

Yoshimura, A. *et al.* Myosin-Va Facilitates the Accumulation of mRNA/Protein Complex in Dendritic Spines. *Curr. Biol.* **16**, 2345–2351 (2006).

-Z-

Zhang, D., Paley, A. J. & Childs, G. The transcriptional repressor, ZFM1 interacts with and modulates the ability of EWS to activate transcription. *J. Biol. Chem.* **273**, 18086–18091 (1998).

Zhang, F., Chen, Y., Li, M. & Yu, X. The oligonucleotide/oligosaccharide-binding fold motif is a poly(ADP-ribose)-binding domain that mediates DNA damage response. *Proc. Natl. Acad. Sci. U. S. A.* **111**, 7278–7283 (2014).

Zhang, F., Shi, J., Bian, C. & Yu, X. Poly(ADP-Ribose) Mediates the BRCA2-Dependent Early DNA Damage Response. *Cell Rep.* **13**, 678–689 (2015).

Zhang, T. *et al.* FUS Regulates Activity of MicroRNA-Mediated Gene Silencing. *Mol. Cell* **69**, 787–801.e8 (2018).

Zhang, Y., Wang, J., Ding, M. & Yu, Y. Site-specific characterization of the Asp- and Glu-ADP-ribosylated proteome. *Nat. Methods* **10**, 981–984 (2013).

Zhang, Z. C. & Chook, Y. M. Structural and energetic basis of ALS-causing mutations in the atypical proline-tyrosine nuclear localization signal of the Fused in Sarcoma protein (FUS). *Proc. Natl. Acad. Sci. U. S. A.* **109**, 12017–12021 (2012).

Zhao, M., Kim, J.R., van Bruggen, R. & Park, J. RNA-binding proteins in amyotrophic lateral sclerosis. *Molecules and cells* **41**, 818 (2018).

Zhou, Y., Liu, S., Öztürk, A. & Hicks, G. G. FUS-regulated RNA metabolism and DNA damage repair. **2**, e29515 (2014).

Zinszner, H., Albalat, R. & Ron, D. A novel effector domain from the RNA-binding protein TLS or EWS is required for oncogenic transformation by CHOP. *Genes Dev.* **8**, 2513–2526 (1994).

Zinszner, H., Sok, J., Immanuel, D., Yin, Y. & Ron, D. TLS (FUS) binds RNA in vivo and engages in nucleo-cytoplasmic shuttling. *J. Cell Sci.* **110**, 1741–1750 (1997).